

Singularity-Invariant Leg Rearrangements in Stewart-Gough Platforms



Júlia Borràs Sol

Institut de Robòtica i Informàtica Industrial

Universitat Politècnica de Catalunya

Consejo Superior de Investigaciones Científicas

Thesis advisor:

Federico Thomas

A thesis submitted for the degree of

Doctor of Philosophy

Barcelona, 2011

Universitat Politècnica de Catalunya

Institut d'Organització i Control de Sistemes Industrials

Programa de doctorat:
Automatització Avançada i Robòtica

Aquesta tesi ha estat realitzada a:

Institut de Robòtica i Informàtica Industrial, CSIC-UPC

Director de tesi:
Federico Thomas

© Júlia Borràs Sol 2011

A la meva família,
pel seu recolzament incondicional.

Agraïments

M'agradaria expressar la meva sincera gratitud al professor Federico Thomas. La seva inestimable guia al llarg d'aquests 4 anys m'ha permès no només realitzar aquesta tesi, sinó aprendre que és la recerca i a estimar la professió a través del seu entusiasme en els projectes però també de la seva mirada crítica, sempre constructiva.

També voldria agrair a la professora Carme Torras el temps que m'ha dedicat, al llarg de tots els treballs que hem fet junts, pels seus punts de vista sovint diferents que m'han donat més perspectiva i per deixar-me aprendre de la seva professionalitat i versatilitat.

La Maria Alberich també mereix el meu agraïment, per haver-me presentat al Federico, i mostrar-me el camí cap a l'Institut i el món de la investigació, així com també pels seus consells al llarg d'aquest temps, des de la carrera fins avui.

Finalment, també vull agrair a tots els companys de l'Institut de Robòtica i Informàtica Industrial, pel bon ambient, els bons moments, les opinions compartides i el recolzament moral i professional. I a la meva família i al Joan, per estar sempre al meu costat.

Abstract

The Stewart-Gough platform was first introduced by E. Gough in 1954 and, since then, it has been used for many applications thanks to its great stiffness, accuracy and robustness in comparison with serial manipulators. It has triggered the research on parallel manipulators and continues to be the center of many researches because, despite its simple geometry, its analysis translates into challenging mathematical problems. One of the most challenging ones is the geometric interpretation of its singularities, that is, those positions where the platform loses stiffness. A complete geometric characterization of these unstable poses is still an open problem.

The present thesis provides new insight into this problem from a completely new approach: finding *singularity-invariant leg rearrangements*.

Finding all the transformations that leave the solution of a problem invariant does not solve it, but it provides a lot of information that contribute to its resolution. In the Stewart-Gough platform context, this indirect approach consists in the characterization of all the leg rearrangements that leave the platform singularity locus invariant. Such singularity-invariant leg rearrangements are shown to be a powerful tool to obtain kinematically equivalent manipulators, to help to visualize at a glance the complexity of its kinematics and to provide a common and original framework for the study of both pose-dependent singularities and architectural singularities of Stewart-Gough platforms.

The thesis analyzes all the rigid components that a Stewart-Gough platform can contain on a case-by-case basis. Then, it is shown how some of the most simple components admit any leg rearrangement that preserves the lines and planes that their attachments define. On the contrary, other more complex components only admit rearrangements that preserve some extra geometric constraints. This apparently restrictive fact will provide interesting geometric information about the kinematics and the topology of the singularity locus of the analyzed platforms.

In sum, this dissertation presents a new way to arrive at the geometric interpretations of Stewart-Gough platform singularities, a classification of these platforms depending on their singularities, and an inherent classification of all the architectural singularities, as well as some practical applications of these theoretical results.

Resum

La plataforma de Stewart-Gough va aparèixer per primer cop el 1954 de la mà de E. Gough, i des de llavors s'ha usat en moltes aplicacions gràcies a la seva rigidesa, la gran precisió en els seus moviments i la seva robustesa comparada amb els manipuladors sèrie. Ha liderat la recerca sobre robots paral·lels perquè, tot i el seu disseny geomètric senzill, el seu anàlisi dóna lloc a problemes matemàtics molt complexos. Un dels més estimulants és la descripció geomètrica de les seves singularitats, és a dir, aquelles posicions on el mecanisme perd la rigidesa. La completa caracterització geomètrica d'aquestes posicions inestables és encara un problema obert.

Aquesta tesi aporta més llum sobre aquest problema des d'una òptica completament nova: trobar els rearranjaments de potes que mantenen les singularitats invariants (en anglès, *singularity-invariant leg rearrangements*).

Trobar aquelles transformacions que mantenen invariants les solucions d'un problema matemàtic no ens en dóna la solució, però sí que ens proporciona molta informació que ajuda en la resolució del problema. En el context dels robots paral·lels, aquest plantejament indirecte consisteix en trobar els canvis en les posicions de les potes que no modifiquen la localització de les singularitats. Els anomenats *singularity-invariant leg rearrangements* demostren ser una eina potent per a obtenir manipuladors cinemàticament equivalents, ajuden a visualitzar la complexitat de l'anàlisi d'un manipulador en un cop d'ull, i proporcionen un marc comú per a l'estudi de les singularitats dependents de la posició i les dependents de l'arquitectura de les plataformes de Stewart-Gough.

El treball analitza totes les components rígides que una plataforma de Stewart-Gough pot contenir. Es mostra com les components més senzilles admeten qualsevol rearranjament que mantingui les rectes i plans definits pels punts d'ancoratge de les potes. D'altra banda, les components més complexes només admeten rearranjaments

que satisfan restriccions addicionals. Aquest fet pot semblar més restrictiu, però proporciona informació geomètrica rellevant sobre la cinemàtica i la topologia de la hipersuperfície de singularitats de la plataforma.

En resum, aquesta tesi presenta una nova manera d'obtenir interpretacions geomètriques de les singularitats, de classificar les plataformes paral·leles depenent de les seves singularitats i proporciona una classificació inherent de les singularitats arquitectòniques, així com algunes aplicacions pràctiques d'aquests resultats.

Contents

1	Introduction	1
1.1	Motivation	1
1.2	Objectives	5
2	Preliminary concepts	9
2.1	Kinematics and singularities of Stewart-Gough platforms	9
2.2	Classifications of Stewart-Gough platforms	15
2.3	Architectural singularities of Stewart-Gough platforms	17
2.4	Manipulability, dexterity and other performance indexes	19
2.5	Summary of open problems and related work	21
3	Singularity-invariant leg rearrangements	23
3.1	Notation	23
3.2	Singularity-invariant leg rearrangement: Definition	24
3.2.1	Methodology I: Finding an affine relation between leg lengths	25
3.2.2	Methodology II: Rewriting the singularity polynomial	28
4	The Point-Line, Point-Plane and Line-Line components	31
4.1	Finding the affine relation between leg lengths	31
4.2	The affine relation for the Point-Plane component	34
4.3	The affine relation for the Line-Line component	35

4.4	Architectural singularities in Line-Line components	37
4.5	Examples	38
4.5.1	The Zhang-Song platform	38
4.5.2	The Griffis-Duffy Platform	43
4.6	More on the Point-Plane component	49
4.7	More on the Line-Line component	52
4.8	Application to the implementation of an octahedral manipulator	55
5	The Line-Plane component	61
5.1	Pentapods	61
5.2	Finding the affine relation between leg lengths	63
5.3	Finding the rearrangements by rewriting the Jacobian determinant	66
5.3.1	Static Analysis	66
5.3.2	Singularity-invariant leg rearrangement condition	68
5.4	Singularity-invariant leg rearrangement rules	69
5.5	Geometric interpretation of parallel singularities in Line-Plane components	74
5.6	Classifying pentapods by their singularities	76
5.6.1	Pentapod families with identical singularities	76
5.6.2	Three possible topologies for the singularity locus	77
5.6.3	Forward kinematics: Quartically, cubically and quadratically-solvable cases	79
5.6.4	A quadratically-solvable pentapod	82
5.7	Architecture singularities	85
5.7.1	Algebraic characterization	85
5.7.2	Geometric interpretation	86
5.7.3	Proximity to architectural singularities	88
5.7.4	An example	90

5.8	The role of cross-ratios	94
5.9	Examples	97
5.9.1	Uncoupled parallel manipulator	97
5.9.2	Elimination of multiple spherical joints	98
5.9.3	Numerical example of a quadratically-solvable pentapod	98
5.10	Non-generic cases	102
5.10.1	One attachment in \mathcal{B}	102
5.10.2	Two attachments in \mathcal{B}	103
5.10.3	Four aligned attachments	107
5.11	Applications on reconfigurable pentapods	109
5.11.1	A design free from architectural singularities	112
5.11.2	A pentaglide with parallel arrangement of guides	116
6	The Line-Body component	121
6.1	Rewriting the Jacobian matrix determinant	121
6.2	Singularity-invariant leg rearrangements rules	123
6.3	Classification of Line-Body designs	126
6.3.1	No consistent real roots	127
6.3.2	One consistent real root	128
6.3.3	Two consistent real roots	130
6.3.4	Three consistent real roots	132
6.4	Architectural singularities	133
6.5	Examples	134
6.5.1	No consistent real roots	135
6.5.2	One consistent real root	136
6.5.3	Two consistent real roots	137
6.5.4	Three consistent real roots	139

7 The Plane-Plane component	143
7.1 Finding the affine relation between leg lengths	143
7.1.1 Generalizing and simplifying the condition	146
7.2 Singularity-invariant leg rearrangement rules	147
7.3 Examples	149
7.3.1 A doubly-planar Stewart-Gough platform	149
7.3.2 Platform with degenerate cubic curves	151
7.3.3 Griffis-Duffy platforms	154
7.4 Classification of doubly-planar Stewart-Gough platforms	159
7.4.1 General doubly-planar manipulators	159
7.4.2 Families of doubly-planar 3-3 manipulators	167
7.5 Rewriting the Jacobian matrix determinant	171
7.6 Architectural Singularities	172
7.6.1 Algebraic characterization	172
7.6.2 Geometric interpretation	173
7.6.3 Comparison with previous results	176
8 The Plane-Body and the Body-Body components	179
8.1 The Plane-Body component	180
8.2 The Body-Body component	181
8.3 Example of a non-generic case: a decoupled Stewart-Gough platform . .	182
9 Conclusions: contributions and prospects for further research	185
Appendices	187
A Cayley-Menger determinants and Distance Geometry	188
B Cross-ratios and Projective Geometry	191

List of Figures

1.1	First implementation of the Gough platform to test tyres.	2
1.2	Applications of the Stewart-Gough platform.	3
1.3	All rigid components that a Stewart-Gough platform can contain.	6
2.1	A general Stewart-Gough platform.	10
2.2	Static analysis of a Stewart-Gough platform.	13
2.3	The three possible 3-3 Stewart-Gough platforms.	16
2.4	Over-actuated components of Stewart-Gough platforms.	18
3.1	A single-leg rearrangement of a general Stewart-Gough platform.	24
4.1	A point-line component formed by legs l_1 and l_2	32
4.2	Point-Plane singularity-invariant leg rearrangement.	34
4.3	Singularity-invariant leg rearrangements on the Line-Line component.	36
4.4	Transformation from the basic flagged to the Zhang-Song platform.	39
4.5	An architecturally singular Zhang-Song platform.	40
4.6	Self-motion of the architecturally singular Zhang-Song platform.	41
4.7	Eigenvalues of $\mathbf{J}^T \mathbf{J}$ for the architecturally-singular Zhang-Song platform.	42
4.8	Rearrangement from the octahedral platform into a Griffis-Duffy platform.	44
4.9	An architecturally singular Griffis-Duffy platform.	45
4.10	Self-motion of the architecturally singular Griffis-Duffy platform.	47

LIST OF FIGURES

4.11 Eigenvalues of $\mathbf{J}^T\mathbf{J}$ for the architecturally-singular Griffis-Duffy platform.	48
4.12 The self-motion discretization using CUIK.	49
4.13 Leg rearrangements in the Point-Plane component.	50
4.14 Base triangles of a Point-Plane component before and after a leg rearrangement.	51
4.15 A generic Line-Line component.	52
4.16 Approximation to the octahedral manipulator that avoid double-ball joints.	56
4.17 A 6-6 platform kinematically equivalent to the octahedral manipulator.	58
4.18 Representation of all architecturally singular Griffis-Duffy platforms. . .	59
4.19 Prototype of a 6-6 parallel manipulator.	60
5.1 A pentapod.	61
5.2 A 5-axis milling machine developed by Metrom Mechatronische	62
5.3 A generic Line-Plane component with an additional leg in gray.	63
5.4 Schematic representation of a pentapod.	67
5.5 One-to-one correspondence between the attachments in the platform line and the lines of the pencil centered at \mathcal{B}	70
5.6 Representation of singularity surface of the Line-Plane component. . . .	72
5.7 Singularity-invariant leg rearrangement rules for the Line-Plane component.	73
5.8 Geometric interpretation of the parallel singularities of the Line-Plane component.	75
5.9 Planar geometric construction that defines all the geometric parameters in a pentapod.	77
5.10 Quartically, cubically and quadratically-solvable pentapods (left), with their corresponding \mathcal{B} -surfaces (right).	78
5.11 The composition of the \mathcal{B} -correspondence and the \mathcal{C}_5 -correspondence. .	89
5.12 The pentapod analyzed in Section 5.7.4.	90

LIST OF FIGURES

5.13 Singular conics, \mathcal{C}_i , for $i = 1, \dots, 5$ for the pentapod in Fig. 5.12.	92
5.14 Self-motion of the analyzed architecturally singular pentapod.	93
5.15 The role of cross-ratios in the Line-Plane component.	95
5.16 Rearrangement from a Line-Plane component to an uncoupled manipu- lator.	97
5.17 Elimination of multiple spherical joints.	99
5.18 Pentapod analyzed in Section 5.9.3.	100
5.19 Singular conics of the pentapod appearing in Fig. 5.18.	101
5.20 The pentapod described in Section 5.7.4, and its singular conics.	104
5.21 Another non-generic pentapod.	105
5.22 Degenerate conics for the analyzed non-generic pentapod.	106
5.23 A Line-Plane component containing a Line-Line subcomponent.	107
5.24 A reconfigurable leg along a guide.	110
5.25 A reconfigurable pentapod free from architectural singularities.	112
5.26 Singular conics of the pentapod appearing in Fig. 5.25.	114
5.27 A reconfigurable Line-Plane prototype.	116
5.28 Prototype of the reconfigurable quadratically-solvable pentapod.	120
6.1 Notation associated with a Line-Body component.	122
6.2 Singularity-invariant leg substitutions in the Line-Body component.	126
6.3 One-to-one correspondence between the line and the cubic curve attached to the base.	128
6.4 Generic pentapod analyzed in Section 6.5.1 with its corresponding at- tachment coordinates.	135
6.5 Pentapod analyzed in Section 6.5.2.	136
6.6 A pentapod with two real consistent roots.	138
6.7 A Line-Body with locus formed by 3 space lines crossing two by two.	139

LIST OF FIGURES

6.8	Pentapod analyzed in Section 6.5.4 and its attachment coordinates. . . .	140
6.9	The base attachments can be moved along the lines without modifying the singularity locus of the pentapod.	141
7.1	Notation associated with a Plane-Plane component.	143
7.2	Manipulator analyzed in Section 7.3.1 with its corresponding attachment coordinates.	149
7.3	The base and the platform curves defined in (7.11).	150
7.4	Platform described in Table 7.1.	151
7.5	The base and the platform curves defined by (7.13).	152
7.6	Possible leg substitutions are shown in gray.	154
7.7	Griffis-Duffy type I platform and its equivalent octahedral manipulator.	155
7.8	Griffis-Duffy type II platform and its equivalent platform after removing all collinearities.	157
7.9	The basic 3-3 Stewart-Gough manipulators.	167
7.10	A doubly-planar Stewart-Gough platform and its corresponding attachment coordinates.	173
7.11	The pencil of cubics through the first five platform and base attachments and the 3 singular points.	178
8.1	A decoupled manipulator with non-planar platform and its corresponding attachment coordinates.	182
8.2	Singularity-invariant leg rearrangements from the example in Fig. 8.1. .	184
B.1	Cross-ratios of points on a line or a conic, and cross-ratios of lines in a pencil.	192

Chapter 1

Introduction

1.1 Motivation

Even when there is no known solution to a given mathematical problem, it is always possible to try to find the set of transformations that leave its solution invariant. Although this does not solve the problem itself, it provides insight into its nature. This way of thinking is at the root of the development of Group Theory and it is the one applied herein for the characterization of the singularity loci of Stewart-Gough platforms.

The Stewart-Gough platform is a parallel robot defined as a 6-DoF parallel mechanism with six identical extensible legs connected to a base and a moving platform through ball-and-socket joints [40, 94]. It triggered the research on parallel manipulators, and it has remained one of the most widely studied because, despite its geometric simplicity, its analysis translates into challenging mathematical problems [26].

The first implementation of this platform was done by E. Gough in 1954 [40]. He developed the *Universal Tire-Testing Machine*, a moving platform to which a tire was attached. It was linked to the ground by 6 links with varying lengths. Each link had a ball-and-socket joint at the base and a universal joint at the platform, so that changing the link lengths, the position and the orientation of the moving platform (and of the attached wheel) was modified. The wheel was driven by a conveyor belt and the mechanism allowed the operator to measure the tire wear and tear under combined loads. Gough died in 1972 but his testing machine continued to be used up until the late 1980 (Fig. 1.1).

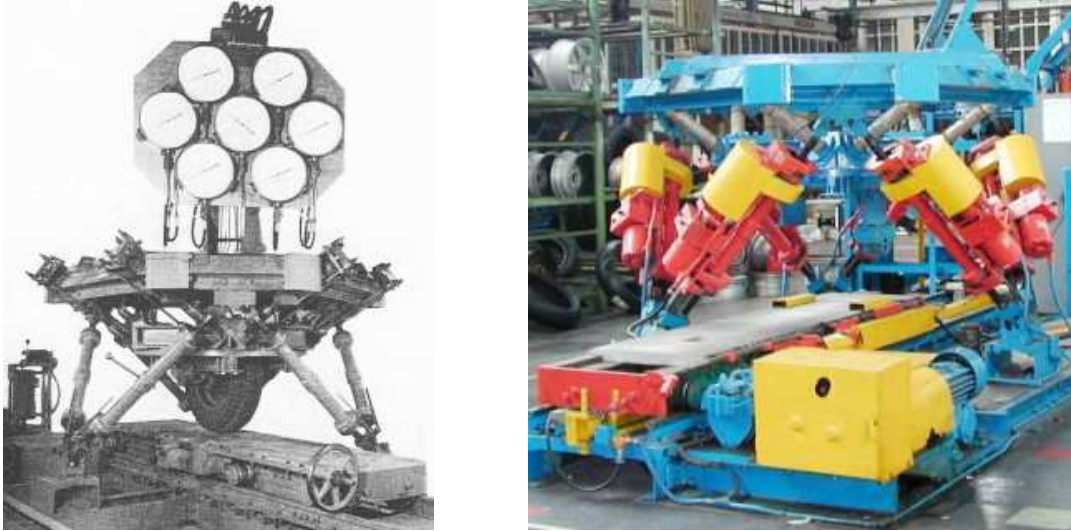


Figure 1.1: First implementation of the Gough platform to test tyres, and an actual implementation of the same machine, used in the Dunlop Tyres company.

In 1965, D. Stewart suggested a 6-DoF mechanism capable of reproduce general motion in space [94], in other words, a flight simulator. Stewart's mechanism consisted of a triangular platform supported by ball joints over three legs of adjustable lengths and angular altitudes connected to the ground through two-axis joints. Stewart's paper received many reviews, one of them by E. Gough, who suggested the use of six linear actuators all in parallel, similarly to his tire testing machine. This suggestion made the platform manipulator a fully parallel actuated mechanism that, nowadays, is known as the Stewart-Gough platform.

Since the 1980's, the research on parallel manipulators has attracted the interest of many researchers and is still the focus of several important research projects. In particular, applications of the Stewart-Gough platforms appear in machine tool technology, coordinate measuring machines, crane technology, force sensors, telescopes and medical robots. For example, in Fig. 1.2-(a) appears a micro-positioning device developed by the PI company (Piezo Nano Positioning) that provides significantly higher accuracy and resolution than hydraulically driven systems. Parallel kinematics precision positioning systems have many advantages over serial kinematics stages, such as lower inertia, improved dynamics, smaller package size and higher stiffness (see [81] for more positioning devices based on the Stewart-Gough platform). In the leisure in-

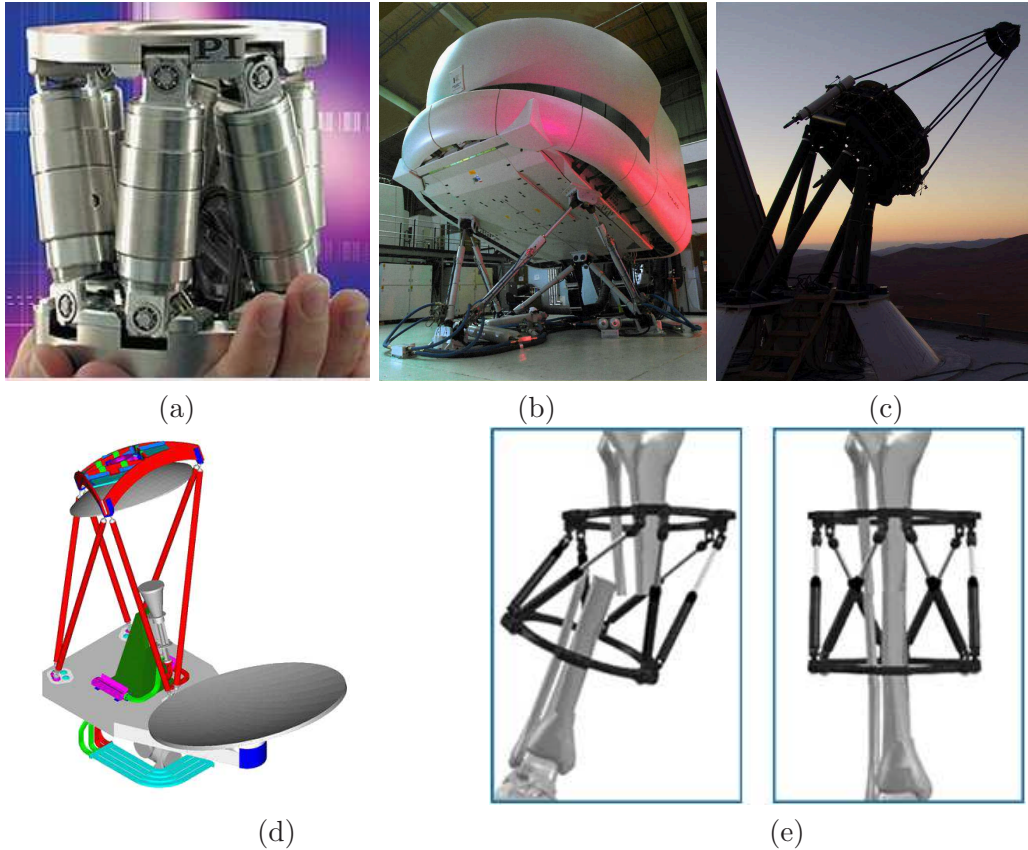


Figure 1.2: Applications of the Stewart-Gough platform in positioning devices, flight simulators, telescopes and orthopedic surgery.

dustry, numerous parallel structures are used for flight simulators [Fig. 1.2-(b)]. Many companies offer movement simulators in various dimensions, and this domain is one of the most successful for parallel structures. Fig. 1.2-(c) shows an hexapod telescope in OCA (Observatorio Cerro Armazones), mounted on a Stewart-Gough platform structure, allowing it to move in all six spatial degrees of freedom and also providing strong structural integrity. As a result, the ratio of bearing pressure and its own weight is very high. Furthermore, the six-leg structure allows very precise positioning and repeatability [88]. Satellite communications require very accurate pointing systems, Fig. 1.2-(d) shows a pointing system for double reflector antenna developed by Alcatel Alenia Space company and the Catania University that uses a Stewart-Gough platform. Finally, as an example of medical robot, the Stewart-Gough platform has been used to develop the Taylor Spatial Frame [96], an external fixator used in orthopedic surgery for the

correction of bone deformities and treatment of complex fractures [Fig. 1.2-(e)].

One important part of the analysis that have to be done to obtain a well-conditioned Stewart-Gough platform corresponds to the characterization of its singularities [28]. When a parallel platform is on a singularity, it gains degrees of freedom even though their actuators are locked. Therefore, the characterization of these unstable poses is essential for several aspects. To improve the robot design, one needs manipulators with as few singularities as possible, or located outside of the reachable workspace. For dynamics and control, it is also necessary to improve the robot behavior near a singularity, and for workspace computation and path planning, it is essential to detect efficiently how near the robot is to a singular pose. In addition, a different type of singularities, called architectural, have also deserved a special attention in the lately literature [64]. Architecturally singular Stewart-Gough platforms are always in a singularity independently of their leg lengths. In general, they are of no practical interest because they cannot be controlled. Thus, their characterization is important to avoid them in the early design process.

The geometric and topological characterization of the singularity locus of a given Stewart-Gough platform in its six-dimensional configuration space is, in general, a huge task which has only been completely solved for some specializations —*i.e.*, designs in which some spherical joints in the platform, the base, or both, coalesce to form multiple spherical joints [2, 5, 30, 79]. The geometrical interpretation of the singularity conditions allow to better understand and more efficiently detect the closeness to a singular pose. Similarly, architectural singularities are usually characterized by algebraic conditions [53, 54, 108], and only few of them have been geometrically interpreted.

In this context, it seems reasonable to find leg rearrangements in a given Stewart-Gough platform that leave its singularity locus invariant for several reasons:

- If the singularity locus of the platform at hand has already been characterized, it could be interesting to modify the location of its legs to optimize some other platform characteristics without altering such locus (such as stiffness, avoidance of leg collisions or elimination of multiple spherical joints). For example, they can be used to improve the robot behavior near a singularity.

- If the singularity locus of the analyzed platform has not been characterized yet, it could be of interest to simplify the platform's geometry by changing the location of its legs, thus easing the task of obtaining this characterization.
- Analyzing all possible leg rearrangements, one could identify all equivalent platforms, to avoid repeating analyses that actually correspond to the same manipulator (as occurs in the literature).
- The characterization of singularity-invariant leg rearrangement provide information about the kinematics of the platform, that can be used to obtain new geometric characterizations of its singularities.
- Because of their geometric nature, singularity-invariant leg rearrangements provide indirectly geometric interpretations of architectural singularities.

In conclusion, singularity-invariant leg rearrangements are shown to be a general useful tool for the design and kinematic analysis of all Stewart-Gough platforms.

1.2 Objectives

The main goal of this thesis is the characterization of the geometric transformations on the locations of the leg attachments of a Stewart-Gough platform that leave its singularities invariant. In general, substituting one leg of a Stewart-Gough platform by another arbitrary leg modifies the platform singularity locus in a rather unexpected way. Nevertheless, in those cases in which the considered platform contains rigid sub-assemblies, or *components* [57], legs can be rearranged so that the singularity locus remains unaltered provided that the kinematics of the components are not modified.

The legs involved in a rigid component fix the relative position between two geometric entities (points, lines, planes or bodies). A singularity-invariant leg rearrangement defined for a rigid component can be applied to any Stewart-Gough platform that contains it.

This thesis is structured following the component classification (Fig. 1.3) as follows:

- (a) The Point-Line component. It is the most simple one. It can appear up to 6 times in one Stewart-Gough platform.

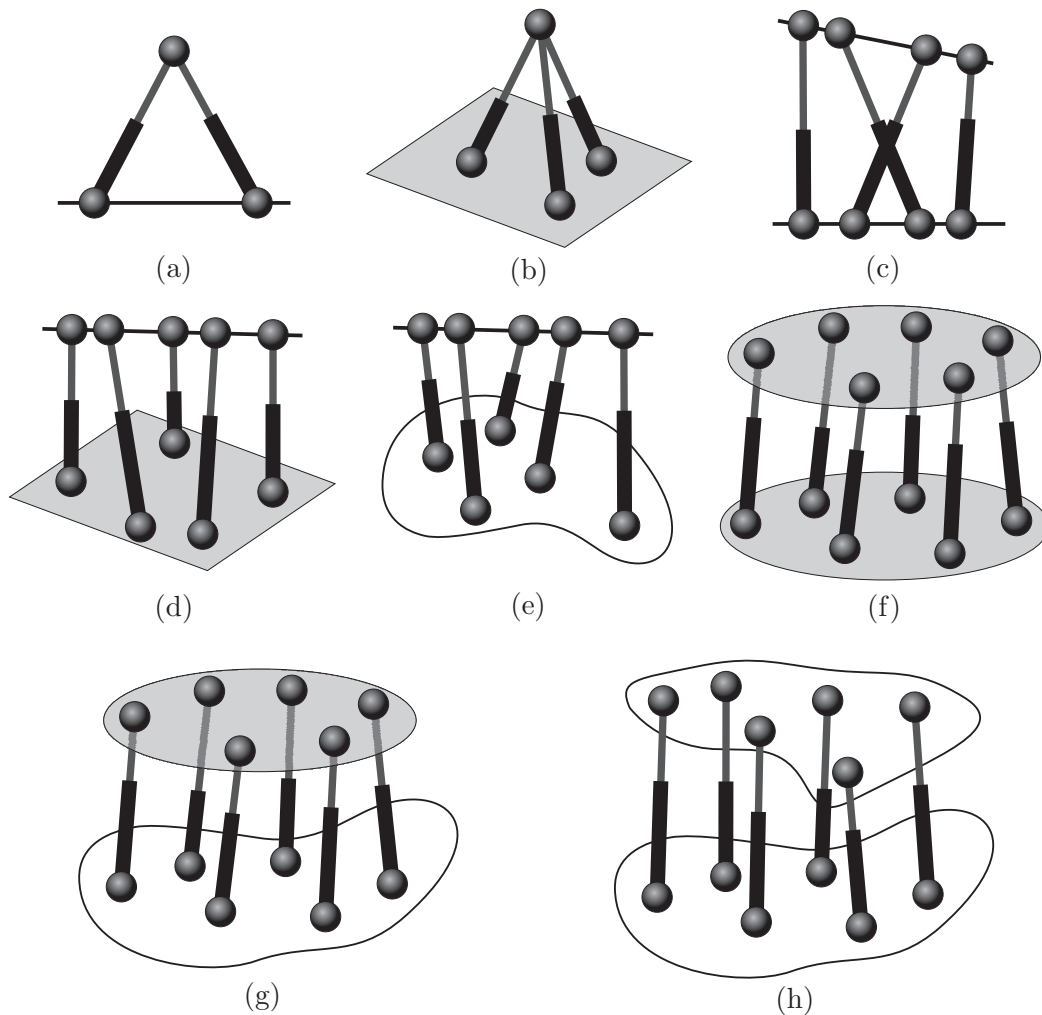


Figure 1.3: All rigid components that a Stewart-Gough platform can contain.

- (b) The Point-Plane component. Formed by 3 legs, it can only appear twice in a Stewart-Gough platform.
- (c) The Line-Line component. It involves 4 legs and it is the first that presents complex singularities.
- (d) The Line-Plane component. Involves 5 legs and can be considered for itself as a manipulator, called pentapod, with practical interest when working with axisymmetric tools.
- (e) The Line-Body component. It is the generalization of the Line-Plane component

and thus, it is equivalent to general pentapods.

- (f) The Plane-Plane component. Involving 6 legs, it is the first component that represents a full Stewart-Gough platform.
- (g) The Plane-Body and the Body-Body components. They correspond to the most general Stewart-Gough platforms, it will be shown how they do not admit any singularity-invariant leg rearrangement for a generic configuration of their leg attachments.

The possible leg rearrangements for each of the above components are studied from Chapter 4 to Chapter 8, respectively. It will be shown how the complete characterization of all the singularity-invariant leg rearrangements, and the identification of the geometric rules to perform them, will permit to:

1. Generate families of Stewart-Gough platforms with equivalent singularity locus without the limitations of previous classification which do not consider the possibility of collinear or coplanar attachments.
2. Classify and characterize all architectural singularities arising in Stewart-Gough platforms. All possible singularity-invariant leg rearrangements that can be obtained by continuous transformations in the location of the attachments of a Stewart-Gough platform can lead to architectural singularities by properly adjusting the involved geometric parameters and, conversely, all architecturally singular platforms can be obtained by applying a degenerate singularity-invariant leg rearrangement to a non-singular platform.
3. Decouple the problem of locating the singularities of a Stewart-Gough platform to that of improving, for example, its dexterity in a given region of its configuration space. This would be possible because singularity-invariant leg rearrangements permit modifying the value of the platform Jacobian determinant by a constant factor.
4. Optimize the design of a given parallel platform to improve its manoeuvrability or to avoid possible collisions between its legs, in a given region of its configuration space, without altering its singularity locus. This includes the possibility of eliminating multiple spherical joints which are always difficult to implement.

5. Design reconfigurable platforms whose attachments can be modified statically or dynamically to adapt them to different tasks. Since the legs lengths, before and after such kind of transformations, would be in one-to-one correspondence, the control of such reconfigurable platforms would not be increased notably by the possibility of reconfiguring them.

At the beginning of this thesis a conjecture was formulated:

All singularity-invariant leg rearrangements, under degenerate circumstances, can lead to architectural singularities and, conversely, all architecturally singular platforms can be obtained by applying a degenerate singularity-invariant leg rearrangement to a non architecturally-singular platform.

At the end of the completion of this thesis, it was possible to assert that, indeed, all architectural singularities have been detected as a degenerate singularity-invariant leg rearrangement, and the other way round, any singularity-invariant leg rearrangement can lead to an architectural singularity. In addition, singularity-invariant leg rearrangements provide the tools to detect any other architectural singularity for any non-generic case.

The thesis is organized as follows. Chapter 2 presents the state of the art in the kinematic analysis on Stewart-Gough platforms and in parallel robots in general. Chapter 3 provides the two methodologies that will be applied in the successive chapters. As stated before, Chapters from 4 to 8 present the singularity-invariant leg rearrangements for each component, some of them presenting practical applications of singularity-invariant leg rearrangements, such as design optimizations for very well-known manipulators, reconfigurable robot designs and two prototypes that have been constructed at Institut de Robòtica i Informàtica Industrial using the theory presented here. The conclusions summarize the main contributions and propose prospects for further research.

Chapter 2

Preliminary concepts

2.1 Kinematics and singularities of Stewart-Gough platforms

There is a large number of publications regarding the kinematics of Stewart-Gough platforms, both for particular configurations of the attachments [30, 90, 98, 111], and for the general case [34, 47].

Contrary to what happens to serial manipulators, the forward kinematics of Stewart-Gough platforms is a very challenging problem, while their inverse kinematics is trivial.

The resolution of the forward kinematics problem is essential for control, on-line simulation and for performance analysis. For a Stewart-Gough platform, it consist in finding the position and orientation (*i.e.*, the pose) of the platform, given its leg lengths.

Let A_i and B_i , for $i = 1, \dots, 6$, denote the center points of the leg attachments and let \mathbf{a}_i and $\tilde{\mathbf{b}}_i$ be their position vectors, in the base and platform reference frames respectively (refer to Fig. 2.1). Given the position $\mathbf{p} = (p_x, p_y, p_z)^T$ and the orientation $\mathbf{R} = R(\alpha_x, \alpha_y, \alpha_z)$, the location of the platform attachments in the base reference frame can be expressed as $\mathbf{b}_i = \mathbf{p} + \mathbf{R}\tilde{\mathbf{b}}_i$, for $i = 1, \dots, 6$. For the sake of simplicity, in this thesis the center points of the leg attachments will be denoted by their position vectors.

Geometrically, the forward kinematic problem is equivalent to the problem of placing a rigid body such that six given points of the body lie on six given spheres. Algebraically, this can be expressed as:

$$\|\mathbf{a}_i - \mathbf{b}_i\|^2 = l_i^2, \quad i = 1, \dots, 6, \quad (2.1)$$

2.1 Kinematics and singularities of Stewart-Gough platforms

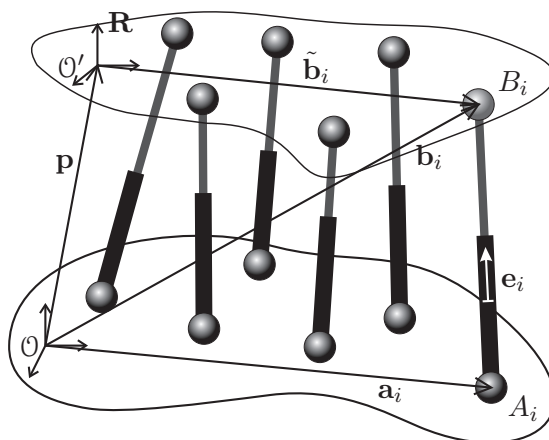


Figure 2.1: A general Stewart-Gough platform with base attachments A_i and platform attachments at B_i , $i = 1, \dots, 6$.

where l_i is the length of the i th leg.

In general, the above system of six equations can have several solutions. In other words, there are several poses for which the corresponding leg lengths are the same. Each valid pose is called an assembly mode. The number of assembly modes depends on how the attachments are arranged. The topology of a given arrangement of attachments is called an architecture and each architecture has an associated maximum number of assembly modes. This number ranges from 8 to 40.

For some particular architectures, a closed-form solution for their forward kinematics is known [79, 98, 111]. Closed-form solutions simplify the corresponding error analysis, and provide accurate and fast computations. For these particular architectures, either several attachments merge into multiple spherical joints or some alignment or coplanarity constraints must be satisfied between attachments.

For the general case, it was proved that the maximum number of assembly modes was 40 [61, 82, 86]. In fact, a 40th degree polynomial allowing to calculate (numerically) all possible assembly modes was found by Husty in 1994 [47]. Later, Dietmaier, in 1998, found a Stewart-Gough platform with 40 real assembly modes for a particular set of leg lengths using continuation techniques [27].

More recently, Distance Geometry has appeared as a new approach to deal with kinematic problems. Indeed, it has immediate relevance where distances between points

2.1 Kinematics and singularities of Stewart-Gough platforms

are determined or considered. It started to receive a lot of attention twenty years ago with the advent of molecular magnetic resonance experiments to obtain distances between atoms in rigid molecules [24], and more recently in Robotics to obtain intrinsic formulations of different kinematics problems, thus avoiding the introduction of arbitrary reference frames [77, 98], or the problems derived from the tangent half-angle substitution [59, 85]. Interval analysis and linear relaxation techniques have also been used for general position analysis solvers, giving box approximation solutions for general serial and parallel manipulators [69, 71, 80, 97].

If the system of equations in (2.1) is rewritten as an implicit relation between the leg lengths, $\Theta = (l_1, \dots, l_6)$, and the pose of the platform, \mathbf{X} , which depends on the position vector (p_x, p_y, p_z) and the chosen orientation parameters [72], it reads as

$$F(\mathbf{X}, \Theta) = 0.$$

When differentiating this expression with respect to time, it yields

$$\mathbf{P}\dot{\mathbf{X}} + \mathbf{S}\dot{\Theta} = 0 \tag{2.2}$$

where $\mathbf{P} = \frac{\partial F}{\partial \mathbf{X}}$ and $\mathbf{S} = \frac{\partial F}{\partial \Theta}$. The most accepted classification of Stewart-Gough platform singularities was introduced in 1990 by Gosselin and Angeles [38] using this formulation and consists in three categories:

- Type I (called *serial singularities* in [68]): They arise when $|\frac{\partial F}{\partial \Theta}| = 0$. They occur when the manipulator reaches the boundary of the workspace or internal boundaries limiting different subregions of the workspace. In such singularities, there exist nonzero $\dot{\Theta}$ for which $\dot{\mathbf{X}} = 0$. In other words, there are velocities that cannot be reproduced at the output. One can say that, at type I singularities, the manipulator loses degrees of freedom.
- Type II (called *parallel singularities* in [68]): They arise when $|\frac{\partial F}{\partial \mathbf{X}}| = 0$. They occur when the platform is locally movable even when the actuated joints are locked and happens within the workspace. That is, if $\dot{\Theta} = 0$, $\dot{\mathbf{X}}$ is not necessarily zero. One can say that, at type II singularities, the manipulator gains degrees of freedom.

2.1 Kinematics and singularities of Stewart-Gough platforms

- Type III: When both $|\frac{\partial F}{\partial \Theta}| =$ and $|\frac{\partial F}{\partial \mathbf{X}}| = 0$. They occur when the end-effector may be moved while the actuators are locked, and vice versa.

Ma and Angeles made a further distinction for type II singularities in [64] by introducing the concept of *architectural singularities*. These are manipulators whose geometric parameters make $\det(\mathbf{P}) = 0$ for any position of the workspace. In this situation, the manipulator exhibits a self-motion for any set of leg lengths.

It was shown in [38] that the Stewart-Gough platforms have very simple type I singularities, as matrix \mathbf{S} is singular only when any of the leg lengths is zero. This, in practice, can never happen due to joint limits. In fact, type I singularities only happen at the limits of the prismatic joints, just because at the limit of the workspace some velocities cannot be reproduced by the platform, but without losing the capability of controlling it.

On the other hand, in [91] it was proved that the type II singularities are much more complicated and much research efforts have been put on the characterization of this type of singularities.

Equation (2.2) can be reformulated using the Jacobian matrix, that is, the matrix that relates the velocities of the actuated joints with the linear and angular velocities of the platform. The linear and angular velocities of a rigid body are normally described with a twist, $\mathcal{T} = (\mathbf{v}, \boldsymbol{\Omega})^T$, where \mathbf{v} stands for the linear velocity and $\boldsymbol{\Omega}$ for the angular velocity. The orientation parameters should be chosen so that the derivative of the pose vector is directly the platform twist. If not, it will be related to it through a matrix, $\mathcal{T} = \mathbf{H}\dot{\mathbf{X}}$ [68].

Equation (2.2) can be written as

$$\dot{\Theta} = \mathbf{J}^{-1}\dot{\mathbf{X}}. \quad (2.3)$$

If \mathbf{J}^{-1} is singular, there exists $\dot{\mathbf{X}} \neq 0$ so that $\dot{\Theta} = 0$. Matrix \mathbf{J}^{-1} can be written in terms of matrices \mathbf{P} and \mathbf{S} as $\mathbf{J}^{-1} = -\mathbf{S}^{-1}\mathbf{P}$, but, as for Stewart-Gough platforms $\mathbf{S} = \text{Diag}(l_1, \dots, l_6)$ [38], the study of singularities normally reduces to the study of matrix \mathbf{P} , and in an abuse of language, it is normally called \mathbf{J} .

Due to the reciprocity relation between linear velocities (angular velocities) and forces (torques), matrix \mathbf{J} in (2.3) can also be obtained through the statics study

2.1 Kinematics and singularities of Stewart-Gough platforms

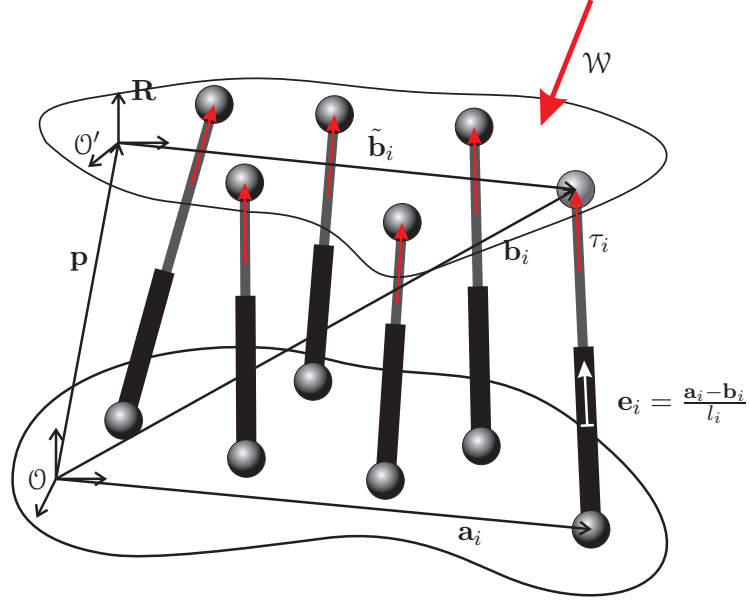


Figure 2.2: The force applied to the platform must be equal to the resultant force exerted by the legs.

of Stewart-Gough platforms (Fig. 2.2). If a wrench $\mathcal{W} = (\mathbf{F}, \mathbf{T})^T$ is applied to the moving platform, where \mathbf{F} stands for the force and \mathbf{T} the torque, the system will be in equilibrium if the resultant force exerted by the legs compensate \mathcal{W} . Indeed, following [68], the equations of equilibrium of the moving platform in its global reference frame can be expressed as:

$$\mathbf{F} = \sum_{i=1}^6 \tau_i \frac{\mathbf{a}_i - \mathbf{b}_i}{l_i}$$

$$\mathbf{T} = \sum_{i=1}^6 \tau_i \frac{(\mathbf{a}_i - \mathbf{b}_i) \times (\mathbf{b}_i - \mathbf{p})}{l_i} = \sum_{i=1}^6 \tau_i \frac{(\mathbf{a}_i - \mathbf{b}_i) \times \mathbf{R}\tilde{\mathbf{b}}_i}{l_i}$$

where τ_i is the force exerted by the actuated joint i for $i = 1, \dots, 6$. In matrix form, these two equations can be rewritten as

$$\mathcal{W} = \mathbf{K} \begin{pmatrix} \tau_1 \\ \vdots \\ \tau_6 \end{pmatrix} \quad (2.4)$$

where

$$\mathbf{K} = \begin{pmatrix} \frac{1}{l_1} & \cdots & 0 \\ \vdots & \ddots & \vdots \\ 0 & \cdots & \frac{1}{l_6} \end{pmatrix} \begin{pmatrix} \mathbf{a}_1 - \mathbf{b}_1 & \cdots & \mathbf{a}_6 - \mathbf{b}_6 \\ (\mathbf{a}_1 - \mathbf{b}_1) \times \mathbf{R}\tilde{\mathbf{b}}_1 & \cdots & (\mathbf{a}_6 - \mathbf{b}_6) \times \mathbf{R}\tilde{\mathbf{b}}_6 \end{pmatrix}$$

2.1 Kinematics and singularities of Stewart-Gough platforms

Then, due to the reciprocity relation between forces and velocities, $\mathbf{K} = \mathbf{J}^{-T}$ and, thus, equation (2.4) can be rewritten as

$$\mathcal{W} = \mathbf{J}^{-T} \boldsymbol{\tau}.$$

By solving this linear system for τ_1, \dots, τ_6 , it is clear that the forces exerted by the legs are values divided by the Jacobian matrix determinant. As a consequence, in a singular position, forces on the actuated joints may go to infinite, and near a singular configuration, they may become very large.

An important property of Stewart-Gough platforms was shown by Merlet in [66]: the rows of \mathbf{J}^{-1} are the Plücker coordinates of the leg lines. Indeed, the Plücker coordinates of a line through a point P with position vector \mathbf{p} and director vector \mathbf{d} are defined as

$$(\mathbf{d}, \mathbf{d} \times \mathbf{p}).$$

Note that an equivalent expression of the line coordinates can be obtained by changing the chosen point P . Thus, the i th row of the Jacobian matrix

$$(\mathbf{a}_i - \mathbf{b}_i, (\mathbf{a}_i - \mathbf{b}_i) \times \mathbf{R}\tilde{\mathbf{b}}_i) \tag{2.5}$$

can be interpreted as the Plücker coordinates of the line through A_i and B_i . As a consequence, the study of singular poses can be reduced to the study of the linear dependence between the Plücker coordinates of 6 lines. A further simplification of the Jacobian matrix can be obtained with an equivalent expression of the same line coordinates, obtained changing the chosen point:

$$((\mathbf{b}_i - \mathbf{a}_i), ((\mathbf{b}_i - \mathbf{a}_i) \times \mathbf{a}_i)). \tag{2.6}$$

Thus, if the rows of \mathbf{J}^{-1} are substituted by these Plücker coordinates, a simpler matrix is obtained, whose determinant has the same roots as the determinant of \mathbf{J}^{-1} .

Several works deal with singularities of Stewart-Gough platforms by studying the line complexes formed by their legs [65, Ch. 12],[25, 109] and the study of screw systems [36, 37].

An analytic characterization of singularities was provided in [41, 63, 91] using Laplace expansions of the Jacobian matrix determinant. Although an analytic expression is obtained, it does not say much about the nature and the topology of the

2.2 Classifications of Stewart-Gough platforms

singularity loci in the configuration space of the platform with respect to the base. The only Stewart-Gough platforms for which a cell decomposition of their singularity loci is available are the flagged and partially-flagged parallel manipulators (a particular architecture detailed in [2, 99]). In most cases the objective is to find geometric interpretations of the singular configurations for particular architectures and efficient graphical representations of the singularity-locus.

Closely related to the works based on Laplace expansions are those dealing with syzygies, relations between 4×4 determinants involving the homogeneous coordinates of sets of four attachments called brackets. White used them in [105] to obtain an expression of the Jacobian matrix determinant taking into account the representation of Plücker coordinates as determinants of 2×2 matrices whose elements are coordinates of the attachments. The obtained expression is a linear combination of products of 3 brackets, with the advantage that each bracket can be directly interpreted as the volume of the tetrahedron formed by 4 attachments. This formula, known as *superbracket*, or the *pure condition*, is the base of those works based on Grassman-Cayley algebra that succeeded to obtain geometric interpretations of singular poses for several architectures [3, 4, 5, 12].

2.2 Classifications of Stewart-Gough platforms

One of the existing classifications of Stewart-Gough platforms is based on treating them as bipartite graphs (see Fig. 2.3 for several examples using such representation). For example, an architecture with m and n different attachments either on the base or the platform is referred to as an $m - n$ Stewart-Gough platform. Using this nomenclature, the simplest architecture is of type 3-3 and the most general one of type 6-6. Using this approach, an incomplete classification appeared in [51]. Later on, Faugère and Lazard made a detailed classification of all $m - n$ classes of Stewart-Gough platforms with all possible combinations of connections between attachments [33]. They enumerated 35 different classes representing all possible Stewart-Gough platforms, giving the maximum number of assembly modes for each of them. Nowadays, this classification is widely used when describing Stewart-Gough architectures [68, Table 4.6]. Unfortunately, it does not take into account non-generic cases, that is, architectures with alignment or coplanarity restrictions in their attachments which are very common in many implementations.

2.2 Classifications of Stewart-Gough platforms

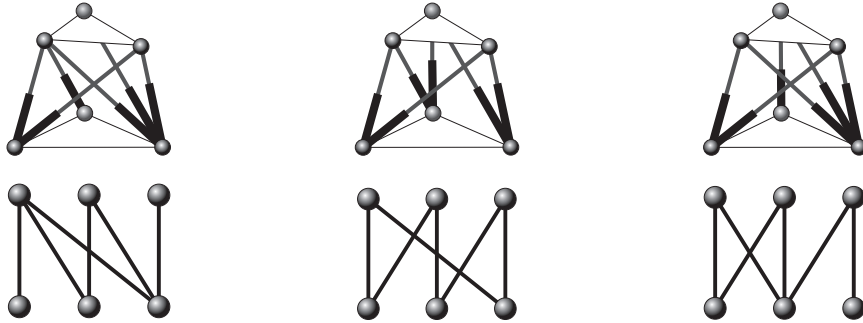


Figure 2.3: The three possible 3-3 Stewart-Gough platforms (top) and their symbolic representation as bipartite graphs (bottom).

Kong and Gosselin presented a different classification [57]. They define rigid substructures with less than 6 legs (called components) and then they form manipulators by joining different components. These components are:

PP: Point-Point (a single leg);

PL: Point-Line (two legs sharing a spherical joint);

PB: Point-Body (three legs sharing a spherical joint);

LL: Line-Line (four legs, their endpoints lying on two lines); and

LB: Line-Body (five legs, an endpoint from each lying on a line).

The idea of Kong and Gosselin was to solve the forward kinematics of each component and then, given a platform, solve its forward kinematics from the solution of each of its components. The existence of a rigid component in a platform greatly simplifies its analysis, but it is not clear how to put together the solution to the forward kinematics of each of its components to form the solution for the entire manipulator.

A large number of publications deal with particular architectures, many of them being kinematically and singularity equivalent. The lack of a singularity-preserving classification in the literature increases the volume of works that could be applied simultaneously to many equivalent manipulators. This thesis presents a tool that allows to compare and detect kinematically equivalent Stewart-Gough platforms.

2.3 Architectural singularities of Stewart-Gough platforms

Special attention has been paid to the characterization of architectural singularities. Such singularities must be avoided in the design process, as architecturally singular manipulators cannot be controlled in any position of its workspace. Any architecturally singular manipulator gains one (or more) degrees of freedom and thus it is capable to perform a movement, called *self-motion*, while their actuated joints remain locked.

As it was stated by Merlet in [66], singularities of Stewart-Gough manipulators happen when their leg lines form a linear complex (*i.e.* a system of linear dependent lines [25]). Then, architecturally singular platforms are manipulators whose legs are always forming a linear complex. X. Kong in [56] distinguishes between two kinds of architecturally singular components. On the one hand, those components that, by construction, have legs forming a linear complex are called over-actuated components and must be avoided in the design process for obvious reasons (Fig. 2.4) and on the other hand, those components that are only architecturally singular when their attachments hold some kind of condition, the *architecturally-singular condition*. These kind of components can be used to form Stewart platforms because the attachments, in general position, form a non-singular structure. The whole literature about architectural singularities focuses on describing such condition. Lately, architecturally singular manipulators have gained interest in the context of compliant manipulators and construction of complex joints [83].

A further division is possible. Manipulators have been divided into two big categories depending on whether their bases and moving platforms are planar, usually referred to as planar and non-planar platforms. Non-planar platforms have been studied in [49], [49] and [54]. M. Husty and A. Karger present a list of non-planar architecturally singular Stewart-Gough platforms. All of them have some kind of alignment on the base and/or on the platform, and they state that any architecturally singular non-planar Stewart-Gough platform has this kind of alignment restriction on the attachments. In particular, they give algebraic characterizations of the architectural singularities for the Line-Line and the Line-Plane components, with a vague geometrical interpretation. The works of A. Karger and M. Husty are closely connected to the work done by the French mathematicians R. Bricard and E. Borel at the beginning of

2.3 Architectural singularities of Stewart-Gough platforms

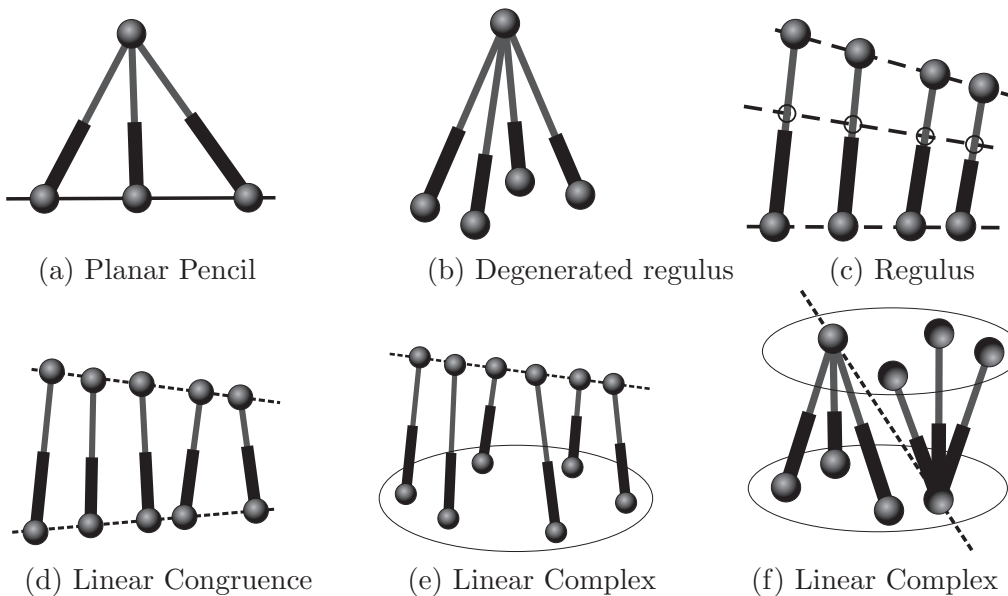


Figure 2.4: Over-actuated components are architecturally singular manipulators because, independently on how one distributes their leg attachments, they are always forming legs whose supporting lines define a linear complex.

the XXth century [7, 21], which studied all the movements that a rigid body can perform when some of its points are supported by rigid bars, and thus, perform spherical trajectories. Such spherical trajectories correspond to the so-called self-motions of the architecturally singular manipulators.

The major part of publications on architectural singularities deal with the second category: planar-platforms. They include those working with planar polygonal platforms [64], using the theory of linear manifolds of correlations [87], imposing zeros on the Jacobian matrix determinant [107, 108], or imposing some kind of algebraic relation between the platform attachments and the base attachments [58]. All these works can be unified with an important theorem that has been used to characterize architectural singularities on planar-platform manipulators [52, 55, 106]. The theorem published in 1851 by M. Chasles [22], states that

“Given any two conic sections in space between which a projective correspondence p exists, straight lines connecting p -corresponding points on the conics belong to a linear complex.”

2.4 Manipulability, dexterity and other performance indexes

Later, in 1896, R. Bricard reformulated it in the context of kinematics, relating the stability of the position of a rigid body supported by 6 rigid bars.

All the works dealing with planar platforms listed above are particular cases in which a projective correspondence between platform and base attachments exists, and hence, the Chasles theorem can be applied: The manipulator is architecturally singular if, and only if, the platform and base attachments lie on a conic. A. Karger studied in [53] the characterization of architectural singularities when such projectivity does not exist.

Although a lot of work dealing with architectural singularities has been done, it is based in algebraic methods that study the analytical coefficients of the Jacobian matrix determinant on a case by case basis. Thus, the existing characterizations are based on very complicated and nonintuitive demonstrations, and, as a consequence, the geometrical interpretation of such singularities is still an open problem.

Finally, an alternative approach to analyze the singularities of a given architecture and, in particular, its possible architectural singularities, is due to P. Ben-Horin and M. Shoham based on Grassman-Cayley algebra [4]. This algebra was first used in Robotics to solve kinetostatic problems [92]. It has also been successfully used at characterizing the singularities of the octahedral manipulator (a 3-3 architecture) [30], and at simplifying the analysis of platforms with aligned attachments [4].

2.4 Manipulability, dexterity and other performance indexes

One of the major difficulties in the workspace and dexterity analysis of the Stewart-Gough platforms is the strong coupling between position and orientation. Furthermore, such an analysis should preferably be done in association with the singularity analysis because a workspace segmented by singularity barriers will not be fully usable in practice. In addition, it must be taken into account the crucial role of leg collision in limiting the platform workspace [67].

To define a well-conditioned workspace it is necessary to define indexes representing the “distance” to singularities. As no mathematical distance can be defined because

2.4 Manipulability, dexterity and other performance indexes

of the simultaneous use of variables representing translations and orientations, several indexes have been proposed instead [70].

Assuming that the errors on the actuated joints are limited, $\|\Delta\Theta\| \leq 1$, and using the Jacobian matrix definition, the manipulability ellipsoid is defined as

$$\Delta\mathbf{X}^T \mathbf{J}^{-T} \mathbf{J}^{-1} \Delta\mathbf{X} \leq 1. \quad (2.7)$$

When this ellipsoid is a sphere, the platform is said to be isotropic. An isotropic manipulator is optimally well-conditioned, but no Stewart-Gough platform can be constructed to be isotropic all over its workspace.

Using equation (2.7), in [110] the manipulability index is defined as

$$m(\mathbf{J}) = \sqrt{|\mathbf{J}\mathbf{J}^T|}.$$

On the other hand, the isotropy condition can be written as

$$\sqrt{\frac{\lambda_{max}}{\lambda_{min}}} = 1,$$

where λ_{min} and λ_{max} are the minimum and maximum eigenvalues of matrix $\mathbf{J}\mathbf{J}^T$. This value is also known as the inverse of the condition number

$$\kappa(\mathbf{J}) = \kappa(\mathbf{J}^{-1}) = |\mathbf{J}^{-1}| \cdot |\mathbf{J}|,$$

which is another index commonly used to indicate the factor of error amplification, define the accuracy/dexterity of the robot, and also the closeness of a pose to a singularity. Moreover, it has been used as a performance index for optimal design, and also an index to determine the useful workspace [70].

However, due to the complexity of the obtained expressions for these indexes, they have only been computed analytically for a limited number of platforms. Furthermore, all of them are sensitive to the chosen units and norm. As a consequence, none of them can be used to properly represent positioning accuracy [70].

In short, determining the geometry of a platform to ensure that a given region of its workspace is free from singularities is a difficult problem that has only been solved for some simple architectures.

A critical issue for parallel robots is the dimensional synthesis in the design process. This dimensioning can be formulated as an multiobjective optimization problem

in which it is necessary to take into account aspects such as positioning accuracy, repeatability, stiffness, vibration, workspace volume and singularities. Most of the indexes that have been proposed to quantify them rely on the Jacobian matrix or its inverse. Therefore, the characterization of singular-invariant transformation, that is, transformations that are able to alter the value of the determinant of the Jacobian except when its value is zero, is of clear interest to decouple the problem of locating the singularities to that of improving, for example, the accuracy in a given region of the configuration space.

2.5 Summary of open problems and related work

In conclusion, a great deal of research has been carried out on the kinematics of Stewart-Gough platforms. So far, as the issues of singularity and workspace analysis are concerned, partial answers to many questions are available, but a complete analysis is yet to be performed.

It is usually assumed that most kinematics problems have already been solved so that only more clear and intuitive solutions to old problems can be provided. Nevertheless, three areas related to the kinematics of Stewart-Gough platforms can benefit from the exhaustive analysis of all possible singularity-invariant leg rearrangements. Namely,

- Existing classifications provide only partial information, as each manipulator must be studied separately and independently of the class to which it belongs. This is because two platforms in the same class do not necessarily have the same forward kinematics nor the same singularity structure. The present thesis, on the contrary, comes up with transformations that preserve the platform's singularities, thus opening up the possibility of classifying platforms in families sharing the same singularity structure.
- Despite the amount of work published on the characterization of architectural singularities, their geometrical interpretation is still not clear. Contributions on this topic are presented in this thesis.

2.5 Summary of open problems and related work

- The characterization of the singularity-free regions of the workspace is an important problem for the design of useful Stewart-Gough platforms. Contributions on this topic are obtained in this thesis by using singularity-invariant leg rearrangements. There are very few works on the systematic design of Stewart-Gough platforms. As a consequence, a step in this direction is important for the enhancement and realization of its potential.

Until the moment, no other similar concept to singularity-invariant leg rearrangements has been found in the literature, except for [48, 74], where the authors solve the problem of obtaining redundant legs to a manipulator without modifying its kinematics. Obviously, their obtained results regarding the locus of possible locations for that redundant legs are similar to those obtained for singularity-invariant leg rearrangements, but the authors do not explore all the consequences.

Chapter 3

Singularity-invariant leg rearrangements

3.1 Notation

A general Stewart-Gough platform is a 6-SPS platform. In other words, it has six actuated prismatic legs \mathbf{l}_i with lengths l_i , $i = 1, \dots, 6$, connecting two spherical passive joints centered at $\mathbf{a}_i = (x_i, y_i, z_i)^T$ and $\tilde{\mathbf{b}}_i = (r_i, s_i, t_i)^T$, given in base and platform reference frames, respectively (see Fig. 2.2). The pose of the platform is defined by a position vector $\mathbf{p} = (p_x, p_y, p_z)^T$ and a rotation matrix \mathbf{R}

$$\mathbf{R}(\alpha_x, \alpha_y, \alpha_z) = (\mathbf{i}, \mathbf{j}, \mathbf{k}) = \begin{pmatrix} i_x & j_x & k_x \\ i_y & j_y & k_y \\ i_z & j_z & k_z \end{pmatrix},$$

so that the platform attachments can be written in the base reference frame as $\mathbf{b}_i = \mathbf{p} + \mathbf{R}\tilde{\mathbf{b}}_i$, for $i = 1, \dots, 6$ (Fig. 3.1). To simplify the notation, the same name will be used to denote a point and its position vector.

There are three types of parameters that fully define a Stewart-Gough platform as

$$\text{Pose parameters } \mathbf{X} = (p_x, p_y, p_z, i_x, i_y, i_z, j_x, j_y, j_z, k_x, k_y, k_z)$$

$$\text{Geometric parameters } \mathcal{G} = (x_1, y_1, z_1, r_1, s_1, t_1, \dots, x_6, y_6, z_6, r_6, s_6, t_6)$$

$$\text{Joint parameters } \Theta = (l_1, \dots, l_6)$$

Finally, it will be useful to introduce a 6-dimensional space defined by the coordinates (x, y, z, r, s, t) , called *the space of leg attachments*. Each point of this space

3.2 Singularity-invariant leg rearrangement: Definition

defines a leg that goes from base attachment $\mathbf{a} = (x, y, z)^T$ to platform attachment $\tilde{\mathbf{b}} = (r, s, t)^T$.

From now on, the above notation will be used to describe all Stewart-Gough plat-
forms, with some variations on the names of the local coordinates.

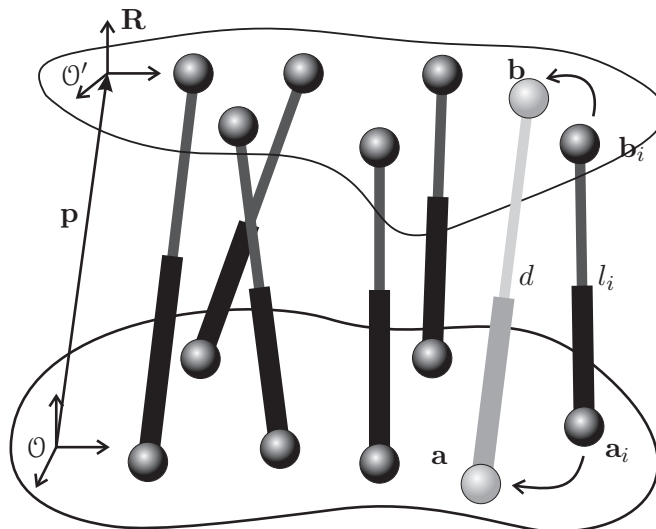


Figure 3.1: A general Stewart-Gough platform with base attachments \mathbf{a}_i and platform attachments at \mathbf{b}_i , $i = 1, \dots, 6$. A single leg rearrangement consist in the substitution of one of the legs by a new one, in gray in the drawing.

3.2 Singularity-invariant leg rearrangement: Definition

A leg rearrangement consists in a relocation of the attachments of the manipulator, without modifying the pose of the platform, and thus, leading to new leg lengths d_1, d_2, \dots, d_6 . In general, such rearrangement completely modifies the kinematics of the manipulator and also the location of its singularities.

For a general Stewart-Gough platform, the forward kinematics problem consists in finding the pose of the moving platform given the leg lengths. This entails solving the quadratic system

$$(\mathbf{a}_i - \mathbf{b}_i)^2 = l_i^2, i = 1, \dots, 6. \quad (3.1)$$

Furthermore, the linear actuator velocities, $\dot{l}_1, \dot{l}_2, \dots, \dot{l}_6$, can be expressed in terms

3.2 Singularity-invariant leg rearrangement: Definition

of the platform velocity vector (\mathbf{v}, Ω) as follows:

$$\mathbf{S} \begin{pmatrix} \dot{l}_1 \\ \dot{l}_2 \\ \vdots \\ \dot{l}_6 \end{pmatrix} = \mathbf{J} \begin{pmatrix} \mathbf{v} \\ \Omega \end{pmatrix} \quad (3.2)$$

where

$$\mathbf{S} = \begin{pmatrix} l_1 & \dots & 0 \\ \vdots & \ddots & \vdots \\ 0 & \dots & l_6 \end{pmatrix}$$

and \mathbf{J} is the matrix of non-normalized Plücker coordinates of the six leg lines [68]. The serial and parallel singularities, as explained in the previous chapter, are given by those configurations in which $\det(\mathbf{S}) = 0$ and $\det(\mathbf{J}) = 0$, respectively [38].

After an arbitrary leg rearrangement, the forward kinematics of the rearranged platform should be solved again, which would lead to a different number of assembly modes and to a different set of singularities. Next, two methodologies to obtain singularity-invariant leg rearrangements are described.

3.2.1 Methodology I: Finding an affine relation between leg lengths

Now suppose that exist a relocation of the base and platform attachments so that the squared leg lengths before and after such rearrangement are related through the affine relation

$$\begin{pmatrix} d_1^2 \\ d_2^2 \\ \vdots \\ d_6^2 \end{pmatrix} = \mathbf{A} \begin{pmatrix} l_1^2 \\ l_2^2 \\ \vdots \\ l_6^2 \end{pmatrix} + \mathbf{b}, \quad (3.3)$$

where \mathbf{A} and \mathbf{b} are a constant matrix and a constant vector, respectively. In such case, the forward kinematics can be solved by just computing the corresponding values l_1, \dots, l_6 through the affine relation (3.3) and then solving system (3.1). In other words, there is a one-to-one correspondence between the sets of leg lengths, and thus, the solution of the forward kinematics is essentially the same.

Furthermore, the singularities also remain unchanged. Indeed, differentiating with

3.2 Singularity-invariant leg rearrangement: Definition

respect to time the affine relation in (3.3) gives

$$\begin{pmatrix} d_1 & \dots & 0 \\ \vdots & \ddots & \vdots \\ 0 & \dots & d_6 \end{pmatrix} \begin{pmatrix} \dot{d}_1 \\ \dot{d}_2 \\ \vdots \\ \dot{d}_6 \end{pmatrix} = \mathbf{A} \begin{pmatrix} l_1 & \dots & 0 \\ \vdots & \ddots & \vdots \\ 0 & \dots & l_6 \end{pmatrix} \begin{pmatrix} \dot{l}_1 \\ \dot{l}_2 \\ \vdots \\ \dot{l}_6 \end{pmatrix} \quad (3.4)$$

and substituting equation (3.2), the linear actuators's velocities of the rearranged platform are related to the platform velocity through

$$\begin{pmatrix} d_1 & \dots & 0 \\ \vdots & \ddots & \vdots \\ 0 & \dots & d_6 \end{pmatrix} \begin{pmatrix} \dot{d}_1 \\ \dot{d}_2 \\ \vdots \\ \dot{d}_6 \end{pmatrix} = \mathbf{A}\mathbf{J} \begin{pmatrix} \mathbf{v} \\ \boldsymbol{\Omega} \end{pmatrix}. \quad (3.5)$$

Thus, the parallel singularities of the platform after the rearrangement correspond to those configurations in which $\det(\mathbf{A}\mathbf{J}) = \det(\mathbf{A})\det(\mathbf{J}) = 0$. As $\det(\mathbf{A})$ is a constant not-null factor, the singularity locus of the platform before and after such rearrangement remains unchanged. Such constant factor that multiplies the singularity polynomial after a rearrangement will be called *singularity factor*.

The other way round, if the parallel singularities between two manipulators are equivalent, *i.e.*, the singularity polynomial only changes in a constant factor, one can relate the velocities $\dot{l}_1, \dot{l}_2, \dots, \dot{l}_6$ with $\dot{d}_1, \dot{d}_2, \dots, \dot{d}_6$ as in (3.4), which can be integrated to obtain an affine relation between the leg lengths of the two platforms.

In conclusion, a leg rearrangement is singularity-invariant if, and only if, it satisfies an affine relation of the form given in (3.3). This affine relation not only guaranties that the singularities will remain unchanged, but also the forward kinematics solution, the number of assembly modes and in summary, all the platform kinematic properties.

When $\det(\mathbf{A}) = 0$, the affine relation is no longer one-to-one, so both the forward kinematics and the singularities change, but such rearrangement has interest because it introduces an *architectural singularity*, *i.e.*, the resulting platform is always in a singularity independently of its leg lengths [64].

3.2.1.1 Single leg rearrangement

Given a rigid component between two geometric entities (for example, two planes for the Plane-Plane component), suppose that the length of any additional leg from one

3.2 Singularity-invariant leg rearrangement: Definition

entity to the other, say d , can be computed independently of the pose of the platform entity, as follows

$$d^2 = a_1 l_1^2 + a_2 l_2^2 + a_3 l_3^2 + a_4 l_4^2 + a_5 l_5^2 + a_6 l_6^2 + b, \quad (3.6)$$

where a_i are constant coefficients for $i = 1, \dots, 6$. Then, the affine relation in equation (3.3) has the form

$$\begin{pmatrix} d^2 \\ d_2^2 \\ \vdots \\ d_6^2 \end{pmatrix} = \begin{pmatrix} a_1 & a_2 & \dots & a_6 \\ 0 & 1 & \dots & 0 \\ & & \ddots & \vdots \\ 0 & 0 & \dots & 1 \end{pmatrix} \begin{pmatrix} l_1^2 \\ l_2^2 \\ \vdots \\ l_6^2 \end{pmatrix} + \begin{pmatrix} b \\ 0 \\ \vdots \\ 0 \end{pmatrix}$$

This corresponds to the rearrangement of only one leg: the substitution of leg \mathbf{l}_i by the new leg \mathbf{d} (Fig. 3.1), which leads to a singularity invariant leg rearrangement as long as the determinant of the above matrix is different from zero.

In most of the cases, this thesis deals with the rearrangement of a single leg, as in practice, it simplifies the computations and it gives equivalent solutions. Only for the Point-Line component it will be shown how some rearrangements can only be performed as the simultaneous application of single leg rearrangements. This will be studied in detail in Chapter 4.

3.2.1.2 Conditional vs. unconditional rearrangements

In the next chapters it will be shown how the analysis of the Point-Line, the Point-Plane and the Line-Line components lead directly to an affine relation of the form (3.6), from which it will be concluded that the rearranged leg attachments can be placed anywhere in the involved geometric entities (point, line or plane). Therefore, they are called *unconditional rearrangements*. On the contrary, in the computation of leg rearrangements for the rest of the components, the new leg length is only affinely related to the original leg lengths when the rearranged leg attachments are placed at specific locations. These are called *conditional rearrangements*. For these components, the condition that has to be fulfilled to guarantee the singularity-invariance gives relevant geometric information about the component that plays a relevant role in the geometric interpretation of singularities.

3.2.2 Methodology II: Rewriting the singularity polynomial

For those components with conditional rearrangements, there is an alternative methodology to obtain the singularity-invariant leg rearrangements which consists in rewriting the determinant of the Jacobian matrix in a convenient form.

Suppose that the singularity polynomial resulting from expanding the determinant of the Jacobian matrix has been rewritten as the determinant of a new matrix of the form

$$\det(\mathbf{J}) = \det(\mathbf{T}) = \begin{vmatrix} r_P(\mathbf{X}) \\ r_G(\mathcal{G}) \end{vmatrix} = 0 \quad (3.7)$$

where $r_P(\mathbf{X})$ are a set of row vectors depending only on the pose parameters and $r_G(\mathcal{G})$ are a set of row vectors depending only on geometric parameters so that, if each row depends only on the local coordinates of the attachments of a single leg, then, we define

$$\widehat{\mathbf{T}} = (r_G(\mathcal{G})) = \begin{pmatrix} r_G(x_1, y_1, z_1, r_1, s_1, t_1) \\ \vdots \\ r_G(x_6, y_6, z_6, r_6, s_6, t_6) \end{pmatrix}.$$

This fact would give a clear cut distinction between the parallel singularities, defined by the root locus of $\det(\mathbf{T})$, and architectural singularities, which will happen whenever $\widehat{\mathbf{T}}$ loses rank. Note that the rows ($r_P(\mathbf{X})$) must be full rank independently of the pose.

Rewriting the singularity polynomial in such a way has been achieved for 2 of the 3 components for which it is believed to be possible. It will be shown how, for a manipulator containing a Line-Plane or a Line-Body component (both components involve 5 legs), the singularity polynomial factorizes into

$$\det(\mathbf{J}) = F_1(\mathbf{c}_1, \dots, \mathbf{c}_5) F_2(\mathbf{c}_6)$$

where factor F_2 is

$$(p_x - x_6)k_x + (p_y - y_6)k_y + (p_z - z_6)k_z$$

that depends on $\mathbf{k} = \mathbf{i} \times \mathbf{j}$ ($\mathbf{R} = (\mathbf{i}, \mathbf{j}, \mathbf{k})$ being the rotation of the platform). Hence, this factor only depends on the sixth leg, and $F_1(\mathbf{c}_1, \dots, \mathbf{c}_5)$ accounts for the singularities of the component embedded in the considered platform. The present thesis presents the reformulation of this factor as

$$F_1(\mathbf{c}_1, \dots, \mathbf{c}_5) = \det(\mathbf{T}),$$

3.2 Singularity-invariant leg rearrangement: Definition

where \mathbf{T} has the same form given in equation (3.7). Work towards a similar formulation for the singularity polynomial of the Plane-Plane component has been done without conclusive results.

Rewriting the singularity polynomial in the presented way is one of the contributions of the present thesis. Indeed, it proves to be useful not only to define singularity-invariant leg rearrangements as explained below, but also to characterize architectural singularities.

Once matrix \mathbf{T} is obtained, it is clear that all the coefficients of the singularity polynomial are minors of matrix $\widehat{\mathbf{T}}$ ¹.

Assuming that only one leg is rearranged, one of the legs will be substituted by a new leg, whose base and platform attachments have local coordinates $\mathbf{a} = (x, y, z)$ and $\tilde{\mathbf{b}} = (r, s, t)$. Then, a singularity invariant leg rearrangement is defined by those $\{x, y, z, r, s, t\}$ for which the matrix

$$\begin{pmatrix} r_G(x_1, y_1, z_1, r_1, s_1, t_1) \\ \vdots \\ r_G(x_6, y_6, z_6, r_6, s_6, t_6) \\ r_G(x, y, z, r, s, t) \end{pmatrix} \quad (3.8)$$

loses rank, where $r_G(x, y, z, r, s, t)$ has the same shape as the rest of the rows, after substituting $(x_i, y_i, z_i, r_i, s_i, t_i)$ by (x, y, z, r, s, t) . When this happens, any row in $\widehat{\mathbf{T}}$ can be substituted by the new row $r_G(x, y, z, r, s, t)$. The resulting matrix will have the same minors, up to a constant multiple. As a consequence, the coefficients of the singularity polynomial of equation (3.7) will be also the same, up to a constant multiple, and thus, its roots will not change.

The rank condition on matrix (3.8) translates into a system of equations that define an hypersurface in the space of leg attachments in implicit form. Thus, only the leg attachments defined by points of this hypersurface will maintain singularities invariant.

Finally, it will be shown that matrix $\widehat{\mathbf{T}}$ coincides with the matrix of the linear system associated with the forward kinematic problem. Given the system (3.1), one can always subtract one of the equations from all the others, thus simplifying quadratic terms. Adding some additional unknowns the bilinear terms can also be simplified,

¹A minor of a matrix is the determinant of some smaller square submatrix, obtained from removing one or more of its rows or columns.

3.2 Singularity-invariant leg rearrangement: Definition

thus obtaining a linear system of equations that involves only part of the unknowns. This will be called the linear system associated with the quadratic system (3.1). The matrix of this system is equivalent to matrix $\widehat{\mathbf{T}}$, in the sense that one can be obtained from the other using only linear row operations.

This methodology will be explained in detail in Chapters 5 and 6.

Chapter 4

The Point-Line, Point-Plane and Line-Line components

4.1 Finding the affine relation between leg lengths

Consider a Gough-Stewart platform containing a Point-Line component defined by two legs with lengths l_1 and l_2 [Fig. 4.1-(left)]. Now, introduce a third leg with length d_1 , as shown in the same figure. Lengths l_1 , l_2 , and d_1 are not independent and the relation between them can be straightforwardly obtained by realizing that the volume of the tetrahedron defined by \mathbf{a}_1 , \mathbf{a}_2 , \mathbf{a}_3 , and \mathbf{b}_1 is null, *i.e.*, all four points are coplanar. Then, using Euler's formula for the volume of a tetrahedron in terms of the square of its edge lengths [29, Problem 68], gives:

$$f(l_1, l_2, d_1) = \begin{vmatrix} 0 & 1 & 1 & 1 & 1 \\ 1 & 0 & (m+n)^2 & l_1^2 & m^2 \\ 1 & (m+n)^2 & 0 & l_2^2 & n^2 \\ 1 & l_1^2 & l_2^2 & 0 & d_1^2 \\ 1 & m^2 & n^2 & d_1^2 & 0 \end{vmatrix} = 0. \quad (4.1)$$

The above determinant can be recognized as the Cayley-Menger determinant of four points (see Appendix A for details). The Cayley-Menger determinant of m points is proportional to the squared volume of the simplex that these points define in \mathbb{R}^{m-1} .

Expanding the determinant (4.1) and factorizing the result, the affine relation between l_1 , l_2 and d is obtained:

$$f(l_1, l_2, d_1) = nl_1^2 + ml_2^2 - (m+n)d_1^2 - mn(m+n) = 0.$$

4.1 Finding the affine relation between leg lengths

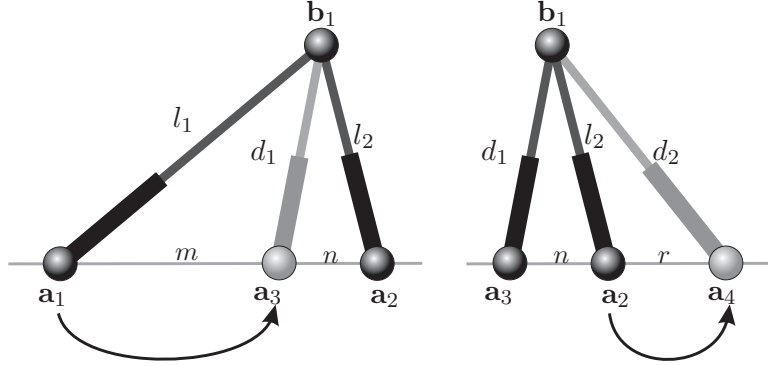


Figure 4.1: A point-line component formed by legs l_1 and l_2 . Two Point-Line rearrangements can be applied to move the two attachments, \mathbf{a}_1 and \mathbf{a}_2 , along the line.

Note that the same equation for 4 general coplanar points does not factor, it is necessary the collinearity of \mathbf{a}_1 , \mathbf{a}_2 and \mathbf{a}_3 .

Thus, when rearranging a single leg, the affine relation in (3.3) has the form

$$\begin{pmatrix} d_1^2 \\ l_2^2 \\ \vdots \\ d_6^2 \end{pmatrix} = \mathbf{A} \begin{pmatrix} l_1^2 \\ l_2^2 \\ \vdots \\ l_6^2 \end{pmatrix} + \mathbf{b}$$

where

$$\mathbf{A} = \begin{pmatrix} \frac{n}{m+n} & \frac{m}{m+n} & \dots & 0 \\ 0 & 1 & \dots & 0 \\ \vdots & \vdots & \ddots & \vdots \\ 0 & 0 & \dots & 1 \end{pmatrix}$$

whose determinant is

$$\det(\mathbf{A}) = \frac{n}{m+n}.$$

As a consequence, the singularity polynomial of the platform after this leg rearrangement, say $\det(\mathbf{J}_1)$, can be expressed in terms of the singularity polynomial of the original platform, say $\det(\mathbf{J}_0)$, as:

$$\det(\mathbf{J}_1) = \frac{n}{m+n} \cdot \det(\mathbf{J}_0). \quad (4.2)$$

Thus, the singularity polynomial, after the rearrangement, is equal to the original one multiplied by the distance between the two attachments, divided by the same

4.1 Finding the affine relation between leg lengths

distance before the rearrangement, and affected by a sign change if the order of the attachments is permuted.

The above Point-Line rearrangement was defined as a Δ -transform in [11]. In what follows, a Point-Line rearrangement will be denoted by Δ^{l_i, l_j, l_k} indicating that a point-line component formed by l_i and l_j is substituted by the one formed by l_i and l_k .

By applying a Point-Line rearrangement, one of its two attachments has been moved on the line. The other can be moved by applying one more Point-Line rearrangement. For example, on the result of the above Point-Line rearrangement, substitute \mathbf{l}_2 by \mathbf{d}_2 , as shown in Fig. 4.1-(right). Then, following the same reasoning as for the first rearrangement, the singularity polynomial of the resulting platform, say $\det(\mathbf{J}_2)$, can be expressed as:

$$\det(\mathbf{J}_2) = \frac{n+r}{n} \cdot \det(\mathbf{J}_1) = \frac{n+r}{m+n} \cdot \det(\mathbf{J}_0). \quad (4.3)$$

Observe that the above two rearrangements can be applied simultaneously to move both attachments on the line at the same time. In this case, the relationship between the leg lengths can be expressed as:

$$\begin{aligned} f_1(l_1, l_2, d_1) &= nl_1^2 + ml_2^2 - (m+n)d_1^2 - mn(m+n) = 0 \\ f_2(l_1, l_2, d_2) &= rl_1^2 + (m+n)d_2^2 - (m+n+r)l_2^2 - r(m+n)(m+n+r) = 0. \end{aligned}$$

Thus, the affine relation is

$$\begin{pmatrix} d_1^2 \\ d_2^2 \\ \vdots \\ l_6^2 \end{pmatrix} = \mathbf{A} \begin{pmatrix} l_1^2 \\ l_2^2 \\ \vdots \\ l_6^2 \end{pmatrix} + \mathbf{b} = \begin{pmatrix} \frac{n}{m+n} & \frac{m}{m+n} & \cdots & 0 \\ -\frac{r}{m+n} & \frac{m+n+r}{m+n} & \cdots & 0 \\ \vdots & \vdots & \ddots & \vdots \\ 0 & 0 & \cdots & 1 \end{pmatrix} \begin{pmatrix} l_1^2 \\ l_2^2 \\ \vdots \\ l_6^2 \end{pmatrix} + \mathbf{b} \quad (4.4)$$

whose determinant is

$$\det(\mathbf{A}) = \frac{n(m+n+r) + mr}{(m+n)^2} = \frac{nm + n^2 + rn + rm}{(m+n)^2} = \frac{(n+r)(m+n)}{(m+n)^2} = \frac{n+r}{m+n}.$$

In conclusion, the singularity polynomial of the platform after this double leg rearrangement can be expressed as in (4.3). Thus, the result is the same if the two rearrangements are applied either sequentially or simultaneously. Nevertheless, there are some circumstances in which a set of rearrangements can only be applied simultaneously. This will become evident in the next examples.

4.2 The affine relation for the Point-Plane component

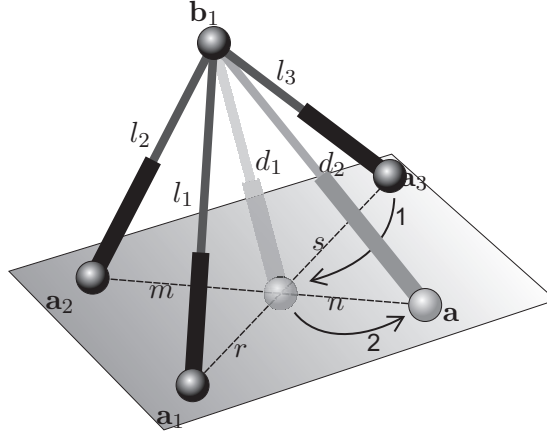


Figure 4.2: A base attachment in a Point-Plane component can be placed anywhere in the plane after two Point-Line rearrangements.

In what follows, a set of Point-Line rearrangements will be denoted

$$\{\Delta^{l_1, l_2, l_3} \Delta^{l_4, l_5, l_6} \dots\},$$

when applied sequentially, and

$$\left\{ \begin{array}{c} \Delta^{l_1, l_2, l_3} \\ \Delta^{l_4, l_5, l_6} \\ \vdots \end{array} \right\},$$

when applied simultaneously.

4.2 The affine relation for the Point-Plane component

The Point-Plane component consists in three legs meeting at a point, so it is also known as a tripod. In the Point-Plane component, any base attachment can be moved to any other point of the base plane by performing sequentially two Point-Line rearrangements.

For instance, if the base attachment \mathbf{a}_3 has to be moved to \mathbf{a} , the set of Point-Line rearrangements that can be applied is

$$\{\Delta^{l_3 l_1 d_1}, \Delta^{l_2 d_1 d_2}\},$$

with corresponding relations for the involved leg lengths:

$$f_1 = s l_1^2 + r l_3^2 - (s + r) d_1^2 - s r (s + r) = 0 \quad (4.5)$$

4.3 The affine relation for the Line-Line component

and

$$f_2 = nl_2^2 + md_2^2 - (m+n)d_1^2 - mn(m+n) = 0, \quad (4.6)$$

respectively (see Fig. 4.2). Writing them in the form of equation (3.3), taking into account that the substituted leg is \mathbf{l}_3 , one obtains

$$\begin{pmatrix} l_1^2 \\ l_2^2 \\ d_1^2 \\ \vdots \\ l_6^2 \end{pmatrix} = \mathbf{A}_1 \begin{pmatrix} l_1^2 \\ l_2^2 \\ l_3^2 \\ \vdots \\ l_6^2 \end{pmatrix} + \mathbf{b} = \begin{pmatrix} 1 & 0 & 0 & \dots & 0 \\ 0 & 1 & 0 & \dots & 0 \\ \frac{s}{s+r} & 0 & \frac{r}{s+r} & \dots & 0 \\ \vdots & \vdots & \vdots & \ddots & 0 \\ 0 & 0 & 0 & \dots & 1 \end{pmatrix} \begin{pmatrix} l_1^2 \\ l_2^2 \\ l_3^2 \\ \vdots \\ l_6^2 \end{pmatrix} + \mathbf{b}$$

and

$$\begin{pmatrix} l_1^2 \\ l_2^2 \\ d_2^2 \\ \vdots \\ l_6^2 \end{pmatrix} = \mathbf{A}_2 \begin{pmatrix} l_1^2 \\ l_2^2 \\ d_1^2 \\ \vdots \\ l_6^2 \end{pmatrix} + \mathbf{b} = \begin{pmatrix} 1 & 0 & 0 & \dots & 0 \\ 0 & 1 & 0 & \dots & 0 \\ 0 & \frac{-n}{m} & \frac{m+n}{m} & \dots & 0 \\ \vdots & \vdots & \vdots & \ddots & 0 \\ 0 & 0 & 0 & \dots & 1 \end{pmatrix} \begin{pmatrix} l_1^2 \\ l_2^2 \\ d_1^2 \\ \vdots \\ l_6^2 \end{pmatrix} + \mathbf{b}$$

respectively. After applying both rearrangements

$$\det(\mathbf{J}_2) = \det(\mathbf{A}_1)\det(\mathbf{A}_2)\det(\mathbf{J}_0) = \frac{(m+n)r}{(s+r)m}\det(\mathbf{J}_0). \quad (4.7)$$

Note that in this example the sequence of two Point-Line rearrangements has to be applied sequentially, as the second one needs the result of the first one. In Section 4.6 it will be shown that such rearrangements can be done in a single step by computing directly the affine relation between the involved leg lengths.

4.3 The affine relation for the Line-Line component

The Line-Line component consist of 4 legs with collinear attachments both in the base and the platform. A Line-Line component involving four attachments appears in Fig. 4.3-(left). If Point-Line rearrangements are applied sequentially to it, the last rearrangement would always yield a double spherical joint that cannot be split. But if the following simultaneous rearrangements

$$\left\{ \begin{array}{l} \Delta^{l_3, l_1, d_1} \\ \Delta^{l_1, l_2, d_3} \\ \Delta^{l_4, l_3, d_3} \\ \Delta^{l_3, l_4, d_4} \end{array} \right\} \quad (4.8)$$

4.3 The affine relation for the Line-Line component

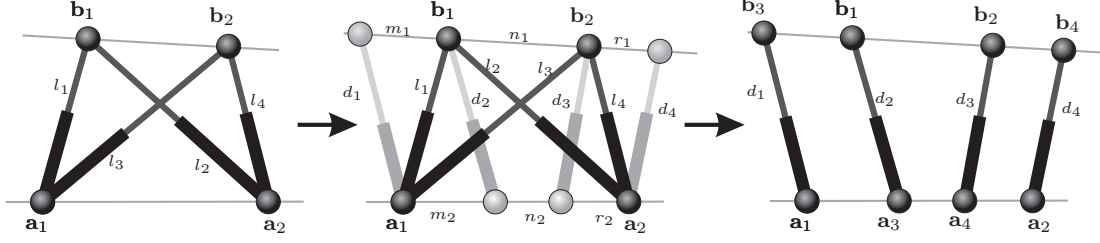


Figure 4.3: Singularity-invariant leg rearrangements on the Line-Line component using Point-Line rearrangements.

are applied, all double attachments can be split into single spherical joints [Fig. 4.3-(right)]. This has practical consequences when trying to eliminate multiple spherical joints.

The corresponding affine relations for the above rearrangements appear in Table. 4.1. Then, the corresponding affine relation entailing all of them at the same time is:

$$\begin{pmatrix} d_1^2 \\ d_2^2 \\ d_3^2 \\ \vdots \\ l_6^2 \end{pmatrix} = \mathbf{A} \begin{pmatrix} l_1^2 \\ l_2^2 \\ l_3^2 \\ \vdots \\ l_6^2 \end{pmatrix} + \mathbf{b}$$

$$= \begin{pmatrix} \frac{m_1+n_1}{n_1} & 0 & -\frac{m_1}{n_1} & 0 & \cdots & 0 \\ \frac{n_2+r_2}{m_2+n_2+r_2} & \frac{m_2}{m_2+n_2+r_2} & 0 & 0 & \cdots & 0 \\ 0 & 0 & \frac{r_2}{m_2+n_2+r_2} & \frac{m_2+n_2}{m_2+n_2+r_2} & \cdots & 0 \\ 0 & -\frac{r_1}{n_1} & 0 & \frac{n_1+r_1}{n_1} & \cdots & 0 \\ \vdots & \vdots & \vdots & \vdots & \ddots & \vdots \\ 0 & 0 & 0 & 0 & & 1 \end{pmatrix} \begin{pmatrix} l_1^2 \\ l_2^2 \\ l_3^2 \\ \vdots \\ l_6^2 \end{pmatrix} + \begin{pmatrix} m_1(n_1 + m_1) \\ -m_2(n_2 + r_2) \\ -r_2(m_2 + n_2) \\ r_1(r_1 + n_1) \\ 0 \\ 0 \end{pmatrix} \quad (4.9)$$

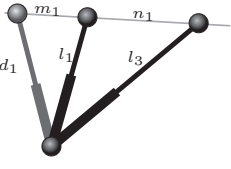
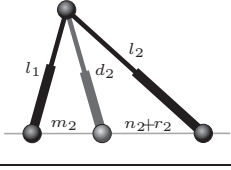
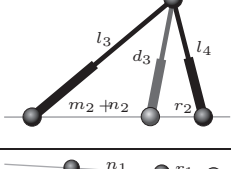
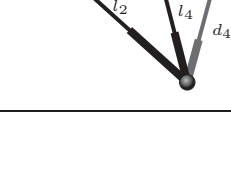
and thus, the resulting singularity polynomial is

$$\det(\mathbf{J}_1) = \det(\mathbf{A})\det(\mathbf{J}) = \frac{(m_1 + n_1)(n_1 + r_1)m_2r_2 - (m_2 + n_2)(n_2 + r_2)m_1r_1}{n_1^2(m_2 + n_2 + r_2)^2} \det(\mathbf{J}). \quad (4.10)$$

Note that the attachments can be placed anywhere on the lines by applying the above four rearrangements simultaneously, but with this methodology, no transformations could be applied to the general 4-4 Line-Line component, that is, the one containing no multiple spherical joints [Fig. 4.3-(right)]. In Section 4.7 it will be shown how a

4.4 Architectural singularities in Line-Line components

Table 4.1: Δ -transforms in the Line-Line component of Fig. 4.3

rearrangement	Affine relation
	$n_1 d_1^2 + m_1 l_3^2 - (m_1 + n_1) l_1^2 - m_1 n_1 (n_1 + m_1) = 0$
	$(n_2 + r_2) l_1^2 + m_2 l_2^2 - (m_2 + n_2 + r_2) d_2^2 - m_2 (n_2 + r_2) (m_2 + n_2 + r_2) = 0$
	$(m_2 + n_2) l_4^2 + r_2 l_3^2 - (m_2 + n_2 + r_2) d_3^2 - r_2 (m_2 + n_2) (m_2 + n_2 + r_2) = 0$
	$r_1 l_2^2 + n_1 d_4^2 - (n_1 + r_1) l_4^2 - r_1 n_1 (r_1 + n_1) = 0$

Line-Line singularity invariant leg rearrangement can be performed without relying on Point-Line rearrangements.

4.4 Architectural singularities in Line-Line components

It is important to realize that factor (4.10) vanishes if, and only if,

$$\frac{|\mathbf{a}_3 - \mathbf{a}_1| |\mathbf{a}_2 - \mathbf{a}_4|}{|\mathbf{a}_1 - \mathbf{a}_2| |\mathbf{a}_3 - \mathbf{a}_4|} = \frac{|\mathbf{b}_3 - \mathbf{b}_1| |\mathbf{b}_2 - \mathbf{b}_4|}{|\mathbf{b}_1 - \mathbf{b}_2| |\mathbf{b}_3 - \mathbf{b}_4|}, \quad (4.11)$$

that is, if the cross-ratio [75] of \mathbf{a}_1 , \mathbf{a}_4 , \mathbf{a}_3 , and \mathbf{a}_2 equals that of \mathbf{b}_1 , \mathbf{b}_4 , \mathbf{b}_3 , and \mathbf{b}_2 (see Appendix B). When this happens, the singularity factor is identically zero. In this case, the platform is said to be *architecturally singular*. In other words, it is always in a singularity independently of its leg lengths. Alternatively, it is also said that the platform exhibits a *self-motion*, *i.e.*, it is movable while keeping its leg lengths constant. This architectural singularity was already studied in [56], and it also appears as the fifth type of singularity in Theorem 1 of [49] or equivalently type 8 in Theorem 3 of

[54]. The cross-ratio singularity condition was also found in [4] and [10] using much more involved derivations than the one above.

4.5 Examples

4.5.1 The Zhang-Song platform

4.5.1.1 Leg rearrangements

Zhang and Song identified in [111] a whole family of special Gough-Stewart platforms with closed-form formulation for their forward kinematics. One member of this family appears in Fig. 4.4-(d) which is of interest because it has five aligned attachments both in the base and the platform. Next, the singularity polynomial of this platform will be proved to be equal to that of the platform in Fig. 4.4-(a) (known as 3-2-1 platform [35] or flagged platform [2]) multiplied by a constant factor. Both the Zhang and Song platform and the 3-2-1 manipulator are composed by a Line-Line component and two additional legs.

Let first apply the sequence of rearrangements to the 3-2-1 platform in Fig. 4.4-(a)

$$\{\Delta^{p_1, p_3, q_3} \Delta^{p_2, p_4, q_4}\}$$

which leads to the platform in Fig. 4.4-(b). Now, apply the sequence

$$\{\Delta^{q_1, q_2, l_2} \Delta^{q_3, q_4, l_4}\}$$

which leads to the platform in Fig. 4.4-(c).

Therefore, using (4.2) four times, the singularity polynomial of the platform in Fig. 4.4-(c) is that of the 3-2-1 platform in Fig. 4.4-(a) multiplied by:

$$\frac{n_1^2}{n_{11}^2} \frac{(m_2 + n_2 + r_2)^2}{(m_2 + n_{21})^2}. \quad (4.12)$$

Now, the same four rearrangements given by (4.8) can be applied to the Line-Line component, thus obtaining the singularity factor appearing in equation (4.10). As a consequence, the singularity factor of the platform in Fig. 4.4-(d) is:

$$\frac{n_1^2}{n_{11}^2} \frac{(m_2 + n_2 + r_2)^2}{(m_2 + n_{21})^2} \frac{(m_1 + n_1)(n_1 + r_1)m_2r_2 - (m_2 + n_2)(n_2 + r_2)m_1r_1}{n_1^2(m_2 + n_2 + r_2)^2}.$$

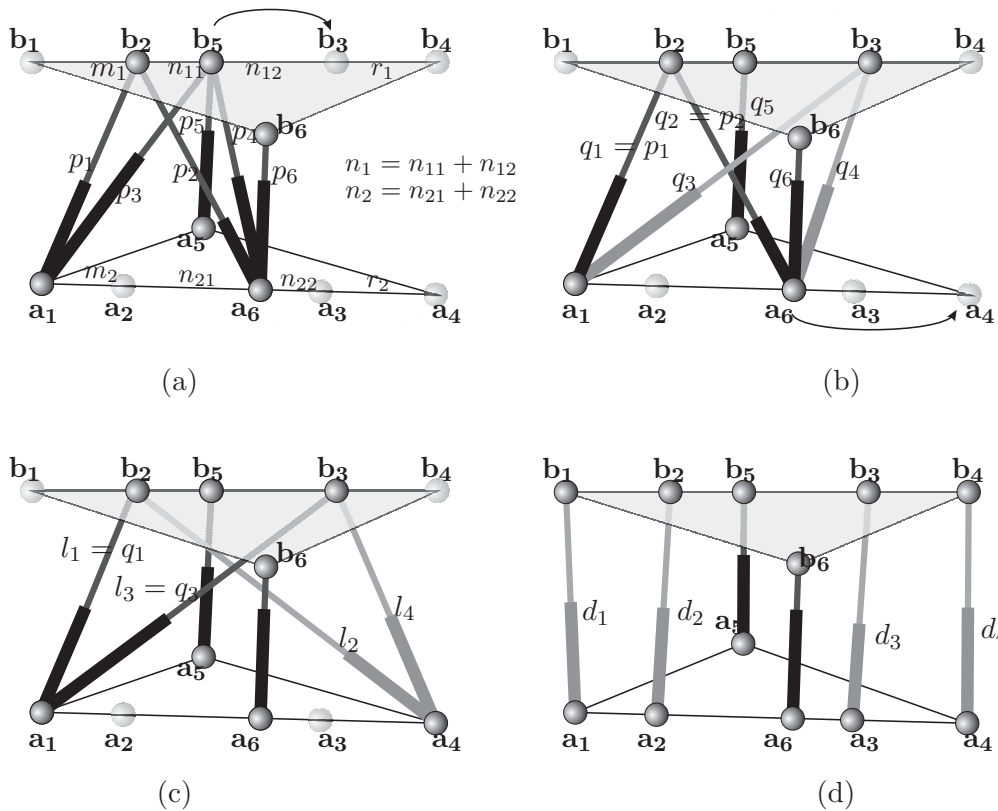
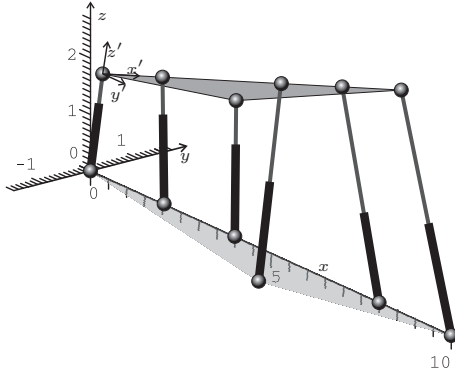


Figure 4.4: The basic flagged platform in (a) can be transformed through a set of Point-Line rearrangements into the Zhang-Song platform in (d).

4.5.1.2 Architecturally singular Zhang-Song platform

A Stewart-Gough platform is architecturally-singular when one of its components is architecturally singular. As before, the Line-Line component becomes architecturally singular when the cross-ratio of the aligned platform attachment locations is equal to the cross-ratio of the aligned base attachment locations.

A parameterization of the self-motions resulting from architectural singularities introduced by a sequence of Point-Line rearrangements can always be found by proceeding backwards. That is, by undoing the rearrangements and introducing parameters when needed. For example, for the Zhang-Song platform (Fig. 4.5) with the leg attachment coordinates appearing in Table I, the cross-ratio condition in (4.11) is satisfied. Hence, the platform is architecturally singular and, as a consequence, it will exhibit



i	\mathbf{a}_i	\mathbf{b}_i	d_i^2
1	(0, 0, 0)	(0, 0, 0)	22
2	(2, 0, 0)	(1, 0, 0)	$15 - \sqrt{2}$
3	(8, 0, 0)	(4, 0, 0)	$54 - 28\sqrt{2}$
4	(10, 0, 0)	(5, 0, 0)	$87 - 45\sqrt{2}$
5	(6, -1, 0)	(3, 0, 0)	$28 - 12\sqrt{2}$
6	(4, 0, 0)	(2, 2, 0)	$16 - (6 + \sqrt{3})\sqrt{2}$

Figure 4.5: An architecturally singular Zhang-Song platform and the corresponding table of attachment coordinates

a self-motion. To obtain a parameterization of this self-motion, observe that, for the Zhang-Song architecturally singular platform, using (4.9), it can be concluded:

$$\begin{pmatrix} -4 & 0 & 1 & 0 \\ 8 & 2 & 0 & 0 \\ 0 & 0 & 2 & 8 \\ 0 & 1 & 0 & -4 \end{pmatrix} \begin{pmatrix} l_1^2 \\ l_2^2 \\ l_3^2 \\ l_4^2 \end{pmatrix} = \begin{pmatrix} 12 - 3d_1^2 \\ 160 + 10d_2^2 \\ 160 + 10d_3^2 \\ 12 - 3d_4^2 \end{pmatrix}.$$

Given fixed values for d_1^2, \dots, d_4^2 , the above linear system is underconstrained, as expected. In other words, there is an infinite set of values for l_1^2, \dots, l_4^2 compatible with a set of values for d_1^2, \dots, d_4^2 . This set can be parameterized, for the values of d_i^2 in Fig. 4.5, by taking one of the leg lengths as parameter (l_4^2 has been chosen here) yielding

$$\begin{aligned} l_1^2 &= -l_4^2 + 101 - 35\sqrt{2} \\ l_2^2 &= 4l_4^2 - 249 + 135\sqrt{2} \\ l_3^2 &= -4l_4^2 + 350 - 140\sqrt{2} \end{aligned}$$

The above leg lengths correspond to the self-motion of the manipulator in Fig. 4.4-(c). It is necessary to proceed undoing the four other rearrangements to obtain the leg lengths for the corresponding 3-2-1 parallel platform in Fig. 4.4-(a). The result is:

$$\begin{aligned} p_1^2 &= 101 - 35\sqrt{2} - l_4^2 \\ p_2^2 &= -63 + 33\sqrt{2} + l_4^2 \\ p_3^2 &= -3l_4^2 + 265 - 105\sqrt{2} \\ p_4^2 &= -l_4^2 + 101 - 45\sqrt{2} \\ p_5^2 &= 28 - 12\sqrt{2} \\ p_6^2 &= 16 - (6 + \sqrt{3})\sqrt{2} \end{aligned}$$

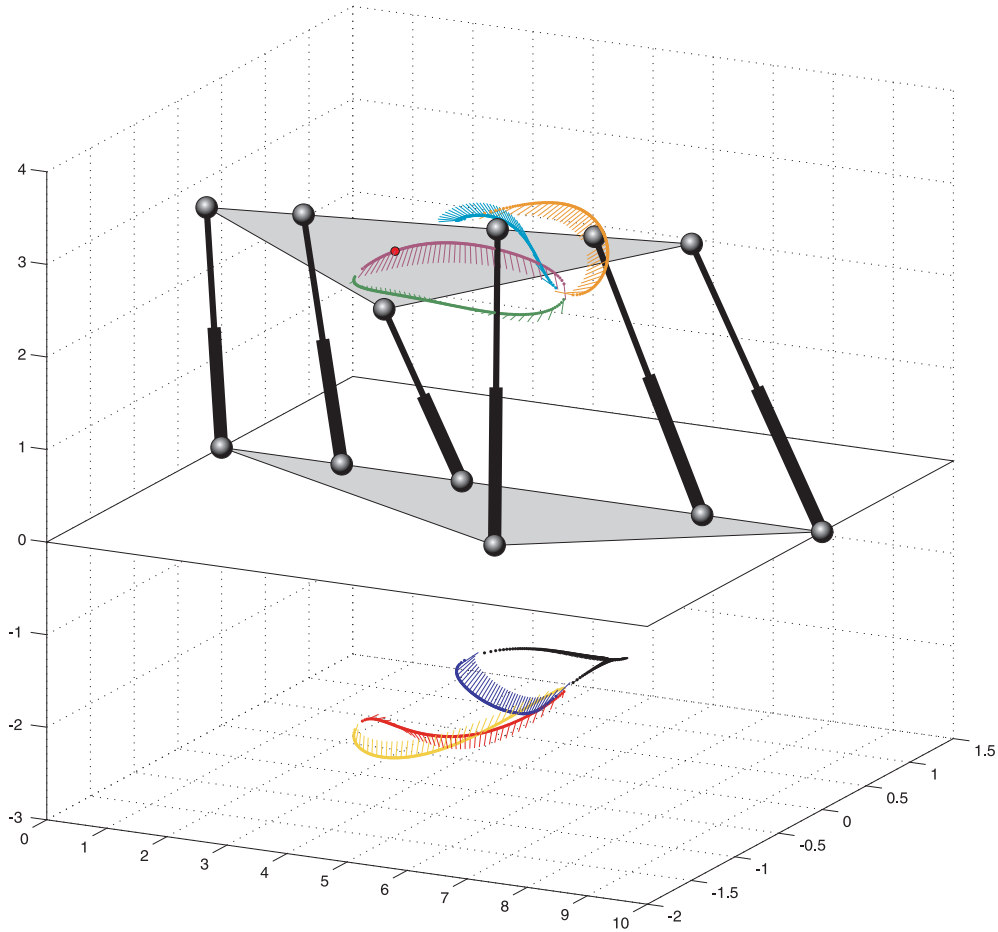


Figure 4.6: Curve traced by the barycenter of the triangular platform in Fig. 4.5 when it is moved along its self-motion, and the normal direction to the platform plane. Each color corresponds to one branch of the forward kinematics generated as the parameter is swept.

The 3-2-1 parallel platform can have up to eight assembly modes which can be expressed in closed-form in terms of its leg lengths [2]. Thus, by sweeping l_4^2 in the range $(0, \infty)$, eight curves in the configuration space of the platform are traced. This provides a complete characterization of the sought self-motion. Fig. 4.6 depicts the location of the barycenter of the triangular moving platform for the obtained self-motion.

Each value of the parameter l_4^2 defines a unique point in joint space (a set of leg lengths), which leads to eight solutions of the forward kinematics (one for each assembly mode) in configuration space. Note that these solutions may be real only for some

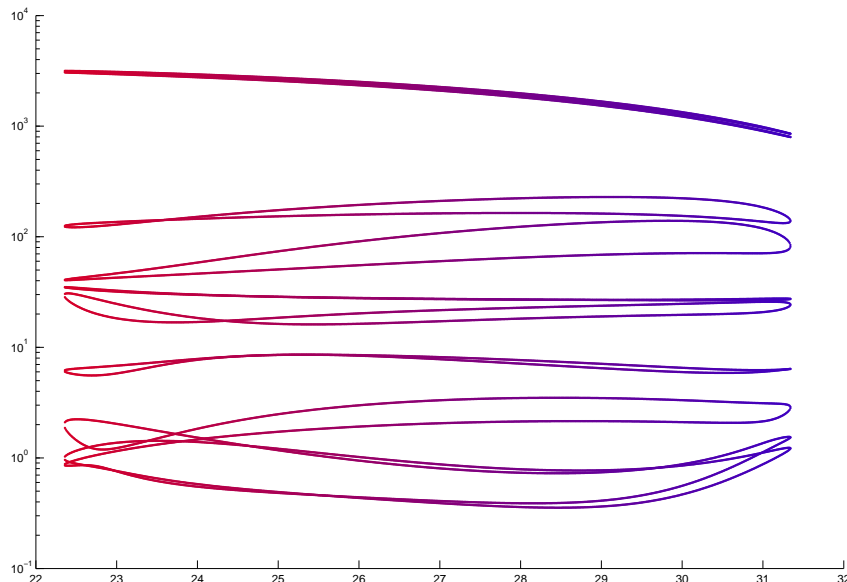


Figure 4.7: All eigenvalues for all assembly modes, excluding the one that is always zero, of $\mathbf{J}^T \mathbf{J}$, where \mathbf{J} is the Jacobian matrix of the analyzed architecturally-singular Zhang-Song platform, as a function of l_4^2 .

ranges of the parameter. In the example, the parameter in the interval (22.35, 31.34) yields the real solutions plotted in Fig. 4.6. The extremes of this interval correspond to transition points between different assembly modes (marked with a change of color in the figure). Nevertheless, such transition points do not correspond to higher-order singularities of the architecturally-singular Zhang-Song platform. Indeed, if the eigenvalues of $\mathbf{J}\mathbf{J}^T$, where \mathbf{J} is the Jacobian matrix of the architecturally-singular Zhang-Song platform, are computed along its self-motion, five of them are always different from zero. Fig. 4.7 plots in logarithmic scale all eigenvalues, excluding the one that is always zero, for all assembly modes as a function of l_4^2 . Note that none of them vanishes.

4.5.2 The Griffis-Duffy Platform

4.5.2.1 Leg rearrangements

Consider the octahedral parallel platform in Fig. 4.8-(top), also known as 2-2-2 platform [46]. Now, apply the following set of rearrangements to it

$$\left\{ \begin{array}{l} \Delta^{l_2, l_1, d_1} \\ \Delta^{l_3, l_2, d_2} \\ \Delta^{l_4, l_3, d_3} \\ \Delta^{l_5, l_4, d_4} \\ \Delta^{l_6, l_5, d_5} \\ \Delta^{l_1, l_6, d_6} \end{array} \right\} \quad (4.13)$$

The resulting platform is the Griffis-Duffy platform [42] appearing in Fig. 4.8-(bottom).

The affine relations resulting from the rearrangements in (4.13) are:

$$\begin{aligned} f_1 &= m_1 l_2^2 + m_2 l_1^2 - (m_1 + m_2) d_1^2 - m_1 m_2 (m_1 + m_2) \\ f_2 &= n_2 l_2^2 + n_1 l_3^2 - (n_1 + n_2) d_2^2 - n_1 n_2 (n_1 + n_2) \\ f_3 &= m_3 l_4^2 + m_4 l_3^2 - (m_3 + m_4) d_3^2 - m_3 m_4 (m_3 + m_4) \\ f_4 &= n_4 l_4^2 + n_3 l_5^2 - (n_3 + n_4) d_4^2 - n_3 n_4 (n_3 + n_4) \\ f_5 &= m_5 l_6^2 + m_6 l_5^2 - (m_5 + m_6) d_5^2 - m_5 m_6 (m_5 + m_6) \\ f_6 &= n_6 l_6^2 + n_5 l_1^2 - (n_6 + n_5) d_6^2 - n_6 n_5 (n_5 + n_6). \end{aligned} \quad (4.14)$$

Then, the affine relation including all legs can be expressed as

$$\begin{pmatrix} d_1^2 \\ d_2^2 \\ d_3^2 \\ d_4^2 \\ d_5^2 \\ d_6^2 \end{pmatrix} = \begin{pmatrix} \frac{m_2}{m_1+m_2} & \frac{m_1}{m_1+m_2} & 0 & 0 & 0 & 0 \\ 0 & \frac{n_2}{n_1+n_2} & \frac{n_1}{n_1+n_2} & 0 & 0 & 0 \\ 0 & 0 & \frac{m_4}{m_3+m_4} & \frac{m_3}{m_3+m_4} & 0 & 0 \\ 0 & 0 & 0 & \frac{n_4}{n_3+n_4} & \frac{n_3}{n_3+n_4} & 0 \\ 0 & 0 & 0 & 0 & \frac{m_6}{m_5+m_6} & \frac{m_5}{m_5+m_6} \\ \frac{n_5}{n_5+n_6} & 0 & 0 & 0 & 0 & \frac{n_6}{n_5+n_6} \end{pmatrix} \begin{pmatrix} l_1^2 \\ l_2^2 \\ l_3^2 \\ l_4^2 \\ l_5^2 \\ l_6^2 \end{pmatrix} - \begin{pmatrix} m_1 m_2 \\ n_1 n_2 \\ m_3 m_4 \\ n_3 n_4 \\ m_5 m_6 \\ n_6 n_5 \end{pmatrix}. \quad (4.15)$$

The resulting singularity factor is:

$$\det(\mathbf{A}) = \frac{m_2 m_4 m_6 n_2 n_4 n_6 - m_1 m_3 m_5 n_1 n_3 n_5}{(m_1 + m_2)(m_3 + m_4)(m_5 + m_6)(n_1 + n_2)(n_3 + n_4)(n_5 + n_6)} \quad (4.16)$$

Therefore, the singularity-polynomial of the platform in Fig. 4.8-(right) is that of Fig. 4.8-(left) multiplied by factor (4.16). Note that this factor is constant: it only

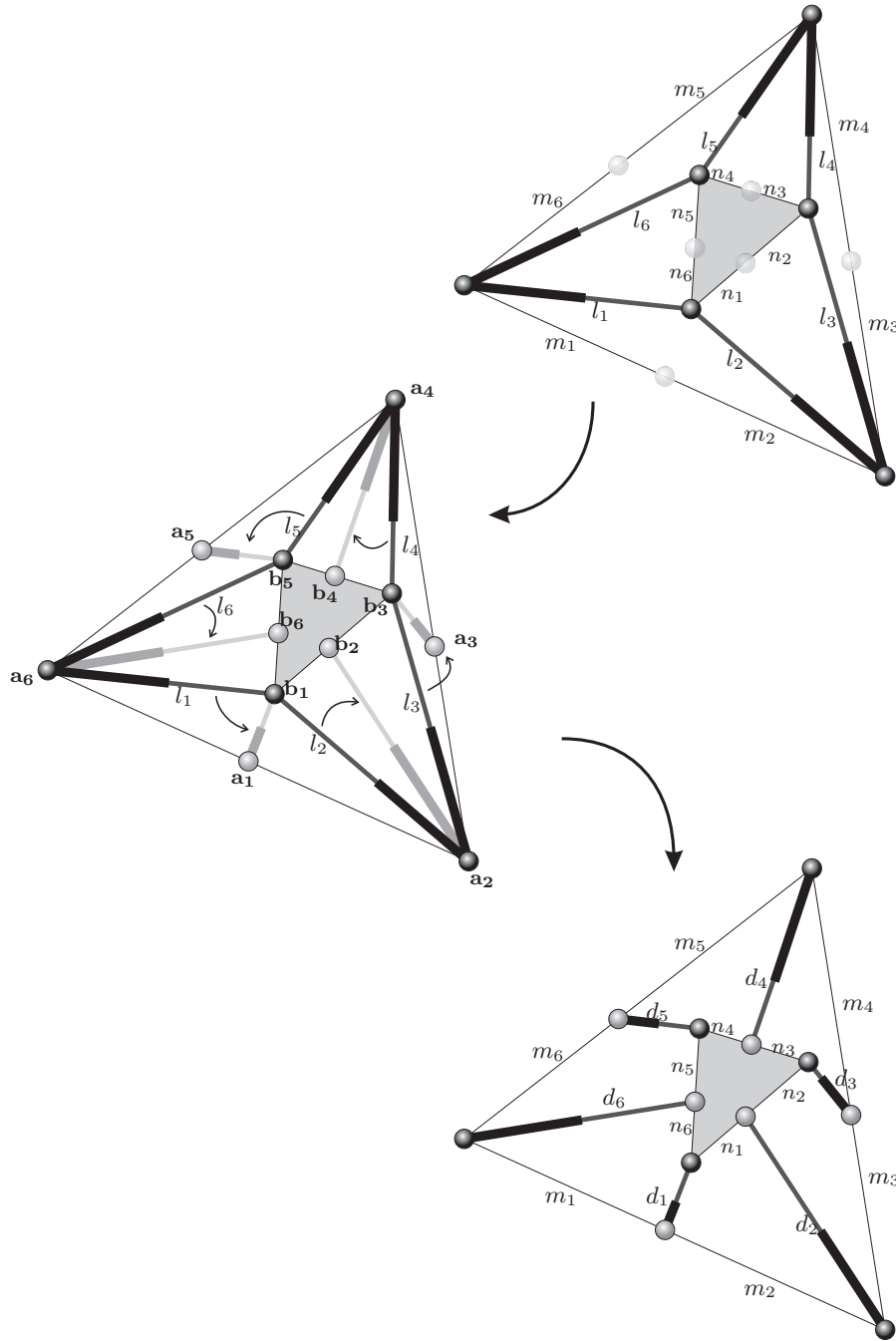


Figure 4.8: The simultaneous application of 6 Δ -transforms transforms an octahedral platform into a Griffis-Duffy platform.

depends on geometric parameters. It is easy to check that it vanishes if, and only if,

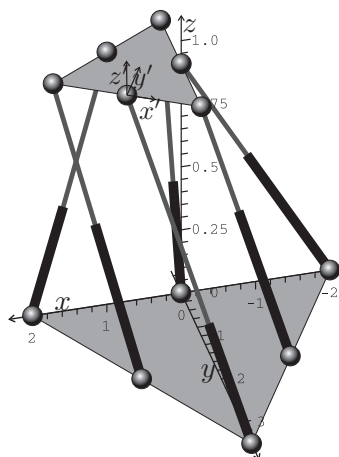
$$\frac{|\mathbf{a}_2, \mathbf{a}_6, \mathbf{a}_3| |\mathbf{a}_1, \mathbf{a}_5, \mathbf{a}_4|}{|\mathbf{a}_2, \mathbf{a}_6, \mathbf{a}_4| |\mathbf{a}_1, \mathbf{a}_5, \mathbf{a}_3|} = \frac{|\mathbf{b}_2, \mathbf{b}_6, \mathbf{b}_3| |\mathbf{b}_1, \mathbf{b}_5, \mathbf{b}_4|}{|\mathbf{b}_2, \mathbf{b}_6, \mathbf{b}_4| |\mathbf{b}_1, \mathbf{b}_5, \mathbf{b}_3|}, \quad (4.17)$$

where $|\mathbf{a}_i, \mathbf{a}_j, \mathbf{a}_k|$ is the area of the triangle defined by points \mathbf{a}_i , \mathbf{a}_j and \mathbf{a}_k . It is worth noting that these cross-ratios between areas are projective invariants whose role for coplanar points is similar to that of the cross-ratios between distances for collinear points [112].

Using rather more complicated arguments, the algebraic condition derived from factor (4.16) to detect architectural singularities in Griffis-Duffy platforms was already found in [50]. In this latter reference, the reader can also find an alternative geometric interpretation which, from our point of view, is not as elegant as the one given above in terms of cross-ratios between areas. Another interpretation of the same factor (4.16) can be found in [108]. In [53] the same manipulator was used as a particular case example of a general theorem on architectural singularities.

An important consequence of this result is that, if factor (4.16) is different from zero, the singularity locus of a Griffis-Duffy platform is the same as that of an octahedral platform. If it is zero, the platform is architecturally singular.

4.5.2.2 An architecturally singular Griffis-Duffy platform



i	\mathbf{a}_i	\mathbf{b}_i	d_i^2
1	$(0, 0, 0)$	$(0, \sqrt{3}, 0)$	$3 - \sqrt{3}$
2	$(2, 0, 0)$	$(-1/2, \sqrt{3}/2, 0)$	2
3	$(1, \sqrt{3}, 0)$	$(-1, 0, 0)$	$5 - \sqrt{3}$
4	$(0, 2\sqrt{3}, 0)$	$(0, 0, 0)$	$15 - 4\sqrt{3}$
5	$(-1, \sqrt{3}, 0)$	$(1, 0, 0)$	$11 - 5\sqrt{3}$
6	$(-2, 0, 0)$	$(1/2, \sqrt{3}/2, 0)$	$11 - 3\sqrt{3}$

Figure 4.9: An architecturally singular Griffis-Duffy platform and the corresponding table of attachment coordinates.

As an example of architecturally singular Griffis-Duffy platform, consider the platform with the leg attachment coordinates appearing in Fig. 4.9. In this case, the singularity factor (4.16) is identically zero. Hence, the platform is architecturally singular and, as a consequence, it will exhibit a self-motion. To obtain a characterization

of this self-motion, we will proceed as in the previous section. First, observe that, for the Griffis-Duffy architecturally singular platform, using the system of equations in (4.15), it can be concluded that:

$$\begin{pmatrix} 2 & 2 & 0 & 0 & 0 & 0 \\ 0 & 1 & 1 & 0 & 0 & 0 \\ 0 & 0 & 2 & 2 & 0 & 0 \\ 0 & 0 & 0 & 1 & 1 & 0 \\ 0 & 0 & 0 & 0 & 2 & 2 \\ 1 & 0 & 0 & 0 & 0 & 1 \end{pmatrix} \begin{pmatrix} l_1^2 \\ l_2^2 \\ l_3^2 \\ l_4^2 \\ l_5^2 \\ l_6^2 \end{pmatrix} = \begin{pmatrix} 16 + 4d_1^2 \\ 2 + 2d_2^2 \\ 16 + 4d_3^2 \\ 2 + 2d_4^2 \\ 16 + 4d_5^2 \\ 2 + 2d_6^2 \end{pmatrix}.$$

Since the above matrix is rank defective, there is an infinite number of values for l_1^2, \dots, l_6^2 compatible with d_1^2, \dots, d_6^2 . Substituting the values of d_1^2, \dots, d_6^2 in the table of Fig. 4.9 and solving the above system taking l_6^2 as parameter, yields:

$$\begin{aligned} l_1^2 &= -l_6^2 + 24 - 6\sqrt{3} \\ l_2^2 &= l_6^2 - 10 + 4\sqrt{3} \\ l_3^2 &= -l_6^2 + 16 - 4\sqrt{3} \\ l_4^2 &= l_6^2 + 2 + 2\sqrt{3} \\ l_5^2 &= -l_6^2 + 30 - 10\sqrt{3} \end{aligned}$$

The octahedral platform can have up to 16 assembly modes which can be obtained as the roots of an eight-degree polynomial in the square of the unknown [100, p. 161]. Thus, no algebraic formula exists for the forward kinematics of the octahedral platform. Nevertheless, the self-motion can be characterized by sweeping l_6^2 in the range $(0, \infty)$ and obtaining the roots of the biotic polynomial numerically. The 16 solutions obtained for each value of l_6^2 form eight pairs of manipulator postures, one being the mirror image of another about the base plane.

Fig. 4.10 shows the location of the barycenter of the triangular moving platform for the obtained self-motion. The color of the plotted points encodes the parameter sweep from its lower value (pure red) to its upper value (pure blue). It is interesting to note that four assembly modes are real for $l_6^2 \in (3.89, 6.025)$ and eight for $l_6^2 \in (6.025, 8.9)$. The platform cannot be assembled for l_6^2 outside the range $(3.89, 8.9)$. As in the example of the previous section, the configurations obtained for the value of the parameter that lead to changes in the number of assembly modes do not correspond to higher-order singularities of the architecturally-singular platform. Indeed, if the eigenvalues of $\mathbf{J}\mathbf{J}^T$, where \mathbf{J} is the Jacobian matrix of the architecturally-singular Griffis-Duffy platform, are

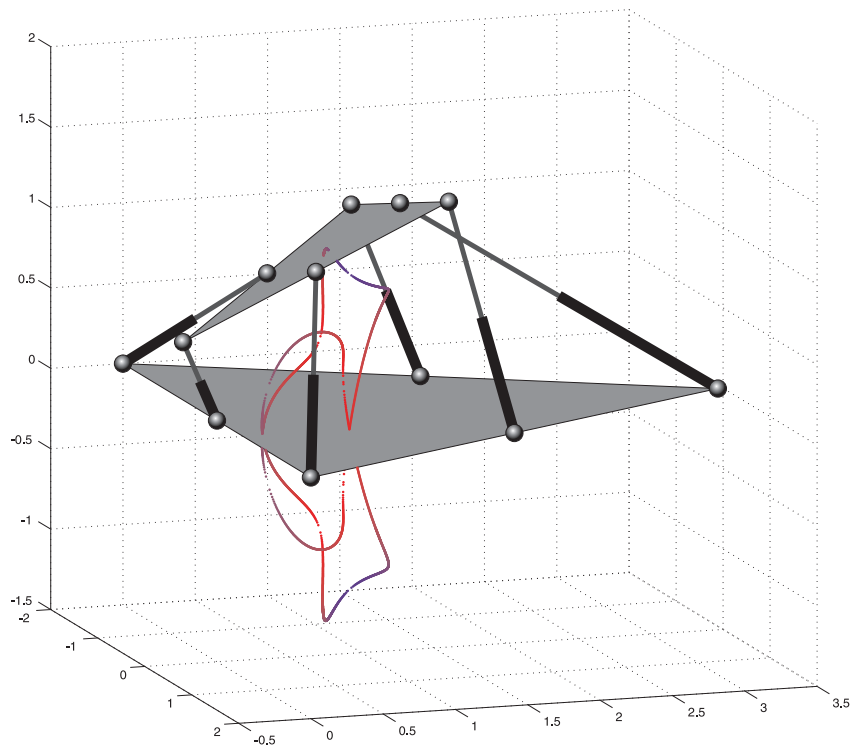


Figure 4.10: Curve traced by the barycenter of the triangular platform in Fig. 4.9 when it is moved along its self-motion. The color corresponds to the value of the parameter swept from its lower value (pure red) to its upper value (pure blue). It consists of two symmetric disjoint components with respect to the plane $z = 0$ (the base plane). Note that for the same color different points are obtained, corresponding to different assembly modes.

computed along the self-motion, five of them are always different from zero. Fig. 4.11 plots in logarithmic scale all eigenvalues, excluding the one that is always zero, for all assembly modes as a function of the chosen parameter. Note that none of them vanishes.

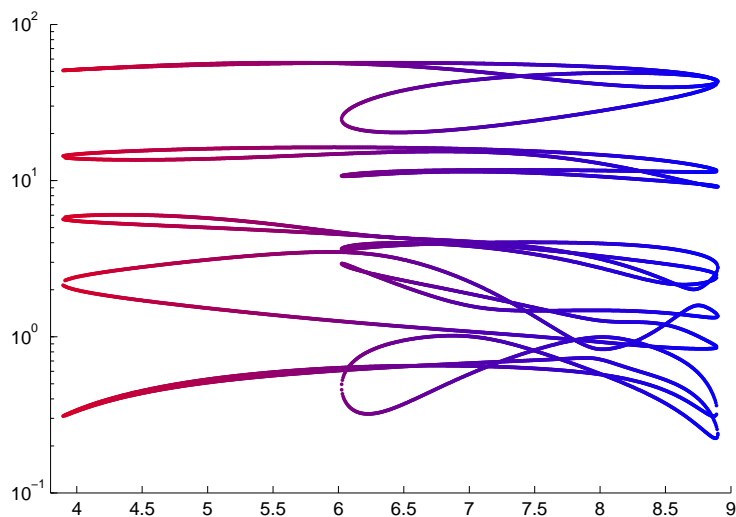


Figure 4.11: All eigenvalues for all assembly modes, excluding the one that is always zero, of $\mathbf{J}^T \mathbf{J}$, where \mathbf{J} is the Jacobian matrix of the analyzed architecturally-singular Griffis-Duffy platform, as a function of l_6^2 .

In order to validate the obtained self-motions, the results obtained have been compared using the proposed parameterization technique and those obtained using the CUIK software package. CUIK uses linear relaxation techniques to discretize the space of all the configurations that a multiloop linkage can adopt [80]. The obtained results for the attachment coordinates and the leg lengths of the Griffis-Duffy manipulator in [80] (also available online at [97]) appear in Fig. 4.12. The solution obtained using CUIK consists of a list of boxes approximating the self-motion with a resolution of 10^{-1} . It can be checked that the sampled points obtained using the proposed technique are all included in these boxes.

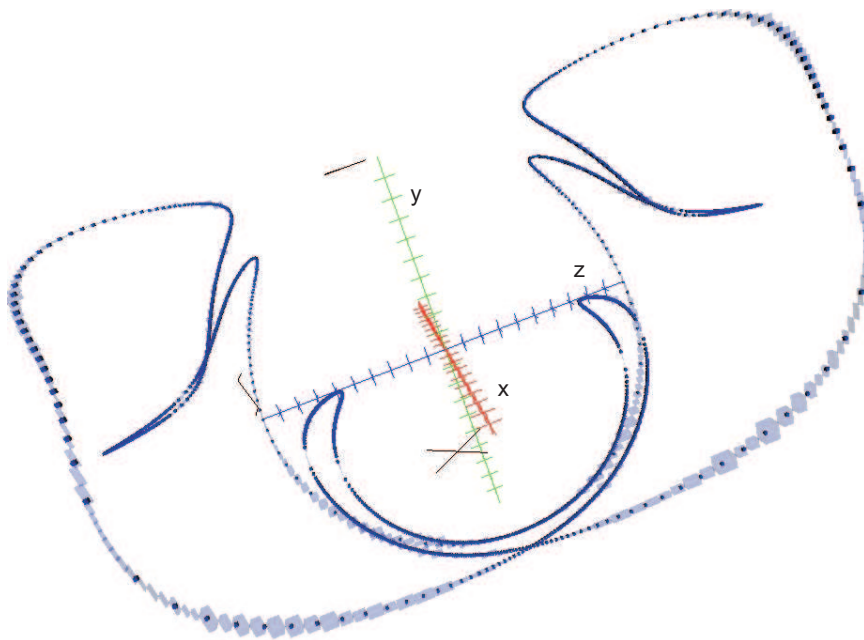


Figure 4.12: The self-motion discretization of an architecturally-singular Griffis-Duffy platform obtained using CUIK is plotted in light transparent blue, and the samples obtained with the presented parametrization in dark blue.

4.6 More on the Point-Plane component

There are several ways to compute the affine relation between the leg lengths of a tripod in Fig. 4.2. In the past section, the two relations given by the Point-Line leg rearrangement in equations (4.5) and (4.6) are combined to obtain an affine relation between them [17]. Now, Cayley-Menger determinants will be used to obtain such relation (see Appendix A for details on Cayley-Menger determinants). This methodology might be more involved than the previous one, but it is much easier to find a geometric interpretation of the singularity factor. In [9], several components were analyzed using this technique.

The Point-Plane component involves 3 legs and 4 attachments (Fig. 4.13). To find the affine relation, the length d of an additional leg must be computed with respect to the other leg lengths. To this end, consider the component with the additional leg. It involves the 5 attachments \mathbf{a}_1 , \mathbf{a}_2 , \mathbf{a}_3 , \mathbf{a} and \mathbf{b}_1 , and the corresponding Cayley-Menger

determinant gives the volume of the 4-dimensional simplex defined by the 5 points. As they are embedded in \mathbb{R}^3 , the simplex volume is null.

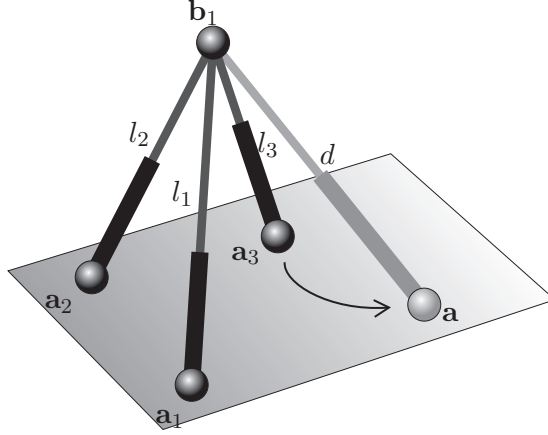


Figure 4.13: Leg l_1 can be substituted by d without modifying the singularity locus.

Using the notation introduced in Appendix A, the 5-point Cayley-Menger determinant is $D(\mathbf{a}_1, \mathbf{a}_2, \mathbf{a}_3, \mathbf{b}_1, \mathbf{a}) = 0$. Applying Jacobi's theorem, using the same partition as in equation (A.5), leads to

$$D(\mathbf{a}_1, \mathbf{a}_2, \mathbf{a}_3, \mathbf{b}_1, \mathbf{a}) = \frac{D(\mathbf{a}_1, \mathbf{a}_2, \mathbf{a}_3, \mathbf{b}_1)D(\mathbf{a}_1, \mathbf{a}_2, \mathbf{a}_3, \mathbf{a}) - D(\mathbf{a}_1, \mathbf{a}_2, \mathbf{a}_3, \mathbf{b}_1; \mathbf{a}_1, \mathbf{a}_2, \mathbf{a}_3, \mathbf{a})^2}{D(\mathbf{a}_1, \mathbf{a}_2, \mathbf{a}_3)} = 0.$$

Since all Cayley-Menger determinants are proportional to squared volumes of simplexes, $D(\mathbf{a}_1, \mathbf{a}_2, \mathbf{a}_3) \neq 0$ because the area of the base triangle must be different from zero for any non-architecturally singular tripod. Furthermore, since $D(\mathbf{a}_1, \mathbf{a}_2, \mathbf{a}_3, \mathbf{a}) = 0$ because the four points are in the same plane, the above equation becomes linear in d^2 :

$$D(\mathbf{a}_1, \mathbf{a}_2, \mathbf{a}_3, \mathbf{b}_1; \mathbf{a}_1, \mathbf{a}_2, \mathbf{a}_3, \mathbf{a}) = 0, \tag{4.18}$$

that is,

$$\begin{vmatrix} 0 & 1 & 1 & 1 & 1 \\ 1 & 0 & d(\mathbf{a}_1, \mathbf{a}_2)^2 & d(\mathbf{a}_1, \mathbf{a}_3)^2 & d(\mathbf{a}, \mathbf{a}_1)^2 \\ 1 & d(\mathbf{a}_2, \mathbf{a}_1)^2 & 0 & d(\mathbf{a}_2, \mathbf{a}_3)^2 & d(\mathbf{a}, \mathbf{a}_2)^2 \\ 1 & d(\mathbf{a}_3, \mathbf{a}_1)^2 & d(\mathbf{a}_3, \mathbf{a}_2)^2 & 0 & d(\mathbf{a}, \mathbf{a}_3)^2 \\ 1 & l_1^2 & l_2^2 & l_3^2 & d^2 \end{vmatrix} = 0.$$

where $d(\mathbf{a}_i, \mathbf{a}_j)^2$ stands for the square distance between the two attachments \mathbf{a}_i and \mathbf{a}_j . Using the Laplace expansion of the elements of the last row, all coefficients can

4.6 More on the Point-Plane component

be reinterpreted in terms of Cayley-Menger determinants, except for the independent term, giving the following affine relation:

$$\begin{aligned}
 -D(\mathbf{a}_1, \mathbf{a}_2, \mathbf{a}_3; \mathbf{a}_2, \mathbf{a}_3, \mathbf{a})l_1^2 + D(\mathbf{a}_1, \mathbf{a}_2, \mathbf{a}_3; \mathbf{a}_1, \mathbf{a}_3, \mathbf{a})l_2^2 \\
 -D(\mathbf{a}_1, \mathbf{a}_2, \mathbf{a}_3; \mathbf{a}_1, \mathbf{a}_2, \mathbf{a})l_3^2 + D(\mathbf{a}_1, \mathbf{a}_2, \mathbf{a}_3)d^2 + D = 0
 \end{aligned}$$

where D is a constant that does not depend either on l_i , for $i = 1, 2, 3$, or d .

Thus, if leg \mathbf{l}_3 is substituted by the new leg with length d , the singularity factor is

$$\frac{D(\mathbf{a}_1, \mathbf{a}_2, \mathbf{a}_3; \mathbf{a}_1, \mathbf{a}_2, \mathbf{a})}{D(\mathbf{a}_1, \mathbf{a}_2, \mathbf{a}_3)}. \quad (4.19)$$

The advantage of this formulation, with respect to the one using two Point-Line rearrangements, is that all terms in the obtained singularity factor can be described in terms of volumes of simplexes, using equation (A.3). Actually, this factor is the area of the new base triangle divided by the area of the old base triangle. Next, it will be seen how this is equivalent to the singularity factor obtained in the previous chapter after sequentially applying two Point-Line rearrangements.

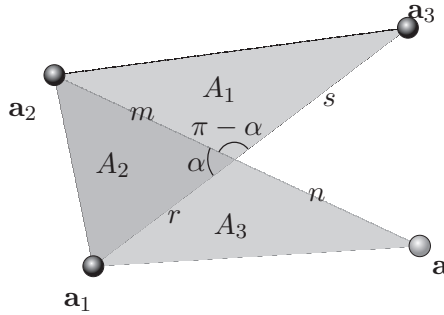


Figure 4.14: Base triangles of a Point-Plane component before and after a leg rearrangement. The notation used is the same as in Fig. 4.2

Using the notation in Fig. 4.14, the quotient of the areas obtained in equation (4.19) is

$$\frac{D(\mathbf{a}_1, \mathbf{a}_2, \mathbf{a}_3; \mathbf{a}_1, \mathbf{a}_2, \mathbf{a})}{D(\mathbf{a}_1, \mathbf{a}_2, \mathbf{a}_3)} = \frac{(A_2 + A_3)(A_1 + A_2)}{(A_1 + A_2)^2} = \frac{A_2 + A_3}{A_1 + A_2}. \quad (4.20)$$

Computing such areas depending on α gives

$$\begin{aligned}
 A_1 &= ms \sin(\pi - \alpha) = ms \sin(\alpha), \\
 A_2 &= mr \sin(\alpha), \\
 A_3 &= rn \sin(\alpha).
 \end{aligned}$$

Substituting these values in (4.20) yields

$$\frac{\sin(\alpha)r(m+n)}{\sin(\alpha)m(r+s)}$$

which is the same result obtained in Section 4.2, in equation (4.7).

When the singularity factor is zero, an architectural singularity is introduced. In this case, if the resulting area of the base triangle is zero, the point-plane become architecturally singular, as their legs belong to a planar pencil of lines [Fig. 2.4-(a)].

4.7 More on the Line-Line component

In Section 4.3, it has been shown how the legs of a Line-Line component can be rearranged by computing several Point-Line rearrangements. Nevertheless, such rearrangements can only be performed when the Line-Line contains at least one Point-Line component. In this section, the affine relation between the leg lengths for a generic Line-Line component will be obtained.

According to Fig. 4.15 and following the notation introduced in Chapter 3, adapted to the dimension of the problem, local coordinates of the base attachments in the base reference frame are $\mathbf{a}_i = (x_i, 0, 0)$. The pose of the platform line with respect to the base can be described by the position vector $\mathbf{p} = (p_x, p_y, p_z)^T$ and the unit director vector $\mathbf{i} = (i_x, i_y, i_z)^T$. Thus, the coordinates of the leg attachments in the platform line, expressed in the base reference frame, can be written as $\mathbf{b}_i = \mathbf{p} + z_i\mathbf{i}$, for $i = 1, \dots, 4$.

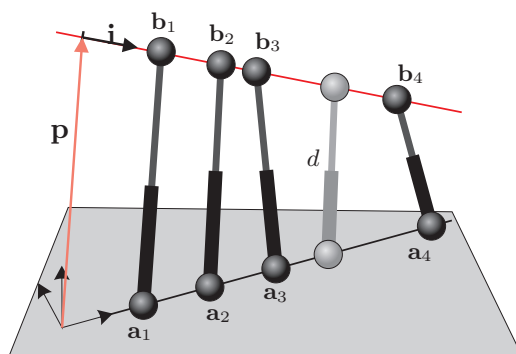


Figure 4.15: A generic Line-Line component does not contain any Point-Line component.

4.7 More on the Line-Line component

Suppose now that the length of a new leg going from $\mathbf{a} = (x, 0, 0)$ to $\mathbf{b} = \mathbf{p} + z\mathbf{i}$ has to be computed (in gray in 4.15). Taking the distance equations of the four legs $l_i^2 = \|\mathbf{b}_i - \mathbf{a}_i\|^2$, for $i = 1, \dots, 4$, together with that of the new leg $d^2 = \|\mathbf{b} - \mathbf{a}\|^2$, leads to a system of 5 quadratic equations. The subtraction of equation $i_x^2 + i_y^2 + i_z^2 = 1$ from the other five cancels all quadratic terms in i_x , i_y and i_z , yielding

$$\begin{aligned} z_i t - x_i p_x - x_i z_i i_x + \frac{1}{2}(p_x^2 + p_y^2 + p_z^2 + x_i^2 + z_i^2 - l_i^2) &= 0, \text{ for } i = 1, \dots, 4 \\ z t - x p_x - x z_i i_x + \frac{1}{2}(p_x^2 + p_y^2 + p_z^2 + x^2 + z^2 - d^2) &= 0, \end{aligned}$$

where $t = \mathbf{p} \cdot \mathbf{i}$. In addition, subtracting the first equation from the others, quadratic terms in p_x , p_y and p_z cancel too, and the following linear system is obtained:

$$\begin{pmatrix} z_1 - z_2 & x_2 - x_1 & x_2 z_2 - x_1 z_1 & 0 \\ z_1 - z_3 & x_3 - x_1 & x_3 z_3 - x_1 z_1 & 0 \\ z_1 - z_4 & x_4 - x_1 & x_4 z_4 - x_1 z_1 & 0 \\ z_1 - z & x - x_1 & x z - x_1 z_1 & \frac{1}{2} \end{pmatrix} \begin{pmatrix} t \\ p_x \\ i_x \\ d^2 \end{pmatrix} = \frac{1}{2} \begin{pmatrix} x_2^2 + z_2^2 - l_2^2 - x_1^2 - z_1^2 + l_1^2 \\ x_3^2 + z_3^2 - l_3^2 - x_1^2 - z_1^2 + l_1^2 \\ x_4^2 + z_4^2 - l_4^2 - x_1^2 - z_1^2 + l_1^2 \\ x^2 + z^2 - x_1^2 - z_1^2 + l_1^2 \end{pmatrix}. \quad (4.21)$$

Now, d^2 can be obtained by solving the above system using Cramer's rule:

$$d^2 = \frac{\begin{vmatrix} z_1 - z_2 & x_2 - x_1 & x_2 z_2 - x_1 z_1 & x_2^2 + z_2^2 - l_2^2 - x_1^2 - z_1^2 + l_1^2 \\ z_1 - z_3 & x_3 - x_1 & x_3 z_3 - x_1 z_1 & x_3^2 + z_3^2 - l_3^2 - x_1^2 - z_1^2 + l_1^2 \\ z_1 - z_4 & x_4 - x_1 & x_4 z_4 - x_1 z_1 & x_4^2 + z_4^2 - l_4^2 - x_1^2 - z_1^2 + l_1^2 \\ z_1 - z & x - x_1 & x z - x_1 z_1 & x^2 + z^2 - x_1^2 - z_1^2 + l_1^2 \end{vmatrix}}{\begin{vmatrix} z_1 - z_2 & x_2 - x_1 & x_2 z_2 - x_1 z_1 \\ z_1 - z_3 & x_3 - x_1 & x_3 z_3 - x_1 z_1 \\ z_1 - z_4 & x_4 - x_1 & x_4 z_4 - x_1 z_1 \end{vmatrix}}. \quad (4.22)$$

Expanding the determinants involved in the above equation leads to the affine relation

$$d^2 = c_1 l_1^2 + c_2 l_2^2 + c_3 l_3^2 + c_4 l_4^2 + c_0, \quad (4.23)$$

where all the coefficients depend on known constant coordinates. Thus, any leg rearrangement within a Line-Line component leaves singularities invariant.

To compute the singularity factor resulting from the above rearrangement coefficient c_1 in (4.23) must be computed. To this aim, elementary row operations will be applied

4.7 More on the Line-Line component

to the determinants in (4.22), which permit to rewrite them as

$$d^2 = \frac{\begin{vmatrix} -z_1 & x_1 & x_1 z_1 & x_1^2 + z_1^2 - l_1^2 & 1 \\ z_1 - z_2 & x_2 - x_1 & x_2 z_2 - x_1 z_1 & x_2^2 + z_2^2 - l_2^2 - x_1^2 - z_1^2 + l_1^2 & 0 \\ z_1 - z_3 & x_3 - x_1 & x_3 z_3 - x_1 z_1 & x_3^2 + z_3^2 - l_3^2 - x_1^2 - z_1^2 + l_1^2 & 0 \\ z_1 - z_4 & x_4 - x_1 & x_4 z_4 - x_1 z_1 & x_4^2 + z_4^2 - l_4^2 - x_1^2 - z_1^2 + l_1^2 & 0 \\ z_1 - z & x - x_1 & xz - x_1 z_1 & x^2 + z^2 - x_1^2 - z_1^2 + l_1^2 & 0 \end{vmatrix}}{\begin{vmatrix} -z_1 & x_1 & x_1 z_1 & 1 \\ z_1 - z_2 & x_2 - x_1 & x_2 z_2 - x_1 z_1 & 0 \\ z_1 - z_3 & x_3 - x_1 & x_3 z_3 - x_1 z_1 & 0 \\ z_1 - z_4 & x_4 - x_1 & x_4 z_4 - x_1 z_1 & 0 \end{vmatrix}}$$

Now, the first row can be added to all the others, without changing the values of the determinants. This yields to the following equivalent expression of d^2 :

$$d^2 = \frac{\begin{vmatrix} -z_1 & x_1 & x_1 z_1 & x_1^2 + z_1^2 - l_1^2 & 1 \\ -z_2 & x_2 & x_2 z_2 & x_2^2 + z_2^2 - l_2^2 & 1 \\ -z_3 & x_3 & x_3 z_3 & x_3^2 + z_3^2 - l_3^2 & 1 \\ -z_4 & x_4 & x_4 z_4 & x_4^2 + z_4^2 - l_4^2 & 1 \\ -z & x & xz & x^2 + z^2 & 1 \end{vmatrix}}{\begin{vmatrix} -z_1 & x_1 & x_1 z_1 & 1 \\ -z_2 & x_2 & x_2 z_2 & 1 \\ -z_3 & x_3 & x_3 z_3 & 1 \\ -z_4 & x_4 & x_4 z_4 & 1 \end{vmatrix}} \quad (4.24)$$

This is a simple linear algebra technique that will be used several times to simplify equations.

Studying the expansion of the determinant in the numerator of (4.24), it is easy to see that the coefficient multiplying l_1^2 in (4.23) is the cofactor corresponding to the element (1, 4) of the matrix in the numerator, multiplied by -1 , that is,

$$c_1 = -(-1)^{1+3} \frac{\begin{vmatrix} -z_2 & x_2 & x_2 z_2 & 1 \\ -z_3 & x_3 & x_3 z_3 & 1 \\ -z_4 & x_4 & x_4 z_4 & 1 \\ -z & x & xz & 1 \end{vmatrix}}{\begin{vmatrix} -z_1 & x_1 & x_1 z_1 & 1 \\ -z_2 & x_2 & x_2 z_2 & 1 \\ -z_3 & x_3 & x_3 z_3 & 1 \\ -z_4 & x_4 & x_4 z_4 & 1 \end{vmatrix}} = (-1)^{1+3} \frac{\begin{vmatrix} -z & x & xz & 1 \\ -z_2 & x_2 & x_2 z_2 & 1 \\ -z_3 & x_3 & x_3 z_3 & 1 \\ -z_4 & x_4 & x_4 z_4 & 1 \end{vmatrix}}{\begin{vmatrix} -z_1 & x_1 & x_1 z_1 & 1 \\ -z_2 & x_2 & x_2 z_2 & 1 \\ -z_3 & x_3 & x_3 z_3 & 1 \\ -z_4 & x_4 & x_4 z_4 & 1 \end{vmatrix}}, \quad (4.25)$$

where the rows of the determinant have been reordered using multi-linear properties of determinants.

4.8 Application to the implementation of an octahedral manipulator

It is clear than the numerator and the denominator correspond to an equivalent expression, before and after the substitution of leg \mathbf{l}_1 by \mathbf{d} . This expression is the architectural singularity condition. It is zero if, and only if, the cross-ratios of the four base attachments is equal to the cross-ratio of the four platform attachments. This is the same condition found in Section 4.4. Indeed, when one imposes the equality between the cross-ratio $\{\mathbf{b}_1, \mathbf{b}_2; \mathbf{b}_3, \mathbf{b}_4\}$ with $\{\mathbf{a}_1, \mathbf{a}_2; \mathbf{a}_3, \mathbf{a}_4\}$ (using equation (B.1)), one gets

$$\frac{(z_3 - z_1)(z_4 - z_2)}{(z_4 - z_1)(z_3 - z_2)} = \frac{(x_3 - x_1)(x_4 - x_2)}{(x_4 - x_1)(x_3 - x_2)}$$

or equivalently,

$$\begin{aligned} & (z_3 - z_1)(z_4 - z_2)(x_4 - x_1)(x_3 - x_2) - (x_3 - x_1)(x_4 - x_2)(z_4 - z_1)(z_3 - z_2) \\ &= \begin{vmatrix} -z_1 & x_1 & x_1 z_1 & 1 \\ -z_2 & x_2 & x_2 z_2 & 1 \\ -z_3 & x_3 & x_3 z_3 & 1 \\ -z_4 & x_4 & x_4 z_4 & 1 \end{vmatrix} = 0 \end{aligned}$$

When the cross-ratio of the platform attachments is equal to the cross-ratio of the base attachments, the singularity factor is zero and the manipulator is architecturally singular. Having the same cross-ratio means that the leg lines follow a projective one-to-one correspondence between the two lines that define the component (more details in Appendix B). Then, the four leg lines belong to a regulus that can be defined by any 3 legs [Fig. 2.4-(c)]. A regulus is a linear complex of rank 3 [25, Figure 3A in Table 4].

4.8 Application to the implementation of an octahedral manipulator

One of the most famous 3-3 Stewart-Gough platforms consists of six double-ball-ended legs thereby forming a zigzag pattern. For symmetry reasons, this topology is either taken as it stands or is approximated in most implementations of the Stewart-Gough platform. Since the 12 lines that join the double-ball-joints can be interpreted as the eight triangular faces of an octahedron, the term *octahedral manipulator* was coined in [46] to name it.

Clearly, it is advantageous to have multiple spherical joints sharing the same center of rotation in a parallel manipulator to simplify its kinematics. However, difficulties

4.8 Application to the implementation of an octahedral manipulator

always arise in constructing such spherical joints. There have been several attempts to construct them (see [19] and the references therein), but none of them use off-the-self mechanical elements. Another disadvantage of this kind of joints is that the range of action of the leg actuators is reduced because of the risk of mechanical interference. In [62], kinematic substitutions are introduced to provide a way around this problem where it is shown, for example, that the manipulator appearing in Fig. 4.16(a), that avoids the double-ball-joints in the base, is kinematically equivalent to the octahedral manipulator. This particular arrangement of joints is also known as the triple arm mechanism [101].

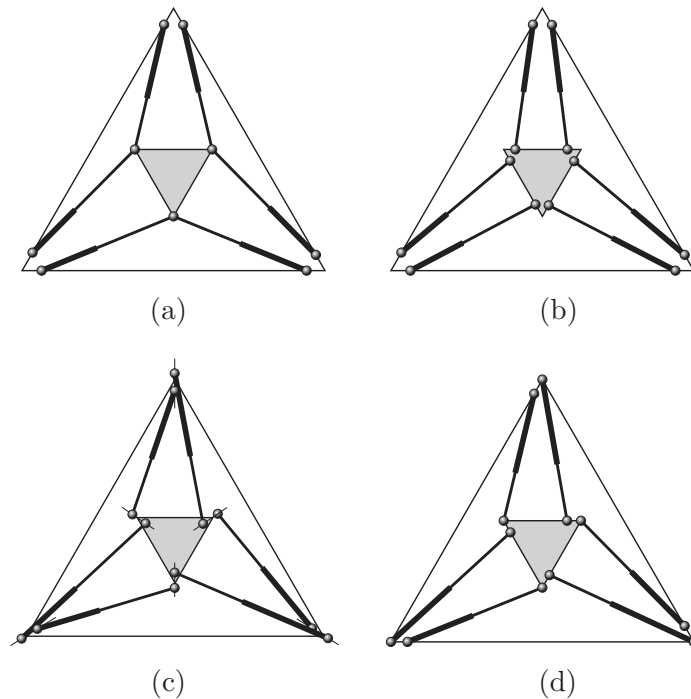


Figure 4.16: The triple arm mechanism (a), the standard approximation to the octahedral manipulator that avoids all double-ball-joints (b), the Stoughton-Arai approximation intended to also improve the dexterity of the manipulator (c), and the Griffis-Duffy modification (d).

Most implementations avoid the difficulty of constructing multiple spherical joints by approximating them with a collection of single spherical joints with small offsets between the centers of rotation of the links, as shown in Fig. 4.16(b). Such offsets change the kinematics of the mechanism, resulting in one of two possible problems, as pointed

4.8 Application to the implementation of an octahedral manipulator

out in [19]. First, if the offsets are included in the kinematics of the mechanism, the kinematic equations may become very complex and thus very difficult to solve. Second, if the offsets are neglected, thus simplifying the kinematic equations, errors arise. These errors may have a significant impact in precision applications, or in manipulators such as the Tetrobot [43] that consists in stacking multiple octahedral manipulators resulting in the accumulation of errors if such offsets are introduced and neglected.

The modification of the octahedral manipulator proposed by Stoughton and Arai consist in separating the six double-ball joints alternatively inward and outward radially [95], as shown in Fig. 4.16(c). Each double-ball-joint is separated by the same amount into a pair of spherical joints whose centers are equidistant to the original center.

In Section 4.5.2 it has been shown that, if this six double-ball joints are alternatively separated not radially but following the edges of the base and platform triangles, as shown in Fig. 4.16(d), the resulting manipulator is kinematically equivalent to the original octahedral one. This fact was already acknowledged by Griffis and Duffy in [42] (without giving an explicit formulation) but it has been overlooked, even by the same authors, in subsequent publications where alternatives to avoid these joints are discussed [62].

According to Fig. 4.17 and the results in Section 4.5.2, the affine relation between leg lengths of the resulting 6-6 platform and the original octahedral manipulator can be expressed as:

$$\begin{pmatrix} m_1^2 \\ m_2^2 \\ m_3^2 \\ m_4^2 \\ m_5^2 \\ m_6^2 \end{pmatrix} = \mathbf{A} \begin{pmatrix} l_1^2 \\ l_2^2 \\ l_3^2 \\ l_4^2 \\ l_5^2 \\ l_6^2 \end{pmatrix} - \mathbf{b} \quad (4.26)$$

where

$$\mathbf{A} = \begin{pmatrix} \frac{d_{12}-\delta_1}{d_{12}} & \frac{\delta_1}{d_{12}} & 0 & 0 & 0 & 0 \\ 0 & \frac{d_{45}-\delta_2}{d_{45}} & \frac{\delta_2}{d_{45}} & 0 & 0 & 0 \\ 0 & 0 & \frac{d_{23}-\delta_3}{d_{23}} & \frac{\delta_3}{d_{23}} & 0 & 0 \\ 0 & 0 & 0 & \frac{d_{56}-\delta_4}{d_{56}} & \frac{\delta_4}{d_{56}} & 0 \\ 0 & 0 & 0 & 0 & \frac{d_{13}-\delta_5}{d_{13}} & \frac{\delta_5}{d_{13}} \\ \frac{\delta_6}{d_{46}} & 0 & 0 & 0 & 0 & \frac{d_{46}-\delta_6}{d_{46}} \end{pmatrix} \quad (4.27)$$

4.8 Application to the implementation of an octahedral manipulator

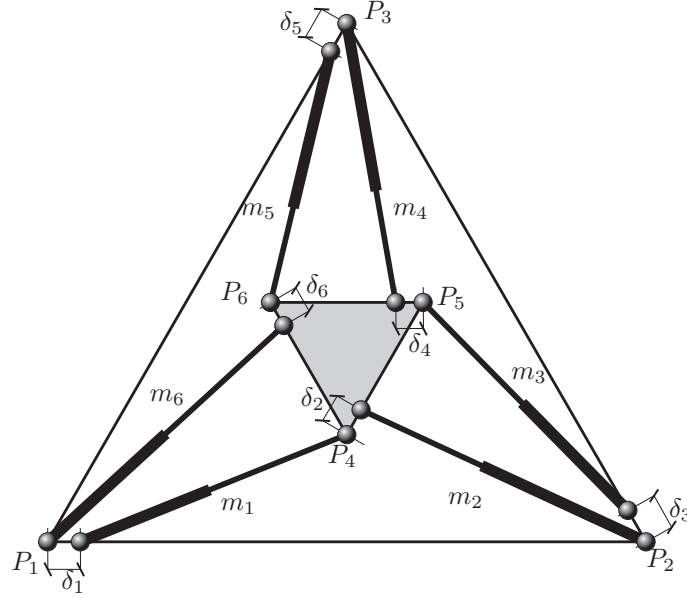


Figure 4.17: Contrary to what happens to the Stoughton-Arai approximation, the proposed modification leads to a 6-6 platform kinematically equivalent to the octahedral manipulator.

and

$$\mathbf{b} = \begin{pmatrix} \delta_1(d_{12} - \delta_1) \\ \delta_2(d_{45} - \delta_2) \\ \delta_3(d_{23} - \delta_3) \\ \delta_4(d_{56} - \delta_4) \\ \delta_5(d_{13} - \delta_5) \\ \delta_6(d_{46} - \delta_6) \end{pmatrix}$$

If $\det(\mathbf{A}) \neq 0$, there is a one-to-one correspondence between (m_1^2, \dots, m_6^2) and (l_1^2, \dots, l_6^2) . Remind that \mathbf{A} is constant as it only depends on architectural parameters.

For example, consider a parallel manipulator with the same topology as the one depicted in Fig. 4.17 with the following geometric parameters: $d_{12} = d_{23} = d_{13} = 12$, $d_{46} = d_{45} = d_{56} = 6$, $\Delta_1 = \delta_1 = \delta_3 = \delta_5$, and $\Delta_2 = \delta_2 = \delta_4 = \delta_6$. Substituting these values in (4.27) and computing its determinant, one obtains

$$\begin{aligned} \det(\mathbf{A}) = & -\frac{1}{20736}\Delta_1^3\Delta_2^2 - \frac{1}{10368}\Delta_1^2\Delta_2^3 + \frac{1}{3456}\Delta_1^3\Delta_2 + \frac{1}{576}\Delta_1^2\Delta_2^2 + \frac{1}{864}\Delta_1\Delta_2^3 - \frac{1}{1728}\Delta_1^3 \\ & - \frac{1}{96}\Delta_1^2\Delta_2 - \frac{1}{48}\Delta_1\Delta_2^2 - \frac{1}{216}\Delta_2^3 + \frac{1}{48}\Delta_1^2 + \frac{1}{8}\Delta_1\Delta_2 + \frac{1}{12}\Delta_2^2 - \frac{1}{4}\Delta_1 - \frac{1}{2}\Delta_2 + 1. \end{aligned}$$

Fig. 4.18 plots $\det(\mathbf{A})$ as a function of Δ_1 and Δ_2 . When $\Delta_1 + \Delta_2 = 12$, the

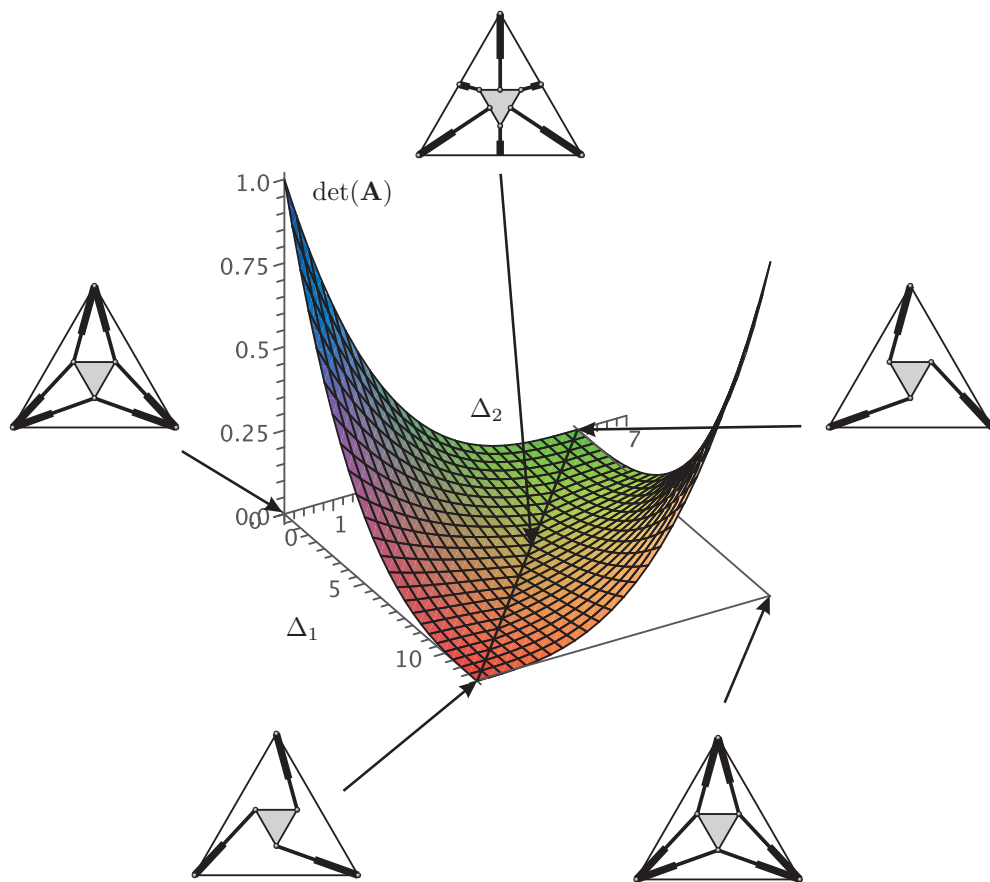


Figure 4.18: By properly choosing the offsets $\Delta_1 = \delta_1 = \delta_3 = \delta_5$ and $\Delta_2 = \delta_2 = \delta_4 = \delta_6$ in Fig. 4.17, it is possible to reach architecturally singular platforms including the trivial situations in which couples of legs coincide and the architecturally singular Griffis-Duffy platform.

4.8 Application to the implementation of an octahedral manipulator

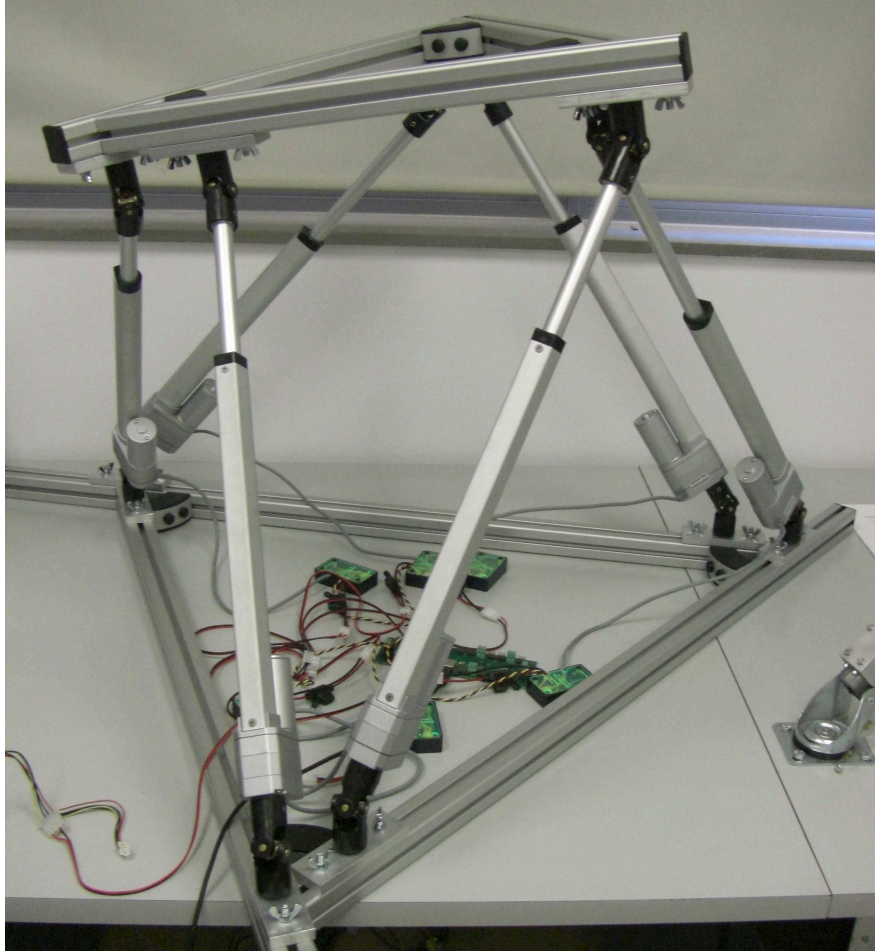


Figure 4.19: Prototype of a 6-6 parallel manipulator.

introduced offsets lead to an architecturally singular platform as $\det(\mathbf{A}) = 0$.

This prototype has been implemented at IRI (Fig. 4.19) [84].

Chapter 5

The Line-Plane component

5.1 Pentapods

The Line-Plane component is normally studied as a part of a Stewart-Gough platform, but it has also interest as an independent manipulator. Indeed, a pentapod is usually defined as a 5-degree-of-freedom fully-parallel manipulator with an axial spindle as moving platform. This kind of manipulators have revealed as an interesting alternative to serial robots handling axisymmetric tools. Their particular geometry permits that, in one tool axis, inclination angles of up to 90 degrees are possible thus overcoming the orientation limits of the classical Stewart-Gough platform.

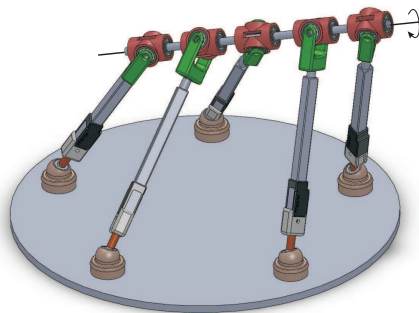


Figure 5.1: A pentapod. While the axis defined by these universal joints is rigidly linked to the base for fixed leg lengths, any tool attached to it can freely rotate.

A pentapod is well suited to handling an axisymmetric tool because the moving platform can freely rotate around the axis defined by the five aligned revolute joints (Fig 5.1). If this rotation axis is made coincident with the symmetry axis of the tool,

the uncontrolled motion becomes irrelevant in most cases. Indeed, there are important industrial tasks requiring a tool to be perpendicular to a 3D free-form surface along a given trajectory without caring about its axial orientation. They include, for example, 5-axis milling, laser-engraving, spray-based painting, surface polishing and water-jet cutting. Alternatively, this uncontrolled rotation motion can always be eliminated by blocking one of the five aligned revolute joints. The study of the kinematics properties of pentapods is thus highly relevant for many applications [20, 76, 102].

There are some variations on the basic described pentapod that consists in substituting the universal joints by two consecutive revolute joints. The axes of the last revolute joints remain collinear with the axis of the tool while the axis of the other revolute joint axis no longer intersect with the tool axis. This is the joint arrangement used by Metrom in its Pentapod machine (Fig. 5.2). This arrangement simplifies the construction of the resulting pentapod but its kinematic analysis is far from trivial. Actually, the solutions to its direct kinematics are given by the roots of a system of 5 polynomials of degree 4 together with a quadratic normalizing condition. Therefore, the number of solutions is not greater than 2048 [20], [103]. When this number is compared to the 16 possible direct kinematic solutions of the basic pentapod, one also gets an idea of the relative complexity between the singularity loci of the basic and the modified design.



Figure 5.2: A 5-axis milling machine, based on a pentapod, developed by Metrom Mechatronische Maschinen GmbH (reproduced with permission).

The present chapter about the Line-Plane component deals with pentapods with coplanar base attachments, while the following one, about the Line-Body component,

5.2 Finding the affine relation between leg lengths

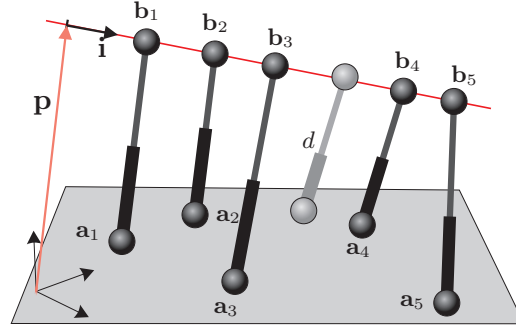


Figure 5.3: A generic Line-Plane component with an additional leg in gray.

studies the kinematics of a general pentapod. Both chapters complete the first studies appeared in [8, 15] and in [18] about the Line-Plane and Line-Body components, respectively. All are valid both considering the component as an independent manipulator or as a rigid component of a Stewart-Gough platform.

5.2 Finding the affine relation between leg lengths

Consider the 5-legged parallel platform appearing in Fig. 5.3. Following the notation introduced in Chapter 3 adapted to the dimension of the problem, the local coordinates of the base attachments expressed in the base reference frame are $\mathbf{a}_i = (x_i, y_i, 0)$. The pose of the platform with respect to the base plane can be described by the position vector $\mathbf{p} = (p_x, p_y, p_z)^T$ and the unit vector $\mathbf{i} = (i_x, i_y, i_z)^T$. Thus, the coordinates of the leg attachments in the platform line, expressed in the base reference frame, can be written as $\mathbf{b}_i = \mathbf{p} + z_i \mathbf{i}$, for $i = 1, \dots, 5$.

Proceeding in a similar way as for the Line-Line component, the length of a new leg introduced by the rearrangement depends on the lengths of the five legs. The derived system has now 5 equations, $l_i^2 = |\mathbf{b}_i - \mathbf{a}_i|^2$, for $i = 1, \dots, 5$, plus the one for the additionally introduced leg, $d^2 = |\mathbf{b} - \mathbf{a}|^2$. Then, subtracting the equation $\|\mathbf{i}\|^2 = i_x^2 + i_y^2 + i_z^2 = 1$ from the expression for l_i^2 , $i = 1, \dots, 5$, quadratic terms in i_x , i_y and i_z cancel out yielding

$$z_i t - x_i p_x - y_i p_y - x_i z_i i_x - y_i z_i i_y + \frac{1}{2}(p_x^2 + p_y^2 + p_z^2 + x_i^2 + y_i^2 + z_i^2 - l_i^2) = 0, \quad (5.1)$$

for $i = 1, \dots, 5$, where $t = \mathbf{p} \cdot \mathbf{i}$. Subtracting the first equation from the others, quadratic terms in p_x , p_y and p_z cancel out as well. Then, the resulting system of equations can

5.2 Finding the affine relation between leg lengths

be written in matrix form as

$$\begin{pmatrix} x_2 - x_1 & y_2 - y_1 & x_2 z_2 - x_1 z_1 & y_2 z_2 - y_1 z_1 & 0 \\ x_3 - x_1 & y_3 - y_1 & x_3 z_3 - x_1 z_1 & y_3 z_3 - y_1 z_1 & 0 \\ x_4 - x_1 & y_4 - y_1 & x_4 z_4 - x_1 z_1 & y_4 z_4 - y_1 z_1 & 0 \\ x_5 - x_1 & y_5 - y_1 & x_5 z_5 - x_1 z_1 & y_5 z_5 - y_1 z_1 & 0 \\ x - x_1 & y - y_1 & xz - x_1 z_1 & yz - y_1 z_1 & \frac{1}{2} \end{pmatrix} \begin{pmatrix} p_x \\ p_y \\ i_x \\ i_y \\ d^2 \end{pmatrix} = \begin{pmatrix} (z_2 - z_1)t + N_2 \\ (z_3 - z_1)t + N_3 \\ (z_4 - z_1)t + N_4 \\ (z_5 - z_1)t + N_5 \\ (z - z_1)t + N \end{pmatrix}, \quad (5.2)$$

where

$$N_i = 1/2(x_i^2 + y_i^2 + z_i^2 - l_i^2 - x_1^2 - y_1^2 - z_1^2 + l_1^2), \text{ for } i = 1, \dots, 5 \text{ and}$$

$$N = 1/2(x^2 + y^2 + z^2 - x_1^2 - y_1^2 - z_1^2 + l_1^2).$$

If the resulting system is degenerate (*i.e* it is rank-deficient), a different unknown can be chosen as a parameter, either p_x , p_y , i_x or i_y . For any non-architecturally-singular manipulator, there will be always an associated non-degenerate linear system by properly choosing the right parameter (this will be seen in detail in the next sections).

In a similar way as in the previous chapter, (5.2) can be solved for d^2 using Cramer's rule, yielding

$$d^2 = \frac{2(rt + s)}{C}. \quad (5.3)$$

where C is the determinant of the matrix in (5.2),

$$r = \begin{vmatrix} x_2 - x_1 & y_2 - y_1 & x_2 z_2 - x_1 z_1 & y_2 z_2 - y_1 z_1 & z_2 - z_1 \\ x_3 - x_1 & y_3 - y_1 & x_3 z_3 - x_1 z_1 & y_3 z_3 - y_1 z_1 & z_3 - z_1 \\ x_4 - x_1 & y_4 - y_1 & x_4 z_4 - x_1 z_1 & y_4 z_4 - y_1 z_1 & z_4 - z_1 \\ x_5 - x_1 & y_5 - y_1 & x_5 z_5 - x_1 z_1 & y_5 z_5 - y_1 z_1 & z_5 - z_1 \\ x - x_1 & y - y_1 & xz - x_1 z_1 & yz - y_1 z_1 & z - z_1 \end{vmatrix}, \quad (5.4)$$

and

$$s = \begin{vmatrix} x_2 - x_1 & y_2 - y_1 & x_2 z_2 - x_1 z_1 & y_2 z_2 - y_1 z_1 & N_2 \\ x_3 - x_1 & y_3 - y_1 & x_3 z_3 - x_1 z_1 & y_3 z_3 - y_1 z_1 & N_3 \\ x_4 - x_1 & y_4 - y_1 & x_4 z_4 - x_1 z_1 & y_4 z_4 - y_1 z_1 & N_4 \\ x_5 - x_1 & y_5 - y_1 & x_5 z_5 - x_1 z_1 & y_5 z_5 - y_1 z_1 & N_5 \\ x - x_1 & y - y_1 & xz - x_1 z_1 & yz - y_1 z_1 & N \end{vmatrix}.$$

Note how the numerator in (5.3) has been expressed as the sum of two determinants using the formula $|c_1 \dots (tc_{i_1} + c_{i_2}) \dots c_n| = |c_1 \dots c_{i_1} \dots c_n|t + |c_1 \dots c_{i_2} \dots c_n|$. Furthermore, using simple matrix row operations, both matrices have been simplified in a similar way as in the previous chapter.

5.2 Finding the affine relation between leg lengths

Equation (5.3) is not an affine relation because it depends on $t = \mathbf{p} \cdot \mathbf{i}$. However, imposing $r = 0$, the squared length of the new leg given by (5.3) can be rewritten as

$$d^2 = \frac{1}{C} \begin{vmatrix} x & y & xz & yz & x^2 + y^2 + z^2 & 1 \\ x_1 & y_1 & x_1 z_1 & y_1 z_1 & x_1^2 + y_1^2 + z_1^2 - l_1^2 & 1 \\ x_2 & y_2 & x_2 z_2 & y_2 z_2 & x_2^2 + y_2^2 + z_2^2 - l_2^2 & 1 \\ x_3 & y_3 & x_3 z_3 & y_3 z_3 & x_3^2 + y_3^2 + z_3^2 - l_3^2 & 1 \\ x_4 & y_4 & x_4 z_4 & y_4 z_4 & x_4^2 + y_4^2 + z_4^2 - l_4^2 & 1 \\ x_5 & y_5 & x_5 z_5 & y_5 z_5 & x_5^2 + y_5^2 + z_5^2 - l_5^2 & 1 \end{vmatrix}. \quad (5.5)$$

After Laplace expansion by the elements of the 5th column, the above expression leads to the affine relation

$$d^2 = c_1 l_1^2 + c_2 l_2^2 + c_3 l_3^2 + c_4 l_4^2 + c_5 l_5^2 + c_0,$$

where again all the coefficients depend on known constant coordinates.

In conclusion, the Line-Plane component is the first one for which a general leg rearrangement is not unconditionally singularity-invariant. To be so, the new leg attachments $\mathbf{a} = (x, y, 0)$ and $\mathbf{b} = \mathbf{p} + z\mathbf{i}$ must satisfy the condition $r = 0$.

Now, is it possible to proceed as in the previous chapter to compute the singularity factor resulting from substituting the leg with length l_1 by the leg with length d , that is, the coefficient of l_1^2 in the affine relation (5.5), which corresponds to the cofactor of the element (2, 5) of the matrix in (5.5):

$$c_1 = \frac{\begin{vmatrix} x & y & xz & yz & 1 \\ x_2 & y_2 & x_2 z_2 & y_2 z_2 & 1 \\ x_3 & y_3 & x_3 z_3 & y_3 z_3 & 1 \\ x_4 & y_4 & x_4 z_4 & y_4 z_4 & 1 \\ x_5 & y_5 & x_5 z_5 & y_5 z_5 & 1 \end{vmatrix}}{\begin{vmatrix} x_1 & y_1 & x_1 z_1 & y_1 z_1 & 1 \\ x_2 & y_2 & x_2 z_2 & y_2 z_2 & 1 \\ x_3 & y_3 & x_3 z_3 & y_3 z_3 & 1 \\ x_4 & y_4 & x_4 z_4 & y_4 z_4 & 1 \\ x_5 & y_5 & x_5 z_5 & y_5 z_5 & 1 \end{vmatrix}}$$

Again, it is clear than the numerator and the denominator correspond to an equivalent expression, before and after the performed rearrangement. In the previous chapters, it was shown how when the singularity factor is identically zero, the platform, after the rearrangement, become architecturally singular. Nevertheless, in this case, the situation is a bit more complicated because it is a conditional leg rearrangement. That

5.3 Finding the rearrangements by rewriting the Jacobian determinant

is, to have an architecturally singular Line-Plane component, not only this singularity factor has to be zero, but the condition $r = 0$ has also to be fulfilled. Architectural singularities of the Line-Plane component will be studied in detail in Section 5.7.

5.3 Finding the rearrangements by rewriting the Jacobian determinant

Up to this point, all singularity-invariant leg rearrangements have been deduced by finding an affine relation. Next, it will be shown how the alternative methodology described in Chapter 3 can be applied to obtain the same rearrangement and to provide, at the same time, convenient equations to deal with singularities and to relate the forward kinematics problem with the singularity locus of the manipulator.

It is well known that the Jacobian matrix of a Stewart-Gough platform (*i.e.*, the matrix relating the leg velocities to those of the platform itself) is the matrix whose columns are the Plücker coordinates of the leg lines. When a 6-legged Stewart-Gough platform contains a Line-Plane component, the resulting Jacobian matrix determinant factors into two components, one related only to the geometric and pose parameters of the Line-Plane component, and the other only to the geometric parameters of the 6th leg, plus the pose parameters of the platform. Next, it is shown how the Jacobian matrix of a Line-Plane component can be independently derived by performing its statics analysis.

5.3.1 Static Analysis

Consider the pentapod appearing in Fig. 5.4, whose base and platform attachments lay on plane Π and line Λ , respectively. Let Π coincide with the xy -plane of the base reference frame. Using the same notation as before, attachment locations are given by $\mathbf{a}_i = (x_i, y_i, 0)^T$ and $\mathbf{b}_i = \mathbf{p} + z_i \mathbf{i}$, $i = 1, \dots, 5$ and the leg lengths l_1, \dots, l_5 respectively.

In static equilibrium, any external force $\mathbf{F} = (f_1, f_2, f_3)^T$ applied at the platform point $\mathbf{q} = \mathbf{p} + z_F \mathbf{i}$ must be compensated by the forces applied along the legs. Let τ_i denote the magnitude of these forces. Then, in static equilibrium situations,

$$\mathbf{F} + \sum_{i=1}^5 \tau_i \mathbf{e}_i = \mathbf{0}. \quad (5.6)$$

5.3 Finding the rearrangements by rewriting the Jacobian determinant

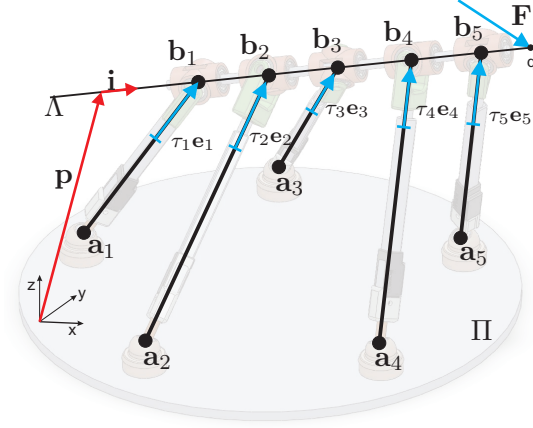


Figure 5.4: Schematic representation of a pentapod.

Likewise, the balance of torques with respect to the origin of the platform reference frame should also be null, that is,

$$\mathbf{F} \times (\mathbf{q} - \mathbf{p}) + \sum_{i=1}^5 \tau_i \mathbf{e}_i \times (\mathbf{b}_i - \mathbf{p}) = 0.$$

In other words,

$$z_F \mathbf{F} \times \mathbf{i} + \sum_{i=1}^5 \tau_i z_i \mathbf{e}_i \times \mathbf{i} = 0. \quad (5.7)$$

Since the platform can freely rotate around Λ , only the torques around two axes perpendicular to \mathbf{i} are important. They can be taken, without loss of generality, as

$$\mathbf{v}_1 = \left(0, \frac{i_z}{\sqrt{i_z^2 + i_y^2}}, -\frac{i_y}{\sqrt{i_z^2 + i_y^2}} \right)^T,$$

$$\mathbf{v}_2 = \mathbf{i} \times \mathbf{v}_1.$$

Then, projecting (5.7) onto these two axes, one gets two scalar equations which, together with (5.6), leads to a system of five scalar equations equations in τ_1, \dots, τ_5 . In matrix form, it can be expressed as

$$\mathbf{J} \begin{pmatrix} \tau_1 \\ \vdots \\ \tau_5 \end{pmatrix} = \begin{pmatrix} f_1 \\ f_2 \\ f_3 \\ \frac{z_F((i_z^2 + i_y^2)f_1 - i_x(i_z f_3 - i_y f_2))}{\sqrt{i_z^2 + i_y^2}} \\ \frac{z_F(i_z f_2 - i_y f_3)}{\sqrt{i_z^2 + i_y^2}} \end{pmatrix} \quad (5.8)$$

5.3 Finding the rearrangements by rewriting the Jacobian determinant

where \mathbf{J} is a 5×5 matrix with columns

$$\begin{pmatrix} p_x + z_i i_x - x_i \\ p_y + z_i i_y - y_i \\ p_z + z_i i_z \\ \frac{z_i}{i_y} \frac{(i_x - i_z)(p_y + z_i i_y - y_i) - (i_y + (i_x + i_z)i_z)(p_x + z_i i_x - x_i) + (i_y - i_x(i_x + i_z))(p_z + z_i i_z)}{\sqrt{2 + \frac{(i_x + i_z)^2}{i_y^2}}} \\ \frac{z_i}{i_y} \frac{(i_x^2 + i_y^2 + i_z^2)((i_x + i_z)(y_i - p_y) + i_y(p_z + p_x - x_i))}{\sqrt{2 + \frac{(i_x + i_z)^2}{i_y^2}}} \end{pmatrix}.$$

When an external force applied on the platform cannot be balanced by the forces exerted by the legs, the pentapod is in a singularity. Mathematically, this corresponds to those configurations in which $\det(\mathbf{J}) = 0$. It can be checked, using a symbolic computational tool, that

$$\det(\mathbf{J}) = \frac{(i_x^2 + i_y^2 + i_z^2)\det(\mathbf{T})}{l_1 l_2 l_3 l_4 l_5} = \frac{\det(\mathbf{T})}{l_1 l_2 l_3 l_4 l_5} \quad (5.9)$$

where

$$\mathbf{T} = \begin{pmatrix} i_z p_z & i_z(p_z i_x - p_x i_z) & i_z(p_z i_y - p_y i_z) & p_z(p_x i_z - p_z i_x) & p_z(p_y i_z - p_z i_y) & -i_z^2 \\ z_1 & x_1 & y_1 & x_1 z_1 & y_1 z_1 & 1 \\ z_2 & x_2 & y_2 & x_2 z_2 & y_2 z_2 & 1 \\ z_3 & x_3 & y_3 & x_3 z_3 & y_3 z_3 & 1 \\ z_4 & x_4 & y_4 & x_4 z_4 & y_4 z_4 & 1 \\ z_5 & x_5 & y_5 & x_5 z_5 & y_5 z_5 & 1 \end{pmatrix}. \quad (5.10)$$

In what follows, let $\hat{\mathbf{T}}$ denote the 5×6 matrix resulting from removing the first row of \mathbf{T} . It is important to realize that this matrix depends only on the coordinates of the leg attachments, whereas the first row of \mathbf{T} depends on the pose of the manipulator. This leads to a clear-cut distinction of two types of singularities, architectural and parallel, the former depending exclusively on $\hat{\mathbf{T}}$, whereas the latter depending also on the pose.

5.3.2 Singularity-invariant leg rearrangement condition

For non-architecturally-singular manipulators, *i.e.*, those for which $\hat{\mathbf{T}}$ is not rank defective, the condition $\det(\mathbf{T}) = 0$ characterizes the set of robot poses lacking stiffness.

5.4 Singularity-invariant leg rearrangement rules

Expanding $\det(\mathbf{T})$ by its first row, the following polynomial equation is obtained:

$$C_1 i_z p_z + C_2 i_z (p_z i_x - p_x i_z) + C_3 i_z (p_z i_y - p_y i_z) + C_4 p_z (p_x i_z - p_z i_x) + C_5 p_z (p_y i_z - p_z i_y) - C_6 i_z^2 = 0, \quad (5.11)$$

where C_i for $i = 1, \dots, 5$ are the cofactors of the elements of the first row of \mathbf{T} . This defines the singularity hypersurface in the configuration space of the pentapod.

The attachments of the i -th leg can be characterized by a single point in \mathbb{R}^3 with coordinates (x_i, y_i, z_i) . This *3D space of leg attachments* will play an important role in the analysis of Line-Plane rearrangements.

Consider the following surface in this space of leg attachments:

$$\{(x, y, z) \in \mathbb{R}^3 \mid \begin{vmatrix} z & x & y & xz & yz & 1 \\ z_1 & x_1 & y_1 & x_1 z_1 & y_1 z_1 & 1 \\ z_2 & x_2 & y_2 & x_2 z_2 & y_2 z_2 & 1 \\ z_3 & x_3 & y_3 & x_3 z_3 & y_3 z_3 & 1 \\ z_4 & x_4 & y_4 & x_4 z_4 & y_4 z_4 & 1 \\ z_5 & x_5 & y_5 & x_5 z_5 & y_5 z_5 & 1 \end{vmatrix} = 0\}. \quad (5.12)$$

The last five rows of this determinant coincide with that of matrix $\hat{\mathbf{T}}$, thus the coefficients of this polynomial coincide with those in (5.11). Furthermore, if any of the legs is substituted by a new leg with attachments (x, y, z) satisfying (5.12), then the coefficients of the polynomial in (5.11) will be the same up to a constant multiple. In other words, its roots will not change.

In conclusion, equation (5.12) defines singularity-invariant leg rearrangements. Note that this result coincides with the condition found in Section 5.2, with the condition $r = 0$ where r is defined in (5.4).

5.4 Singularity-invariant leg rearrangement rules

Using two different methodologies, the same result has been obtained. In the Line-Plane component, a leg rearrangement that substitutes one of the legs by a new one going from $\mathbf{a} = (x, y, 0)$ to $\mathbf{b} = \mathbf{p} + z\mathbf{i}$ is singularity invariant, if, and only if, x , y , and

5.4 Singularity-invariant leg rearrangement rules

z satisfy,

$$\begin{vmatrix} z & x & y & xz & yz & 1 \\ z_1 & x_1 & y_1 & x_1z_1 & y_1z_1 & 1 \\ z_2 & x_2 & y_2 & x_2z_2 & y_2z_2 & 1 \\ z_3 & x_3 & y_3 & x_3z_3 & y_3z_3 & 1 \\ z_4 & x_4 & y_4 & x_4z_4 & y_4z_4 & 1 \\ z_5 & x_5 & y_5 & x_5z_5 & y_5z_5 & 1 \end{vmatrix} = 0. \quad (5.13)$$

In this section, this condition is analyzed in order to understand, from a purely geometric point of view, how the legs of a pentapod can be rearranged without modifying its singularity locus. The above condition will reveal a hidden geometric structure that will help us in the next section, to give a geometric interpretation of parallel singularities, architectural singularities, and even to classify Line-Plane pentapods into 3 families.

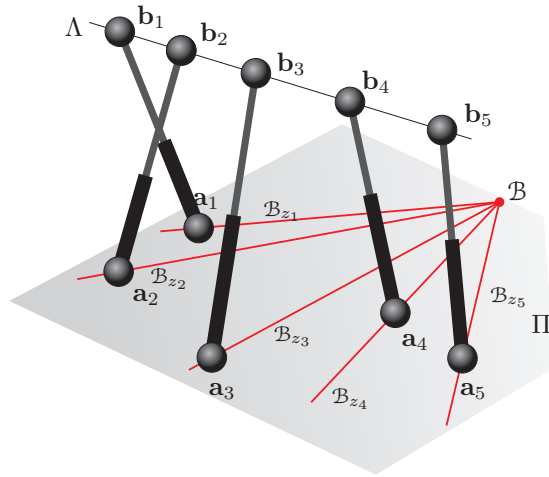


Figure 5.5: One-to-one correspondence between the attachments in the platform line and the lines of the pencil centered at \mathcal{B} . Each value of z_i defines a point $\mathbf{b}_i = \mathbf{p} + z_i\mathbf{i}$ in the platform line, and a line, \mathcal{B}_{z_i} , in the base plane.

Expanding the determinant in (5.13) by its first row yields:

$$C_1z + C_2x + C_3y + C_4xz + C_5yz + C_6 = 0, \quad (5.14)$$

which can be seen as the implicit form equation of a surface in the space of leg attachments (see an example of such surface in Fig. 5.6). Equation (5.14) in turn can be

5.4 Singularity-invariant leg rearrangement rules

rewritten in vector form as:

$$[(C_2 \ C_3 \ C_6) + z(C_4 \ C_5 \ C_1)] \begin{pmatrix} x \\ y \\ 1 \end{pmatrix} = 0. \quad (5.15)$$

Interpreting this surface in the 3D space of leg attachments —where (x, y) and z are the coordinates of the attachments in the base plane Π and the platform line Λ , respectively— equation (5.13) defines a one-to-one correspondence between points in Λ and lines of a pencil embedded in Π (refer to Fig. 5.5). Indeed, a point in Λ with coordinate z determines the line

$$(C_2 + C_4z)x + (C_3 + C_5z)y + C_6 + C_1z = 0$$

in Π and, by varying z , a pencil of lines with focus located at:

$$\mathcal{B} = \left(\frac{C_3C_1 - C_6C_5}{C_2C_5 - C_4C_3}, -\frac{C_2C_1 - C_4C_6}{C_2C_5 - C_4C_3}, 0 \right) \quad (5.16)$$

is obtained. On the way round, each line of the pencil, *i.e.*, a line through \mathcal{B} and $(x, y, 0)$, determines a point in Λ with coordinate

$$z = -\frac{C_2x + C_3y + C_6}{C_4x + C_5y + C_1}. \quad (5.17)$$

It can be checked how the same z value is obtained for all the points $(x, y, 0)$ on the same line through \mathcal{B} .

In what follows, a line of the pencil will be called \mathcal{B} -line and denoted by \mathcal{B}_z , where z is the coordinate of its corresponding point on Λ . The one-to-one correspondence between points in Λ and \mathcal{B} -lines in Π , defined by equation (5.13), will be called \mathcal{B} -*correspondence*. Moreover, the surface defined by (5.14) will be called \mathcal{B} -*surface* when interpreted in the 3D space of leg attachments.

Of particular interest is the \mathcal{B} -line \mathcal{B}_∞ ,

$$\mathcal{B}_\infty = \{(x, y) \mid C_4x + C_5y + C_1 = 0\}. \quad (5.18)$$

because in practice no attachment in Π can be located on it (with the exception of \mathcal{B}), as the corresponding attachment on Λ should have to be moved to infinity. With the introduced notation, any line of the pencil can be seen as a linear combination of the line corresponding to $z = 0$ and the line corresponding to $z = \infty$.

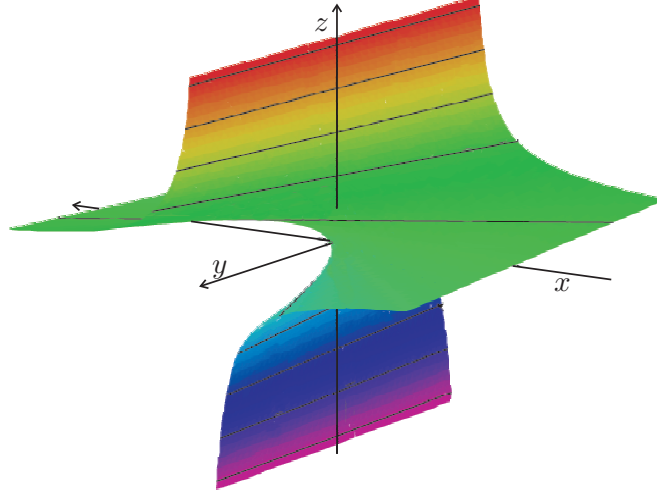


Figure 5.6: Representation of surface (5.14) with the origin placed at point (5.16), and the y -axis placed at line (5.18).

Fig. 5.6 shows that the \mathcal{B} -surface defined by (5.14) has the shape of a spiral-like ruled surface around a vertical axis passing through point \mathcal{B} (5.16) in the xy -plane, and approaching a line parallel to (5.18) as z tends to ∞ . This can be recognized as a hyperbolic paraboloid with two directing lines at infinity, which are obtained by intersecting the planes $z = 0$ and $C_4x + C_5y + C_1 = 0$ with the plane at infinity.

Finally, two simple rules to move the attachments without altering the singularity locus naturally arise (Fig. 5.7):

- all attachments in the plane can be freely moved along their \mathcal{B} -lines, and
- an attachment in the line can be freely moved if, and only if, the other attachment of the corresponding leg is located at \mathcal{B} .

Following these two rules, it is possible to move any base attachment, say \mathbf{a}_i , to any arbitrary location on Π , say \mathbf{a}'_i , in three steps:

- move \mathbf{a}_i along the corresponding \mathcal{B} -line until it meets \mathcal{B} ,
- move \mathbf{b}_i till its coordinate in the line determines a \mathcal{B} -line that contains \mathbf{a}'_i , and
- move \mathbf{a}_i along the \mathcal{B} -line that contains \mathbf{a}'_i .

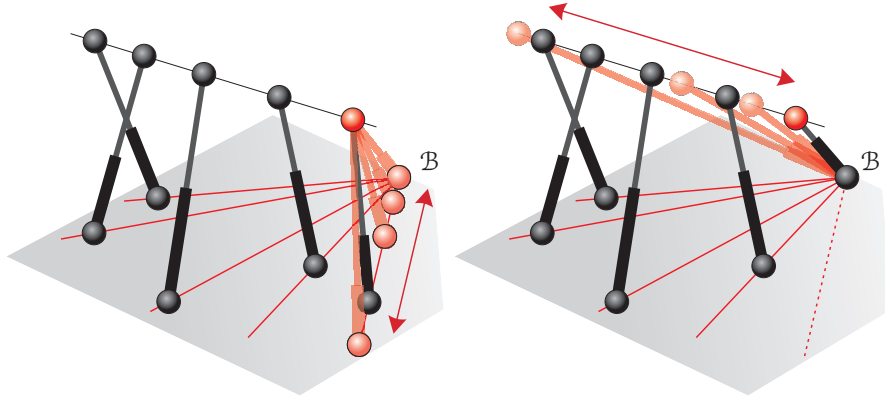


Figure 5.7: Singularity-invariant leg rearrangement rules for the Line-Plane component.

In practice, any base attachment can be freely relocated on the plane, as long as its corresponding platform attachment is relocated in the corresponding platform coordinate. Thus, it is possible to carry out many complex transformations, but special attention must be paid to avoid that, at each step,

- no three attachments in the plane are located in the same \mathcal{B} -line because three leg lengths would become dependent [Fig. 2.4-(a)], and
- no four attachments in the plane are collinear as, in this case, the line-plane subassembly would contain an architecturally singular Line-Line component. This rather surprising result will become evident at the end of Section 5.8 where the proposed transformations are interpreted in terms of cross-ratios.
- the manipulator does not fall into an architectural singularity, which will be studied in detail in Section 5.7.

Finally, two more remarks may ease the practical application of the above leg rearrangement rules:

- There can be at most two coincident attachments on the base plane, which must lie on point \mathcal{B} . Otherwise, the manipulator either would contain a Line-Line rigid component or it would be architecturally singular.

5.5 Geometric interpretation of parallel singularities in Line-Plane components

- Along a design process, the location of point \mathcal{B} may be conveniently specified by placing two coincident attachments, which can be separated later by using appropriate leg rearrangements.

5.5 Geometric interpretation of parallel singularities in Line-Plane components

The singularity polynomial in equation (5.11) can be rewritten in vector form as:

$$[i_z(C_2 \ C_3 \ C_6) - p_z(C_4 \ C_5 \ C_1)] \begin{pmatrix} p_x i_z - p_z i_x \\ p_y i_z - p_z i_y \\ i_z \end{pmatrix} = 0. \quad (5.19)$$

The parallel singularities of the analyzed pentapod correspond to those configurations, defined by $\mathbf{p} = (p_x, p_y, p_z)$ and $\mathbf{i} = (i_x, i_y, i_z)$, that satisfy the above equation. Then, two situations arise:

- If $i_z \neq 0$, (5.19) yields

$$[(C_2 \ C_3 \ C_6) + \mu(C_4 \ C_5 \ C_1)] \begin{pmatrix} p_x + \mu i_x \\ p_y + \mu i_y \\ 1 \end{pmatrix} = 0, \quad (5.20)$$

where $\mu = -p_z/i_z$. The first term of the equation defines a pencil of lines, the same pencil obtained in the previous section. Now, observe that Λ intersects Π at:

$$\mathcal{A} = (p_x + \mu i_x, p_y + \mu i_y, 0). \quad (5.21)$$

Then, according to (5.20), the singularity occurs when point \mathcal{A} lies on the line defined by $\mathcal{B}_0 + \mu\mathcal{B}_\infty$, that is, the line of the pencil corresponding to $z = -p_z/i_z$. Note that, if \mathcal{A} coincides with \mathcal{B} , the focus of the pencil, the manipulator would be singular for any value of p_z and i_z , because \mathcal{A} would simultaneously lay on all lines of the pencil.

5.5 Geometric interpretation of parallel singularities in Line-Plane components

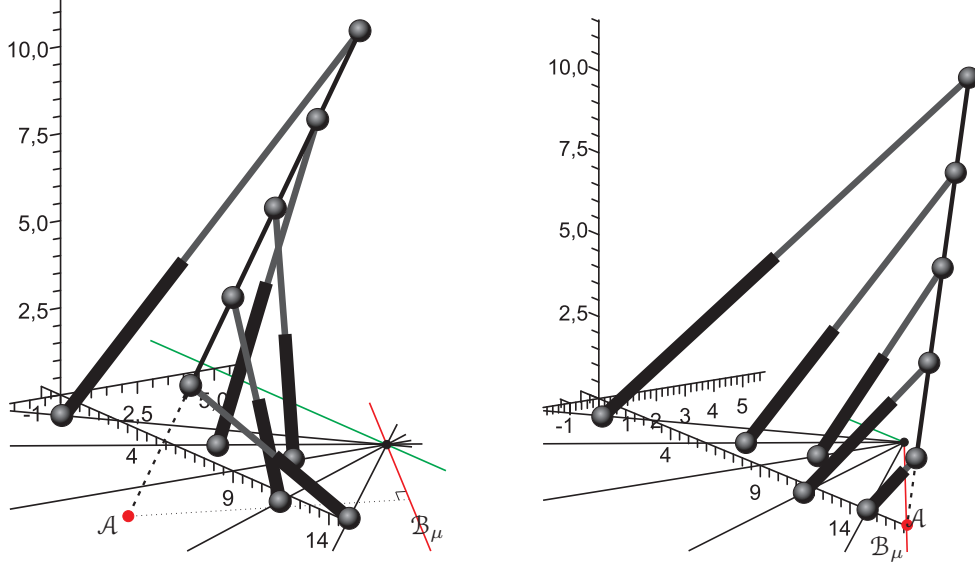


Figure 5.8: Left: For $\mathbf{p} = (5, 8, 13)$ and $\mathbf{i} = (1/3, -2/3, -2/3)$ the manipulator is not in a singular pose. Right: A singular pose is reached when $\mathbf{p} = (7\sqrt{6} - 7, 4, 14)$ and $\mathbf{i} = (\frac{\sqrt{6}}{6}, \frac{-\sqrt{6}}{6}, \frac{-\sqrt{6}}{3})$.

- If $i_z = 0$, (5.19) yields

$$(C_4 \ C_5) \begin{pmatrix} p_z i_x \\ p_z i_y \end{pmatrix} = 0. \quad (5.22)$$

In this case, the manipulator is singular when Λ is parallel to \mathcal{B}_∞ , that is, when $\mathbf{i} = \pm \frac{1}{\sqrt{C_4^2 + C_5^2}}(C_5, -C_4, 0)$. If, in addition, $p_z = 0$, Λ necessarily lies on Π , which is a trivial singularity.

In sum, the Line-Plane pentapod is in a singular configuration iff the platform point $\mathbf{p} + z\mathbf{i}$ intersecting the base does so precisely at its corresponding \mathcal{B} -line \mathcal{B}_z (Fig. 5.8). Note that this includes the cases in which $i_z = 0$.

The above geometric interpretation has two very interesting implications. First, a configuration is singular iff a leg can attain zero length through a singularity-invariant leg rearrangement. After such rearrangement, the two attachments of the leg will both coincide with the point where the platform intersects the base (and so, it will have zero length). Second, this zero-length leg condition holding at singularities permits equating the coordinates of attachments in the base $\mathbf{a} = (x, y, 0)^T$ and platform $\mathbf{b} = \mathbf{p} + z\mathbf{i}$ at

5.6 Classifying pentapods by their singularities

point \mathcal{A} ,

$$\begin{aligned} x &= p_x - \frac{p_z}{i_z} i_x \\ y &= p_y - \frac{p_z}{i_z} i_y \\ p_z + z i_z &= 0, \end{aligned}$$

leading to the following change of variables:

$$\begin{aligned} x i_z &= p_x i_z - p_z i_x \\ y i_z &= p_y i_z - p_z i_y \\ z i_z &= -p_z \end{aligned} \tag{5.23}$$

which, if applied to equation (5.11), yields:

$$(-i_z^2)(C_1 z + C_2 x + C_3 y + C_4 z x + C_5 z y + C_6) = 0. \tag{5.24}$$

When $i_z \neq 0$, this reduces to equation (5.14). Therefore, except for configurations in which the platform lies parallel to the base, the \mathcal{B} -surface (5.14) in the 3D space of leg attachments provides a characterization of singularities equivalent to the hypersurface equation (5.11) in the 5D robot configuration space.

5.6 Classifying pentapods by their singularities

5.6.1 Pentapod families with identical singularities

The obtained Line-Plane rearrangements permit classifying pentapods into families that share the same singularity locus. To achieve this, first it is necessary to identify the geometric entities that fully describe the singularity locus.

First of all, note that it is possible to locate a copy of Λ onto Π , parallel to the line \mathcal{B}_∞ ,

$$\Lambda^+ = \left\{ (x, y) \mid C_4 x + C_5 y + C_1 + \frac{C_2 C_5 - C_3 C_4}{\sqrt{C_4^2 + C_5^2}} = 0 \right\}, \tag{5.25}$$

so that each attachment in Λ^+ lies on its associated \mathcal{B} -line in Π (Fig. 5.9). Then the geometric analysis of the manipulator can be reduced to a planar problem. Indeed, denote the coordinates of the intersections of Λ^+ with \mathcal{B}_{z_i} by \mathbf{b}_i^+ . Notice that \mathbf{b}_i^+ , $i = 1, \dots, 5$, are spaced at the same distances in Λ^+ as \mathbf{b}_i , $i = 1, \dots, 5$, in Λ . Then, Λ^+ is a privileged line in Π that represents a possible location for Λ so that the attachments in it coincide with their corresponding \mathcal{B} -lines. Then, given a particular manipulator, point \mathcal{B} , line \mathcal{B}_∞ and line Λ^+ can be computed using (5.16), (5.18) and (5.25),

5.6 Classifying pentapods by their singularities

respectively. These determine the five \mathcal{B} -lines passing through the base attachments, and their intersections with Λ^+ , \mathbf{b}_i^+ , $i = 1, \dots, 5$, determine also the location of the attachments \mathbf{b}_i , $i = 1, \dots, 5$ in Λ (see Fig. 5.9).

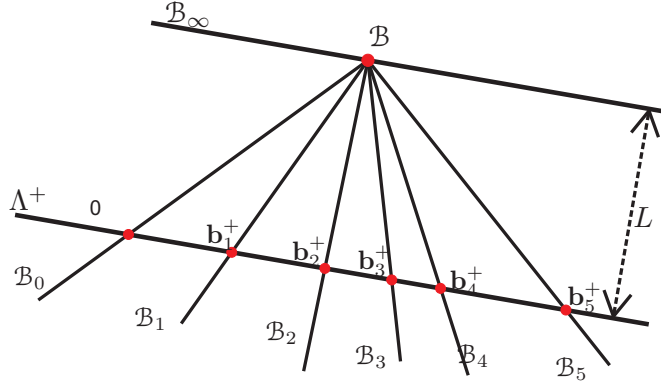


Figure 5.9: Planar geometric construction that defines all the geometric parameters in a pentapod.

As a consequence, point \mathcal{B} , line \mathcal{B}_∞ and line Λ^+ characterize a family of pentapods having exactly the same singularity locus. Furthermore, assuming that point \mathcal{B} is finite, a planar affine transformation that moves \mathcal{B} to the origin and line \mathcal{B}_∞ to the y -axis can always be applied. Then, the \mathcal{B} -surfaces associated with two non-architecturally singular 5-SPU manipulators differ at most on a *scaling factor*, namely the distance of \mathcal{B} to Λ^+ (named L in Fig. 5.9). This factor regulates the attachments spacing in the platform line in relation to the attachments spacing in the base plane.

Therefore, all non-architecturally singular pentapods with finite \mathcal{B} have associated \mathcal{B} -surfaces with the same topology. Moreover, through the change of variables in (5.23), the singularity loci of all these manipulators have also the same topology.

5.6.2 Three possible topologies for the singularity locus

So far, point \mathcal{B} was assumed to be finite. Now, suppose that it is taken to infinity. According to equation (5.16), this implies that $C_2C_5 - C_4C_3 = 0$. By introducing this constraint into equation (5.14), one obtains:

$$(C_4z + C_2)x + (C_3/C_2)(C_4z + C_2)y + C_1z + C_6 = 0. \quad (5.26)$$

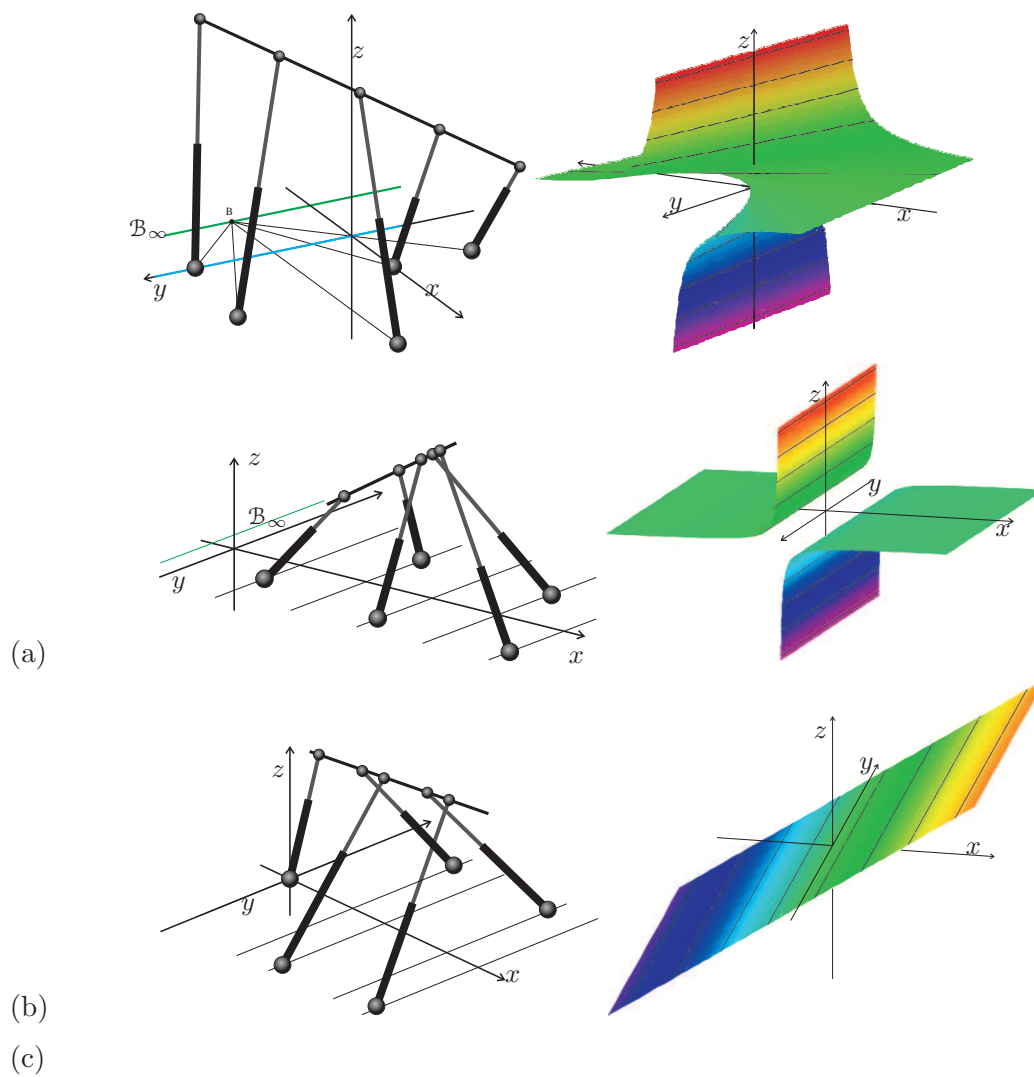


Figure 5.10: Quaternally, cubically and quadratically-solvable pentapods (left), with their corresponding \mathcal{B} -surfaces (right).

5.6 Classifying pentapods by their singularities

It turns out that all \mathcal{B} -lines have now the same slope, $C_3/C_2 = C_5/C_4$, and, therefore, they are all parallel to \mathcal{B}_∞ . Fig. 5.10-(b) shows the corresponding \mathcal{B} -surface with the y -axis placed parallel to line \mathcal{B}_∞ . Now, note that the \mathcal{B} -surface approaches asymptotically line \mathcal{B}_∞ as z tends to $+\!/\!-\infty$. Moreover, the \mathcal{B} -line associated with the value of z for which $C_4z + C_2 = 0$ is the line at infinity. This appears as the surface asymptotically approaching the horizontal plane $C_4z + C_2 = 0$ in the central 3D plot in Fig. 5.10.

It is worth remarking that, in the one-to-one correspondence between points in Λ and lines in Π , a finite point in Λ has its associated \mathcal{B} -line at infinity, while the point at infinity in Λ is associated with the finite \mathcal{B}_∞ line.

In this context, it seems reasonable to make these two lines to be coincident, i.e., \mathcal{B}_∞ is taken to infinity. Then, since point $\mathcal{B} \in \mathcal{B}_\infty$, \mathcal{B} also stays at infinity as before. This further condition implies that $C_4 = C_5 = 0$, and equation (5.26) reduces to:

$$C_2x + C_3y + C_1z + C_6 = 0. \quad (5.27)$$

Of course, all \mathcal{B} -lines continue to be parallel, but observe that their spacing has now become a linear function of z , namely, $C_1z + C_6$. Thus, the \mathcal{B} -surface is a plane in this case. Fig. 5.10-(c) shows this planar \mathcal{B} -surface with \mathcal{B} -lines parallel to the y -axis. Note that the \mathcal{B} -surface approaches line \mathcal{B}_∞ linearly as z tends to $+\!/\!-\infty$.

In sum, there are only three possible topologies for the \mathcal{B} -surfaces associated with non-architecturally singular pentapods: one when point \mathcal{B} is finite [Fig. 5.10-(a)], another when \mathcal{B} is taken to infinity but \mathcal{B}_∞ remains finite [Fig. 5.10-(b)], and the third when both point \mathcal{B} and line \mathcal{B}_∞ are taken to infinity [Fig. 5.10-(c)]. Again, through the change of variables in (5.23), it can be concluded that the manipulators in each of these three families have singularity loci with the same topology.

5.6.3 Forward kinematics: Quartically, cubically and quadratically-solvable cases

Thanks to the obtained expression of the singularity polynomial as the determinant of matrix \mathbf{T} , is it possible to relate the forward kinematic solution with the singularity polynomial, and thus, with the singularity classification done in the previous section, obtaining interesting results for each of the three derived families.

5.6 Classifying pentapods by their singularities

The forward kinematics of a pentapod can be solved by writing the leg lengths as $l_i^2 = \|\mathbf{b}_i - \mathbf{a}_i\|^2$, for $i = 1, \dots, 5$, as done to define the affine relation in Section 5.2. Then, subtracting from the expression for l_i^2 , $i = 1, \dots, 5$, the equation $\|\mathbf{i}\|^2 = i_x^2 + i_y^2 + i_z^2 = 1$, quadratic terms in i_x , i_y and i_z cancel out yielding

$$z_i t - x_i p_x - y_i p_y - x_i z_i i_x - y_i z_i i_y + \frac{1}{2}(p_x^2 + p_y^2 + p_z^2 + x_i^2 + y_i^2 + z_i^2 - l_i^2) = 0, \quad (5.28)$$

for $i = 1, \dots, 5$, where $t = \mathbf{p} \cdot \mathbf{i}$ (note that this is the same equation as (5.1)).

Subtracting the first equation from the others, quadratic terms in p_x , p_y and p_z cancel out as well. Then, the resulting system of equations can be written in matrix form as

$$\begin{pmatrix} x_2 - x_1 & y_2 - y_1 & x_2 z_2 - x_1 z_1 & y_2 z_2 - y_1 z_1 \\ x_3 - x_1 & y_3 - y_1 & x_3 z_3 - x_1 z_1 & y_3 z_3 - y_1 z_1 \\ x_4 - x_1 & y_4 - y_1 & x_4 z_4 - x_1 z_1 & y_4 z_4 - y_1 z_1 \\ x_5 - x_1 & y_5 - y_1 & x_5 z_5 - x_1 z_1 & y_5 z_5 - y_1 z_1 \end{pmatrix} \begin{pmatrix} p_x \\ p_y \\ i_x \\ i_y \end{pmatrix} = \begin{pmatrix} (z_2 - z_1)t + N_2 \\ (z_3 - z_1)t + N_3 \\ (z_4 - z_1)t + N_4 \\ (z_5 - z_1)t + N_5 \end{pmatrix}, \quad (5.29)$$

where

$$N_i = \frac{1}{2}(x_i^2 + y_i^2 + z_i^2 - l_i^2 - x_1^2 - y_1^2 - z_1^2 + l_1^2).$$

Now, notice that the determinant associated with the linear system (5.29) can be written as

$$\begin{vmatrix} x_1 & y_1 & x_1 z_1 & y_1 z_1 & 1 \\ x_2 & y_2 & x_2 z_2 & y_2 z_2 & 1 \\ x_3 & y_3 & x_3 z_3 & y_3 z_3 & 1 \\ x_4 & y_4 & x_4 z_4 & y_4 z_4 & 1 \\ x_5 & y_5 & x_5 z_5 & y_5 z_5 & 1 \end{vmatrix}, \quad (5.30)$$

which coincides with C_1 in (5.11), that is, the first cofactor of matrix \mathbf{T} . If (5.30) vanishes, either p_x , p_y , i_x , or i_y , can be chosen as parameter, instead of t , to reformulate the linear system (5.29). Since for a non-architecturally singular robot not all cofactors are zero, it can be shown that a non-singular linear system of the form given in (5.29) can always be found by choosing either t , p_x , p_y , i_x , or i_y as parameter.

Solving (5.29) by Cramer's rule, and applying the multilinearity property of determinants, yields

$$\begin{aligned} p_x &= (-C_2 t + E_2)/C_1, \\ p_y &= (-C_3 t + E_3)/C_1, \\ i_x &= (-C_4 t + E_4)/C_1, \\ i_y &= (-C_5 t + E_5)/C_1, \end{aligned} \quad (5.31)$$

5.6 Classifying pentapods by their singularities

where E_i results from substituting the $(i - 1)$ th column vector of C_1 by $(N_1, \dots, N_5)^T$. This solution allows the expression of the forward kinematics in terms of the cofactors of matrix \mathbf{T} , which it turns out that defines both the forward kinematics and the singularities of the manipulator.

From equation $i_x^2 + i_y^2 + i_z^2 = 1$ and equation (5.28) for $i = 1$, it can be concluded that:

$$p_z^2 i_z^2 = (1 - i_x^2 - i_y^2) [2(-z_1 t + x_1 p_x + y_1 p_y + z_1 y_1 i_y + z_1 x_1 i_x) - p_x^2 - p_y^2 - x_1^2 - y_1^2 - z_1^2]. \quad (5.32)$$

One the other hand, from $t = \mathbf{p} \cdot \mathbf{i}$,

$$(p_z i_z)^2 = (t - p_x i_x - p_y i_y)^2. \quad (5.33)$$

Equating the right hand sides of equations (5.32) and (5.33), the following polynomial in t is finally obtained:

$$n_4 t^4 + n_3 t^3 + n_2 t^2 + n_1 t + n_0 = 0, \quad (5.34)$$

where

$$\begin{aligned} n_4 &= -\frac{(C_4 C_3 - C_2 C_5)^2}{C_1^4}, \\ n_3 &= -\frac{2}{C_1^4} (C_1^2 (C_5 C_3 + C_4 C_2) \\ &\quad + C_1 (C_5^2 + C_4^2) (C_2 x_1 + (C_1 + C_4 x_1 + C_5 y_1) z_1 + y_1 C_3) \\ &\quad + (C_4 C_3 - C_5 C_2) (E_5 C_2 + E_2 C_5 - E_4 C_3 - E_3 C_4)). \end{aligned} \quad (5.35)$$

and n_2 , n_1 and n_0 depend also on constant parameters.

Each of the four roots of (5.34) determines a single value for p_x , p_y , i_x , and i_y through (5.31) and two sets of values for p_z and i_z by simultaneously solving $\|\mathbf{i}\| = 1$ and $t = \mathbf{p} \cdot \mathbf{i}$. Thus, up to 8 assembly modes are obtained for a given set of leg lengths.

The polynomial in equation (5.34) is the maximum degree polynomial that has to be solved to obtain the forward kinematics solutions of a pentapod with planar base and a linear platform.

5.6.3.1 Quartic, Cubic and Quadratic cases

It has been shown that solving the forward kinematics of a pentapod with planar base and linear platform leads to a *quartic* polynomial.

Now note that, when point \mathcal{B} lies at infinity, $C_2C_5 - C_4C_3 = 0$, then the leading coefficient n_4 in equation (5.34) vanishes, and the forward kinematic solution becomes *cubic*. Then the platform line Λ has, at most, 6 assembly modes. Finally, if not only \mathcal{B} is at infinity, but also line \mathcal{B}_∞ (that is, $C_4 = C_5 = 0$), it is easy to see that also the coefficient n_3 in (5.34) becomes zero, leading to a *quadratic* polynomial. When this happens, the maximum simplification of the kinematics is obtained: a platform with only up to 4 assembly modes.

Thus, note that the three topologies of the singularity locus derived in the preceding section correspond to the quartically, cubically and quadratically-solvable families of pentapods, respectively (Fig. 5.10).

5.6.4 A quadratically-solvable pentapod

A 5-DoF manipulator whose forward kinematics has a quadratic solution is of interest by itself and also as a component to be included in a general 6-DoF Stewart-Gough platform, as first acknowledged in [14].

Consider a quadratically-solvable manipulator whose line \mathcal{B}_∞ coincides with the p_y -axis, and thus its \mathcal{B} -lines are parallel to this axis. This implies that its leg attachment coordinates can be expressed as $\mathbf{a}_i = (x_i, y_i, 0)$ and $\mathbf{b}_i = \mathbf{p} + z_i\mathbf{i}$, with $\mathbf{p} = (p_x, p_y, p_z)$ and $\mathbf{i} = (u, v, w)$ as before, subject to the constraint

$$z_i = \delta x_i, \tag{5.36}$$

To ease readability of the equations, set $x_1 = y_1 = 0$ without losing generality. Then δ , x_i and y_i , $i = 2, 3, 4, 5$, are left as parameters that characterize the family of pentapods analyzed in this section.

5.6 Classifying pentapods by their singularities

5.6.4.1 Forward Kinematics

Following the computations of Section 5.6.3, with the attachment coordinates given in (5.36), the cofactors of the elements of the first row of \mathbf{T} are:

$$\begin{aligned} C_1 &= \delta^2 F, \\ C_2 &= -\delta^3 F, \\ C_3 &= C_4 = C_5 = C_6 = 0, \end{aligned} \quad (5.37)$$

where F can be written as

$$F = \begin{vmatrix} x_2^2 & x_2 y_2 & x_2 & y_2 \\ x_3^2 & x_3 y_3 & x_3 & y_3 \\ x_4^2 & x_4 y_4 & x_4 & y_4 \\ x_5^2 & x_5 y_5 & x_5 & y_5 \end{vmatrix} \quad (5.38)$$

and the coefficients of polynomial (5.34) are:

$$\begin{aligned} n_4 &= n_3 = 0 \\ n_2 &= \frac{(\delta^2 + 1)\delta^2 F^2 - 2\delta F E_4 - E_5^2}{\delta^2 F^2} \\ n_1 &= 2 \frac{E_2 \delta^4 F^2 - F \delta (E_4 E_2 + E_5 E_3) - E_5 (E_2 E_5 - E_3 E_4)}{\delta^5 F^3} \\ n_0 &= \frac{(E_2^2 + E_3^2 + l_1^2 (E_4^2 + E_5^2)) F^2 \delta^4 - (E_2 E_5 - E_4 E_3)^2}{\delta^8 F^4} - l_1^2 \end{aligned}$$

where E_i were defined in Section 5.6.3. Then, polynomial (5.34) becomes quadratic and, as a consequence, its two roots can be simply expressed as:

$$t = \frac{\delta^4 F^2 E_2 - \delta F (E_2 E_4 + E_5 E_3) + E_5 (E_3 E_4 - E_2 E_5) \pm \sqrt{\Delta}}{\delta^3 F (2\delta F E_4 + E_5^2 - (\delta^2 + 1)\delta^2 F^2)}, \quad (5.39)$$

where the discriminant is

$$\begin{aligned} \Delta &= \delta F (E_5^2 + E_4^2 - \delta^4 F^2) \\ &[2\delta^4 F^2 E_4 l_1^2 + \delta^3 F (E_5^2 l_1^2 + E_3^2) + \delta F (E_2^2 + E_3^2) - (\delta^2 + 1)\delta^5 F^3 l_1^2 + 2E_3 (E_2 E_5 - E_4 E_3)]. \end{aligned} \quad (5.40)$$

Each of the two above roots, say t_1 and t_2 , determines a single value for p_x , p_y , i_x , and i_y through (5.31) and two sets of values for p_z and i_z by simultaneously solving $\|\mathbf{i}\| = 1$ and $t = \mathbf{p} \cdot \mathbf{i}$. The resulting four assembly modes are explicitly given by:

$$\mathbf{p} = \begin{pmatrix} \frac{\delta^3 F t_i + E_2}{\delta^2 F} \\ \frac{E_3}{\delta^2 F} \\ \pm \frac{(E_4 - \delta F)\delta^3 F t_i + E_4 E_2 + E_5 E_3}{\delta^2 F \sqrt{\delta^4 F^2 - E_5^2 - E_4^2}} \end{pmatrix} \quad \text{and} \quad \mathbf{i} = \begin{pmatrix} \frac{E_4}{\delta^2 F} \\ \frac{E_5}{\delta^2 F} \\ \pm \frac{\sqrt{\delta^4 F^2 - E_5^2 - E_4^2}}{\delta^2 F} \end{pmatrix}. \quad (5.41)$$

5.6.4.2 Singularity Analysis

Substituting the values of the cofactors in (5.37) into (5.11), the singular configurations of the studied pentapod are the solutions of the following equation

$$\delta^2 i_z F [\delta p_x i_z - (i_x \delta - 1) p_z] = 0. \quad (5.42)$$

Observe that, except for δ , all other design parameters are embedded in F , whereas the robot pose appears only in the remaining two factors. Thus, if $F = 0$, the manipulator is architecturally singular, *i.e.*, it is always singular independently of its leg lengths.

Now, consider the case $F \neq 0$. Then, given a singular configuration (\mathbf{p}, \mathbf{i}) , with $\mathbf{p} = (p_x, p_y, p_z)$ and $\mathbf{i} = (i_x, i_y, i_z)$, it must satisfy either $i_z = 0$ or $[\delta i_z p_x - (\delta i_x - 1) p_z] = 0$.

Following the geometric interpretation given in Section 5.5, when $i_z = 0$, the manipulator is always in a singularity, because Λ is always parallel to \mathcal{B}_∞ (any line is parallel to a line at infinity, and for the quadratic case, \mathcal{B}_∞ is at infinity). This condition holds for configurations where the platform is parallel to the base plane.

On the other hand, when $i_z \neq 0$ equation (5.20) reads as

$$[(C_2 \ 0 \ 0) + \mu(0 \ 0 \ C_1)] \begin{pmatrix} p_x + \mu i_x \\ p_y + \mu i_y \\ 1 \end{pmatrix} = 0,$$

where $\mu = \frac{-p_z}{i_z}$. This condition holds when the intersection point of Λ with Π , defined as \mathcal{A} in equation (5.21), belongs to the line $C_2 x + \mu C_1 = 0$. In other words, when point \mathcal{A} is at a distance

$$\frac{p_z}{i_z} \frac{C_1}{C_2} = -\frac{p_z}{i_z \delta}$$

from the y -axis, the pentapod is in a singularity.

Note that singularities can also be expressed in joint space \mathbb{R}^5 by using the discriminant (5.40), whose expression only depends on the leg lengths l_i , $i=1, \dots, 5$. When $\Delta = 0$ the two solutions given by (5.39) coincide, yielding a parallel singularity. Note that Δ also consists of two factors, the first one $E_5^2 + E_4^2 - \delta^4 F^2 = 0$ corresponds to the condition $i_z = 0$ and the other is equivalent to $(\delta i_z p_x - (\delta i_x - 1) p_z) = 0$.

An interesting practical consideration is that, if the orientation of the tool is fixed, singularities define a plane in position space:

$$c_1 p_x + c_2 p_z = 0,$$

with $c_1 = \delta i_z^2$ and $c_2 = i_z(1 - i_x \delta)$. For example, if the tool is orthogonal to the base plane, *i.e.* $(i_x, i_y, i_z) = (0, 0, 1)$, then the robot will reach a singularity when $\mathbf{p} = (p_x, p_y, p_z)$, satisfies:

$$\delta p_x + p_z = 0.$$

It follows from the above singularity analysis that, for a fixed value of δ , the whole family of non-architecturally singular pentapods considered have exactly the same singularity locus. In other words, given a member of the family, one can freely move its leg attachments without modifying the singularity locus, provided that two constraints are maintained, namely: the proportionality between x_i and z_i , and $F \neq 0$ [see (5.38)], thus, precluding architecturally singular designs.

5.7 Architecture singularities

5.7.1 Algebraic characterization

This Section, for the sake of simplicity, deals with generic cases, that is, the attachments are in general position. As a consequence, none of the base attachments will be coincident with \mathcal{B} . As will be explained in Section 5.10, the present methodology is also able to handle with non-generic cases, but they must be studied separately.

When $\hat{\mathbf{T}}$ is rank defective, $\det(\mathbf{T})$ is identically zero irrespective of the pose of Λ with respect to Π and, hence, the pentapod is said to be architecturally singular.

If, to check rank defectiveness, Gaussian Elimination¹ is applied on $\hat{\mathbf{T}}$, the last row of the resulting matrix is

$$\frac{1}{D_{5,6}} (0 \ 0 \ 0 \ 0 \ -C_6 \ C_5), \quad (5.43)$$

¹Gaussian Elimination uses elementary row operations to reduce a given matrix into a rank-equivalent one, with an upper triangular shape. Then, rank deficiency occurs when all the elements of the last row are zero.

where C_i are the cofactors of the first row of \mathbf{T} as in equation (5.11), and $D_{i,j}$ is the determinant of the matrix formed by the first four rows of $\hat{\mathbf{T}}$ with the i th and j th columns removed.

By permuting the columns of $\hat{\mathbf{T}}$, it can be concluded that a necessary and sufficient condition for a pentapod to be architecturally singular is that

$$\exists i, j \in \{1, \dots, 6\}, i \neq j, \text{ such that } C_i = C_j = 0 \text{ and } D_{i,j} \neq 0. \quad (5.44)$$

The conditions $C_4 = C_5 = 0$ are in one-to-one correspondence with the two algebraic conditions given by Husty and Karger [49, Theorem 1.6] (after setting $x_1 = y_1 = z_1 = y_2 = 0$, which can always be done without loss of generality by properly placing the reference frames). When the attachments are in general position, $D_{4,5} \neq 0$, and thus Husty and Karger's conditions are equivalent to (5.44). However, for platforms whose attachments are not in a generic position (such as, for instance, the quadratically solvable manipulators defined in Section 5.6.4), it can occur that $C_4 = C_5 = D_{4,5} = 0$ and the manipulator is not architecturally singular (see Section 5.9.3 for an example).

5.7.2 Geometric interpretation

It is not only important to characterize architectural singularities to avoid them, but also to determine how near the manipulator is to this kind of singularities to design manipulators with improved global behavior. With this purpose, a geometric interpretation of condition (5.44) is next derived.

Suppose that one of the legs, say \mathbf{l}_5 , is reconfigured to have the new attachments $\mathbf{a} = (x, y, 0)$ and $\mathbf{b} = \mathbf{p} + z\mathbf{i}$. Assuming that $D_{12} \neq 0$, the manipulator becomes architecturally singular, according to (5.44), when C_1 and C_2 are zero. This defines the

following system of equations in the space of leg attachments:

$$\left. \begin{aligned} \widetilde{C}_1 &= \begin{vmatrix} x & y & xz & yz & 1 \\ x_1 & y_1 & x_1z_1 & y_1z_1 & 1 \\ x_2 & y_2 & x_2z_2 & y_2z_2 & 1 \\ x_3 & y_3 & x_3z_3 & y_3z_3 & 1 \\ x_4 & y_4 & x_4z_4 & y_4z_4 & 1 \end{vmatrix} = 0 \\ \widetilde{C}_2 &= \begin{vmatrix} z & y & xz & yz & 1 \\ z_1 & y_1 & x_1z_1 & y_1z_1 & 1 \\ z_2 & y_2 & x_2z_2 & y_2z_2 & 1 \\ z_3 & y_3 & x_3z_3 & y_3z_3 & 1 \\ z_4 & y_4 & x_4z_4 & y_4z_4 & 1 \end{vmatrix} = 0 \end{aligned} \right\} \quad (5.45)$$

where \widetilde{C}_i equals cofactor C_i when evaluated at $\{x = x_5, y = y_5, z = z_5\}$. Then, the roots of this system define the locus of the 5th leg attachments that make the manipulator architecturally singular. By expanding the determinants in (5.45) by their first rows, the above system results in:

$$\left. \begin{aligned} D_{1,2} x + D_{1,3} y + D_{1,4} zx + D_{1,5} zy + D_{1,6} &= 0 \\ D_{1,2} z + D_{2,3} y + D_{2,4} zx + D_{2,5} zy + D_{2,6} &= 0 \end{aligned} \right\} \quad (5.46)$$

which can be rewritten as

$$\begin{pmatrix} D_{1,4} x + D_{1,5} y & D_{1,2} x + D_{1,3} y + D_{1,6} \\ D_{2,4} x + D_{2,5} y + D_{1,2} & D_{2,3} y + D_{2,6} \end{pmatrix} \begin{pmatrix} z \\ 1 \end{pmatrix} = \begin{pmatrix} 0 \\ 0 \end{pmatrix},$$

which clearly has a solution for z if, and only if,

$$\begin{vmatrix} D_{1,4} x + D_{1,5} y & D_{1,2} x + D_{1,3} y + D_{1,6} \\ D_{2,4} x + D_{2,5} y + D_{1,2} & D_{2,3} y + D_{2,6} \end{vmatrix} = 0. \quad (5.47)$$

In conclusion, there exists a value for z that satisfies (5.45) only for the points on the conic

$$\mathcal{C}_5 = \{(x, y) \mid n_1x^2 + n_2xy + n_3y^2 + n_4x + n_5y + n_6 = 0\},$$

where

$$\begin{aligned} n_1 &= D_{1,2}D_{2,4} \\ n_2 &= D_{2,3}D_{1,4} - D_{1,2}D_{2,5} - D_{1,3}D_{2,4} \\ n_3 &= D_{1,3}D_{2,5} - D_{2,3}D_{1,5} \\ n_4 &= D_{1,2}^2 + D_{1,6}D_{2,4} - D_{2,6}D_{1,4} \\ n_5 &= D_{2,6}D_{1,5} - D_{1,6}D_{2,5} - D_{1,3}D_{1,2} \\ n_6 &= D_{1,6}D_{1,2}. \end{aligned}$$

The other way round, for a given value of z , system (5.45) gives a point on this conic. In other words, system (5.45) defines a one-to-one correspondence between the points in Λ and the points of conic \mathcal{C}_5 embedded in Π .

Actually, five different one-to-one correspondences of the same type exist: the correspondences between points in \mathcal{C}_i and points in Λ , where \mathcal{C}_i is the conic that contains all base attachments but \mathbf{a}_i . Each of these correspondences will be called \mathcal{C}_i -correspondence and the coordinates of \mathbf{a}_j and \mathbf{b}_j , for $j \in \{1, \dots, 5\} \setminus \{i\}$, satisfy it by construction. When the i th leg attachments coordinates also satisfy it, the manipulator becomes architecturally singular. In this particular case, all conics collapse into a single conic, which can be simply expressed as

$$\mathcal{C} = \left\{ (x, y) \mid \begin{vmatrix} x^2 & xy & y^2 & x & y & 1 \\ x_1^2 & x_1y_1 & y_1^2 & x_1 & y_1 & 1 \\ x_2^2 & x_2y_2 & y_2^2 & x_2 & y_2 & 1 \\ x_3^2 & x_3y_3 & y_3^2 & x_3 & y_3 & 1 \\ x_4^2 & x_4y_4 & y_4^2 & x_4 & y_4 & 1 \\ x_5^2 & x_4y_5 & y_5^2 & x_5 & y_5 & 1 \end{vmatrix} = 0 \right\}, \quad (5.48)$$

because five points on a plane define a conic.

5.7.3 Proximity to architectural singularities

Conics \mathcal{C}_i can be used to evaluate the proximity of a pentapod to an architectural singularity, but the resulting algebraic expressions are quite involved. To obtain a deeper geometric insight into the problem, it is necessary to study the relation between the \mathcal{C}_i -correspondences given by equation (5.7.2) and the \mathcal{B} -correspondence defined by (5.13).

Consider the following composition:

$$\begin{array}{ccccc} \mathcal{C}_i & \xleftrightarrow{\mathcal{C}_i\text{-correspondence}} & \Lambda & \xleftrightarrow{\mathcal{B}\text{-correspondence}} & \text{Pencil in } \Pi \\ (x, y) & \xleftrightarrow{\quad} & z & \xleftrightarrow{\quad} & \mathcal{B}_z \end{array} \quad (5.49)$$

First of all, note that any (x, y, z) satisfying the \mathcal{C}_i -correspondence satisfies also the \mathcal{B} -correspondence, *i.e.*, any point $(x, y, 0) \in \mathcal{C}_i$ lies on its corresponding \mathcal{B} -line B_z . This is because, particularizing to \mathcal{C}_5 , (5.45) implies that two cofactors of the elements of the last row of the matrix in (5.13) are zero, which makes its determinant zero irrespective of the values given to (x_5, y_5, z_5) . Therefore, the z coordinate corresponding to $(x, y, 0)$

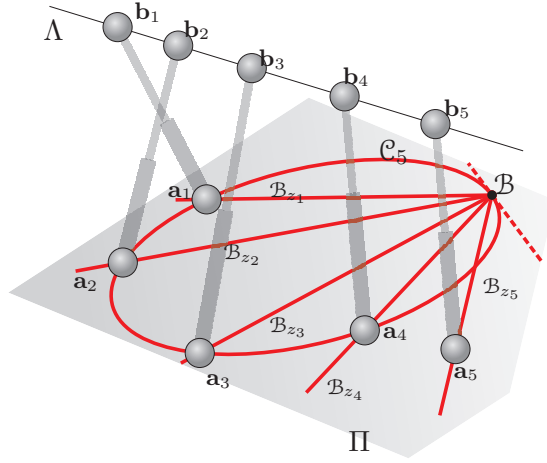


Figure 5.11: The composition of the one-to-one \mathcal{B} -correspondence between points on Λ and \mathcal{B} -lines on Π , and the one-to-one \mathcal{C}_5 -correspondence between points on Λ and points of conic \mathcal{C}_5 . The point on Λ corresponding to the point on the conic coincident with \mathcal{B} necessarily corresponds to the \mathcal{B} -line tangent to \mathcal{C}_5 on \mathcal{B} .

on the conic \mathcal{C}_i is the same as the one corresponding to the \mathcal{B}_z -line through $(x, y, 0)$ (in Fig. 5.11 there is a graphical representation of the \mathcal{C}_5 -correspondence and the \mathcal{B} -correspondence).

As the composition of two one-to-one correspondences is one-to-one, there is a one-to-one correspondence between points in \mathcal{C}_i and lines of the pencil embedded in Π . This fact has two consequences:

1. Point \mathcal{B} lies on the conic, otherwise there would be two points of the conic corresponding to the same \mathcal{B} -line.
2. Point \mathcal{B} has a unique corresponding point in Λ through the \mathcal{C}_i -correspondence, which is necessarily the point corresponding to the \mathcal{B} -line tangent to conic \mathcal{C}_i on \mathcal{B} through the \mathcal{B} -correspondence.

As a consequence, a generic pentapod is architecturally singular when the base attachment \mathbf{a}_i lies on conic \mathcal{C}_i defined by the attachments of the other four legs and \mathcal{B} . This observation is of practical interest to derive a distance to an architectural singularity: the distance from point \mathcal{B} to the conic defined in (5.48). This distance can be evaluated by substituting (x, y) in the conic expression (5.48) by the coordinates of

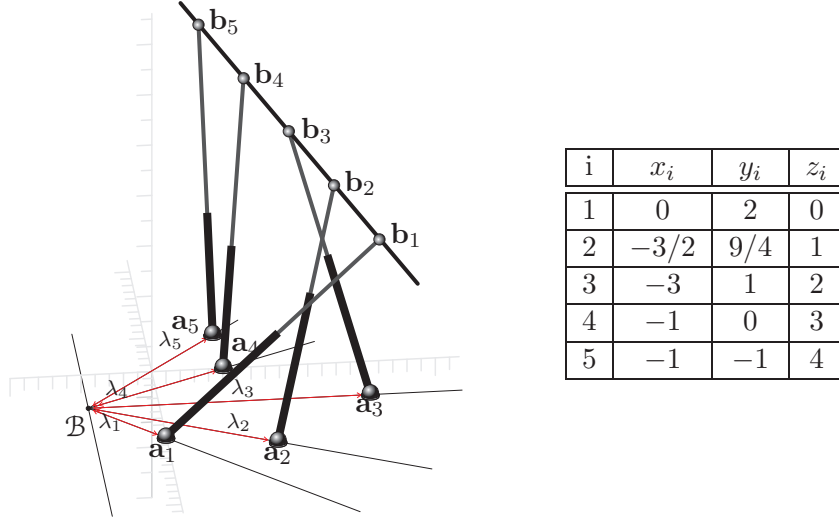


Figure 5.12: The pentapod analyzed in Section 5.7.4 and its attachment coordinates ($\mathbf{a}_i = (x_i, y_i, 0)$ and $\mathbf{b}_i = \mathbf{p} + z_i \mathbf{i}$).

the \mathcal{B} point:

$$\mathcal{C}(b_x, b_y) = \begin{vmatrix} b_x^2 & b_x b_y & b_y^2 & b_x & b_y & 1 \\ x_1^2 & x_1 y_1 & y_1^2 & x_1 & y_1 & 1 \\ x_2^2 & x_2 y_2 & y_2^2 & x_2 & y_2 & 1 \\ x_3^2 & x_3 y_3 & y_3^2 & x_3 & y_3 & 1 \\ x_4^2 & x_4 y_4 & y_4^2 & x_4 & y_4 & 1 \\ x_5^2 & x_4 y_5 & y_5^2 & x_5 & y_5 & 1 \end{vmatrix}, \quad (5.50)$$

where $\mathcal{B} = (b_x, b_y, 0)$.

5.7.4 An example

Consider the pentapod in Fig. 5.12 with the attachments coordinates appearing in the corresponding table.

Let λ_i be the distance between \mathbf{a}_i and \mathcal{B} . Then, for all generic cases, $\lambda_i \neq 0$ for $i = 1, \dots, 5$. The coordinates in Fig. 5.12 correspond to the configuration $\{\lambda_1 = \sqrt{2}, \lambda_2 = 5\sqrt{5}/4, \lambda_3 = 4, \lambda_4 = \sqrt{5}, \lambda_5 = 2\sqrt{2}\}$.

For a general configuration given by $\{\lambda_1, \dots, \lambda_5\}$, the value of the cofactors of matrix \mathbf{T} are

$$\begin{aligned} C_1 &= K, & C_2 &= 2K, & C_3 &= 2K, \\ C_4 &= -K, & C_5 &= 0, & C_6 &= -4K \end{aligned}$$

where

$$K = \frac{\sqrt{10}}{50} (-15\sqrt{2}\lambda_1\lambda_2\lambda_5 + 12\sqrt{5}\lambda_1\lambda_4\lambda_2 - 15\sqrt{2}\lambda_5\lambda_1\lambda_4 - 45\lambda_1\lambda_4\lambda_3 + 8\sqrt{10}\lambda_4\lambda_2\lambda_3 - 45\lambda_5\lambda_2\lambda_3 - 5\lambda_1\lambda_2\lambda_3 + 12\sqrt{5}\lambda_5\lambda_4\lambda_2 + 20\sqrt{10}\lambda_5\lambda_1\lambda_3 - 5\lambda_5\lambda_4\lambda_3). \quad (5.51)$$

which depends only on $\lambda_1, \dots, \lambda_5$. Then, the singularities are given by the roots of

$$\det(\mathbf{T}) = K(i_z p_z - 2i_z(p_x i_z - p_z i_x) - 2i_z(p_y i_z - p_z i_y) - p_z(p_x i_z - p_z i_x) + 4w^2)$$

Hence, this example makes clear how modifying the values of λ_i (i.e., moving the base attachments along their \mathcal{B} -lines) does not modify the singularities of the manipulator.

The distance measure to an architectural singularity is given in equation (5.50). Using the coordinates of \mathbf{a}_i , which can be parametrized depending on λ_i as

$$\mathbf{a}_i = \mathcal{B} + \lambda_i \frac{\mathcal{B} - \mathbf{a}_{0i}}{\|\mathcal{B} - \mathbf{a}_{0i}\|}, \text{ for } i = 1, \dots, 5,$$

where \mathbf{a}_{0i} is the initial location of \mathbf{a}_i , and $\mathcal{B} = (1, 1, 0)$, one obtains

$$\mathcal{C}(b_x, b_y) = (\lambda_1\lambda_2\lambda_3\lambda_4\lambda_5) \frac{K}{10},$$

where $\lambda_i > 0$. If $\lambda_i = 0$, \mathbf{a}_i would be coincident with \mathcal{B} , which does not correspond to an architectural singularity, but it is a non-generic case that must be studied separately. Then, K can be taken as a measure of distance. Note that the greater is the distance to an architectural singularity, the greater is the constant that multiplies the singularity polynomial, and thus, the manipulator will behave better near a singularity.

The constant $\mathcal{C}(b_x, b_y)$ is a measure of distance of point \mathcal{B} to the conic defined by the 5 base attachments. Nonetheless, it can be more intuitive to measure the distance of \mathbf{a}_i to its associated singular conic, that is, the conic formed by the other 4 attachments plus point \mathcal{B} , i.e. \mathcal{C}_i (defined in Section 5.7.2). For the current example, at its initial configuration, the five conics \mathcal{C}_i , $i = 1, \dots, 5$, passing through \mathcal{B} and all base attachments except \mathbf{a}_i are depicted in Fig. 5.13.

Then, if attachment \mathbf{a}_4 is moved along its \mathcal{B} -line, the singularity locus of the analyzed robot remains unaltered, unless it is located on conic \mathcal{C}_4 (the fourth conic in Fig. 5.13). In this case, the manipulator becomes architecturally singular. The new

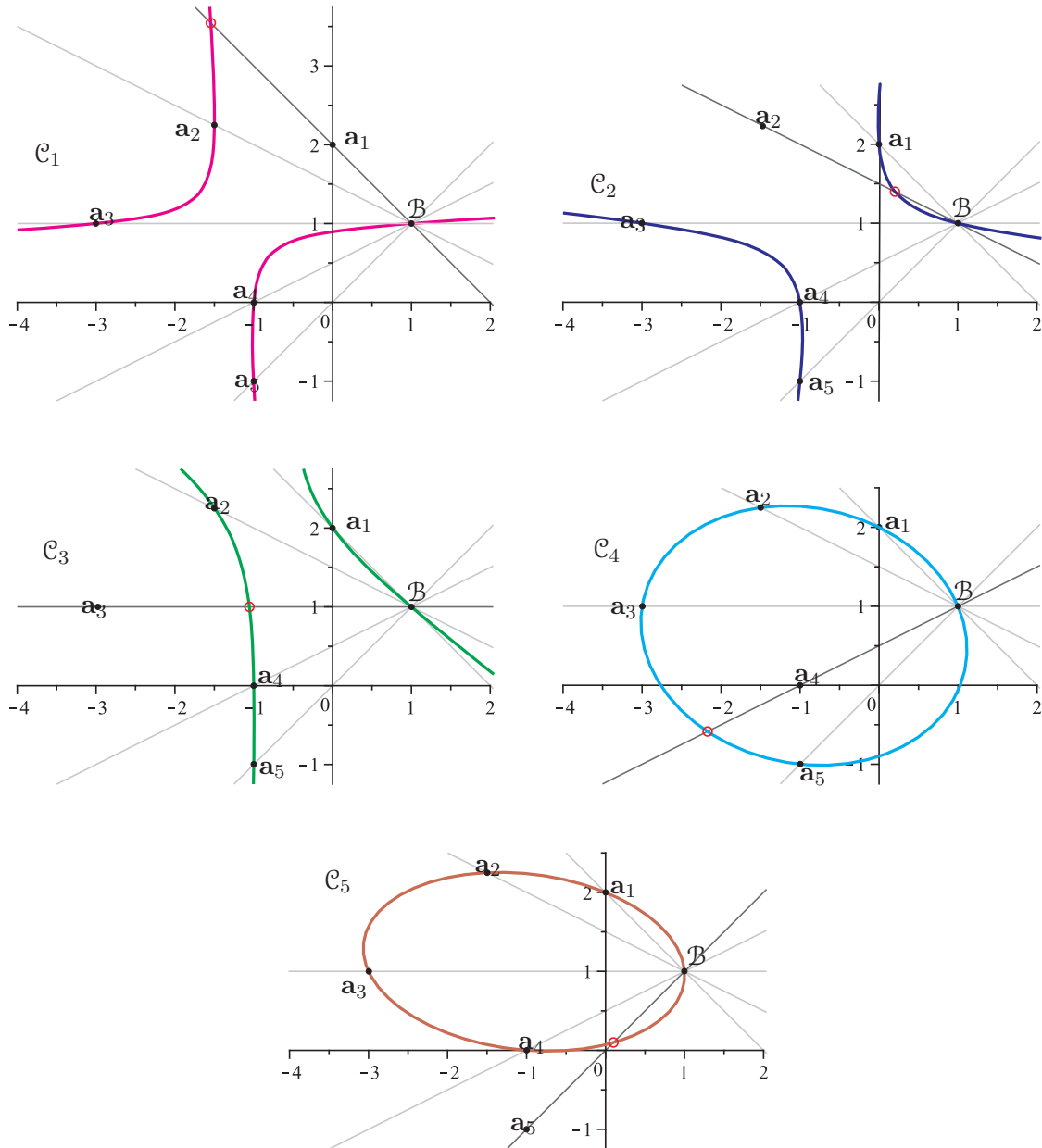


Figure 5.13: Singular conics, \mathcal{C}_i , for $i = 1, \dots, 5$ for the pentapod in Fig. 5.12.

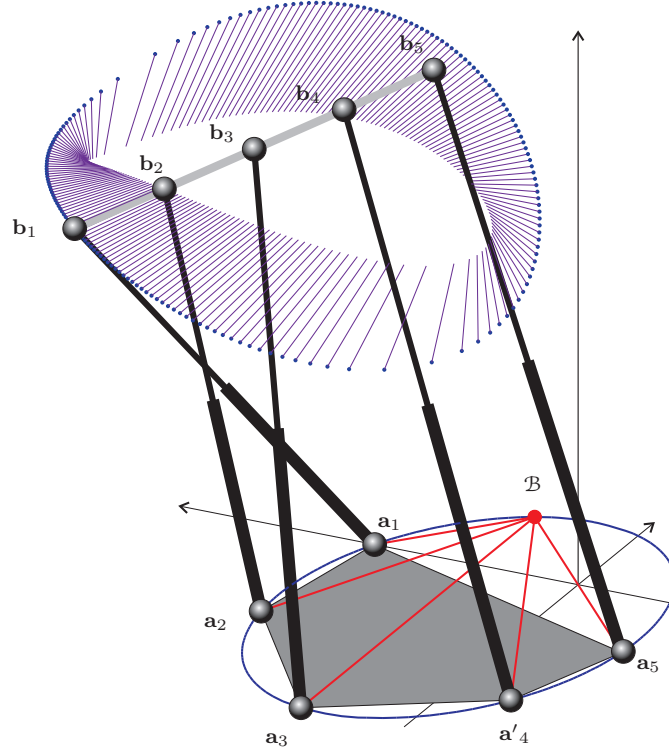


Figure 5.14: Self-motion of the analyzed architecturally singular pentapod.

vector of coordinates for this attachment is $\mathbf{a}'_4 = (-\frac{63}{29}, -\frac{17}{29}, 0)$. Fig. 5.14 shows the self-motion associated with the resulting architecturally singular pentapod with $l_1 = 4.243$, $l_2 = 3.786$, $l_3 = 4.315$, $l_4 = 4.893$, and $l_5 = 5.363$. The reference point $\mathbf{p} = (p_x, p_y, p_z)^T$ and the director vector $\mathbf{i} = (u, v, w)^T$ of Λ is represented along the resulting self-motion. To compute this self-motion, the forward kinematics is expressed as a system of the equations dependent on two of the unknowns, one of them playing the role of a parameter, and then the equations are solved following the procedure described in Section 5.6.3 or [111]. For the detailed computations, see [13].

For the architecturally singular manipulator, the five conics, $\mathcal{C}_1, \dots, \mathcal{C}_5$ are coincident and can be computed using equation (5.48). Moreover, there exists a one-to-one correspondence between the moving platform attachments and the base attachments given by this unique \mathcal{C}_i -correspondence (Section 5.7.2).

5.8 The role of cross-ratios

In Section 5.4 it has been shown that attachment \mathbf{a}_i can be freely relocated on the plane, as long as \mathbf{b}_i is relocated in the corresponding platform location. Nevertheless, special attention must be paid to avoid that, at each step,

- no three attachments in the plane are located in the same \mathcal{B} -line because three leg lengths would become dependent [Fig. 2.4-(a)],
- no four attachments in the plane are collinear as, in this case, the Line-Plane component would contain an architecturally singular Line-Line component, and
- no 5 attachments and \mathcal{B} are in the same conic.

In this section, the last two conditions will be reformulated in terms of cross-ratios.

First of all, note that all the geometric entities involved in this chapter are 1-dimensional projective domains: ranges of points, pencils of lines and conics. Then, the cross-ratio of any set of 4 points (on a conic or on a line) and the cross-ratio of any set of 4 lines of the pencil are well-defined (see Appendix B).

The \mathcal{B} -correspondence is a one-to-one correspondence between the pencil of lines formed by linear combinations of \mathcal{B}_0 and \mathcal{B}_∞ . In other words, if $\{\mathcal{B}_i\}$ is defined as the set of points belonging to the line \mathcal{B}_i , then, the set of points that belong to one of the lines of the pencil is defined by the parameter z in the form

$$\{\mathcal{B}_0\} + z\{\mathcal{B}_\infty\}.$$

Furthermore, each point of the range on Λ is defined by the local coordinate z . Thus, z can be used as the projective parameter for both one-dimensional projective domains, and thus, the correspondence between them is projective¹ (see Appendix B for details). As a consequence, the cross-ratio of any four \mathcal{B} -lines must be equal to the cross-ratio of the corresponding attachments in Λ . This provides an alternative way for computing \mathcal{B} and, what is more important, an alternative way of defining all singularity-invariant changes in the location of the attachments as those that keep invariant the cross-ratios between the \mathcal{B} -lines and their corresponding attachments in Λ .

¹This correspondence is equivalent to the correspondence depicted in Fig. 5.9, which is clearly projective [89, Chapter IV-Theorem 11]

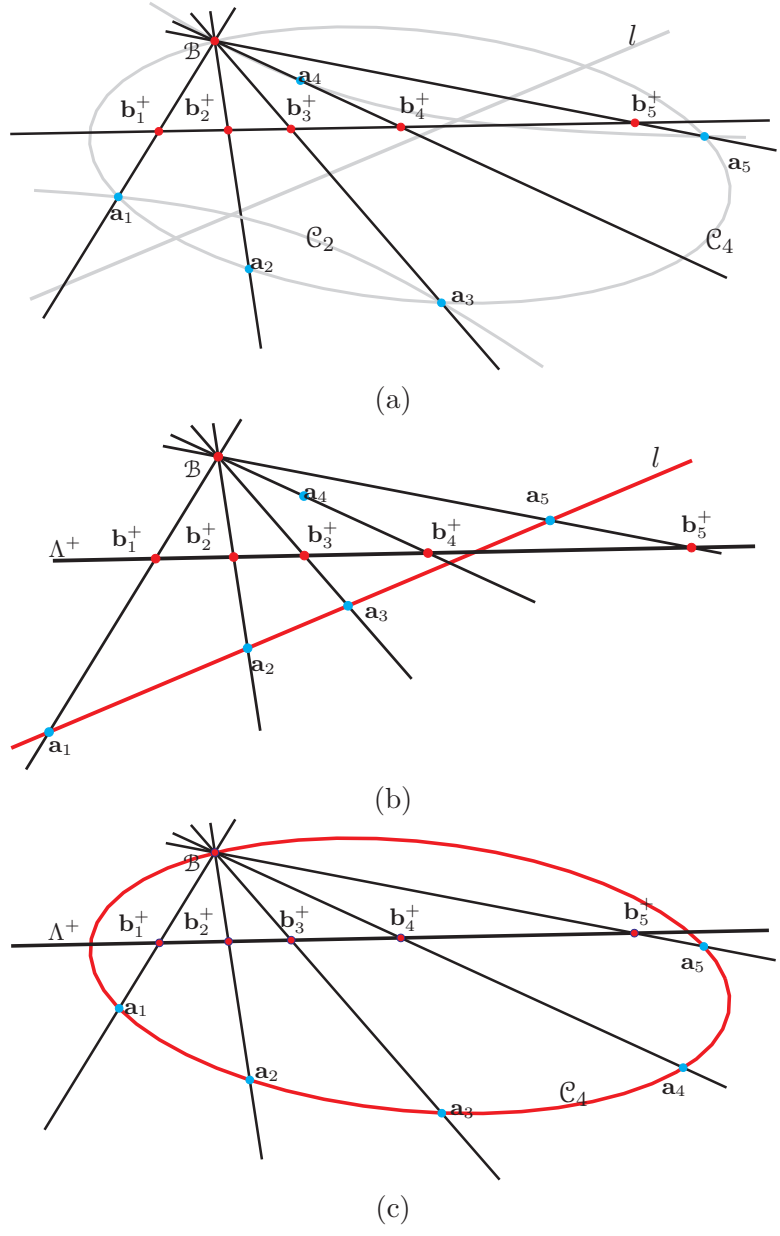


Figure 5.15: (a) The pencil of \mathcal{B} -lines defines a projective one-to-one correspondence between a range of points on Λ , points on any conic through \mathcal{B} and a range of points on any line not through \mathcal{B} (here represented by l). (b) When four attachments are collinear, the cross-ratio between them and their corresponding \mathbf{b}_i^+ is the same. (c) When five base attachments and \mathcal{B} are in the same conic, the cross-ratios of the base attachments is the cross-ratios of their corresponding \mathcal{B} -lines, which at the same time is equal to the cross-ratios of their corresponding \mathbf{b}_i^+ .

In addition, the cross-ratio of points on \mathcal{C}_i can be defined as the cross-ratio of their corresponding \mathcal{B} -lines (as \mathcal{B} always belong to \mathcal{C}_i for $i = 1, \dots, 5$). Then, \mathcal{B} -lines, attachments on conics \mathcal{C}_i and attachments on Λ have equal cross-ratios taken 4 by 4 [Fig. 5.15-(a)]. As a consequence, all \mathcal{C}_i -correspondences are also projective (see Appendix B).

To prevent falling into an architectural singularity, while performing a Line-Plane singularity-invariant leg rearrangement, it is just necessary to avoid two simple conditions:

1. Locate 4 attachments collinearly.
2. Locate the 5 attachments and \mathcal{B} on the same conic.

For the first condition, it has already been shown in Section 4.7 of Chapter 4, that any Line-Line component with equal cross-ratios for the attachments on both lines is architecturally singular. Then, when performing rearrangements following \mathcal{B} -lines, any four attachments located on a line will form a Line-Line component, and they will have the same cross-ratio as their \mathcal{B} -lines, and thus, the same as their corresponding attachments on Λ [Fig. 5.15-(b)].

When the second condition is satisfied [as in Fig. 5.15-(c)], the cross-ratio of any 4 attachments on the base conic are the same than the cross-ratios of their corresponding \mathcal{B} -lines, and the same of their corresponding platform attachments on Λ . Thus, it can be concluded that there exists a projectivity between them (see Appendix B) which is precisely, the \mathcal{C}_i -correspondence. Then, as a line can always be considered a degenerated conic, Chasles theorem (enunciated in Chapter 2) applies: base and platform attachments belong to conic sections in projective correspondence. Thus, the manipulator is architecturally singular.

Now, the first condition can be seen as a particular case of the second because, when 4 attachments are collinear, they belong to a degenerate conic formed by the line they define and the line defined by \mathcal{B} and the remaining non-collinear attachment. Therefore, platform and base attachments are placed in degenerated conic sections in projective correspondence (in Fig. 5.15-(b), such degenerated conic is formed by l and the \mathcal{B}_4 -line).

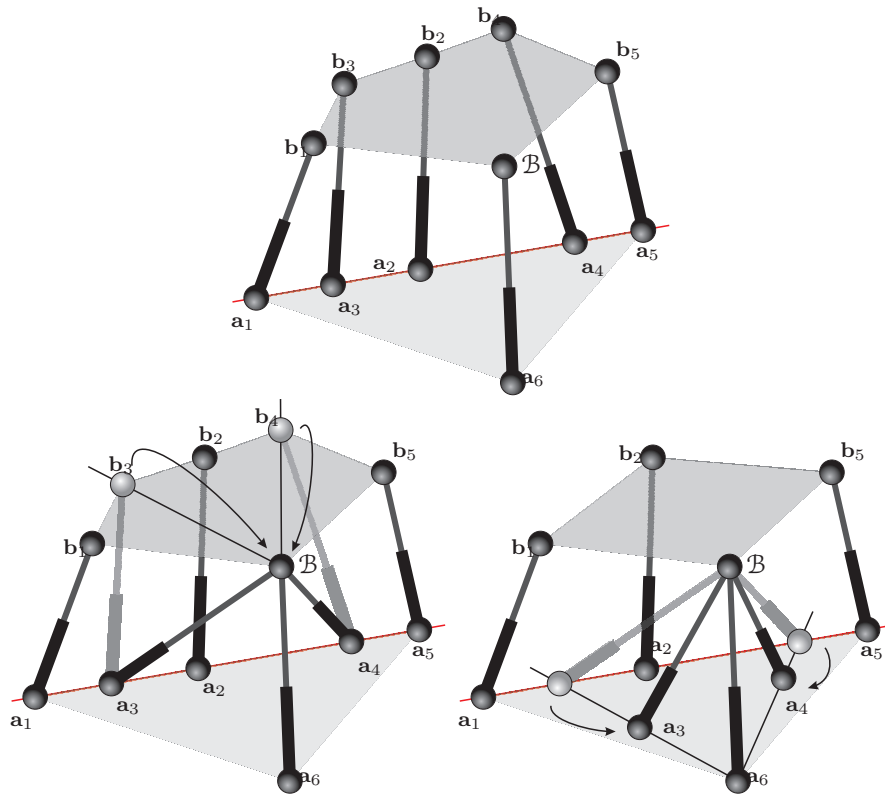


Figure 5.16: The legs of this upside-down Line-Plane component can be rearranged to form an uncoupled manipulator.

5.9 Examples

5.9.1 Uncoupled parallel manipulator

Consider the Stewart-Gough platform in Fig. 5.16-(top). It contains an upside-down Line-Plane component. Hence, the associated pencil of lines lies, in this case, in the platform plane. Moreover, the attachment in the platform of the leg not included in the Line-Plane component is made to be coincident with the focus of the pencil, \mathcal{B} .

According to the results presented in Section 5.4, two platform attachments can be moved along their \mathcal{B} -lines to meet at \mathcal{B} without modifying the singularity locus of the considered platform. A Point-Plane component thus arises [Fig. 5.16-(bottom-left)]. In Chapter 4 it has been shown how the attachments in the plane of a Point-Plane component can be arbitrarily relocated, without changing the singularity locus of the whole platform, provided that no architectural singularities are introduced. As a

consequence, it is possible to misalign two of the base attachments [Fig. 5.16-(bottom-right)]. The result is an uncoupled parallel platform because the legs of the Point-Plane component determine the location of a point in the moving platform and the other three legs, the platform's orientation. It can be said that the resulting uncoupled manipulator contains a concealed Line-Plane component. Thus, it is clear that the presented study transcends that of pentapods.

5.9.2 Elimination of multiple spherical joints

Multiple spherical joints exist in most well-studied Gough-Stewart platforms. Such joints simplify the kinematics and singularity analysis of parallel manipulators, but they are difficult to construct and present small joint ranges, which make them of little practical interest. In this example it is shown how the presented leg rearrangements can be used to eliminate multiple spherical joints from a particular design, as it has been already done in Section 4.5, without losing the advantages of having simple kinematics and maintaining the same singularity locus.

Consider the pentapod depicted in Fig. 5.17-(top), which is clearly of the Line-Plane type studied in this chapter. A set of leg rearrangements can be performed to transform it into a platform with the same singularities, but with no multiple spherical joints. One of the possible sequences of leg rearrangements to attain this goal appears in Fig. 5.17-(bottom).

5.9.3 Numerical example of a quadratically-solvable pentapod

A family of quadratically-solvable manipulators has been introduced in Section 5.6.4. They are characterized by having \mathcal{B} at infinity and the distance between the parallel \mathcal{B} -lines proportional to the distances of the attachments in the platform line. The next example corresponds to one of such manipulators, the one depicted in Fig. 5.18.

The singular conic definitions established in Section 5.7 are also applicable when \mathcal{B} is at infinity, provided that equations are handled using homogeneous coordinates. In this example, the homogeneous coordinates of point \mathcal{B} are $\mathcal{B}_H = (0, 1, 0)_H$, which means that all conics are parabolas or hyperbolas having a vertical asymptote. In Fig. 5.19 the five singular conics are plotted.

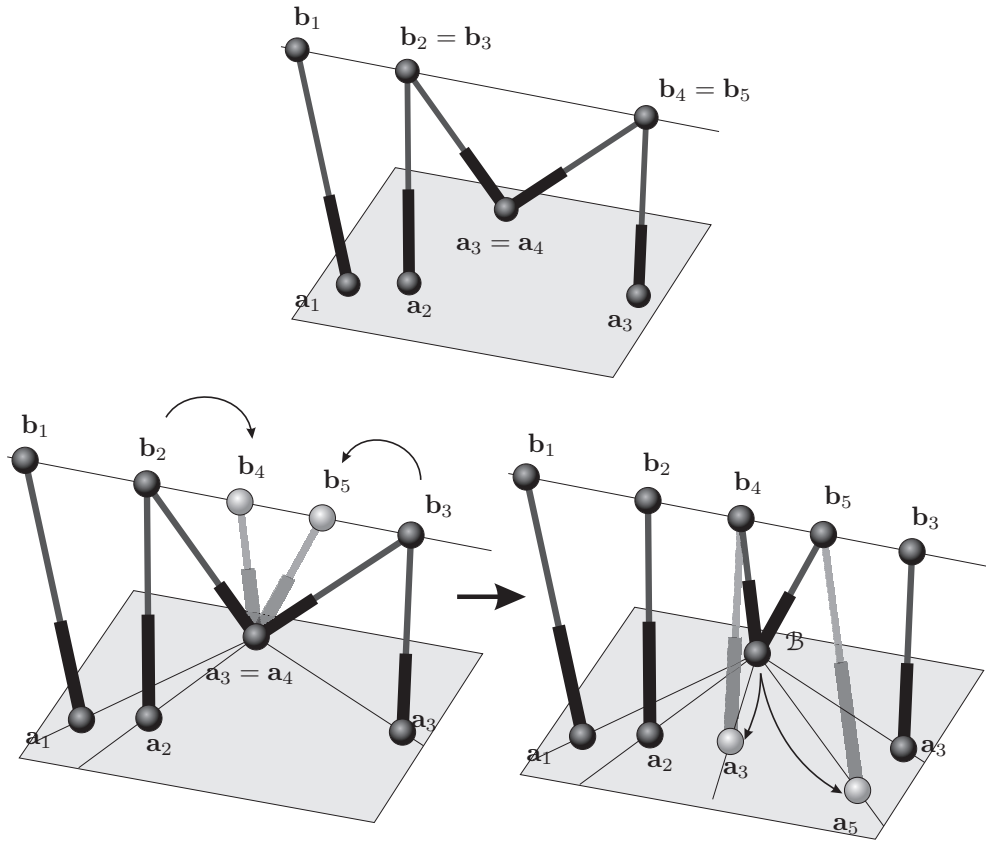


Figure 5.17: Singularity-invariant leg rearrangements can be used at the manipulator design stage to eliminate multiple spherical joints.

Let λ_i denote the distance from each attachment to a line crossing perpendicularly all the \mathcal{B} -lines. By properly choosing the reference frame, all \mathcal{B} -lines are parallel to the y axis, and the crossing line can be selected to be the x axis, so that $\lambda_i = y_i$ for $i = 1, \dots, 5$.

With this parametrization, the cofactors of matrix \mathbf{T} are

$$C_1 = -K, C_2 = K, C_3 = C_4 = C_5 = C_6 = 0,$$

and the Jacobian matrix determinant is given by

$$\det(\mathbf{T}) = K((i_x - 1)p_z - p_x i_z) i_z,$$

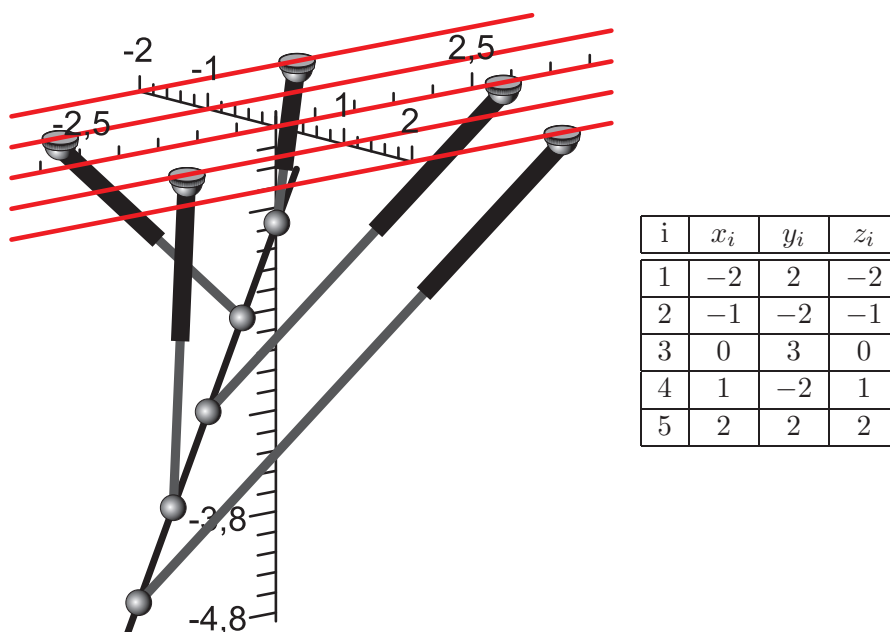


Figure 5.18: Pentapod analyzed in Section 5.9.3 and its attachment coordinates ($\mathbf{a}_i = (x_i, y_i, 0)^T$ and $\mathbf{b}_i = \mathbf{p} + z_i \mathbf{i}$).

where

$$K = 2(9\lambda_2\lambda_5 + \lambda_5\lambda_4 + 6\lambda_3\lambda_4 + \lambda_2\lambda_1 + 9\lambda_1\lambda_4 - 6\lambda_3\lambda_5 + 6\lambda_3\lambda_2 - 6\lambda_3\lambda_1 - 4\lambda_1\lambda_5 - 16\lambda_2\lambda_4).$$

In this case, the distance measure to architectural singularities given in equation (5.50) coincides exactly with the constant factor of the determinant, that is,

$$\mathcal{C}(b_x, b_y) = K.$$

Again, the configuration shown in Fig. 5.18 is the furthest to an architectural singularity, when $-2 \leq \lambda_i \leq 2$ for $i = 1, \dots, 5$. Note that K coincides with the architectural singularity factor found in Section 5.6.4, equation (5.38).

This example is interesting because the two algebraic conditions given by Husty and Karger in [49] are satisfied, as $C_4 = C_5 = 0$, but the manipulator is not architecturally singular. This is not a counter-example because it is not a case in general-position, in the sense that the coordinates of the attachments in the base and in the platform

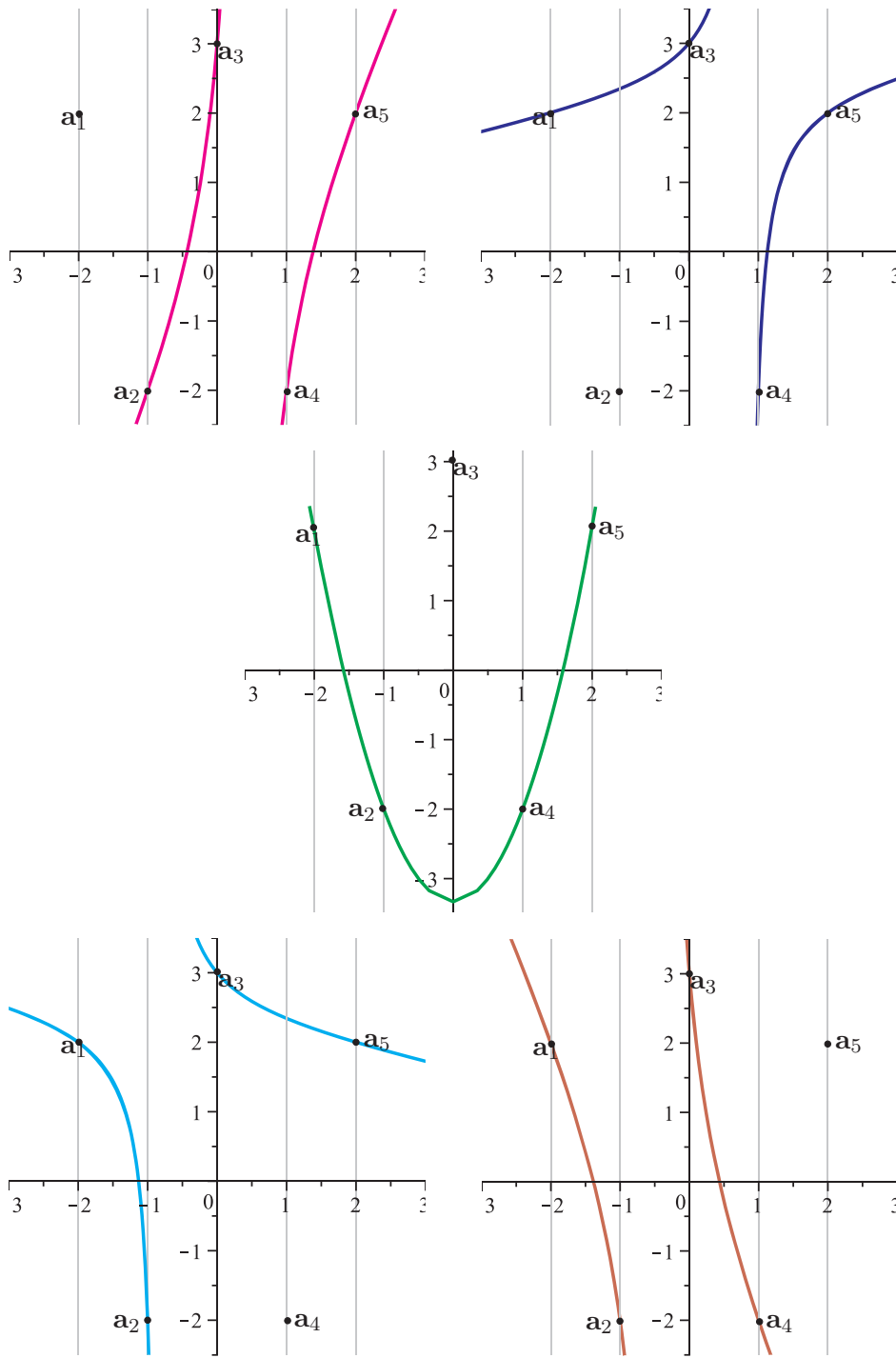


Figure 5.19: C_i , for $i = 1, \dots, 5$, for the pentapod with attachment coordinates appearing in Fig. 5.18.

do satisfy a relation, although a non-trivial one. On the other hand, this example does show that the two algebraic conditions characterizing architectural singularities are only valid when the leg attachments are in general position. They cannot characterize architectural singularities of non-generic pentapods such as, for example, all the members of the family of quadratically-solvable pentapods. On the contrary, both the algebraic generalization and the geometric interpretation provided here allow to identify architectural singularities of all kinds of pentapods with coplanar base attachments.

5.10 Non-generic cases

In the previous sections, generic cases have been considered. In a non-generic case, attachments are not in general position. For example, one of the attachments can be placed coincident with \mathcal{B} . This does not lead to an architectural singularity, but the equation for the distance measure proposed in equation (5.50) cannot be used.

5.10.1 One attachment in \mathcal{B}

Consider the manipulator in Fig. 5.12. In the example analyzed in Section 5.7.4 attachment \mathbf{a}_4 is moved towards its singular conic \mathcal{C}_4 to obtain an architecturally singular manipulator, but if it is moved until it is made coincident with \mathcal{B} instead (with coordinates $(1, 1, 0)$), a non-generic manipulator with the same singularity locus is obtained (Fig. 5.20). As \mathbf{a}_4 is the rearranged attachment, architectural singularities are determined by the \mathcal{C}_4 -correspondence, which is defined similarly to (5.45), but substituting (x_4, y_4, z_4) by (x, y, z) instead of (x_5, y_5, z_5) , that is

$$\left. \begin{aligned} \widetilde{\mathcal{C}}_1 = & \left. \begin{array}{l} \left| \begin{array}{cccc|c} x & y & xz & yz & 1 \\ x_1 & y_1 & x_1z_1 & y_1z_1 & 1 \\ x_2 & y_2 & x_2z_2 & y_2z_2 & 1 \\ x_3 & y_3 & x_3z_3 & y_3z_3 & 1 \\ x_5 & y_5 & x_5z_5 & y_5z_5 & 1 \end{array} \right| = 0 \\ z & y & xz & yz & 1 \\ \widetilde{\mathcal{C}}_2 = & \left. \begin{array}{l} \left| \begin{array}{cccc|c} z & y & xz & yz & 1 \\ z_1 & y_1 & x_1z_1 & y_1z_1 & 1 \\ z_2 & y_2 & x_2z_2 & y_2z_2 & 1 \\ z_3 & y_3 & x_3z_3 & y_3z_3 & 1 \\ z_5 & y_5 & x_5z_5 & y_5z_5 & 1 \end{array} \right| = 0 \end{array} \right\} \end{aligned} \right\}$$

Then, the manipulator is architecturally singular if, and only if, the forth leg attachment coordinates satisfy the above system of equations (remember that $D_{1,2} \neq 0$ for this example). Thus, in this situation, although attachment \mathbf{a}_4 lies on its singular conic, the manipulator is not architecturally singular because the corresponding attachment on Λ , \mathbf{b}_4 , is not on the corresponding location given by the \mathcal{C}_4 -correspondence.

Equation (5.47) can be used to obtain all the singular conics of this manipulator (which are depicted in Fig. 5.20). Thus, two options arise to obtain an architecturally singular manipulator:

- Locate $\mathbf{a}_i \in \{\mathbf{a}_1, \mathbf{a}_2, \mathbf{a}_3 \text{ or } \mathbf{a}_5\}$ on \mathcal{C}_i as in the example of Section 5.7.4, or
- locate \mathbf{b}_4 in Λ so that z_4 makes $C_1 = C_2 = 0$. In other words, locate \mathbf{b}_4 on the point of Λ given by the \mathcal{C}_4 -correspondence.

If the first option is chosen, placing any other attachment on its singular conic would lead to an architecturally singular manipulator with a different self-motion with respect to the example in Section 5.7.4, as the base conic would not be the same.

If the second option is chosen, the corresponding value is $z_4 = \frac{-11}{4}$, which corresponding \mathcal{B} -line must be tangent to \mathcal{C}_4 at \mathcal{B} . If \mathbf{b}_4 is placed on this point, an architecturally singular manipulator is obtained which has exactly the same self-motion as the one in the Section 5.7.4, depicted in Fig. 5.14 because the base conic is the same, with the same leg-lengths except for the new leg $l_4 = 6.318$.

5.10.2 Two attachments in \mathcal{B}

Consider again the example in Fig. 5.12, in which two base attachments are made coincident with \mathcal{B} , for example \mathbf{a}_1 and \mathbf{a}_5 [Fig. 5.21-(a,b,c)]. As long as these two attachments are on \mathcal{B} , the resulting robot cannot be architecturally singular unless other attachments are made coincident, which would lead to a trivial architectural singularity. Next it is discussed why.

The computation of the singular conics (again, equation (5.47) must be used) leads to 3 degenerate conics, \mathcal{C}_2 , \mathcal{C}_3 and \mathcal{C}_4 (Fig. 5.22), which consist of two lines intersecting at \mathcal{B} .

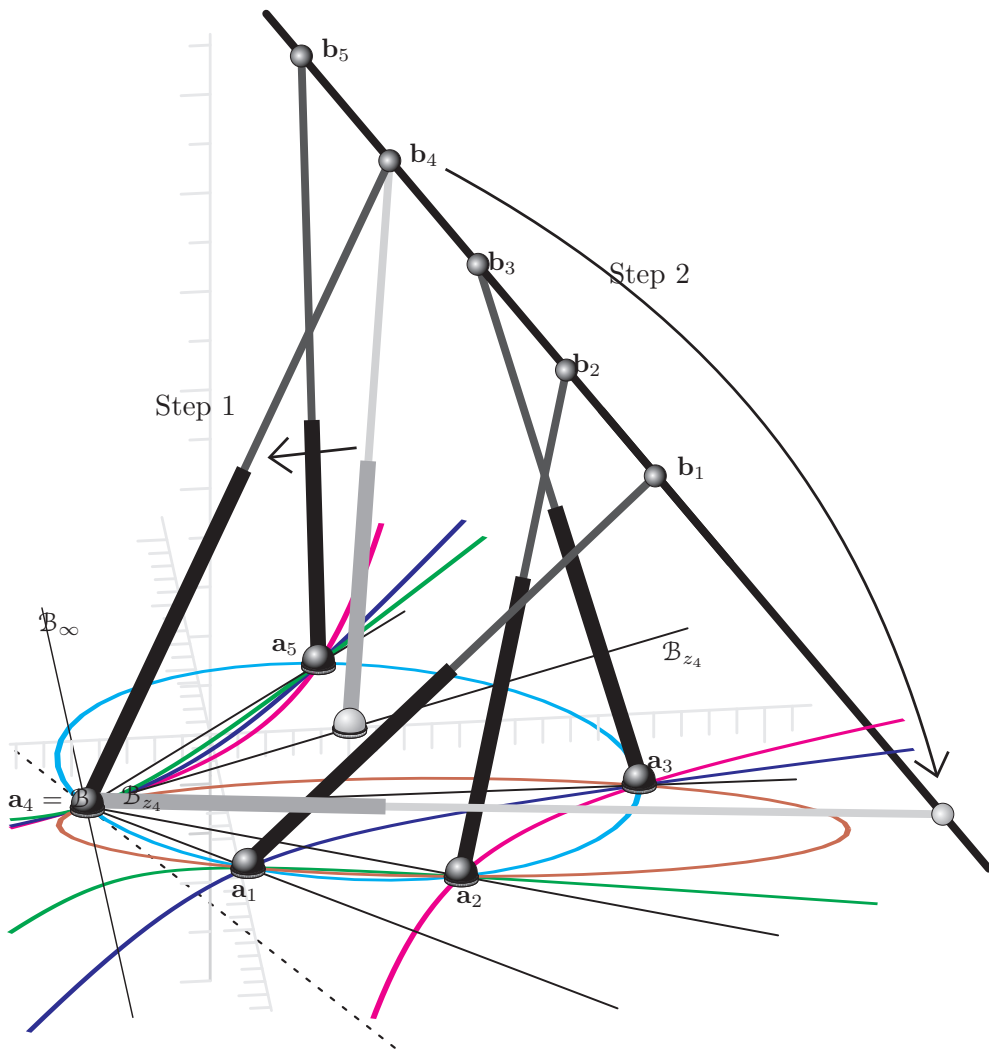


Figure 5.20: The pentapod described in Section 5.7.4, and its singular conics. The first step of the described rearrangement locates \mathbf{a}_4 on \mathcal{B} . Then, to make the manipulator architecturally singular, the second step rearranges \mathbf{b}_4 so that its associated \mathcal{B} -line is tangent to \mathcal{C}_4 at \mathcal{B} (dotted line in the figure).

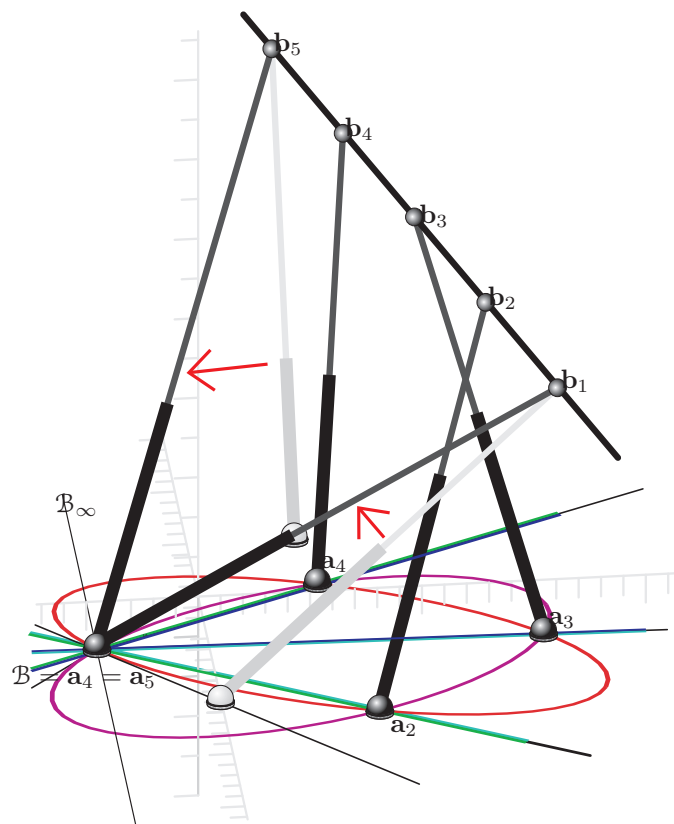


Figure 5.21: The same example as in Section 5.7.4, after rearranging a_4 and a_5 on \mathcal{B} , with their corresponding singular conics.

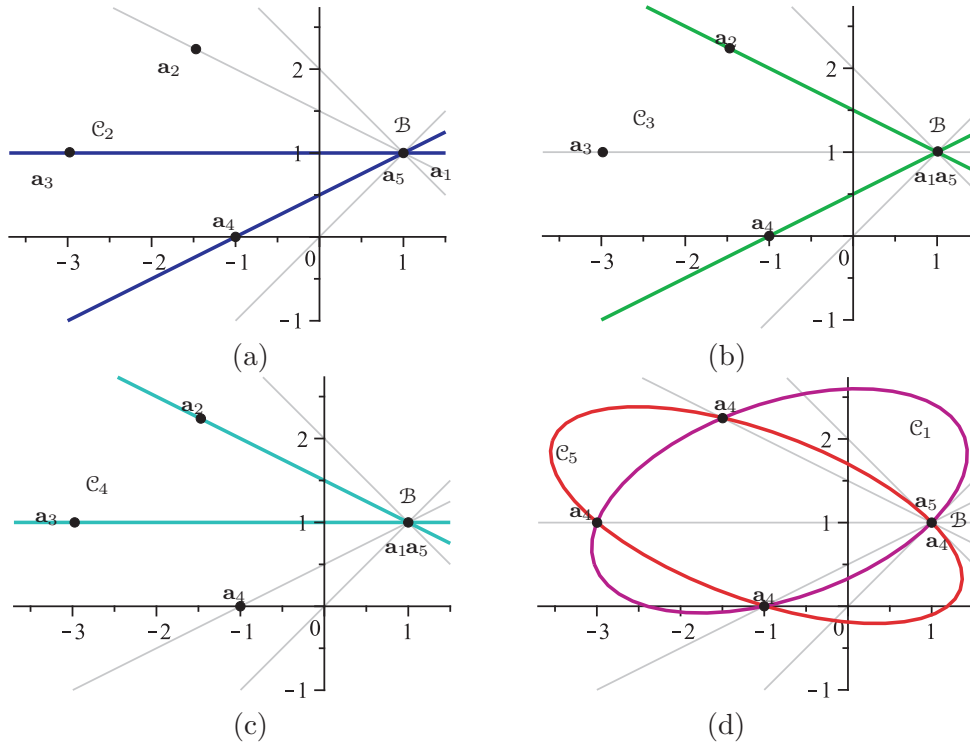


Figure 5.22: When two attachments are made coincident with \mathcal{B} , three of the singular conics are degenerate.

In this case, to obtain an architecturally singular manipulator, the following options arise:

- Locate attachment \mathbf{a}_2 on \mathcal{C}_2 . If \mathbf{a}_2 is moved along its corresponding \mathcal{B} -line, the only intersecting point with \mathcal{C}_2 is \mathcal{B} , but three points on \mathcal{B} form a degenerate inverted tripod.
- Place \mathbf{a}_2 on the \mathcal{B}_3 -line if the corresponding \mathbf{b}_2 is made coincident with \mathbf{b}_3 , which leads to a trivial architecturally singular Line-Line component (shaped $\wedge \setminus \setminus /$, see [25]-Tab. 4-3B).
- The other two singular conics \mathcal{C}_1 and \mathcal{C}_5 are not degenerate but the corresponding attachments are on point \mathcal{B} [Fig. 5.22-(d)]. Thus, to make the manipulator architecturally singular, \mathbf{b}_1 (or \mathbf{b}_5) must be placed to the corresponding point given by the \mathcal{C}_1 -correspondence (or \mathcal{C}_5 -correspondence). The \mathcal{C}_1 -correspondence

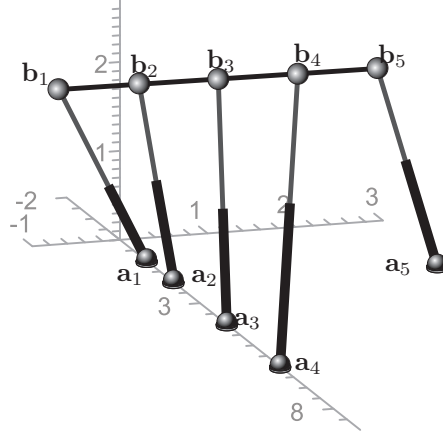


Figure 5.23: A Line-Plane component containing a Line-Line subcomponent.

gives $z = 4$, which is the same coordinate as that of \mathbf{b}_5 . Otherwise, the \mathcal{C}_5 -correspondence gives $z = 0$, which is the coordinate of \mathbf{b}_1 (in other words, the \mathcal{B}_5 -line is tangent to \mathcal{C}_1 , and the \mathcal{B}_1 -line is tangent to \mathcal{C}_5). In conclusion, the only possible architectural singularity is attained by making coincident legs 4 and 5, which is again a trivial singularity.

In short, a Line-Plane component with two attachments coincident on \mathcal{B} cannot be architecturally singular, except for the architectural singularities of lower order (planar pencils involving 3 legs, or regulus involving 4 legs (Fig. 2.4)).

5.10.3 Four aligned attachments

Consider a Line-Plane component containing a Line-Line subcomponent (Fig. 5.23). The nature of the singularities and kinematics of this example is different from the general Line-Plane because this rigid sub-component, but the definition of the singularity-invariant leg rearrangements for the Line-Plane still applies.

When 4 of the attachments are collinear, the reference frame in Π can be placed so that $y_1 = y_2 = y_3 = y_4 = 0$. Then, the \mathcal{B} -correspondence defined in equation (5.13) is

of the form

$$\left\{ (x, y, z) \in \mathbb{R}^3 \mid \begin{vmatrix} z & x & y & xz & yz & 1 \\ z_1 & x_1 & 0 & x_1 z_1 & 0 & 1 \\ z_2 & x_2 & 0 & x_2 z_2 & 0 & 1 \\ z_3 & x_3 & 0 & x_3 z_3 & 0 & 1 \\ z_4 & x_4 & 0 & x_4 z_4 & 0 & 1 \\ z_5 & x_5 & y_5 & x_5 z_5 & y_5 z_5 & 1 \end{vmatrix} = 0 \right\}.$$

The matrix \mathbf{T} cofactors are $C_3 = -y_5 z_5 D_{3,5}$, $C_5 = y_5 D_{3,5}$ and $C_1 = C_2 = C_4 = C_6 = 0$. Thus, the singularity invariant rearrangements are defined by the equation

$$C_3 y + C_5 y z = D_{3,5} y_5 y (z_5 - z) = 0. \quad (5.52)$$

where $D_{i,j}$ is the determinant of the matrix formed by the first 4 rows of $\hat{\mathbf{T}}$ after removing columns i and j .

Then, one of the legs can be substituted by another one going from $\mathbf{a} = (x, y, 0)$ to $\mathbf{b} = \mathbf{p} + z\mathbf{i}$ without modifying the singularity factor as long as

- $y = 0$. This means that the new leg belongs to the Line-Line component, and its corresponding x and z coordinate can take any value. This is coherent with the singularity-invariant leg rearrangements of the Line-Line found in Chapter 4, *i.e.*, attachments can be freely moved along the lines they belong within this component, or
- $z_5 - z = 0$. In other words, if the attachment on Λ of the new leg is located at \mathbf{b}_5 . Then its corresponding attachment on Π can be freely moved on the base plane, because x and y can take any value.

In conclusion, equation (5.52) can be used to define the singularity-invariant leg rearrangements in the Line-Line components, and in addition, the rearrangements of the fifth leg.

Architectural singularities only occur when:

- $y_5 = 0$. Then the fifth base attachment is also collinear, leading to a Linear Congruence [Fig. 2.4-(d)].

5.11 Applications on reconfigurable pentapods

- $D_{3,5} = 0$. This condition written in matrix form is

$$\begin{vmatrix} z_1 & x_1 & x_1 z_1 & 1 \\ z_2 & x_2 & x_2 z_2 & 1 \\ z_3 & x_3 & x_3 z_3 & 1 \\ z_4 & x_4 & x_4 z_4 & 1 \end{vmatrix} = 0,$$

which is exactly the same architectural condition of the Line-Line component found in equation (4.25) (which is zero when the cross-ratios of the base and platform attachments coincide).

This is a degenerate example of a Line-Plane component, where \mathcal{B} is not defined because all the \mathcal{B} lines coincide in a unique line.

Finally, it is important to note that when a general Line-Plane is defined, by performing singularity-invariant leg rearrangements, it is impossible to get a Line-Line subcomponent. Indeed, it has been proved in Section 5.8 that when 4 of the attachments are made collinear, the resulting Line-Line component is architecturally singular by construction, as the cross-ratios of the base and platform attachments will coincide.

5.11 Applications on reconfigurable pentapods

The investment cost to purchase a parallel robot for a particular task could be worth if there is the possibility to reconfigure it for another task. Static and dynamic reconfigurations can be distinguished [93], [60], [44]. Static reconfiguration denotes a manual rebuilding of a robot which might lead to a robot with new kinematic characteristics and a new workspace. Using singularity-invariant leg rearrangements, a less radical approach can be followed. Under this approach some leg attachments can be rearranged so that the geometry of the robot is modified but its kinematic equations are related through an affine relationship between their variables, before and after the reconfiguration. This kind of reconfigurations can be carried out not only statically but also dynamically without increasing significantly the control of the platform.

Consider the singularity-invariant leg rearrangements of the Line-Plane component studied in this chapter. Each base attachment can be rearranged along its \mathcal{B} -line. Then, the base attachments can be placed on actuated guides like in Fig. 5.24, while the moving platform attachments remain unaltered.

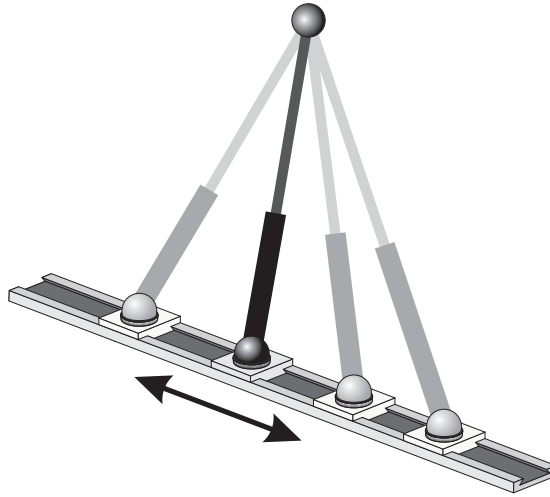


Figure 5.24: A reconfigurable leg along a guide.

In the robotics literature, reconfigurations are normally done to change the location of singularities so that, after a rearrangement, the manipulator can reach positions that were singular before the reconfiguration. Here, a rather different idea is proposed: the singularity locus remains invariant, but the manipulator exhibits an improved behavior because its versatility is increased for different tasks. For example, the static workspace [45] (or usable workspace) can be enlarged locally so that the manipulator can move nearer to the singularity at some locations, or the forces on the legs can be optimally distributed for each task. The advantage is that, while the major part of reconfigurable robots are difficult to control because the kinematic equations change after each reconfiguration, with singularity-invariant rearrangements the kinematic equations will be always the same.

The following two examples show two possible reconfigurable Line-Plane pentapods. The first one is designed such that, it is impossible to fall in an architectural singularity. The second is based on the quadratically-solvable manipulator presented in Section 5.9.3.

For reconfigurable manipulators, the geometric interpretation of architectural singularities becomes more relevant, as the manipulator has to avoid them while reconfiguring.

Let us define λ_i as the distance between \mathcal{B} and \mathbf{a}_i , for $i = 1, \dots, 5$, then, it will be

5.11 Applications on reconfigurable pentapods

shown how the measure of distance to an architectural singularity proposed in equation (5.50) can be expressed as $K = K(\lambda_1, \dots, \lambda_5)$, and that this function appears as a factor in the determinant of the Jacobian matrix computed in Section 5.3. Maximizing K in terms of λ_i , for $i = 1, \dots, 5$, leads to a global optimum which is independent from the pose of the moving platform.

Maximizing K is independent of the manipulator pose. Alternatively, an optimization that takes into account the pose of the robot can be envisaged by considering how a force applied on the moving platform is transmitted to the base through the legs. Consider the external force $\mathbf{F} = (f_1, f_2, f_3)$ applied to a point of the platform in a given pose. To compute the forces transmitted through each leg, τ_i , for $i = 1, \dots, 5$, one has to solve the static equilibrium equations system. This has already been done for the Line-Plane in Section 5.3.1, and the resulting system appears in (5.8). For a specific task, it would be desirable to arrange the legs so that the module of these forces are as close to each other as possible. To this end, the cost function

$$F = F(\lambda_1, \dots, \lambda_5, \mu) = \sum_{i=1}^5 (\tau_i^2 - \mu)^2 \quad (5.53)$$

can be minimized. For comparison purposes, a commonly used local index, the manipulability index defined as

$$M = \sqrt{\det(\mathbf{J}\mathbf{J}^T)}, \quad (5.54)$$

will be also optimized.

Next, optimizations using the above global and local indices will be carried out for two examples. The results are summarized in Tables 5.1 and 5.2. These tables are divided into two parts which correspond to the same pose but to two different applied forces on the platform. In both examples, the first case corresponds to a situation in which a weight hangs at the end of the platform line, and the second one, to a situation in which a force is exerted along the platform line itself. The first row of the tables contains the optima obtained by maximizing $|K|$. The second and the third rows contain the optima obtained by maximizing M and minimizing F , respectively, for a particular pose.

For each optimization, the resulting values of λ_i , the values of $|K|$, F , M , and the resulting distribution of forces are arranged by columns. The rightmost column

5.11 Applications on reconfigurable pentapods

contains a depiction of the resulting leg arrangement. All optimizations are carried out using a gradient descent method taking as starting point the initial configuration defined by the given coordinates.

As expected, it will be seen how the optima resulting from maximizing $|K|$ may not be a good solution in some poses and hence the interest of performing optimizations for particular poses.

5.11.1 A design free from architectural singularities

Thanks to the geometric interpretation of the architectural singularities given in Section 5.7, it is possible to design a reconfigurable pentapod that cannot be architecturally singular in any of its possible configurations. In the next example, point \mathcal{B} is located at the origin, and the \mathcal{B} -lines are radially arranged passing through the vertices of a pentagon.

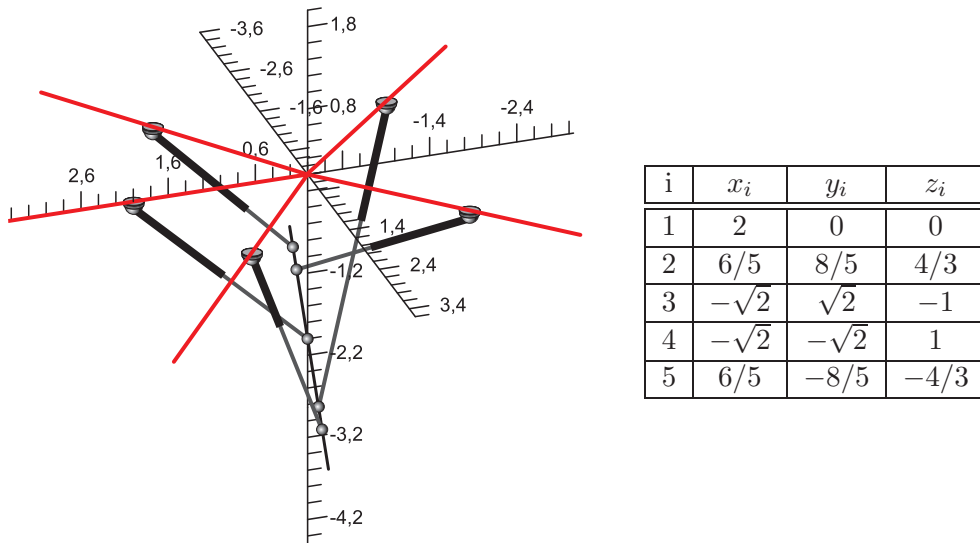


Figure 5.25: A reconfigurable pentapod free from architectural singularities and its corresponding attachment coordinates ($\mathbf{a}_i = (x_i, y_i, 0)^T$ and $\mathbf{b}_i = \mathbf{p} + z_i \mathbf{i}$).

Consider the pentapod appearing in Fig. 5.25 represented in the configuration $\lambda_1 = \lambda_2 = \lambda_3 = \lambda_4 = \lambda_5 = 2$. In Section 5.7 it has been shown that a Line-Plane component is architecturally singular when all the attachments and point \mathcal{B} lie on the same conic. Then, for each attachment, the corresponding singular conics are defined by the rest of

5.11 Applications on reconfigurable pentapods

the attachments and \mathcal{B} , so that the manipulator become architecturally singular when this attachment is located on its singular conic. Such conics are depicted in Fig. 5.26.

If each base attachment is limited to move along half its \mathcal{B} -line, from the origin to infinity, it can never reach its singular conic \mathcal{C}_i and, hence, the manipulator will never be architecturally singular.

For a general configuration given by $\lambda_1, \dots, \lambda_5$, the determinant of the Jacobian computed in Section 5.3 reads as

$$\det(\mathbf{J}) = K(i_z(p_y i_z - i_y p_z) + p_z(p_x i_z - i_x p_z)) \quad (5.55)$$

where

$$K = -\frac{2\sqrt{2}}{225} (192\sqrt{2}\lambda_1\lambda_2\lambda_5 + 42\lambda_2\lambda_3\lambda_5 + 5\lambda_1\lambda_2\lambda_4 + 5\lambda_1\lambda_3\lambda_5 + 245\lambda_1\lambda_4\lambda_5 + 35\sqrt{2}\lambda_2\lambda_3\lambda_4 + 245\lambda_1\lambda_2\lambda_3 + 42\lambda_2\lambda_4\lambda_5 + 35\sqrt{2}\lambda_3\lambda_4\lambda_5 + 150\sqrt{2}\lambda_1\lambda_3\lambda_4).$$

In other words, the cofactor values are $C_1 = C_2 = C_5 = C_6 = 0$, $C_3 = -K$ and $C_4 = K$. Note that, for positive λ_i 's, K is always different from zero and monotone.

For this example, the distance to architectural singularities defined in equation (5.50) reads

$$\mathcal{C}(b_x, b_y) = -\frac{9}{50}\lambda_1\lambda_2\lambda_3\lambda_4\lambda_5 K.$$

Maximizing $|K|$ becomes trivial because the further \mathbf{a}_i is from point \mathcal{B} , the bigger K is. The optimum values always reach the upper limits given to λ_i , $i = 1, \dots, 5$. This may seem a contradiction, as if λ_i , $i = 1, \dots, 5$, grow enough, the manipulator is approaching to a singular pose at which all legs tend to be coplanar. This is because K does not take into account the length of the legs. The manipulability index optimization introduces the dividing leg lengths factor, which quickly corrects this effect. The manipulability index depend on the pose and reads as

$$M = \sqrt{\frac{K^2(i_z(p_y i_z - i_y p_z) + p_z(p_x i_z - i_x p_z))^2}{l_1^2 l_2^2 l_3^2 l_4^2 l_5^2}}$$

where the length of the legs also depend on the given pose (and on λ_i , $i = 1, \dots, 5$). All the results of the optimizations performed for this example can be found in Table 5.1. The limits given for the optimization procedure are $0.5 \leq \lambda_i \leq 6$ for $i = 1, \dots, 5$.

5.11 Applications on reconfigurable pentapods

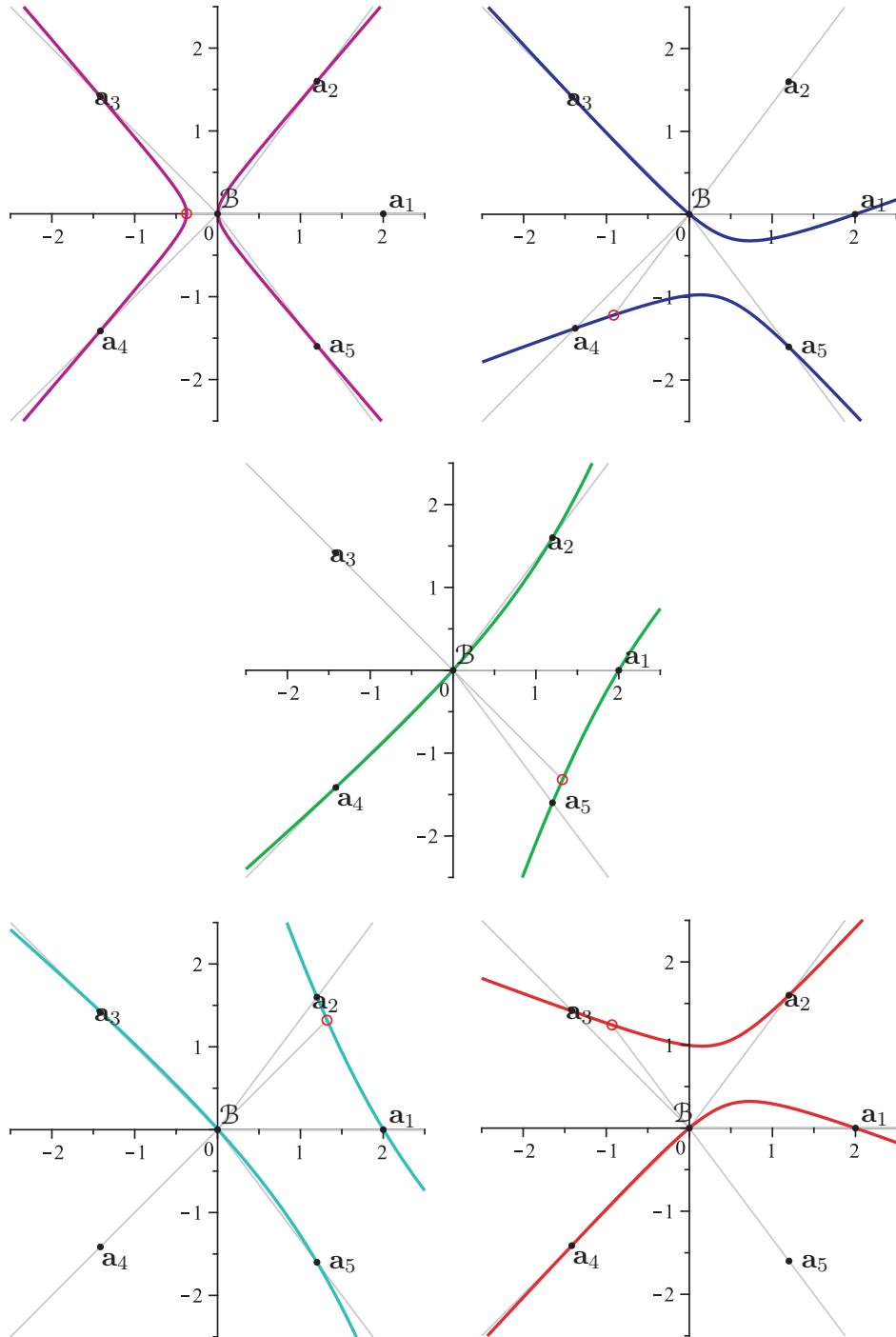


Figure 5.26: \mathcal{C}_i , for $i = 1, \dots, 5$ for the pentapod with attachment coordinates appearing in Fig. 5.25.

5.11 Applications on reconfigurable pentapods

Table 5.1: Optimization results for a reconfigurable pentapod free from architectural singularities.

$\mathbf{p} = (-1, 0, -2), \mathbf{i} = \frac{\sqrt{2}}{6}(1, 1, 4), \mathbf{F} = (0, 0, -1)$				
	Optimum	Values	Forces	
Max($ K $)	$\lambda_1 = 6.0$ $\lambda_2 = 6.0$ $\lambda_3 = 6.0$ $\lambda_4 = 6.0$ $\lambda_5 = 6.0$	$K = -3167.8$ $M = 2.2$ $F = 0.41$	$\tau_1 = -0.23$ $\tau_2 = 0.2$ $\tau_3 = -0.88$ $\tau_4 = 0.05$ $\tau_5 = -0.52$	
Max(M)	$\lambda_1 = 6.0$ $\lambda_2 = 6.0$ $\lambda_3 = 1.68$ $\lambda_4 = 2.47$ $\lambda_5 = 0.5$	$K = -367.1$ $M = 0.45$ $F = 0.58$	$\tau_1 = -0.05$ $\tau_2 = 0.11$ $\tau_3 = -0.94$ $\tau_4 = 0.05$ $\tau_5 = -0.56$	
Min(F)	$\lambda_1 = 1.51$ $\lambda_2 = 0.5$ $\lambda_3 = 4.24$ $\lambda_4 = 1.3$ $\lambda_5 = 1.5$ $\mu = 0.3$	$K = -54.6$ $M = 0.09$ $F = 0.05$	$\tau_1 = -0.51$ $\tau_2 = 0.64$ $\tau_3 = -0.58$ $\tau_4 = -0.35$ $\tau_5 = -0.6$	
$\mathbf{p} = (-1, 0, -2), \mathbf{i} = \frac{\sqrt{2}}{6}(1, 1, 4), \mathbf{F} = -\mathbf{i}$				
	Optimum	Values	Forces	
Max($ K $)	$\lambda_1 = 6.0$ $\lambda_2 = 6.0$ $\lambda_3 = 6.0$ $\lambda_4 = 6.0$ $\lambda_5 = 6.0$	$K = -3167.8$ $M = 0.13$ $F = 0.04$	$\tau_1 = 0.12$ $\tau_2 = -0.03$ $\tau_3 = 0.48$ $\tau_4 = 0.02$ $\tau_5 = 0.29$	
Max(M)	$\lambda_1 = 6.0$ $\lambda_2 = 6.0$ $\lambda_3 = 1.68$ $\lambda_4 = 2.47$ $\lambda_5 = 0.5$	$K = -367.1$ $M = 0.45$ $F = 0.05$	$\tau_1 = 0.02$ $\tau_2 = 0.01$ $\tau_3 = 0.51$ $\tau_4 = 0.04$ $\tau_5 = 0.32$	
Min(F)	$\lambda_1 = 1.67$ $\lambda_2 = 0.5$ $\lambda_3 = 6.0$ $\lambda_4 = 0.5$ $\lambda_5 = 3.64$ $\mu = 0.07$	$K = -64.9$ $M = 0.03$ $F = 0.006$	$\tau_1 = 0.29$ $\tau_2 = -0.21$ $\tau_3 = 0.35$ $\tau_4 = 0.15$ $\tau_5 = 0.31$	

5.11.2 A pentaglidle with parallel arrangement of guides

Consider the quadratically-solvable example developed in Section 5.9.3 for which \mathcal{B} is at infinity and all \mathcal{B} -lines are parallel (its reconfigurable counterpart appears in Fig. 5.27). For this example, λ_i denotes the distance from each attachment to a line crossing perpendicularly all the \mathcal{B} -lines. By choosing properly the reference frame, all \mathcal{B} -lines are parallel to the y axis, and the crossing line coincides with the x axis, so that $\lambda_i = y_i$ for $i = 1, \dots, 5$.

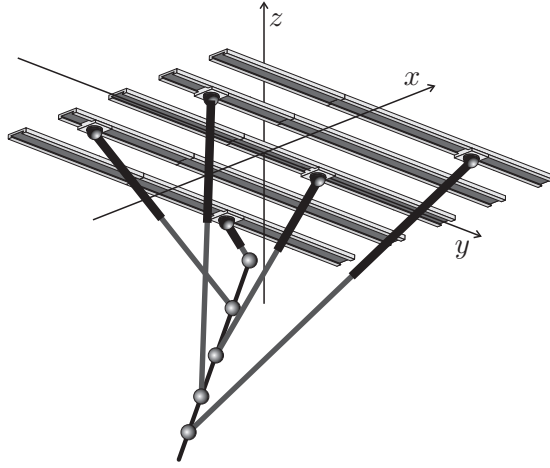


Figure 5.27: A reconfigurable Line-Plane prototype.

With this parametrization, the cofactors of \mathbf{T} are

$$C_1 = -K, C_2 = K, C_3 = \dots = C_6 = 0 \quad (5.56)$$

and the Jacobian matrix determinant is given by

$$\det(\mathbf{J}) = K((u-1)p_z - p_x w)w \quad (5.57)$$

where the constant factor is now given by

$$K = 2(9\lambda_2\lambda_5 + \lambda_5\lambda_4 + 6\lambda_3\lambda_4 + \lambda_2\lambda_1 + 9\lambda_1\lambda_4 - 6\lambda_3\lambda_5 + 6\lambda_3\lambda_2 - 6\lambda_3\lambda_1 - 4\lambda_1\lambda_5 - 16\lambda_2\lambda_4) \quad (5.58)$$

In this case, the distance measure to the architectural singularity, given in equation (5.50), coincides exactly with the constant factor

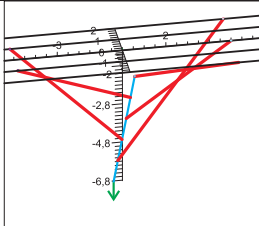
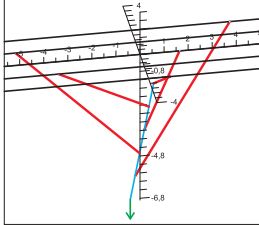
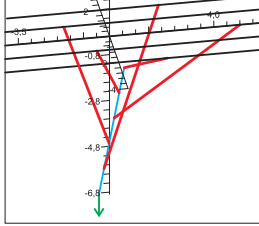
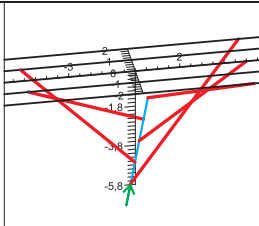
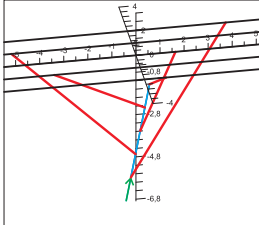
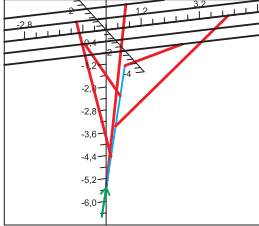
$$\mathcal{C}(B_x, B_y) = K. \quad (5.59)$$

5.11 Applications on reconfigurable pentapods

Optimization results for this example can be found in Table 5.2. The limits given for the guides are $-5 \leq \lambda_i \leq 5$ for $i = 1, \dots, 5$.

5.11 Applications on reconfigurable pentapods

Table 5.2: Optimization of the quadratically-solvable pentapod

$\mathbf{p} = (-1, 0, -3), \mathbf{i} = \frac{\sqrt{2}}{6}(1, 1, 4), \mathbf{F} = (0, 0, -1)$				
	Optimum	Values	Forces	
Max($ K $)	$\lambda_1 = 5.0$ $\lambda_2 = -5.0$ $\lambda_3 = 5.0$ $\lambda_4 = -5.0$ $\lambda_5 = 5.0$	$K = -3200$ $M = 0.96$ $F = 0.03$	$\tau_1 = 0.04$ $\tau_2 = -0.15$ $\tau_3 = -0.45$ $\tau_4 = -0.07$ $\tau_5 = 0.18$	
Max(M)	$\lambda_1 = 0.8982$ $\lambda_2 = -3.5652$ $\lambda_3 = 1.6421$ $\lambda_4 = -5.$ $\lambda_5 = 4.0862$	$K = -1257.1$ $M = 2.26$ $F = 0.08$	$\tau_1 = 0.02$ $\tau_2 = -0.06$ $\tau_3 = -0.57$ $\tau_4 = 0.01$ $\tau_5 = 0.16$	
Min(F)	$\lambda_1 = 1.8652$ $\lambda_2 = -0.6671$ $\lambda_3 = 5.0$ $\lambda_4 = -1.5846$ $\lambda_5 = 2.2309$ $\mu = 0.0470$	$K = -537.5$ $M = 1.46$ $F = 0.002$	$\tau_1 = 0.06$ $\tau_2 = -0.25$ $\tau_3 = -0.25$ $\tau_4 = -0.23$ $\tau_5 = 0.23$	
$\mathbf{p} = (-1, 0, -3), \mathbf{i} = \frac{\sqrt{2}}{6}(1, 1, 4), \mathbf{F} = -\mathbf{i}$				
	Optimum	Values	Forces	
Max($ K $)	$\lambda_1 = 5.0$ $\lambda_2 = -5.0$ $\lambda_3 = 5.0$ $\lambda_4 = -5.0$ $\lambda_5 = 5.0$	$K = -3200$ $M = 0.96$ $F = 0.002$	$\tau_1 = -0.003$ $\tau_2 = 0.09$ $\tau_3 = 0.23$ $\tau_4 = 0.05$ $\tau_5 = -0.03$	
Max(M)	$\lambda_1 = 0.8982$ $\lambda_2 = -3.5652$ $\lambda_3 = 1.6421$ $\lambda_4 = -5.,$ $\lambda_5 = 4.0862$	$K = -1257.1$ $M = 2.26$ $F = 0.006$	$\tau_1 = 0.01$ $\tau_2 = 0.04$ $\tau_3 = 0.30$ $\tau_4 = 0.01$ $\tau_5 = -0.02$	
Min(F)	$\lambda_1 = 1.9677$ $\lambda_2 = -1.0624$ $\lambda_3 = 4.1937$ $\lambda_4 = -0.6947$ $\lambda_5 = 1.3293$ $\mu = 0.0113$	$K = -354.9$ $M = 1.06$ $F = 0.0003$	$\tau_1 = -0.01$ $\tau_2 = 0.13$ $\tau_3 = 0.14$ $\tau_4 = 0.13$ $\tau_5 = -0.05$	

5.11 Applications on reconfigurable pentapods

Based on this architecture, a prototype has been build at IRI [see picture in Fig 5.28-(top)]. The spherical joints of the base are build using universal joints with an additional rotational axis, and they are all on actuated guides as show in Fig. 5.28-(bottom-left). The universal joints of the platform are aligned so that one of their axis is made coincident with the axe of the platform bar [Fig. 5.28-(bottom-right)].

5.11 Applications on reconfigurable pentapods

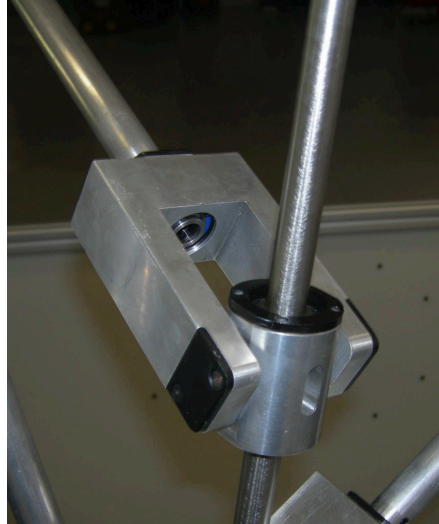
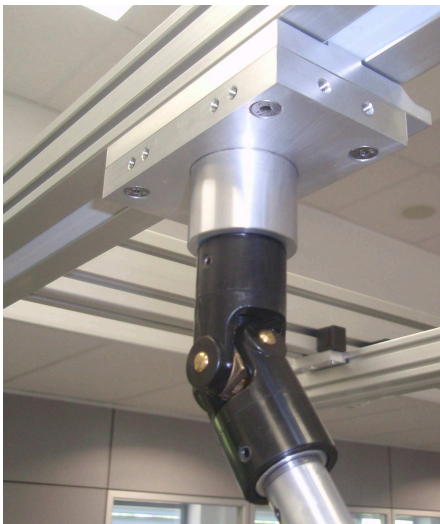


Figure 5.28: Prototype of the reconfigurable quadratically-solvable pentapod and its joint implementations.

Chapter 6

The Line-Body component

6.1 Rewriting the Jacobian matrix determinant

The Line-Body component is formed by five legs attached to a moving platform through collinear attachments. As in the previous section, let Λ denote the line to which these collinear attachments are incident. According to Fig. 6.1, the pose of Λ is defined by a position vector of a point in it, $\mathbf{p} = (p_x, p_y, p_z)^T$, and a unit vector, $\mathbf{i} = (i_x, i_y, i_z)^T$, pointing in its direction. Finally, let leg i have base and platform attachments with coordinates, in the base reference frame, $\mathbf{a}_i = (x_i, y_i, z_i)^T$ and $\mathbf{b}_i = \mathbf{p} + r_i \mathbf{i}$, $i = 1, \dots, 5$, respectively.

Let us assume a Stewart-Gough platform containing a Line-Body component. As it has been discussed before, the singularities of a Stewart-Gough platform are given by the determinant of the Jacobian matrix whose rows are the Plücker coordinates of the leg lines:

$$\mathbf{J} = \begin{pmatrix} \mathbf{c}_1^T \\ \vdots \\ \mathbf{c}_5^T \end{pmatrix} \text{ where } \mathbf{c}_i = \begin{pmatrix} \mathbf{b}_i - \mathbf{a}_i \\ \mathbf{a}_i \times (\mathbf{b}_i - \mathbf{a}_i) \end{pmatrix}.$$

Then, with the introduced notation,

$$\mathbf{c}_i = \begin{pmatrix} p_x + r_i i_x - x_i \\ p_y + r_i i_y - y_i \\ p_z + r_i i_z - z_i \\ z_i(p_y + r_i i_y) - y_i(p_z + r_i i_z) \\ x_i(p_z + r_i i_z) - z_i(p_x + r_i i_x) \\ y_i(p_x + r_i i_x) - x_i(p_y + r_i i_y) \end{pmatrix}$$

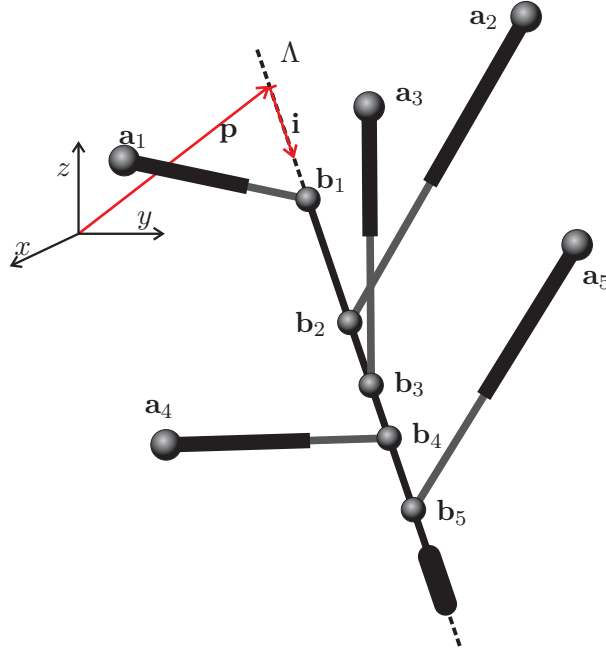


Figure 6.1: Notation associated with a Line-Body component.

for $i = 1, \dots, 5$.

As it has been said before, when a Stewart-Gough platform contains rigid components, the determinant of its Jacobian factors into several terms. For the analyzed platform, the Jacobian determinant factors as follows:

$$\det(\mathbf{J}) = F_1(\mathbf{c}_1, \dots, \mathbf{c}_5)F_2(\mathbf{c}_6), \quad (6.1)$$

where

$$F_2(\mathbf{c}_6) = (p_x - x_6)k_x + (p_y - y_6)k_y + (p_z - z_6)k_z$$

that depends on $\mathbf{k} = \mathbf{i} \times \mathbf{j}$, $\mathbf{R} = (\mathbf{i}, \mathbf{j}, \mathbf{k})$ being the rotation matrix defining the platform orientation. Thus, this factor only depends on the sixth leg, and $F_1(\mathbf{c}_1, \dots, \mathbf{c}_5)$ accounts for the singularities of the Line-Body component embedded in the considered platform. It can be checked, using a computer algebra system, that this polynomial

6.2 Singularity-invariant leg rearrangements rules

can be expressed as the determinant of the following matrix:

$$\mathbf{T} = \begin{pmatrix} 1 & i_x & i_y & i_z & p_x & p_y & p_z & 0 \\ 0 & p_x & p_y & p_z & 0 & 0 & 0 & 1 \\ 0 & 0 & 0 & 0 & i_x & i_y & i_z & 0 \\ r_1 & x_1 & y_1 & z_1 & r_1 x_1 & r_1 y_1 & r_1 z_1 & 1 \\ r_2 & x_2 & y_2 & z_2 & r_2 x_2 & r_2 y_2 & r_2 z_2 & 1 \\ r_3 & x_3 & y_3 & z_3 & r_3 x_3 & r_3 y_3 & r_3 z_3 & 1 \\ r_4 & x_4 & y_4 & z_4 & r_4 x_4 & r_4 y_4 & r_4 z_4 & 1 \\ r_5 & x_5 & y_5 & z_5 & r_5 x_5 & r_5 y_5 & r_5 z_5 & 1 \end{pmatrix}. \quad (6.2)$$

This is a very convenient representation of the singularities of a Line-Body component because the first three rows depend only on its pose and the remaining four, on the coordinates of the attachments.

Let $\hat{\mathbf{T}}$ denote the 5×8 matrix formed by the last five rows of \mathbf{T} . Since the coefficients of the singularity polynomial of the Line-Body component are the 5×4 minors of this matrix, the following two observations arise:

1. If $\hat{\mathbf{T}}$ is rank defective, the Line-Body component will always be singular irrespective of its leg lengths. In other words, it will be architecturally singular.
2. If one of the five rows of $\hat{\mathbf{T}}$ is substituted by another row linearly dependent on these five row vectors, the resulting matrix will have the same 5×5 minors up to a constant multiple. As in the previous chapter, this observation will allow, in the next section, to obtain leg rearrangements that leave the Line-Body component singularities invariant.

6.2 Singularity-invariant leg rearrangements rules

A leg rearrangement consist in the substitution of a leg i by another leg with base and platform attachment coordinates $\mathbf{a} = (x, y, z)^T$ and $\mathbf{b} = \mathbf{p}^T + r\mathbf{i}^T$, respectively. Next, the conditions that (x, y, z, r) must satisfy to leave the singularities of the Line-Body unaltered will be deduced.

6.2 Singularity-invariant leg rearrangements rules

To this end, consider the matrix

$$\mathbf{P} = \begin{pmatrix} r_1 & x_1 & y_1 & z_1 & r_1x_1 & r_1y_1 & r_1z_1 & 1 \\ r_2 & x_2 & y_2 & z_2 & r_2x_2 & r_2y_2 & r_2z_2 & 1 \\ r_3 & x_3 & y_3 & z_3 & r_3x_3 & r_3y_3 & r_3z_3 & 1 \\ r_4 & x_4 & y_4 & z_4 & r_4x_4 & r_4y_4 & r_4z_4 & 1 \\ r_5 & x_5 & y_5 & z_5 & r_5x_5 & r_5y_5 & r_5z_5 & 1 \\ r & x & y & z & rx & ry & rz & 1 \end{pmatrix} \quad (6.3)$$

and take (x, y, z, r) such that \mathbf{P} is rank defective. Then, if you substitute any row in $\hat{\mathbf{T}}$ by $(r, x, y, z, rx, ry, rz, 1)$, all the 5×5 minors of the resulting matrix will be equal to those of $\hat{\mathbf{T}}$ up to a constant multiple. Hence, the corresponding singularity polynomial will be also the same, up to a constant factor. In other words, if any of the legs of the analyzed Line-Body is substituted by another leg whose attachments coordinates are defined by a set of values for (x, y, z, r) that make \mathbf{P} rank defective, the singularity locus of the pentapod will remain unchanged.

If Gaussian Elimination is applied on \mathbf{P} , the last row of the resulting matrix is:

$$\frac{1}{P_{678}} (0 \ 0 \ 0 \ 0 \ 0 \ P_{78} \ P_{68} \ P_{67}),$$

where P_{ij} is the determinant of the matrix obtained from \mathbf{P} after removing the columns i and j , and P_{ijk} the determinant of the matrix formed by the first five rows of \mathbf{P} after removing the columns i , j and k . Then, assuming that $P_{567} \neq 0$, \mathbf{P} is rank defective

6.2 Singularity-invariant leg rearrangements rules

if, and only if,

$$\left. \begin{aligned}
 P_{78} &= \begin{vmatrix} r_1 & x_1 & y_1 & z_1 & r_1x_1 & r_1y_1 \\ r_2 & x_2 & y_2 & z_2 & r_2x_2 & r_2y_2 \\ r_3 & x_3 & y_3 & z_3 & r_3x_3 & r_3y_3 \\ r_4 & x_4 & y_4 & z_4 & r_4x_4 & r_4y_4 \\ r_5 & x_5 & y_5 & z_5 & r_5x_5 & r_5y_5 \\ r & x & y & z & rx & ry \end{vmatrix} = 0 \\
 P_{68} &= \begin{vmatrix} r_1 & x_1 & y_1 & z_1 & r_1x_1 & r_1z_1 \\ r_2 & x_2 & y_2 & z_2 & r_2x_2 & r_2z_2 \\ r_3 & x_3 & y_3 & z_3 & r_3x_3 & r_3z_3 \\ r_4 & x_4 & y_4 & z_4 & r_4x_4 & r_4z_4 \\ r_5 & x_5 & y_5 & z_5 & r_5x_5 & r_5z_5 \\ r & x & y & z & rx & rz \end{vmatrix} = 0 \\
 P_{67} &= \begin{vmatrix} r_1 & x_1 & y_1 & z_1 & r_1x_1 & 1 \\ r_2 & x_2 & y_2 & z_2 & r_2x_2 & 1 \\ r_3 & x_3 & y_3 & z_3 & r_3x_3 & 1 \\ r_4 & x_4 & y_4 & z_4 & r_4x_4 & 1 \\ r_5 & x_5 & y_5 & z_5 & r_5x_5 & 1 \\ r & x & y & z & rx & 1 \end{vmatrix} = 0
 \end{aligned} \right\} \quad (6.4)$$

Since this system is linear in x , y , and z , it can be rewritten, after cofactor expansion, in matrix form as:

$$\begin{pmatrix} P_{278} - P_{578}r & P_{678}r - P_{378} & P_{478} \\ P_{268} - P_{568}r & -P_{368} & P_{678}r + P_{468} \\ P_{267} - P_{567}r & -P_{367} & P_{467} \end{pmatrix} \begin{pmatrix} x \\ y \\ z \end{pmatrix} = \begin{pmatrix} P_{178}r \\ P_{168}r \\ P_{167}r - P_{678} \end{pmatrix}, \quad (6.5)$$

whose solution, using Cramer's rule, yields:

$$x = \frac{f_1(r)}{f(r)}, y = \frac{f_2(r)}{f(r)}, z = \frac{f_3(r)}{f(r)}, \quad (6.6)$$

where $f(r)$, $f_1(r)$, $f_2(r)$ and $f_3(r)$ are cubic polynomials in r . Thus, it can be concluded that all singularity-invariant leg substitutions will be defined by a correspondence between points on Λ and points on a cubic space curve attached to the base (Fig. 6.4).

In other words, for each platform attachment $\mathbf{b} = \mathbf{p} + r\mathbf{i}$, there is a point on the cubic curve defined by the coordinates in equation (6.6).

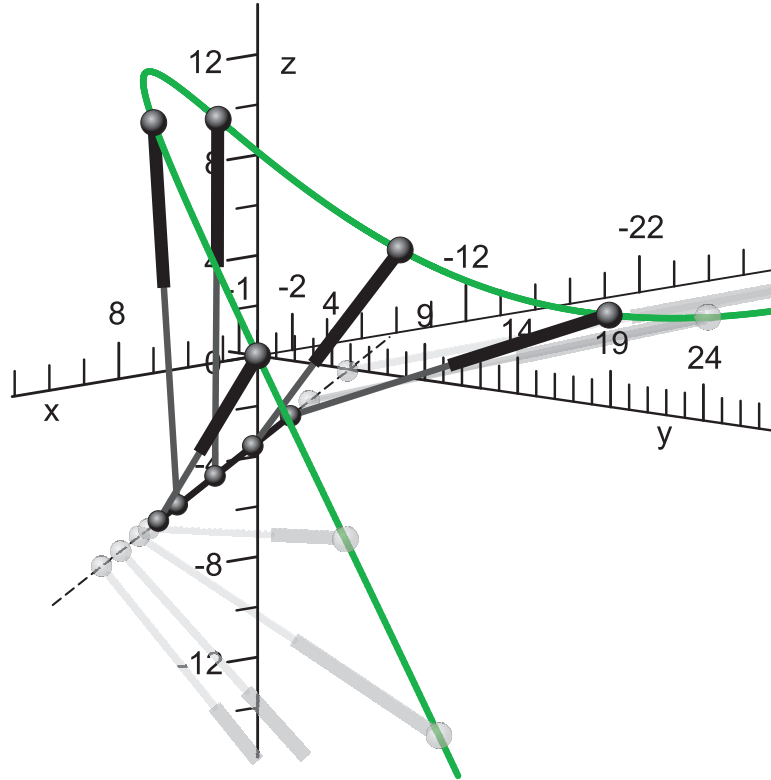


Figure 6.2: In general, a singularity-invariant leg substitution is defined by a 1-1 correspondence between the points on the moving platform and the points on a cubic attached to the base. Some candidates for a leg substitution appear in gray. The coordinates appearing in the graphic correspond to the numeric example in Section 6.5.1.

6.3 Classification of Line-Body designs

Generally, most interesting cases will occur when the cubic curve factor into lower degree terms, which are degenerate cases in which the determinant of the linear system (6.5) is null, *i.e.*, the case in which the solutions given by (6.6) are undefined because $f(r) = 0$ for a given r . In this case, two situations arise:

1. System (6.5) is consistent. One of the equations can be discarded and, for a given value of r , infinitely many solutions can be found for (x, y, z) which correspond to points of a line (as they correspond to the intersection of two planes).
2. System (6.5) is inconsistent. It represents a system of three parallel planes.

6.3 Classification of Line-Body designs

If the determinant of the linear system (6.5) is null, the system is consistent if, and only if, $f_1(r) = 0$, $f_2(r) = 0$, or $f_3(r) = 0$. Lets suppose that ρ_1 is a real root of $f(r) = 0$ that makes the system consistent. Then, one of the equations can be discarded and the system solution is the intersection line between the two remaining plane equations. In other words, if one of the platform attachments of the new leg is placed at $\mathbf{b}_{\rho_1} = \mathbf{p} + \rho_1 \mathbf{i}$, the corresponding base attachment can be placed at any point on the corresponding line in the base. Thus, there is a point-to-line correspondence, in a similar way as in the Point-Line component. Indeed, in this situation, an additional leg can be placed from \mathbf{b}_{ρ_1} to the line, forming a Point-Line component. Thus, the number of real roots of $f(r) = 0$ determine the number of Point-Line components, with the difference, with respect to Chapter 4, that now, a Point-Line component is not necessarily explicit, but it can be obtained through the proper leg rearrangement.

From now on, a distinction between *implicit* and *explicit* components will be made. An explicit component is the one containing all its legs. These components can be detected in a Stewart-Gough platform at a first glance. On the contrary, an implicit component appears after performing a set of singularity-invariant leg rearrangements.

The possible architectures of a pentapod can be classified depending on the number of real roots of $f(r) = 0$ that lead to a consistent linear system. Depending on this number, the cubic curve obtained for the general case degenerates into a plane conic curve and a line, or a set of lines. Table 6.1 summarizes the different possibilities.

Table 6.1: The 4 possible architectures for a pentapod

Number of consistent real roots	Base attachment locus
0	1 cubic curve
1	1 line and 1 plane conic
2	3 non-concurrent lines
3	3 concurrent lines

6.3.1 No consistent real roots

For any non-consistent real root, system (6.5) gives a solution line at infinity, but the finite curve is still of degree 3. This means that there is a finite attachment on the platform for which its corresponding attachment lies at infinity. Fig. 6.3 shows a

manipulator where $r = 2$ is a non-consistent real root of $f(r) = 0$. Same colors in the platform and in the base cubic represent corresponding points through (6.6). Such root appears in the platform as the discontinuity of colors between red and green, which correspond to points of the cubic curve approaching to infinity.

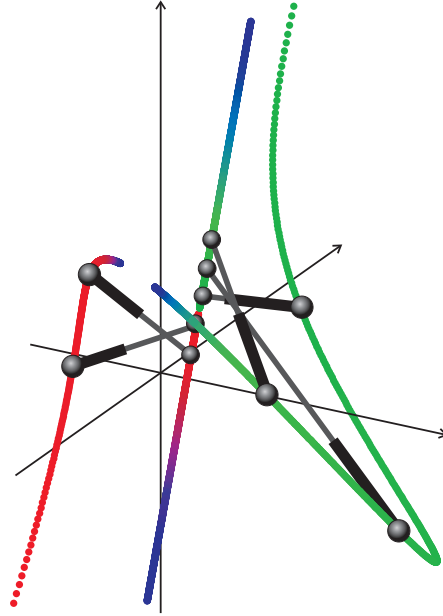


Figure 6.3: Corresponding colors in the platform and in the base cubic illustrate the correspondence when there are no consistent real roots.

This case represents the most general case of pentapods where the space cubic does not factor into lower degree curves. Note that there will always be at least one real root for the polynomial $f(r)$ because it is of degree 3 and complex roots appear in complex conjugate pairs.

6.3.2 One consistent real root

Suppose ρ_1 is the only real consistent root, then

$$\begin{aligned}
 f(r) &= (r - \rho_1)\tilde{f}(r), \\
 f_1(r) &= (r - \rho_1)\tilde{f}_1(r), \\
 f_2(r) &= (r - \rho_1)\tilde{f}_2(r), \\
 f_3(r) &= (r - \rho_1)\tilde{f}_3(r),
 \end{aligned}
 \tag{6.7}$$

6.3 Classification of Line-Body designs

where $\tilde{f}(r)$, $\tilde{f}_1(r)$, $\tilde{f}_2(r)$ and $\tilde{f}_3(r)$ are polynomials of degree 2 for which ρ_1 is not a root, *i.e.* $\tilde{f}(\rho_1) \neq 0$ and $\tilde{f}_i(\rho_1) \neq 0$ for $i = 1, 2, 3$. Then, the system (6.5) has two sets of solutions. First, when $r = \rho_1$, the system becomes degenerate so that only two of its equations are independent. Let p_{ρ_1} and q_{ρ_1} be that two independent equations. Note that they are linear in x , y and z . Then, the first solution set is

$$\Delta = \{(x, y, z, r) \mid r = \rho_1, q_{\rho_1}(x, y, z) = 0, p_{\rho_1}(x, y, z) = 0\}.$$

Interpreting this set of solutions in the space of leg attachments, it can be concluded that, for any attachment with platform coordinate $r = \rho_1$, the corresponding base attachment can be located on any point of the line defined by the intersection of the two planes p_{ρ_1} and q_{ρ_1} , say Λ_1 . Thus, this solution corresponds to a Point-Line component.

The second set of solutions can be obtained substituting (6.7) into the general solution obtained in equation (6.6), yielding

$$\mathcal{L} - \mathcal{C} = \left\{ (x, y, z, r) \mid r = \lambda, x = \frac{\tilde{f}_1(\lambda)}{\tilde{f}(\lambda)}, y = \frac{\tilde{f}_2(\lambda)}{\tilde{f}(\lambda)}, z = \frac{\tilde{f}_3(\lambda)}{\tilde{f}(\lambda)}; \lambda \in \mathbb{R} \right\}. \quad (6.8)$$

Interpreting this set of solutions in the space of leg attachments, a leg belongs to the set $\mathcal{L} - \mathcal{C}$ when its platform attachments lies in a point of Λ while its base attachment belong to a conic with parametric equation $\mathcal{C} = \{(x, y, z) \mid x = \frac{\tilde{f}_1(\lambda)}{\tilde{f}(\lambda)}, y = \frac{\tilde{f}_2(\lambda)}{\tilde{f}(\lambda)}, z = \frac{\tilde{f}_3(\lambda)}{\tilde{f}(\lambda)}; \lambda \in \mathbb{R}\}$. That is, this set represents a one-to-one correspondence between points on line Λ , and points on conic \mathcal{C} .

Note that \mathcal{C} is well defined also when $r = \rho_1$. Then, it can be concluded that line Λ_1 and conic \mathcal{C} have one intersecting point, because the evaluation of (6.8) at $r = \rho_1$ gives a point on the conic that must also belong to Λ_1 , precisely because $r = \rho_1$.

The existence of a factor of degree 1 implies that other factor is of degree 2 and, as a consequence, it defines a planar curve (all quadratic curves are planar). The other way round, if four of the attachments are coplanar, then the cubic factors into a line and a conic. Indeed, suppose that four attachments are coplanar. Then, choosing conveniently the reference frame and renumbering the attachments, $z_i = 0$ for $i = 1, 2, 3, 4$ without loss of generality. In this situation, note that the equation defined by $P_{68} = 0$ in (6.4) factors as

$$P_{68} = z(r - r_5)z_5K.$$

6.3 Classification of Line-Body designs

In other words, the second row of the augmented matrix of system (6.5) has the form

$$(0 \quad 0 \quad (r - r_5)z_5K \quad 0),$$

and hence, $r = r_5$ makes such matrix rank deficient, *i.e.*, $r = r_5$ is a real root that makes the system consistent. The cubic curve attached to the base degenerates into line Λ_1 and conic \mathcal{C} , with one coincident point. Finally, note that there can only be two attachments placed on Λ_1 , whose corresponding platform attachments must coincide, because the solution Δ implies the existence of a Point-Line component. Therefore, three situations can arise

- Two attachments coincident on the platform, whose corresponding base attachments are on line Λ_1 . Then, two legs form an explicit Point-Line component.
- Four base attachments are coplanar and belonging \mathcal{C} . The remaining leg base attachment lies on Λ_1 . Thus, there is an implicit Point-Line component.
- All the base attachments are coplanar and belong to the conic. This would lead to an architectural singularity, because all points belong to a conic section in projective correspondence (the projectivity given by (6.8)).

In Section 6.5.2 a numerical example is presented.

6.3.3 Two consistent real roots

Suppose now that $r = \rho_1$ and $r = \rho_2$ are the only two consistent roots. Then, necessarily, the third one must be non-consistent.

$$\begin{aligned} f(r) &= (r - \rho_1)(r - \rho_2)(r - \rho_3), \\ f_1(r) &= k_1(r - \rho_1)(r - \rho_2)(r - \rho_4), \\ f_2(r) &= k_2(r - \rho_1)(r - \rho_2)(r - \rho_5), \\ f_3(r) &= k_3(r - \rho_1)(r - \rho_2)(r - \rho_6), \end{aligned} \tag{6.9}$$

with $\rho_3 \neq \rho_i$ for $i = 4, 5, 6$. Then, system (6.5) has 3 different solution sets. Two of them corresponding to Point-Line components:

$$\Delta_1 = \{(x, y, z, r) \mid r = \rho_1, q_1(x, y, z) = 0, p_1(x, y, z) = 0\}$$

$$\Delta_2 = \{(x, y, z, r) \mid r = \rho_2, q_2(x, y, z) = 0, p_2(x, y, z) = 0\}$$

6.3 Classification of Line-Body designs

where p_i, q_i are two independent equations from system (6.5) after substituting r by ρ_i (similarly as done in the previous case). Each Point-Line component defines the line Λ_i given by the intersection of planes p_i and q_i , $i = 1, 2$.

The other solution set can be obtained substituting (6.9) in the general solution obtained in (6.6), yielding

$$\mathcal{L} = \left\{ (x, y, z, r) \mid r = \lambda, x = k_1 \frac{\lambda - \rho_4}{\lambda - \rho_3}, y = k_2 \frac{\lambda - \rho_5}{\lambda - \rho_3}, z = k_3 \frac{\lambda - \rho_6}{\lambda - \rho_3}; \lambda \in \mathbb{R} \right\}.$$

Again, interpreting this solution in the space of leg attachments, for each platform point in Λ , described by the coordinate r , the solution set \mathcal{L} gives a point on a parametric line attached to the base (and vice-versa). Let Λ_3 be such line in the base. The platform point with coordinate $r = \rho_3$ corresponds to the point at infinity of Λ_3 .

Again, note that Λ_3 is well defined also when $r = \rho_i$, $i=1,2$. As a consequence, Λ_1 and Λ_2 intersect Λ_3 on the points

$$\left(\frac{k_1(\rho_1 - \rho_4)}{\rho_1 - \rho_3}, \frac{k_2(\rho_1 - \rho_5)}{\rho_1 - \rho_3}, \frac{k_3(\rho_1 - \rho_6)}{\rho_1 - \rho_3} \right) \text{ and } \left(\frac{k_1(\rho_2 - \rho_4)}{\rho_2 - \rho_3}, \frac{k_2(\rho_2 - \rho_5)}{\rho_2 - \rho_3}, \frac{k_3(\rho_2 - \rho_6)}{\rho_2 - \rho_3} \right),$$

respectively.

Finally, Λ_1 and Λ_2 do not intersect. This can be proved by *reductio ad absurdum*. To this end, suppose that Λ_1 and Λ_2 intersect at $\mathbf{a}_0 = (x_0, y_0, z_0)$, this means that one leg can be rearranged to go from \mathbf{a}_0 to $\mathbf{b}_{\rho_1} = \mathbf{p} + \rho_1 \mathbf{i}$ and another leg from \mathbf{a}_0 to \mathbf{b}_{ρ_2} . Then, there is a Point-Line component with the point defined by \mathbf{a}_0 and, using results in Chapter 4, singularity-invariant leg rearrangements can be done so that one of these legs can be substituted by another one from \mathbf{a}_0 to any \mathbf{b}_ρ . This is a contradiction with the solution set \mathcal{L} because, for any value of r , there is only one possible attachment, which is different for each r .

In conclusion, the locus of the cubic curve for this family degenerates into 3 lines in space: two skew lines Λ_1 and Λ_2 and a third line Λ_3 crossing them. In Section 6.5.3 a numerical example is presented.

6.3.4 Three consistent real roots

Proceeding in a similar way as before, the existence of three consistent real roots ρ_1 , ρ_2 and ρ_3 implies that

$$\begin{aligned}
 f(r) &= (r - \rho_1)(r - \rho_2)(r - \rho_3), \\
 f_1(r) &= k_1(r - \rho_1)(r - \rho_2)(r - \rho_3), \\
 f_2(r) &= k_2(r - \rho_1)(r - \rho_2)(r - \rho_3), \\
 f_3(r) &= k_3(r - \rho_1)(r - \rho_2)(r - \rho_3),
 \end{aligned} \tag{6.10}$$

First of all, is it clear that there are 3 Point-Line components corresponding to the solution sets

$$\begin{aligned}
 \Delta_1 &= \{(x, y, z, r) \mid r = \rho_1, q_1(x, y, z) = 0, p_1(x, y, z) = 0\} \\
 \Delta_2 &= \{(x, y, z, r) \mid r = \rho_2, q_2(x, y, z) = 0, p_2(x, y, z) = 0\} \\
 \Delta_3 &= \{(x, y, z, r) \mid r = \rho_3, q_3(x, y, z) = 0, p_3(x, y, z) = 0\}
 \end{aligned}$$

where q_i, p_i are two independent equations from the system (6.5) after substituting r by ρ_i , for $i = 1, 2, 3$. Let Λ_i be the line given by the intersection of the planes q_i and p_i .

Secondly, there is an additional Point-Line component. To find it, substitute (6.10) into the general solution given by (6.6) and consider any value of $r \neq \rho_i$ for $i = 1, 2, 3$. The resulting solution set is

$$\Delta_4 = \{(x, y, z, r) \mid r = \lambda, x = k_1, y = k_2, z = k_3, \lambda \in \mathbb{R}\}$$

which means that any leg whose base attachment is $\mathbf{a} = (k_1, k_2, k_3)$ can be rearranged to any platform attachment $\mathbf{b} = \mathbf{p} + r\mathbf{i}$. In other words, it corresponds to an upside-down Point-Line component, where the line of the component is Λ .

Finally, for any $i = 1, 2, 3$, consider a leg from the platform attachment $\mathbf{b}_{\rho_i} = \mathbf{p} + \rho_i\mathbf{i}$ to the base attachment $\mathbf{a} = (k_1, k_2, k_3)$. On the first hand, these legs belong to the solution set Δ_4 for $\Lambda = \rho_i$ for $i = 1, 2, 3$. On the other hand, they also belong to the solution set Δ_i , thus, \mathbf{a} must be on the line Λ_i . As a consequence, \mathbf{a} belongs to the three lines, Λ_1, Λ_2 and Λ_3 .

In conclusion, the cubic curve degenerates into three lines intersecting at $\mathbf{a} = (k_1, k_2, k_3)$.

Section 6.5.4 shows a numerical example of a manipulator of this type.

6.4 Architectural singularities

The architectural singularities of a Line-Body component will be defined by those geometric parameters that make $\hat{\mathbf{T}}$ rank-deficient. In this section it will be shown how, rearranging a single leg, no architectural singularities can be obtained in general.

Consider the 5×8 matrix

$$\hat{\mathbf{T}} = \begin{pmatrix} r_1 & x_1 & y_1 & z_1 & r_1x_1 & r_1y_1 & r_1z_1 & 1 \\ r_2 & x_2 & y_2 & z_2 & r_2x_2 & r_2y_2 & r_2z_2 & 1 \\ r_3 & x_3 & y_3 & z_3 & r_3x_3 & r_3y_3 & r_3z_3 & 1 \\ r_4 & x_4 & y_4 & z_4 & r_4x_4 & r_4y_4 & r_4z_4 & 1 \\ r_5 & x_5 & y_5 & z_5 & r_5x_5 & r_5y_5 & r_5z_5 & 1 \end{pmatrix}.$$

The rank-deficiency of this matrix can be characterized by performing Gaussian Elimination on it, which leads to a row with 4 zero elements of the form

$$\frac{1}{P_{5678}} (0 \ 0 \ 0 \ 0 \ P_{678} \ P_{578} \ P_{568} \ P_{567})$$

where P_{5678} is the determinant of the matrix obtained from the first 4 rows of \mathbf{P} after removing columns 5, 6, 7 and 8, that is,

$$P_{5678} = \begin{vmatrix} r_1 & x_1 & y_1 & z_1 \\ r_2 & x_2 & y_2 & z_2 \\ r_3 & x_3 & y_3 & z_3 \\ r_4 & x_4 & y_4 & z_4 \end{vmatrix}.$$

Note that $P_{5678} = 0$ if, and only if, \mathbf{a}_i for $i = 1, 2, 3, 4$ are coplanar.

Now suppose that the fifth leg is rearranged, and its new attachment coordinates are (x, y, z, r) . Then, the locus of poses of the fifth leg attachments that make the manipulator architecturally singular is defined by the system $P_{678} = 0, P_{578} = 0, P_{568} = 0, P_{567} = 0$ where x_5, y_5, z_5 and r_5 have been substituted by x, y, z and r .

First of all, note that $\{x = x_i, y = y_i, z = z_i, r = r_i\}$ for $i = 1, 2, 3, 4$ are solutions of the system, because they will make the coordinates of the fifth leg coincide with one of

the existent legs. Therefore, such a rearrangement would lead to a trivial architectural singularity.

Now, it will be shown that the system has no more solutions. First, the system is rearranged in the following matrix form

$$\mathbf{M}(r) \begin{pmatrix} x \\ y \\ z \end{pmatrix} = \mathbf{m}(r)$$

where $\mathbf{M}(r)$ and $\mathbf{m}(r)$ are a matrix and a vector depending on r . The augmented matrix of this system is a 4×4 matrix of the form $(\mathbf{M}|\mathbf{m})$, and the solutions of the system must correspond to zeros of $\det(\mathbf{M}|\mathbf{m})$. In other words, for each solution of the system $\{P_{678} = 0, P_{578} = 0, P_{568} = 0, P_{567} = 0\}$, the corresponding value for r must be a root of $\det(\mathbf{M}|\mathbf{m})$.

Using a symbolic computation tool, it can be checked that

$$\det(\mathbf{M}|\mathbf{m}) = \frac{(r - r_1)(r - r_2)(r - r_3)(r - r_4)K}{P_{5678}}$$

where

$$\begin{aligned} K = & (x_3y_2 - x_3y_4 - x_2y_3 + x_2y_4 - x_4y_2 + x_4y_3)z_1 \\ & + (x_1y_3 - x_3y_1 + x_4y_1 - x_4y_3 - x_1y_4 + x_3y_4)z_2 \\ & + (x_4y_2 + x_1y_4 - x_1y_2 - x_4y_1 + x_2y_1 - x_2y_4)z_3 \\ & + (x_3y_1 - x_1y_3 - x_2y_1 - x_3y_2 + x_1y_2 + x_2y_3)z_4 \end{aligned}$$

is a constant. Thus, the only solutions of the system correspond to the other 4 legs.

For some cases not in general position, rearranging a leg could lead to an architectural singularity. For example, for the family with one real consistent root, the existence of a conic implies that 4 of the attachments are already coplanar. Therefore, $P_{5678} = 0$. Then, in Section 6.3.2, it has been shown that if the fifth leg is made coplanar, the manipulator become architecturally singular.

6.5 Examples

In this section, for each type of pentapod listed in Table 6.1, a numerical example is analyzed.

6.5.1 No consistent real roots

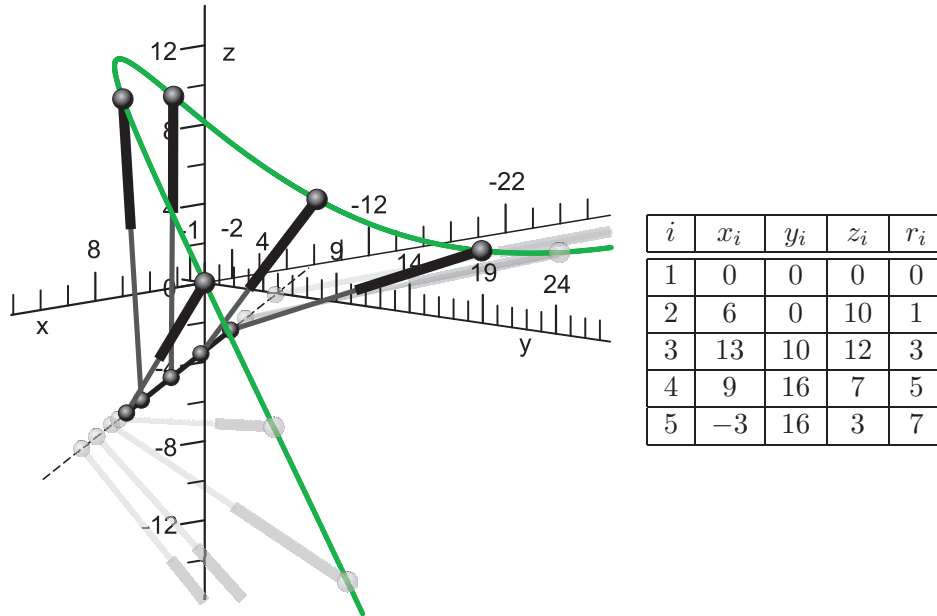


Figure 6.4: Generic pentapod analyzed in Section 6.5.1 with its corresponding attachment coordinates $(\mathbf{a}_i = (x_i, y_i, z_i)^T, \mathbf{b}_i = \mathbf{p} + r_i \mathbf{i})$.

Consider the pentapod in Fig. 6.4. To guarantee the rank-deficiency of \mathbf{P} in (6.3) after substituting the values, the following systems of equations must be satisfied:

$$\begin{pmatrix} 288r - 6612 & 6306 & 5676 \\ -3136 & 288r + 3904 & 3520 \\ 1076 & -2306 & 288r - 1484 \end{pmatrix} \begin{pmatrix} x \\ y \\ z \end{pmatrix} = \begin{pmatrix} 18816r \\ 16384r \\ -5504r \end{pmatrix}, \quad (6.11)$$

whose determinant is $2654208(9r^3 - 131r^2 - r - 1365)$. The roots are 15.22 , $-0.33 + 3.14i$, and $-0.33 - 3.14i$. The evaluation of system (6.11) for $r = 15.22$ yields an inconsistent linear system. As a consequence, the base attachment locus for a leg substituting any of the legs of the analyzed pentapod that would leave its singularity locus invariant is a cubic.

Solving (6.11) using Cramer's rule gives

$$\begin{aligned} x &= \frac{12r(49r^2 - 240r - 553)}{9r^3 - 131r^2 - r - 1365}, \\ y &= \frac{256r(-23r + 2r^2 + 21)}{9r^3 - 131r^2 - r - 1365}, \\ z &= \frac{-4r(-880r + 4557 + 43r^2)}{9r^3 - 131r^2 - r - 1365}. \end{aligned}$$

Fig. 6.4 shows the manipulator and the cubic curve defined by these equations. All legs in gray satisfy the correspondence between r and (x, y, z) through the above curve parameterization, so any of the original pentapod legs can be substituted by any of these legs in gray without modifying the singularity locus of the analyzed pentapod.

For the point of the platform corresponding to the coordinate $r = 15.22$, the system (6.11) in homogeneous coordinates gives the solution line

$$(2.495592037y, y, -0.1308360559y, 0)_H$$

which lies at infinity. In practice, no attachment can be placed on $\mathbf{b} = \mathbf{p} + 15.22\mathbf{i}$.

6.5.2 One consistent real root

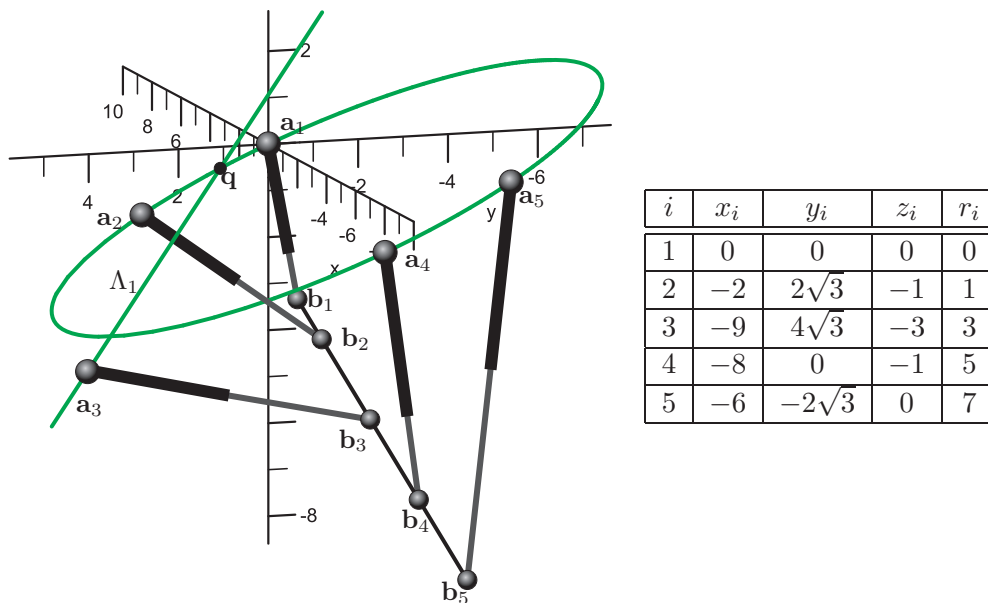


Figure 6.5: Pentapod analyzed in Section 6.5.2 and its corresponding attachment coordinates $(\mathbf{a}_i = (x_i, y_i, z_i)^T, \mathbf{b}_i = \mathbf{p} + r_i\mathbf{i})$. One consistent real root results in a base attachment locus formed by a line and a conic.

Consider the pentapod in Fig. 6.5. To guarantee the rank-deficiency of the matrix \mathbf{P} in (6.3) the following system of equations must be satisfied:

$$\begin{pmatrix} \sqrt{3}(-18r + 70) & 84 & 40\sqrt{3} \\ -144 & 18\sqrt{3}(1 - r) & 72 \\ 20\sqrt{3} & 24 & \sqrt{3}(50 - 18r) \end{pmatrix} \begin{pmatrix} x \\ y \\ z \end{pmatrix} = \begin{pmatrix} 24r\sqrt{3} \\ 216r \\ -24r\sqrt{3} \end{pmatrix}. \quad (6.12)$$

The solution of the above system, obtained using Cramer's rule, is

$$\begin{aligned} x &= \frac{-4r(r+11)}{3r^2-14r+35}, \\ y &= \frac{-12r(r-5)\sqrt{3}}{3r^2-14r+35}, \\ z &= \frac{4r(r-7)}{3r^2-14r+35}. \end{aligned}$$

which corresponds to a conic parameterized in r .

The determinant of system (6.12) is $-5832\sqrt{3}(3r^2-14r+35)(r-3)$. The only real root is $r=3$. After evaluating (6.12) for this real root, a consistent degenerate system is obtained whose solution is:

$$\Lambda_1 = \left\{ (x, y, z) \mid x = \lambda - 6, y = -\frac{2(\lambda-3)\sqrt{3}}{3}, z = \lambda; \lambda \in \mathbb{R} \right\},$$

that is, a line parameterized in λ . Note that the intersecting point of the conic and the line can be obtained substituting $r=3$ on the parameterized conic, yielding the point $\mathbf{q} = \left(\frac{-42}{5}, \frac{18\sqrt{3}}{5}, \frac{-12}{5}\right)$, which can also be obtained evaluating Λ_1 at $\lambda = \frac{-12}{5}$.

Summarizing, the locus of the base attachments consists of a line and a conic (see Fig. 6.5).

In the design process, is it possible to fix the location of the line beforehand, because one can always define a pentapod containing a Point-Line component. When this happens, the cubic curve attached to the platform will factor into a conic and a line, and the line will be defined by the two base attachments belonging to the Point-Line component. Later, the Point-Line can always be made to be implicit by rearranging one of its legs.

6.5.3 Two consistent real roots

In a similar way as in the previous example, a manipulator with two Point-Line components will correspond to the family of two real roots as long as the lines that define these components do not intersect at a point. Consider the pentapod in Fig. 6.6. It has two Point-Line components, the first one from \mathbf{b}_1 to Λ_1 and the second one from \mathbf{b}_3 to Λ_2 , and, thus, the cubic curve must factor into 3 lines.

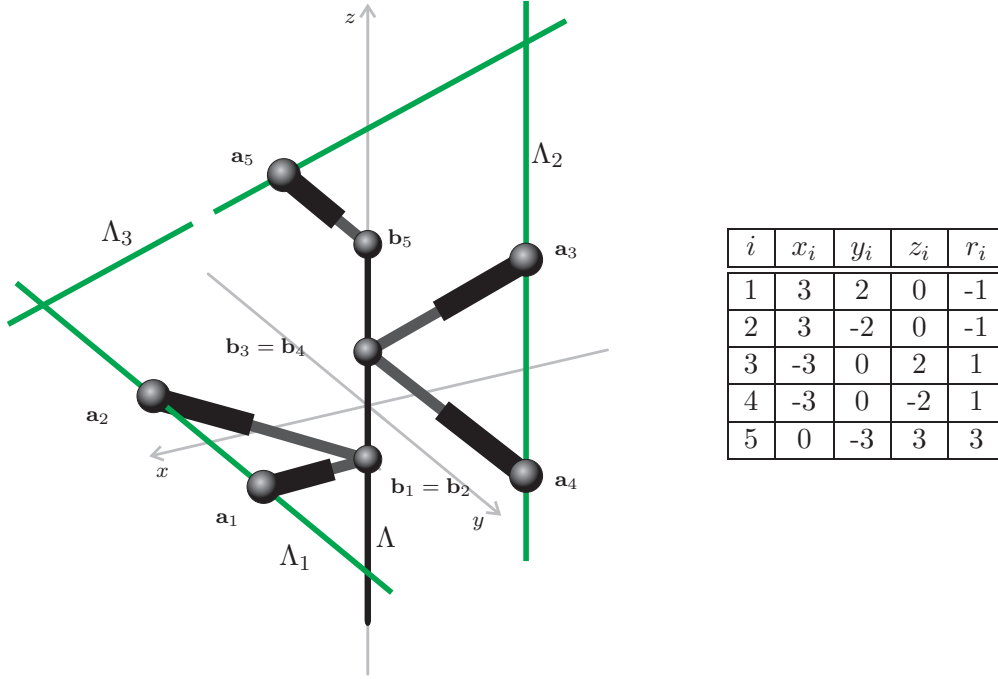


Figure 6.6: A pentapod with two real consistent roots analyzed in Section 6.5.3 and its attachment coordinates ($\mathbf{a}_i = (x_i, y_i, z_i)^T$, $\mathbf{b}_i = \mathbf{p} + r_i \mathbf{i}$).

After substituting the coordinates in equation (6.5), the system reads as

$$\begin{pmatrix} 1152 & 864 + 864r & 0 \\ -576 & 0 & 864r - 864 \\ 288r - 96 & 0 & 0 \end{pmatrix} \begin{pmatrix} x \\ y \\ z \end{pmatrix} = \begin{pmatrix} -3456r \\ 1728r \\ 288r - 864 \end{pmatrix}.$$

and its system determinant is $71663616(-1+3r)(1+r)(-1+r)$. The only non-consistent root is $r = 1/3$. The resolution of the system gives three solution sets:

$$\Delta_1 = \{(x, y, z, r) \mid r = 1, x = -3, y = 0, z = \lambda; \lambda \in \mathbb{R}\},$$

$$\Delta_2 = \{(x, y, z, r) \mid r = -1, x = 3, y = \lambda, z = 0; \lambda \in \mathbb{R}\},$$

$$\mathcal{L} = \{(x, y, z, r) \mid r = \lambda, x = \frac{3(-3+\lambda)}{-1+3\lambda}, y = -\frac{12(\lambda-1)}{3\lambda-1}, z = \frac{6(1+\lambda)}{3\lambda-1}; \lambda \in \mathbb{R}\}$$

Therefore, there are two point-line correspondences, and the last solution gives a point-to-point correspondence between two lines, the platform line Λ and Λ_3 with parametric equation $[x = \frac{3(-3+t)}{-1+3t}, y = -\frac{12(t-1)}{3t-1}, z = \frac{6(1+t)}{3t-1}]$. The legs with platform attachments coordinates $\mathbf{b}_1 = \mathbf{b}_2$ and $\mathbf{b}_3 = \mathbf{b}_4$ correspond to solutions in Δ_1, Δ_2 respectively. The fifth leg attachments correspond to the solution set \mathcal{L} (\mathbf{b}_5 corresponds to \mathbf{a}_5 following the parameterization in \mathcal{L}).

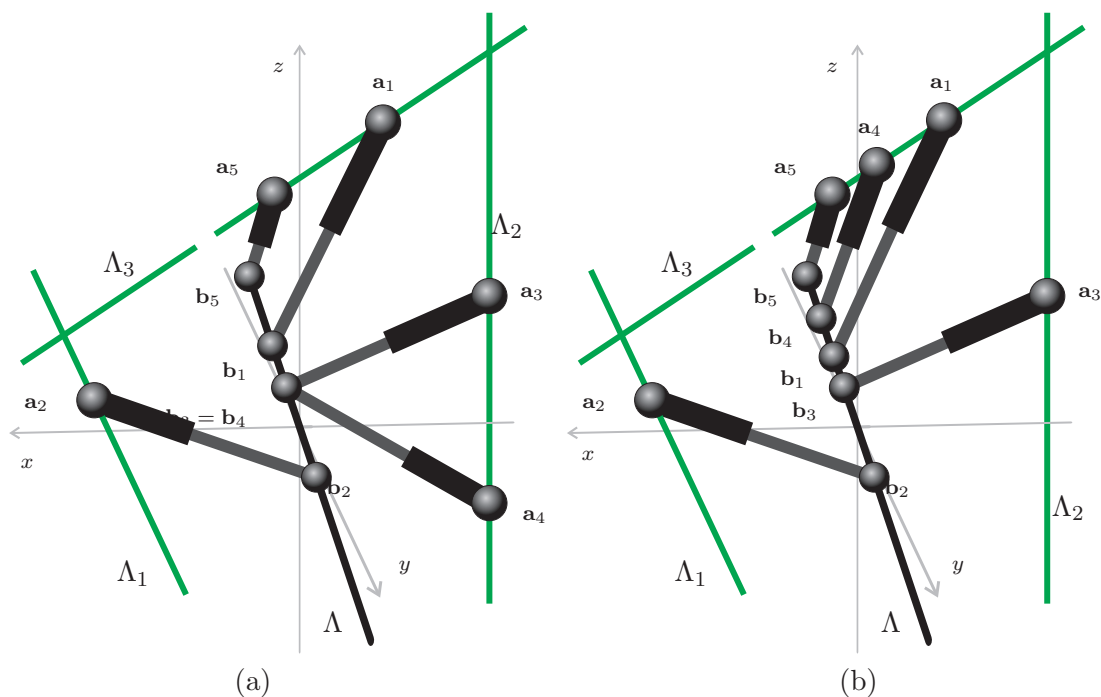


Figure 6.7: Two consistent real root results in a base attachment locus formed by 3 space lines crossing two by two.

Now, two possibilities arise:

- One Point-Line is made to disappear through a rearrangement. Then, the resulting manipulator has one remaining Point-Line component and two legs with attachments going from Λ_3 to Λ . In Fig. 6.7-(a), the first leg has been substituted by a new leg from $r = \frac{7}{5}$ to $(-3/2, -3/2, 9/2)$.
- Two Point-Line components are made to disappear through a rearrangement. Then, the resulting manipulator has three legs with attachments going from from Λ_3 to Λ . In Fig. 6.7-(b), also the fourth leg has been substituted by a leg from $r = 2$ to $(-3/5, -12/5, 18/5)$.

6.5.4 Three consistent real roots

Consider the pentapod in Fig. 6.8. Substituting the table values in (6.5) yields

$$\begin{pmatrix} 2304 - 512r & -128 & 128 \\ -256 & 2688 - 512r & 384 \\ 256 & 384 & 2688 - 512r \end{pmatrix} \begin{pmatrix} x \\ y \\ z \end{pmatrix} = \mathbf{0} \quad (6.13)$$

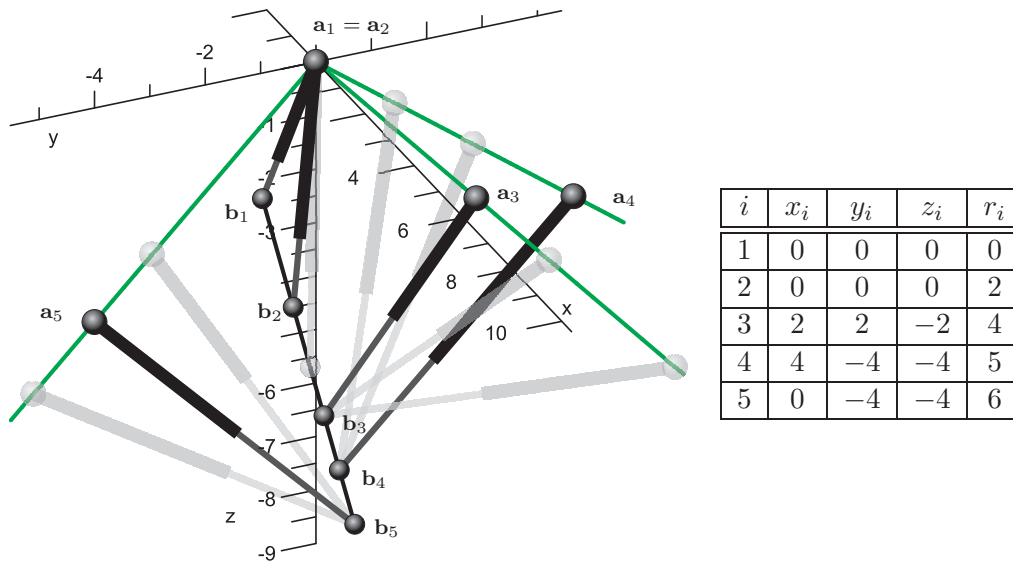


Figure 6.8: Pentapod analyzed in Section 6.5.4 and its attachment coordinates ($\mathbf{a}_i = (x_i, y_i, z_i)^T$, $\mathbf{b}_i = \mathbf{p} + r_i \mathbf{i}$). In this case the cubic curve degenerates into three lines.

whose determinant is $-134217728(r-5)(r-6)(r-4)$. All the roots are real and make the system consistent. This system has the trivial solution $x = y = z = 0$ for any value of r . In other words, any leg can be substituted, without modifying the singularities of the analyzed pentapod, by any other with attachments located at $(0, 0, 0)$ in the base and anywhere in the moving platform.

Now, consider one of the above roots, for example $r = 4$. The substitution of this value in (6.13) yields

$$\left. \begin{aligned} 2x - y + z &= 0 \\ 2x - 5y - 3z &= 0 \\ 2x + 3y + 5z &= 0 \end{aligned} \right\}$$

which is a consistent linear system. That is, the three plane equations intersect at the same line. Solving this system for x and y leads to a parametrization of such line: $\{(x, y, z) \mid x = -t, y = -t, z = t, t \in \mathbb{R}\}$. Proceeding in a similar way for the other two roots, two more line parameterizations are obtained. Summarizing, there are four solution sets, namely:

$$\Delta_1 = \{(x, y, z, r) \mid r = 4, x = -\lambda, y = -\lambda, z = \lambda; \lambda \in \mathbb{R}\}$$

$$\Delta_2 = \{(x, y, z, r) \mid r = 5, x = \lambda, y = -\lambda, z = \lambda; \lambda \in \mathbb{R}\}$$

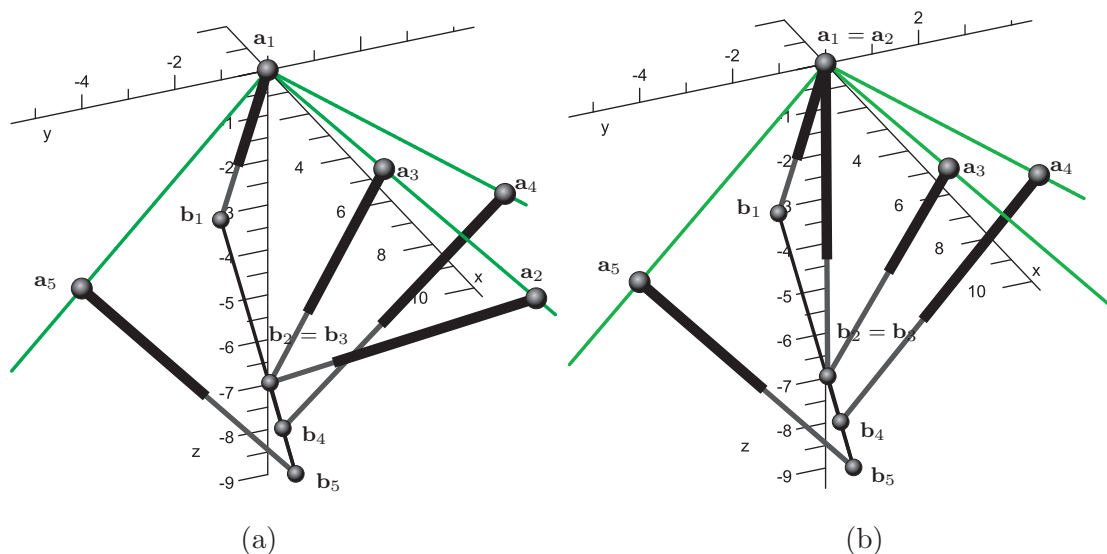


Figure 6.9: The base attachments can be moved along the lines without modifying the singularity locus of the pentapod. This permits coalescing two attachments in the moving platform (a), or two attachments in the base and the platform at the same time (b).

$$\Delta_3 = \{(x, y, z, r) \mid r = 6, x = 0, y = \lambda, z = \lambda; \lambda \in \mathbb{R}\}$$

$$\Delta_4 = \{(x, y, z, r) \mid r = \lambda, x = 0, y = 0, z = 0; \lambda \in \mathbb{R}\}$$

In Fig. 6.8, the legs in gray have attachments whose coordinates are in one of the above solution sets. The legs with platform attachments coordinates \mathbf{b}_3 , \mathbf{b}_4 and \mathbf{b}_5 correspond to solutions in Δ_1 , Δ_2 and Δ_3 , respectively. The solution set Δ_4 corresponds to legs with base attachment at $(0,0,0)$ and platform attachment anywhere in the moving platform line.

Several equivalent manipulators, from the point of view of their singularities, can be obtained by substituting only leg 2. For example, in Fig. 6.9-(a), this leg has been substituted by a leg whose attachments coordinates are in Δ_1 . Its attachments are $\mathbf{a}_2 = (4, 4, -4)$ and $\mathbf{b}_2 = \mathbf{p} + 4\mathbf{i}$, thus making coincident \mathbf{b}_2 and \mathbf{b}_3 . In Fig. 6.9-(b), leg 2 has been substituted by a leg whose attachments coordinates are in Δ_4 . In this case, the new attachments have coordinates $\mathbf{a}_2 = (0, 0, 0)$ and $\mathbf{b}_2 = \mathbf{p} + 4\mathbf{i}$ thus making coincident \mathbf{a}_1 with \mathbf{a}_2 , and \mathbf{b}_2 with \mathbf{b}_3 .

If actuated guides are placed on the lines defined by Δ_1 , Δ_2 , and Δ_3 , the ma-

nipulator can reconfigure its base attachments following singularity-invariant leg rearrangements. This increases its usable workspace because, though singularities remain unchanged, its stiffness does change at each reconfiguration, so that it can be optimized for each specific task at different regions of the workspace.

Chapter 7

The Plane-Plane component

7.1 Finding the affine relation between leg lengths

The Plane-Plane is the first component that represents a full Stewart-Gough platform, generally called doubly-planar Stewart-Gough platform to denote that both base and platform attachments are coplanar. Its singularity-invariant leg rearrangements were first studied in [16]. Here, the results presented therein are extended.

Following the notation introduced in Chapter 3, the Plane-Plane component has, for each leg i , a base attachment with coordinates $\mathbf{a}_i = (x_i, y_i, 0)^T$ and a platform attachment whose coordinates are $\mathbf{b}_i = \mathbf{p} + \mathbf{R}(z_i, t_i, 0)^T$.

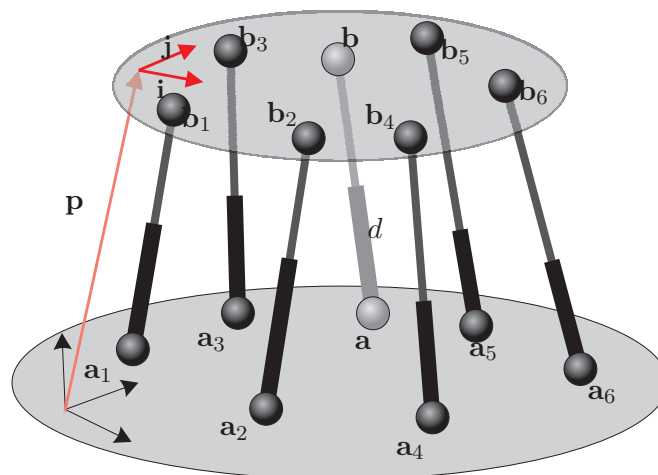


Figure 7.1: Notation associated with a Plane-Plane component.

7.1 Finding the affine relation between leg lengths

In this case, a leg rearrangement with coordinates (x, y, z, t) stands for the substitution of any of the legs by another one going from the base attachment located at $\mathbf{a} = (x, y, 0)^T$ to the platform attachment at $\mathbf{b} = \mathbf{p} + \mathbf{R}(z, t, 0)^T$ (Fig. 7.1). In a similar way as in Section 5.2, the corresponding affine relation will be found by computing the length of the introduced leg, $d^2 = \|\mathbf{b} - \mathbf{a}\|^2$. To this end, consider the system

$$\left. \begin{array}{l} (\mathbf{a}_1 - \mathbf{b}_1)^2 = l_1^2 \\ \vdots \\ (\mathbf{a}_6 - \mathbf{b}_6)^2 = l_6^2 \\ (\mathbf{a} - \mathbf{b})^2 = d^2 \end{array} \right\}$$

Subtracting the equations $i_x^2 + i_y^2 + i_z^2 = 1$ and $j_x^2 + j_y^2 + j_z^2 = 1$, and using the relation $\mathbf{i} \cdot \mathbf{j} = i_x j_x + i_y j_y + i_z j_z = 0$, quadratic terms in the rotation variables cancel out, yielding

$$\left. \begin{array}{l} -\frac{p_x^2 + p_y^2 + p_z^2}{2} - z_1 u - t_1 v + x_1 p_x + y_1 p_y + x_1 z_1 i_x + y_1 z_1 i_y + x_1 t_1 j_x + y_1 t_1 j_y - k_1 = 0 \\ \vdots \\ -\frac{p_x^2 + p_y^2 + p_z^2}{2} - z_6 u - t_6 v + x_6 p_x + y_6 p_y + x_6 z_6 i_x + y_6 z_6 i_y + x_6 t_6 j_x + y_6 t_6 j_y - k_6 = 0 \\ -\frac{p_x^2 + p_y^2 + p_z^2}{2} - z u - t v + x p_x + y p_y + x z i_x + y z i_y + x t j_x + y t j_y - k + d^2/2 = 0 \end{array} \right\}$$

where $u = \mathbf{p} \cdot \mathbf{i}$, $v = \mathbf{p} \cdot \mathbf{j}$, and the constant factors $k_i = \frac{1}{2}(x_i^2 + y_i^2 + z_i^2 + t_i^2 - l_i^2)$ and $k = \frac{1}{2}(x^2 + y^2 + z^2 + t^2)$.

Subtracting the first equation from the others, quadratic terms in p_x , p_y and p_z cancel too, yielding six linear equations in the 9 unknowns p_x , p_y , u , v , i_x , i_y , j_x , j_y and d^2 which can be rewritten in matrix form as:

$$\mathbf{Q} \begin{pmatrix} u \\ v \\ p_x \\ p_y \\ i_x \\ i_y \\ j_x \\ j_y \\ d^2 \end{pmatrix} = \begin{pmatrix} k_2 - k_1 \\ k_3 - k_1 \\ k_4 - k_1 \\ k_5 - k_1 \\ k_6 - k_1 \\ k - k_1 \end{pmatrix}, \quad (7.1)$$

7.1 Finding the affine relation between leg lengths

where

$$\mathbf{Q} = \begin{pmatrix} z_1 - z_2 & t_1 - t_2 & x_2 - x_1 & y_2 - y_1 & x_2 z_2 - x_1 z_1 & y_2 z_2 - y_1 z_1 & x_2 t_2 - x_1 t_1 & y_2 t_2 - y_1 t_1 & 0 \\ z_1 - z_3 & t_1 - t_3 & x_3 - x_1 & y_3 - y_1 & x_3 z_3 - x_1 z_1 & y_3 z_3 - y_1 z_1 & x_3 t_3 - x_1 t_1 & y_3 t_3 - y_1 t_1 & 0 \\ z_1 - z_4 & t_1 - t_4 & x_4 - x_1 & y_4 - y_1 & x_4 z_4 - x_1 z_1 & y_4 z_4 - y_1 z_1 & x_4 t_4 - x_1 t_1 & y_4 t_4 - y_1 t_1 & 0 \\ z_1 - z_5 & t_1 - t_5 & x_5 - x_1 & y_5 - y_1 & x_5 z_5 - x_1 z_1 & y_5 z_5 - y_1 z_1 & x_5 t_5 - x_1 t_1 & y_5 t_5 - y_1 t_1 & 0 \\ z_1 - z_6 & t_1 - t_6 & x_6 - x_1 & y_6 - y_1 & x_6 z_6 - x_1 z_1 & y_6 z_6 - y_1 z_1 & x_6 t_6 - x_1 t_1 & y_6 t_6 - y_1 t_1 & 0 \\ z_1 - z & t_1 - t & x - x_1 & y - y_1 & xz - x_1 z_1 & yz - y_1 z_1 & xt - x_1 t_1 & yt - y_1 t_1 & \frac{1}{2} \end{pmatrix}.$$

Note that only k_i depends on l_i , for $i = 1, \dots, 6$.

Now, let \mathbf{Q}_{ijk} be the square matrix obtained from \mathbf{Q} after deleting columns i , j and k , and Q_{ijk} its determinant. System (7.1) can be solved taking three unknowns as parameters, for example u , v , p_x . The resulting linear system is:

$$\mathbf{Q}_{123} \begin{pmatrix} p_y \\ i_x \\ i_y \\ j_x \\ j_y \\ d^2 \end{pmatrix} = \begin{pmatrix} (z_2 - z_1)u + (t_2 - t_1)v - (x_2 - x_1)p_x + k_2 - k_1 \\ (z_3 - z_1)u + (t_3 - t_1)v - (x_3 - x_1)p_x + k_3 - k_1 \\ (z_4 - z_1)u + (t_4 - t_1)v - (x_4 - x_1)p_x + k_4 - k_1 \\ (z_5 - z_1)u + (t_5 - t_1)v - (x_5 - x_1)p_x + k_5 - k_1 \\ (z_6 - z_1)u + (t_6 - t_1)v - (x_6 - x_1)p_x + k_6 - k_1 \\ (z - z_1)u + (t - t_1)v - (x - x_1)p_x + k - k_1 \end{pmatrix}.$$

Solving this system for d^2 using Cramer's rule and then applying multi-linear properties of determinants to split the determinant of the resulting matrix into 4 determinants yields

$$d^2 = \frac{Q_{239}u + Q_{139}v + Q_{129}p_x + Q_{123}^*}{\frac{1}{2}Q_{123}}, \quad (7.2)$$

where Q_{123}^* is the determinant of \mathbf{Q}_{123} except for the last column that contains the elements $k_i - k_1$ for $i = 2, \dots, 6$ and $k - k_1$. As a result, imposing $Q_{239} = Q_{139} = Q_{129} = 0$, equation (7.2) becomes affine in l_1^2, \dots, l_6^2 . Indeed, expanding Q_{123}^* leads to an expression of the form

$$d^2 = c_1 l_1^2 + c_2 l_2^2 + c_3 l_3^2 + c_4 l_4^2 + c_5 l_5^2 + c_6 l_6^2 + c_0,$$

where all coefficients depend on known constants. Then, any leg rearrangement satisfying $Q_{239} = Q_{139} = Q_{129} = 0$ leaves singularities invariant. In other words, substituting any leg by a new leg with base attachment located at $\mathbf{a} = (x, y, 0)^T$ and platform attachment at $\mathbf{b} = \mathbf{p} + \mathbf{R}(z, t, 0)^T$, the singularities will remain invariant as long as (x, y, z, t) satisfies the system $Q_{239} = Q_{139} = Q_{129} = 0$, where Q_{ijk} can be simplified into a 7×7 determinant using simple row/column operations, yielding a system of the

7.1 Finding the affine relation between leg lengths

following three determinants equated to zero:

$$Q_{239} = \begin{vmatrix} y_1 & x_1z_1 & y_1z_1 & x_1t_1 & y_1t_1 & z_1 & 1 \\ y_2 & x_2z_2 & y_2z_2 & x_2t_2 & y_2t_2 & z_2 & 1 \\ y_3 & x_3z_3 & y_3z_3 & x_3t_3 & y_3t_3 & z_3 & 1 \\ y_4 & x_4z_4 & y_4z_4 & x_4t_4 & y_4t_4 & z_4 & 1 \\ y_5 & x_5z_5 & y_5z_5 & x_5t_5 & y_5t_5 & z_5 & 1 \\ y_6 & x_6z_6 & y_6z_6 & x_6t_6 & y_6t_6 & z_6 & 1 \\ y & xz & yz & xt & yt & z & 1 \end{vmatrix} = 0, \quad (7.3)$$

$$Q_{139} = \begin{vmatrix} y_1 & x_1z_1 & y_1z_1 & x_1t_1 & y_1t_1 & t_1 & 1 \\ y_2 & x_2z_2 & y_2z_2 & x_2t_2 & y_2t_2 & t_2 & 1 \\ y_3 & x_3z_3 & y_3z_3 & x_3t_3 & y_3t_3 & t_3 & 1 \\ y_4 & x_4z_4 & y_4z_4 & x_4t_4 & y_4t_4 & t_4 & 1 \\ y_5 & x_5z_5 & y_5z_5 & x_5t_5 & y_5t_5 & t_5 & 1 \\ y_6 & x_6z_6 & y_6z_6 & x_6t_6 & y_6t_6 & t_6 & 1 \\ y & xz & yz & xt & yt & t & 1 \end{vmatrix} = 0, \quad (7.4)$$

$$Q_{129} = \begin{vmatrix} y_1 & x_1z_1 & y_1z_1 & x_1t_1 & y_1t_1 & -x_1 & 1 \\ y_2 & x_2z_2 & y_2z_2 & x_2t_2 & y_2t_2 & -x_2 & 1 \\ y_3 & x_3z_3 & y_3z_3 & x_3t_3 & y_3t_3 & -x_3 & 1 \\ y_4 & x_4z_4 & y_4z_4 & x_4t_4 & y_4t_4 & -x_4 & 1 \\ y_5 & x_5z_5 & y_5z_5 & x_5t_5 & y_5t_5 & -x_5 & 1 \\ y_6 & x_6z_6 & y_6z_6 & x_6t_6 & y_6t_6 & -x_6 & 1 \\ y & xz & yz & xt & yt & -x & 1 \end{vmatrix} = 0, \quad (7.5)$$

7.1.1 Generalizing and simplifying the condition

The above reasoning fails if $Q_{123} = 0$ but, for a non-architecturally singular manipulator, a set of parameters other than $\{u, v, p_x\}$ can be chosen, leading to a non-degenerate system. However, this may change the expression of the singularity-invariant leg rearrangement condition in equations (7.3)-(7.5). To avoid such ambiguity, the condition can be reformulated in terms of rank deficiency of the matrix \mathbf{Q}_9 (that is, matrix \mathbf{Q} in equation (7.1) without the last column). The submatrix of the 5 first rows of \mathbf{Q}_9 are full rank for any non-architecturally singular manipulator. Furthermore, \mathbf{Q}_9 is rank defective if, and only if, all its submatrices have null determinant. However, it is only necessary to check 3 of its 6×6 submatrices. Thus, the condition given by (7.3)-(7.5) is equivalent to the rank deficiency of \mathbf{Q}_9 . The advantage of this formulation is that any set of 3 6×6 submatrices could be used instead of (7.3)-(7.5).

7.2 Singularity-invariant leg rearrangement rules

To simplify the notation, consider the following matrix:

$$\mathbf{P} = \begin{pmatrix} -z_1 & -t_1 & x_1 & y_1 & x_1 z_1 & y_1 z_1 & x_1 t_1 & y_1 t_1 & 1 \\ -z_2 & -t_2 & x_2 & y_2 & x_2 z_2 & y_2 z_2 & x_2 t_2 & y_2 t_2 & 1 \\ -z_3 & -t_3 & x_3 & y_3 & x_3 z_3 & y_3 z_3 & x_3 t_3 & y_3 t_3 & 1 \\ -z_4 & -t_4 & x_4 & y_4 & x_4 z_4 & y_4 z_4 & x_4 t_4 & y_4 t_4 & 1 \\ -z_5 & -t_5 & x_5 & y_5 & x_5 z_5 & y_5 z_5 & x_5 t_5 & y_5 t_5 & 1 \\ -z_6 & -t_6 & x_6 & y_6 & x_6 z_6 & y_6 z_6 & x_6 t_6 & y_6 t_6 & 1 \\ -z & -t & x & y & xz & yz & xt & yt & 1 \end{pmatrix}. \quad (7.6)$$

Let P_{ij} be the determinant of the submatrix obtained from \mathbf{P} after deleting columns i and j , and P_{ijk} the determinant of the submatrix formed by the first 6 rows of \mathbf{P} after deleting columns i , j and k .

Note that $P_{ij} = Q_{ij9}$ for $i, j \neq 9$ and $P_{ijk} = \frac{1}{2}Q_{ijk}$ for $k \neq 9$. Using these relations, it can be proved that \mathbf{Q}_9 is rank defective if, and only if, \mathbf{P} is also rank defective. Thus, a much simpler condition can now be stated: a leg rearrangement with coordinates (x, y, z, t) leaves singularities invariant as long as matrix \mathbf{P} is rank defective.

Again, to check rank deficiency, Gaussian Elimination is applied on \mathbf{P} . The last row of the resulting matrix has 3 nonzero terms dependent on x, y, z and t . The corresponding 3 equations are equivalent to impose the conditions given by (7.3), (7.4), (7.5). Different equations arise depending on the order of the columns. For example, Gaussian Elimination on matrix \mathbf{P} as it appears in equation (7.6) leads to a matrix whose last row is

$$\frac{1}{P_{789}} (0 \ 0 \ 0 \ 0 \ 0 \ 0 \ P_{89} \ P_{79} \ P_{78}).$$

Then, as long as $P_{789} \neq 0$, the singularity-invariant leg rearrangements are defined by the condition

$$P_{89} = P_{79} = P_{78} = 0. \quad (7.7)$$

Alternatively, if the columns of \mathbf{P} are sorted as $[y, xz, yz, xt, yt, 1, -z, -t, x]$, then the corresponding condition is $P_{23} = P_{13} = P_{12} = 0$, provided that $P_{123} \neq 0$.

7.2 Singularity-invariant leg rearrangement rules

In this section, a geometric interpretation of the singularity-invariant condition is given, in a similar way as in the previous chapters.

7.2 Singularity-invariant leg rearrangement rules

Note that any equation consisting of a submatrix determinant P_{ij} equated to zero will be bilinear in the unknowns, but with different monomials. Consider the condition given in (7.7) which, after cofactor expansion, leads to

$$\left. \begin{aligned} -P_{891}z + P_{892}t + P_{893}x - P_{894}y + P_{895}xz - P_{896}yz + P_{897}xt &= 0 \\ -P_{791}z + P_{792}t + P_{793}x - P_{794}y + P_{795}xz - P_{796}yz + P_{798}yt &= 0 \\ -P_{781}z + P_{782}t + P_{783}x - P_{784}y + P_{785}xz - P_{786}yz + P_{789} &= 0 \end{aligned} \right\} \quad (7.8)$$

As the system is linear both in (x, y) and in (z, t) , it can be rewritten in matrix form as

$$\mathbf{S}_b \begin{pmatrix} z \\ t \\ 1 \end{pmatrix} = \begin{pmatrix} 0 \\ 0 \\ 0 \end{pmatrix}, \quad (7.9)$$

where

$$\mathbf{S}_b = \begin{pmatrix} P_{895}x - P_{896}y - P_{891} & P_{892} + P_{897}x & P_{893}x - P_{894}y \\ P_{795}x - P_{796}y - P_{791} & P_{792} + P_{798}y & P_{793}x - P_{794}y \\ P_{785}x - P_{786}y - P_{781} & P_{782} & P_{783}x - P_{784}y + P_{789} \end{pmatrix}$$

only depends on x and y (b refers to *base*, as x and y are the coordinates of the base attachments). The other way round, the system can also be written as

$$\mathbf{S}_p \begin{pmatrix} x \\ y \\ 1 \end{pmatrix} = \begin{pmatrix} 0 \\ 0 \\ 0 \end{pmatrix}, \quad (7.10)$$

where

$$\mathbf{S}_p = \begin{pmatrix} P_{893} + P_{895}z + P_{897}t & -P_{894} - P_{896}z & P_{892}t - P_{891}z \\ P_{793} + P_{795}z & P_{798}t - P_{794} - P_{796}z & P_{792}t - P_{791}z \\ P_{783} + P_{785}z & -P_{784} - P_{786}z & P_{782}t - P_{781}z + P_{789} \end{pmatrix}$$

only depends on z and t (p refers to *platform*, as z and t are the coordinates of the platform attachments).

From equation (7.9) it is clear that the system has a solution for (z, t) only for those (x, y) that satisfy $\det(\mathbf{S}_b) = 0$, and this solution is unique (assuming that \mathbf{S}_b has rank 2). In the same way, there exists a solution for (x, y) only for those (z, t) that make $\det(\mathbf{S}_p) = 0$. Both determinants define cubic curves on the base and platform planes, respectively. In other words, system (7.8) defines a one-to-one correspondence between generic points on two cubic curves. However, the correspondence may be not one-to-one for special points on the cubics, as will be seen in the example of Section 7.3.2.

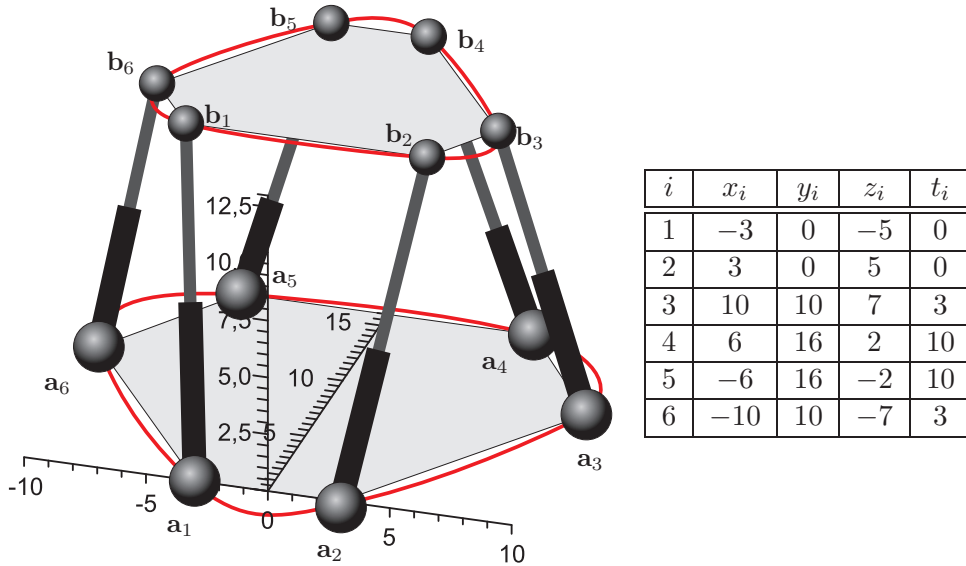


Figure 7.2: Manipulator analyzed in Section 7.3.1 with its corresponding attachment coordinates ($\mathbf{a}_i = (x_i, y_i, 0)^T$, $\mathbf{b}_i = \mathbf{p} + \mathbf{R}(z_i, t_i, 0)^T$).

Depending on the placement of the attachments, these curves can be generic curves of degree 3, or a line and a conic, or even 3 lines crossing 2 by 2. This will be exemplified in the following section.

7.3 Examples

7.3.1 A doubly-planar Stewart-Gough platform

In [48] Husty *et al.* analyzed a Stewart-Gough platform, searching where additional legs could be placed without changing its forward kinematics solution, to obtain a redundant manipulator. The same example is analyzed here. The local coordinates of the attachments are listed in the table of Fig 7.2.

After substituting the corresponding numerical values, the system of equations (7.8) results in:

$$\left. \begin{aligned} 2430z - 4050x + 255yz + 188xt &= 0 \\ -280t + 45y + 13yt &= 0 \\ -70t + 43y - 4xz + 60 &= 0 \end{aligned} \right\}$$

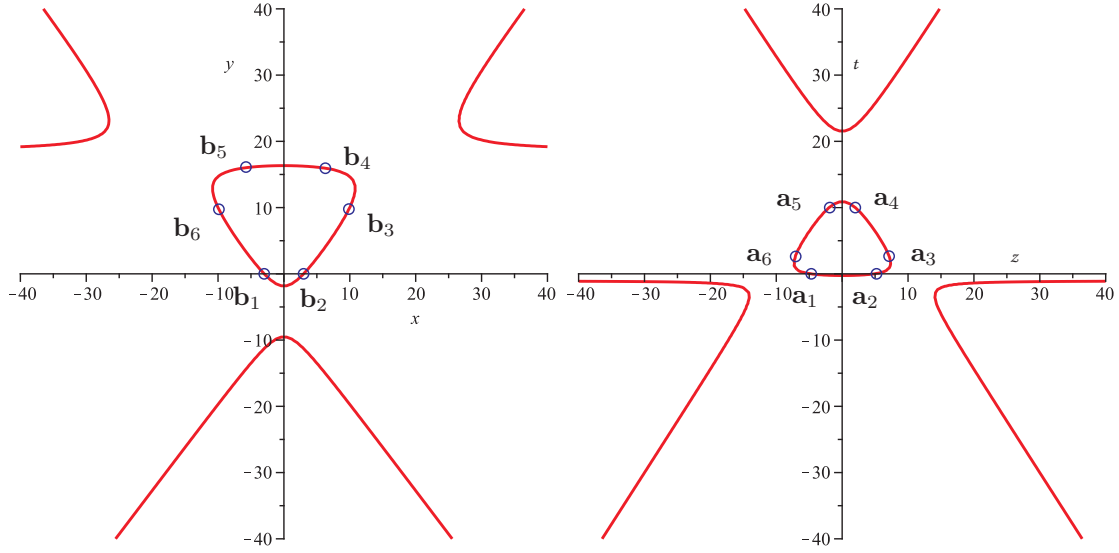


Figure 7.3: The base and the platform curves defined in (7.11).

and, thus, matrices \mathbf{S}_b and \mathbf{S}_p are:

$$\mathbf{S}_b = \begin{pmatrix} 2430 + 255y & 188x & -4050x \\ 0 & 13y - 280 & 45y \\ -4x & -70 & 60 + 43y \end{pmatrix},$$

and

$$\mathbf{S}_p = \begin{pmatrix} 188t - 4050 & 255z & 2430z \\ 0 & 13t + 45 & -280t \\ -4z & 43 & 60 - 70t \end{pmatrix},$$

whose determinants equated to zero give the two equations of cubic curves

$$\begin{aligned} -16296x^2y + 9503y^3 + 302400x^2 - 47312y^2 - 1599420y - 2721600 &= 0, \\ 20598z^2t - 8554t^3 + 21870z^2 + 275173t^2 - 1932795t - 546750 &= 0; \end{aligned} \quad (7.11)$$

plotted in Fig. 7.3. The cubic in the base coincides with the one appearing in [48], whereas the cubic in the platform is not given explicitly there. In [48], the authors propose to add additional legs to obtain redundant manipulators. Instead, here legs are substituted by other legs satisfying the one-to-one correspondence between the base and platform cubics defined by (7.11). The singularity locus will remain unchanged, but other performance indices could thus be improved, such as stiffness, or maneuverability, or even the workspace could be enlarged by reducing the risk of leg collisions.

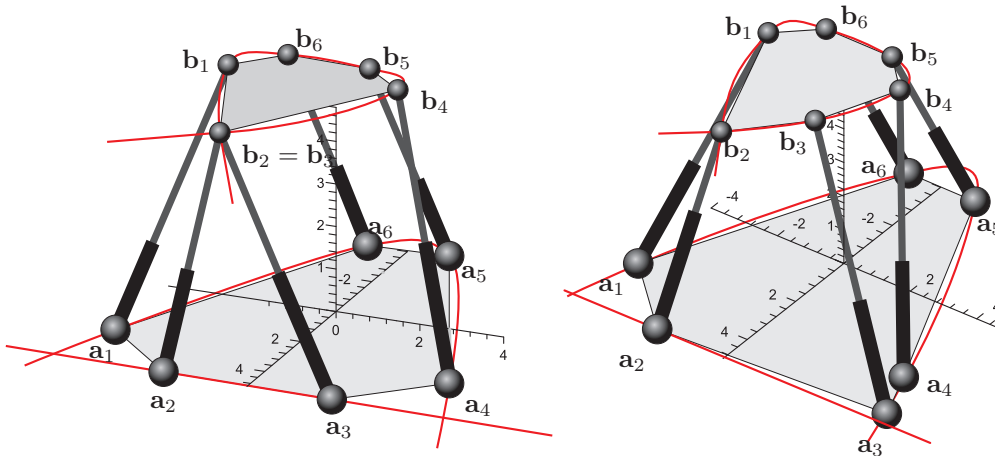


Figure 7.4: Platform described in Table 7.1 (left), and the resulting platform after rearranging its 3rd leg (right).

7.3.2 Platform with degenerate cubic curves

Interesting cases appear when one or both of the curves are degenerate. Consider the example with attachment coordinates given in Table 7.1, where two of the attachments on the platform are made coincident, $\mathbf{b}_2 = \mathbf{b}_3$. The corresponding platform is represented in Fig. 7.4-(left). The two legs sharing an attachment form a Point-Line component and, as it has been proved in Chapter 4, base attachments \mathbf{a}_2 and \mathbf{a}_3 can be rearranged on any point on the line $\mathbf{a}_2\mathbf{a}_3$ without modifying the singularity locus.

Table 7.1: Coordinates of the attachments $\mathbf{a}_i = (x_i, y_i, 0)$ and $\mathbf{b}_i = \mathbf{p} + \mathbf{R}(z_i, t_i, 0)^T$ for the analyzed robot

i	x_i	y_i	z_i	t_i
1	3	-4	-2	-2
2	5	-2	2	-1/2
3	5	2	2	-1/2
4	3	4	-2	2
5	-4	1	-3	1
6	-4	-1	-3	-1

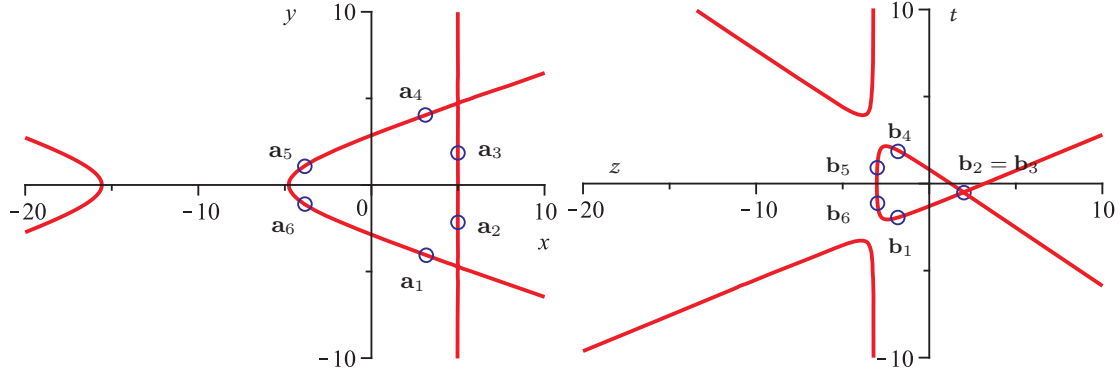


Figure 7.5: The base and the platform curves defined by (7.13).

After applying Gaussian elimination on \mathbf{P} , the following equations are obtained:

$$\left. \begin{aligned} 372z + 18988t + 1302x - 5656y + 527xz + 2828yz + 1212xt &= 0 \\ 5172z + 808t - 2502x + 404y + 257xz + 404yz + 2424yt &= 0 \\ 74z - 44x - 13xz + 202 &= 0 \end{aligned} \right\} \quad (7.12)$$

and the corresponding cubic curves are defined by

$$\begin{aligned} (x - 5)(31x^2 - 280y^2 + 631x + 2308) &= 0, \\ (-132z^3 + 124z^2t + 476zt^2 + 191z^2 + 620zt + 1528t^2 + 1259z + 744t - 1606) &= 0. \end{aligned} \quad (7.13)$$

In other words, the cubic curve in the base factorizes into a conic (an hyperbola) and a line, while the platform curve remains a cubic, but with a singular point (called node) on the point of the Point-Line component. Fig. 7.5 contains the plot of these two curves and the corresponding location of the attachments.

The correspondence between the base line and the platform cubic curve can be derived by solving system (7.12) as follows. Take any point on the base line $\mathbf{a}_2\mathbf{a}_3$, that is, substitute $x = 5$ on the system, then

$$\left. \begin{aligned} 3007z + 25048t + 6510 - 5656y + 2828yz &= 0 \\ +6457z + 808t - 12510 + 404y + 404yz + 2424yt &= 0 \\ 9z - 18 &= 0 \end{aligned} \right\}$$

From the last equation, $z = 2$. Substituting this value into the first two equations and factorizing the result yields

$$\left. \begin{aligned} 12524(1 + 2t) &= 0 \\ 404(1 + 3y)(1 + 2t) &= 0 \end{aligned} \right\}$$

The solution of the system is

$$\Delta = \{(x, y, z, t) \mid x = 5, y = s, z = 2, t = -1/2, s \in \mathbb{R}\},$$

that is, any point on the line $x = 5$ corresponds to the vertex $\mathbf{b}_2 = \mathbf{b}_3$, in accordance with the singularity-invariant leg rearrangements of the Point-Line component (Chapter 4).

For the rest of the points on the cubic curve, the correspondence can be written in terms of a single parameter z . Given a point on the platform cubic

$$\left(z, \frac{-31z^2 - 155z - 186 \pm \sqrt{\delta}}{2(119z + 382)} \right),$$

the corresponding point on the base hyperbola is

$$\left(\frac{2(37z + 101)}{44 + 13z}, \frac{3(z - 2)(16669z^2 + 103981z + 162022) \mp (26z + 88)\sqrt{\delta}}{4(2 - z)(44 + 13z)^2 \pm 2(39z + 132)\sqrt{\delta}} \right), \quad (7.14)$$

where the discriminant $\delta = (16669z^2 + 103981z + 162022)(z - 2)^2$ determines whether points are real or complex. Real points on the platform always correspond to real points on the base, and vice versa. Observe that, for the singular point $z = 2$, (7.14) is apparently undefined. However, terms $(z - 2)$ can be simplified and then the resulting point gives the intersection between the line and the hyperbola. In other words, this parametrization represents the one-to-one correspondence between points on the platform cubic and the base hyperbola, except for the singular platform point $(2, -1/2)$, a double point that corresponds to two points on the hyperbola (the two intersections of the line with the conic).

To avoid multiple spherical joints, here the Point-Line component can be split by substituting any of its legs by another leg going from the conic to the base cubic. For example, take the point on the platform cubic given by $z = 0$ and $t = \frac{-93 + \sqrt{162022}}{382}$, and solve system (7.12) after evaluating it on this point, or equivalently, evaluate expression (7.14) for $z = 0$. The result is:

$$x = \frac{101}{22} \text{ and } y = \frac{243033 - 44\sqrt{162022}}{-3872 + 132\sqrt{162022}}.$$

Hence, the 3rd leg can be substituted by a new leg going from the base point $(\frac{101}{22}, \frac{243033 - 44\sqrt{162022}}{-3872 + 132\sqrt{162022}}, 0)$ to the platform attachment with local coordinates $(0, \frac{-93 + \sqrt{162022}}{382}, 0)$

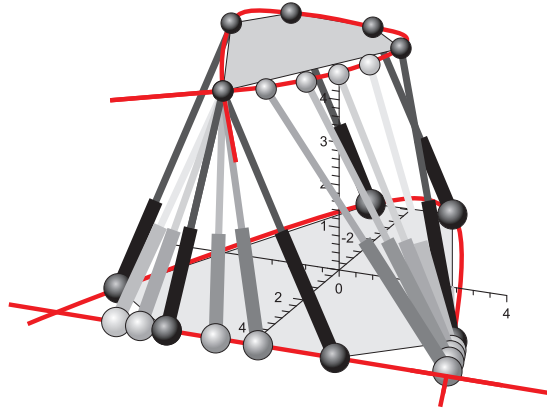


Figure 7.6: Possible leg substitutions are shown in gray.

and the resulting Jacobian determinant is the same as before the rearrangement, but multiplied by $\frac{15990+93\sqrt{162022}}{67232} = 0.794$. After this leg rearrangement, the platform has no coincident attachments [Fig. 7.4-(right)], in other words, the Point-Line component has been made implicit.

In Fig. 7.6, other possible leg rearrangements for this example are shown in gray.

7.3.3 Griffis-Duffy platforms

In 1993, Griffis and Duffy patented two manipulators named thereafter Griffis-Duffy type I and II platforms [42]. Both platforms have their attachments distributed on triangles, three attachments on the vertices and three on the midpoints of the edges. Type I platforms are formed by joining the attachments on the midpoints on the base to the vertices on the platform, and the vertices on the base to midpoints on the platform [Fig. 7.7-(left)]. Type II join midpoints to midpoints and vertices to vertices [Fig. 7.8-(left)].

In Chapter 4.5.2, type I Griffis-Duffy platforms have been shown to be singularity equivalent to the octahedral manipulator. In [50], type II Griffis-Duffy manipulators are shown to be always non-architecturally singular.

Consider the two examples with the attachment coordinates given in Table 7.2, where the same triangles define two Griffis-Duffy manipulators of type I and type II, respectively. A representation of these manipulators can be found in Fig. 7.7 and Fig. 7.8, respectively.

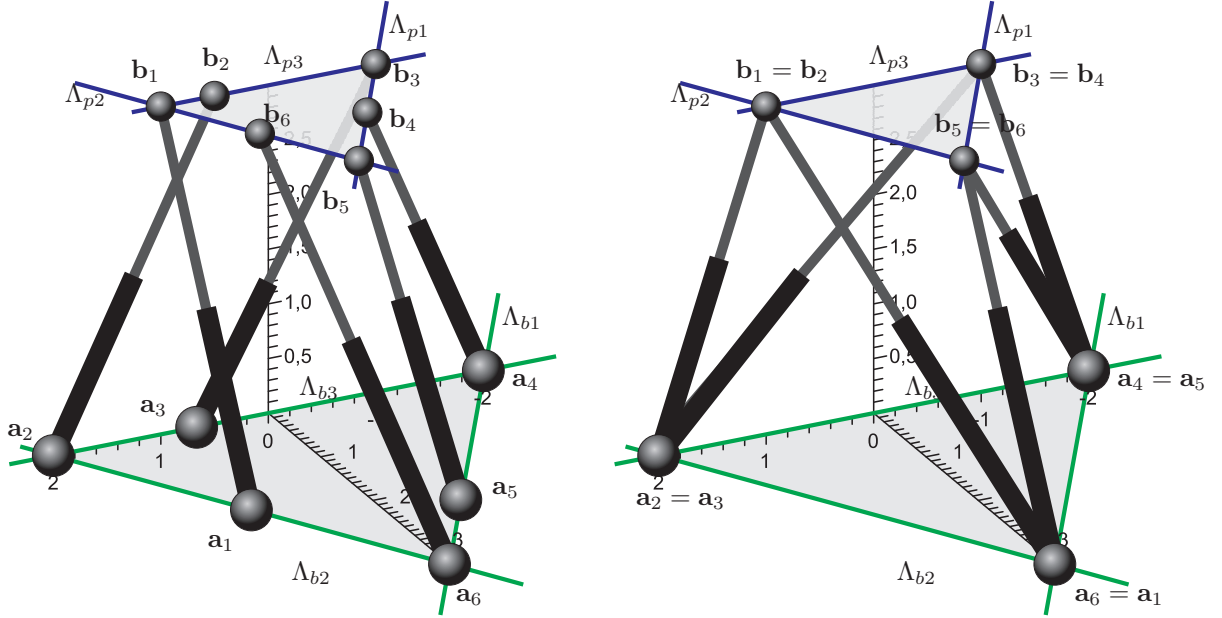


Figure 7.7: Griffis-Duffy type I platform with the attachment coordinates given in in Table 7.2 (left), and its equivalent octahedral manipulator after applying a leg rearrangement (right).

The computation of the base and platform cubic curves factorizes into the 3 same lines for both type I and type II platforms:

$$\begin{aligned} (\sqrt{3}z - t + \sqrt{3})(\sqrt{3}z + t - \sqrt{3})t &= 0, \\ (-3x + \sqrt{3}y - 6)(3x + \sqrt{3}y - 6)y &= 0. \end{aligned} \quad (7.15)$$

Let

- Λ_{p1} be the line on the platform given by equation $\sqrt{3}z - t + \sqrt{3} = 0$,
- Λ_{p2} be the line on the platform given by equation $\sqrt{3}z + t + \sqrt{3} = 0$,
- Λ_{p3} be the line on the platform given by equation $t = 0$,
- Λ_{b1} be the line on the base given by equation $-3x + \sqrt{3}y - 6 = 0$,
- Λ_{b2} be the line on the base given by equation $3x + \sqrt{3}y - 6 = 0$ and
- Λ_{b3} be the line on the base given by equation $y = 0$.

Whereas the obtained lines are the same for type I and II, the system obtained by applying Gaussian elimination on matrix \mathbf{P} results in different equations. The system

Table 7.2: Coordinates of the attachments $\mathbf{a}_i = (x_i, y_i, 0)$ and $\mathbf{b}_i = \mathbf{p} + \mathbf{R}(z_i, t_i, 0)^T$ for the analyzed robots

i	z_i	t_i
1	1	0
2	1/2	0
3	-1	0
4	-1/2	$\sqrt{3}/2$
5	0	$\sqrt{3}$
6	1/2	$\sqrt{3}/2$

i Type I	i Type II	x_i	y_i
2	1	2	0
3	2	2/3	0
4	3	-2	0
5	4	-2/3	$(4/3)\sqrt{3}$
6	5	0	$2\sqrt{3}$
1	6	1	$\sqrt{3}$

corresponding to the type I platform is:

$$\left. \begin{aligned} 2t - y + yz + xt &= 0 \\ (\sqrt{3}z + t - \sqrt{3})y &= 0 \\ -2\sqrt{3}z + 4t + \sqrt{3}x - y + \sqrt{3}xz + 3yz - 2\sqrt{3} &= 0 \end{aligned} \right\} \quad (7.16)$$

whereas that for the type II platform is:

$$\left. \begin{aligned} 2t - y + xt - yz &= 0 \\ 3\sqrt{3}y - 8\sqrt{3}t + \sqrt{3}yz + yt &= 0 \\ 10\sqrt{3}z - 16t - 5\sqrt{3}x + 9y + \sqrt{3}xz + yz - 2\sqrt{3} &= 0 \end{aligned} \right\} \quad (7.17)$$

The resolution of these systems gives correspondences between base and platform attachments that leave the singularities invariant.

Using the same notation as in the previous chapter, for the Griffis-Duffy type I manipulator, system (7.16) has 6 sets of solutions

$$\begin{aligned} \Delta_{b1} &= \{(x, y, z, t) \mid x = \lambda, y = (\lambda + 2)\sqrt{3}, z = 0, t = \sqrt{3}; \lambda \in \mathbb{R}\}, \\ \Delta_{b2} &= \{(x, y, z, t) \mid x = \lambda, y = (2 - \lambda)\sqrt{3}, z = 1, t = 0; \lambda \in \mathbb{R}\}, \\ \Delta_{b3} &= \{(x, y, z, t) \mid x = \lambda, y = 0, z = -1, t = 0; \lambda \in \mathbb{R}\}, \\ \Delta_{p1} &= \{(x, y, z, t) \mid x = -2, y = 0, z = \lambda, t = \sqrt{3}(\lambda + 1); \lambda \in \mathbb{R}\}, \\ \Delta_{p2} &= \{(x, y, z, t) \mid x = 0, y = 2\sqrt{3}, z = \lambda, t = \sqrt{3}(1 - \lambda); \lambda \in \mathbb{R}\}, \\ \Delta_{p3} &= \{(x, y, z, t) \mid x = 2, y = 0, z = \lambda, t = 0; \lambda \in \mathbb{R}\}. \end{aligned}$$

In other words, all the correspondences are between points and lines (in accordance with the results in Chapter 4), that is, to each vertex of the base (platform) triangle

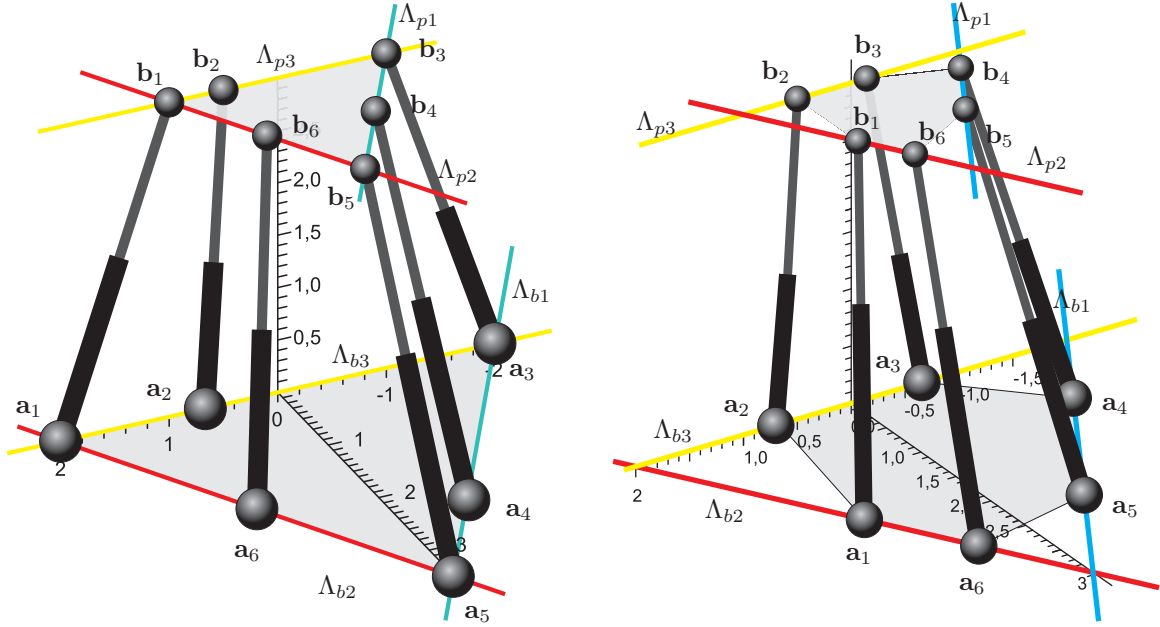


Figure 7.8: Griffis-Duffy type II platform with attachment coordinates given in Table 7.2 (left), and its equivalent platform after removing all collinearities (right).

corresponds a line on the platform (base) triangle. Thus, by moving the six midpoint attachments along their supporting lines, the manipulator can be rearranged into the equivalent octahedral manipulator depicted in Fig. 7.7-(right) (a result in accordance with that in Chapter 4).

On the other hand, for the Griffis-Duffy type II, system (7.17) has three sets of solutions given by

$$\begin{aligned} \mathcal{L}_1 &= \{(x, y, z, t) \mid x = \frac{2\lambda}{\lambda+2}, \quad y = \frac{4(\lambda+1)\sqrt{3}}{\lambda+2}, \quad z = \lambda, \quad t = (\lambda+1)\sqrt{3}, \quad \lambda \in \mathbb{R}\} \\ \mathcal{L}_2 &= \{(x, y, z, t) \mid x = 2\lambda, \quad y = -2(\lambda-1)\sqrt{3}, \quad z = \lambda, \quad t = (1-\lambda)\sqrt{3}, \quad \lambda \in \mathbb{R}\} \\ \mathcal{L}_3 &= \{(x, y, z, t) \mid x = \frac{2-10\lambda}{\lambda-5}, \quad y = 0, \quad z = \lambda, \quad t = 0, \quad \lambda \in \mathbb{R}\} \end{aligned}$$

Each set \mathcal{L}_i defines a one-to-one correspondence between points of Λ_{bi} and Λ_{pi} for $i = 1, 2, 3$.

In conclusion, the same geometrical elements determine the invariance of the singularity locus, but in the first case the correspondence is between points and lines and in the second case it is between points in two lines.

The legs of the type II manipulator can be rearranged following the obtained line-line correspondences, but some rearrangements must be avoided. For example, placing

four legs in the same line-line correspondence would lead to an architecturally singular manipulator, as it would contain a Line-Line component in projective correspondence (see Section 4.4).

An interesting rearrangement consists in removing all collinearities from the type II manipulator. As a result, an equivalent platform such as that shown in Fig. 7.8-(right) is obtained.

To remove collinearities, all legs from vertex to vertex need to be rearranged. The first leg can be placed going from a point on Λ_{b2} to the corresponding point on Λ_{p2} . In other words, take a point on Λ_{b2} , substitute its coordinates in system (7.17) and the solution gives a point on Λ_{p2} :

$$\underbrace{\begin{matrix} x = 1/2 \\ y = (3/2)\sqrt{3} \end{matrix}}_{\text{on } \Lambda_{b2}} \quad \begin{matrix} \text{Substitute in (7.17)} \\ \longrightarrow \\ \text{and solve} \end{matrix} \quad \underbrace{\begin{matrix} z = 1/4 \\ t = (3/4)\sqrt{3} \end{matrix}}_{\text{on } \Lambda_{p2}}$$

The same can be done to substitute the 3rd leg by a leg going from Λ_{b3} to Λ_{p3} :

$$\underbrace{\begin{matrix} x = -2/3 \\ y = 0 \end{matrix}}_{\text{on } \Lambda_{b3}} \quad \begin{matrix} \text{Substitute in (7.17)} \\ \longrightarrow \\ \text{and solve} \end{matrix} \quad \underbrace{\begin{matrix} z = -1/7 \\ t = 0 \end{matrix}}_{\text{on } \Lambda_{p3}}$$

and finally, the 5th leg is substituted by a leg going from a point on Λ_{b1} to a point on Λ_{p1}

$$\underbrace{\begin{matrix} x = -3/2 \\ y = (1/2)\sqrt{3} \end{matrix}}_{\text{on } \Lambda_{b1}} \quad \begin{matrix} \text{Substitute in (7.17)} \\ \longrightarrow \\ \text{and solve} \end{matrix} \quad \underbrace{\begin{matrix} z = -6/7 \\ t = (1/7)\sqrt{3} \end{matrix}}_{\text{on } \Lambda_{p1}}$$

The resulting manipulator, depicted in Fig. 7.8-(right), is equivalent to the one in Fig. 7.8-(left), in terms of both its forward kinematics and its singularity locus.

In conclusion, this proves that it is not necessary that a platform has collinear attachments to behave like a Griffis-Duffy type II manipulator.

7.4 Classification of doubly-planar Stewart-Gough platforms

7.4.1 General doubly-planar manipulators

This section presents a theory that generalizes the results presented in all the previous chapters, as all the singularity-invariant leg rearrangements found between points, lines and planes can be seen as particular cases in Plane-Plane rearrangements. Indeed, in the following table, all possible doubly-planar Stewart-Gough platforms are analyzed, attending to their topology, detecting also all the equivalences between them. In Merlet's book [68, Table 4.6] all Stewart-Gough platforms are listed, attending to their topology, for the general case. Next, the same manipulators will be analyzed, considering all of them with coplanar attachments and analyzing a generic example for each architecture. They will be identified with a number, corresponding to the order of appearance in Merlet's table. For each manipulator, the solution of system (7.8) is given, as well as a representation of the curves defining the singularity invariant leg rearrangements. Finally, equivalences between manipulators are listed so that all the cases of Merlet's table are covered.

The solutions sets for system (7.8) can be of several types:

- Δ A solution set that represents a correspondence between a point and a line (see Chapter 4). In the figures, they are plotted in blue when the line is at the platform, and in green when the line lies at the base.
- \mathcal{T} A solution set that represents a correspondence between a point and a plane, *i.e.*, a Point-Plane component.
- \mathcal{L} A solution set that represents a one-to-one correspondence between points of two lines.
- LL A solution set corresponding to the Line-Line component (see Chapter 4). They are plotted in pink in the figures.
- LP A solution set corresponding to the Line-Plane component (see Chapter 5).
- $\mathcal{C} - \mathcal{F}$ A solution set corresponding to a one-to-one correspondence between a conic and a cubic curve.

7.4 Classification of doubly-planar Stewart-Gough platforms

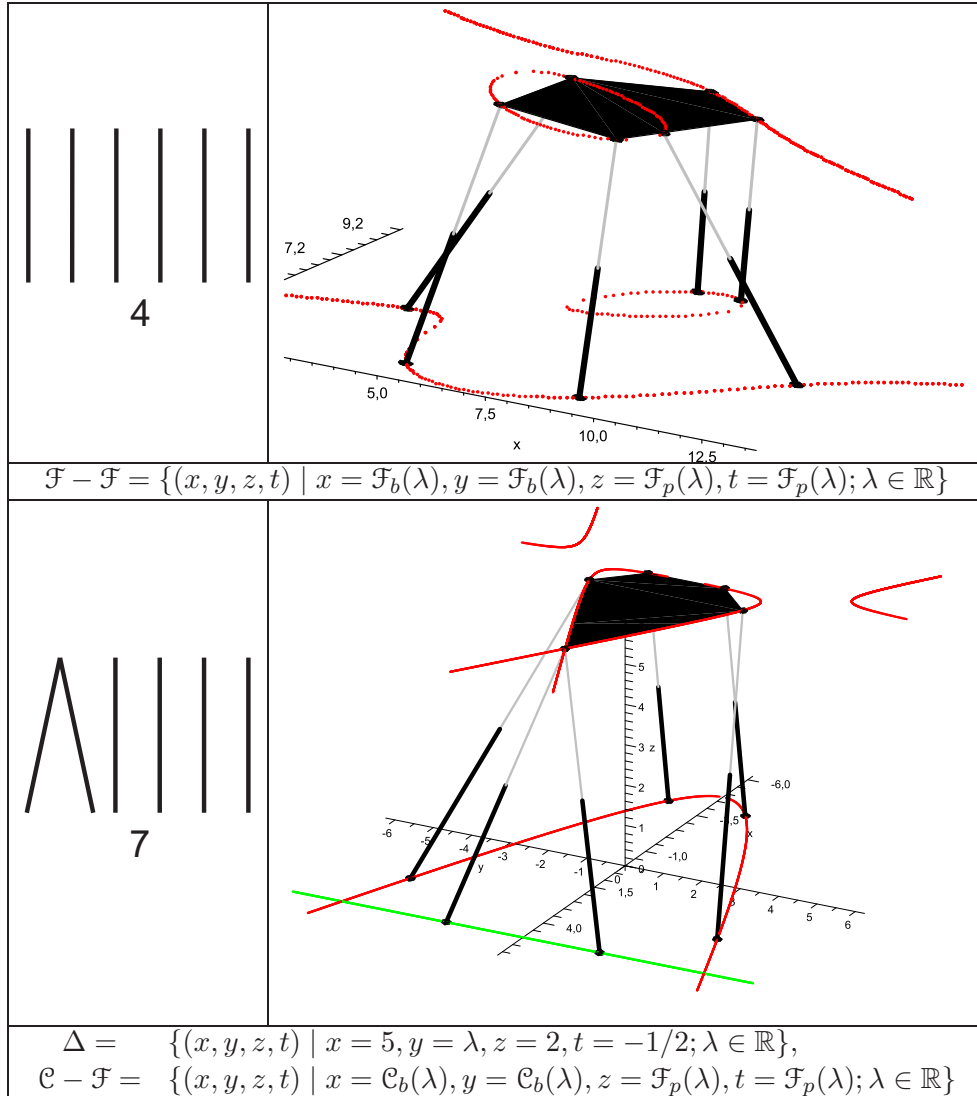
$\mathcal{C} - \mathcal{L}$ A solution set corresponding to a one-to-one correspondence between a conic and a line.

$\mathcal{F} - \mathcal{F}$ The more general case, a one-to-one correspondence between two cubic curves.

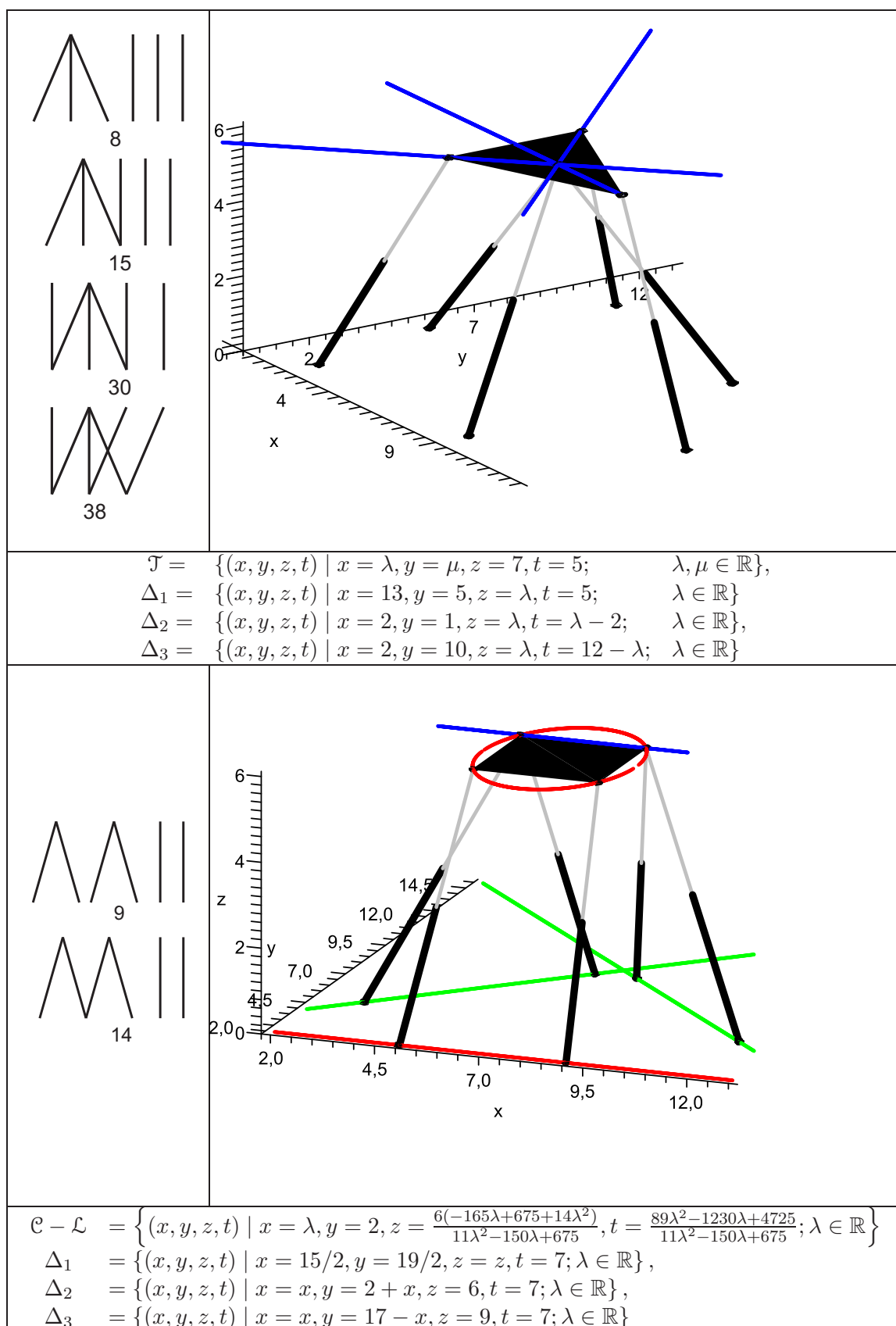
All one-to-one correspondences between points are plotted in red if there is only one, in red and yellow when there are two correspondences, and in red yellow and cyan if three correspondences coexist in the manipulator. For \mathcal{T} and LP solution sets, no curve is shown, as points can belong to any point of the plane. All the pictures correspond to examples of generic manipulators.

This classification also uses the 35 classes defined by Fauger and Lazard in [33], as it is commonly used to identify manipulators. On the other hand, it is quite different from other classifications like that in [57], with 11 classes according to rigid components, but elements of the same class are not necessarily equivalent from the point of view of their kinematics nor their singularities.

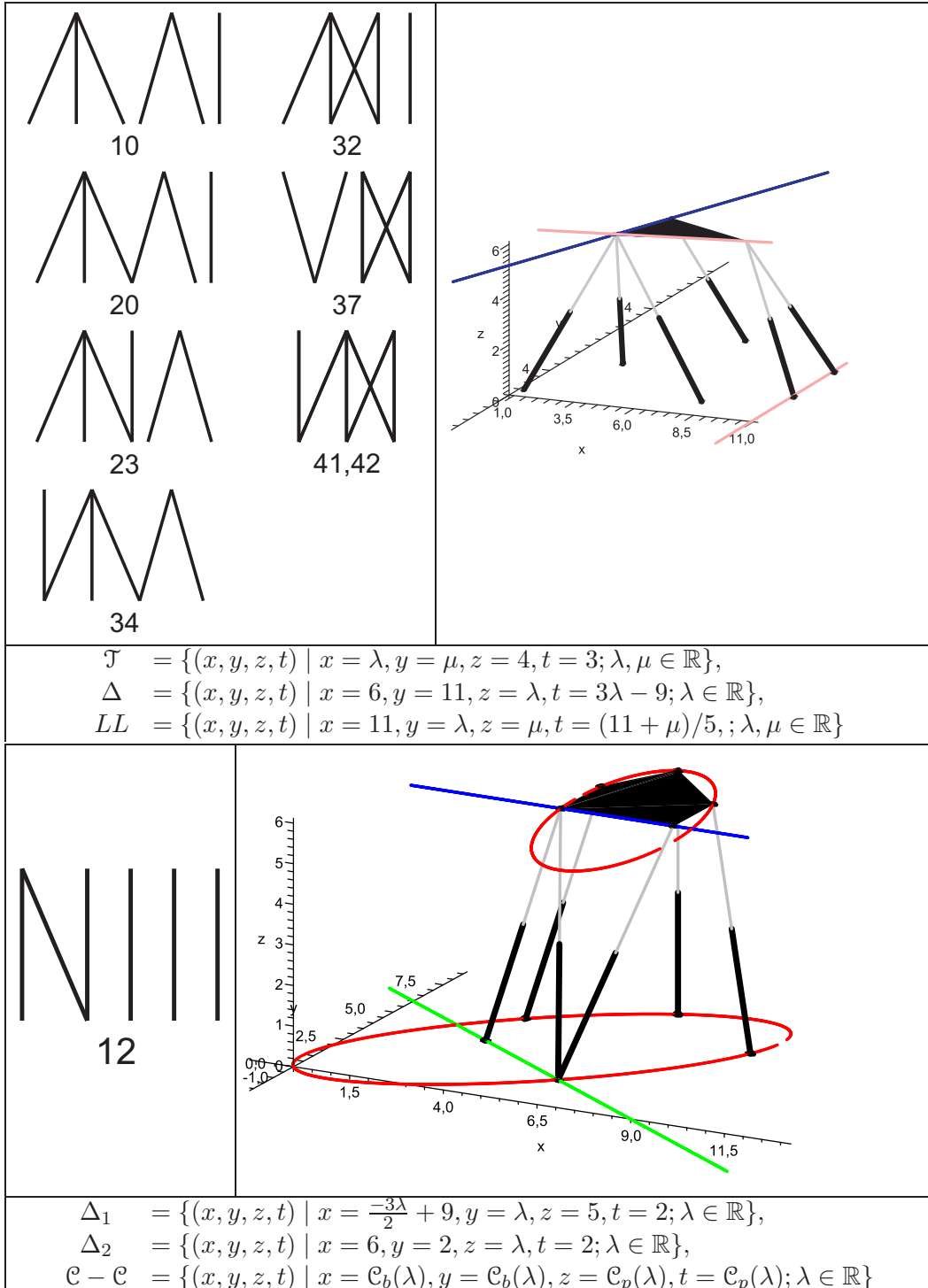
7.4 Classification of doubly-planar Stewart-Gough platforms



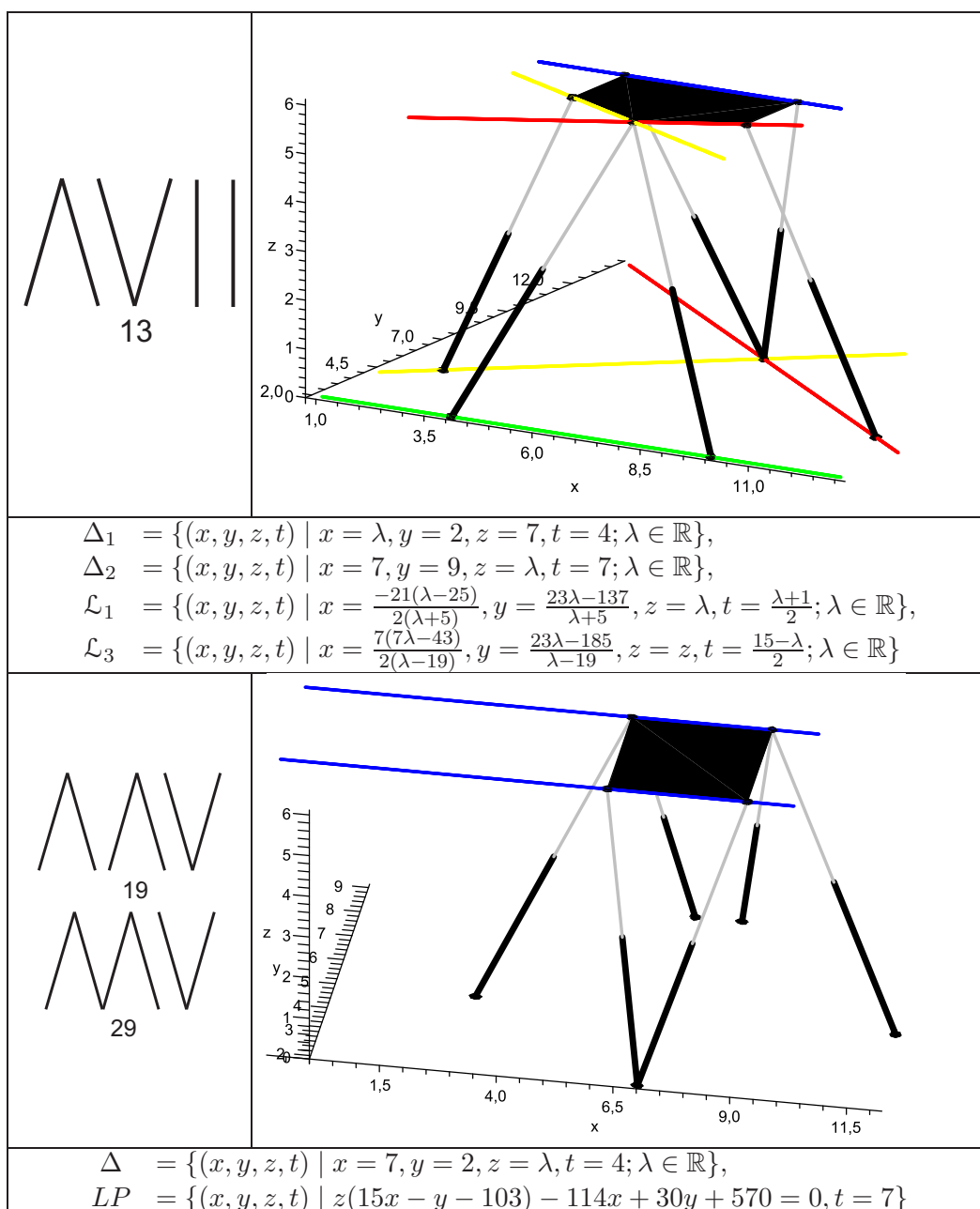
7.4 Classification of doubly-planar Stewart-Gough platforms



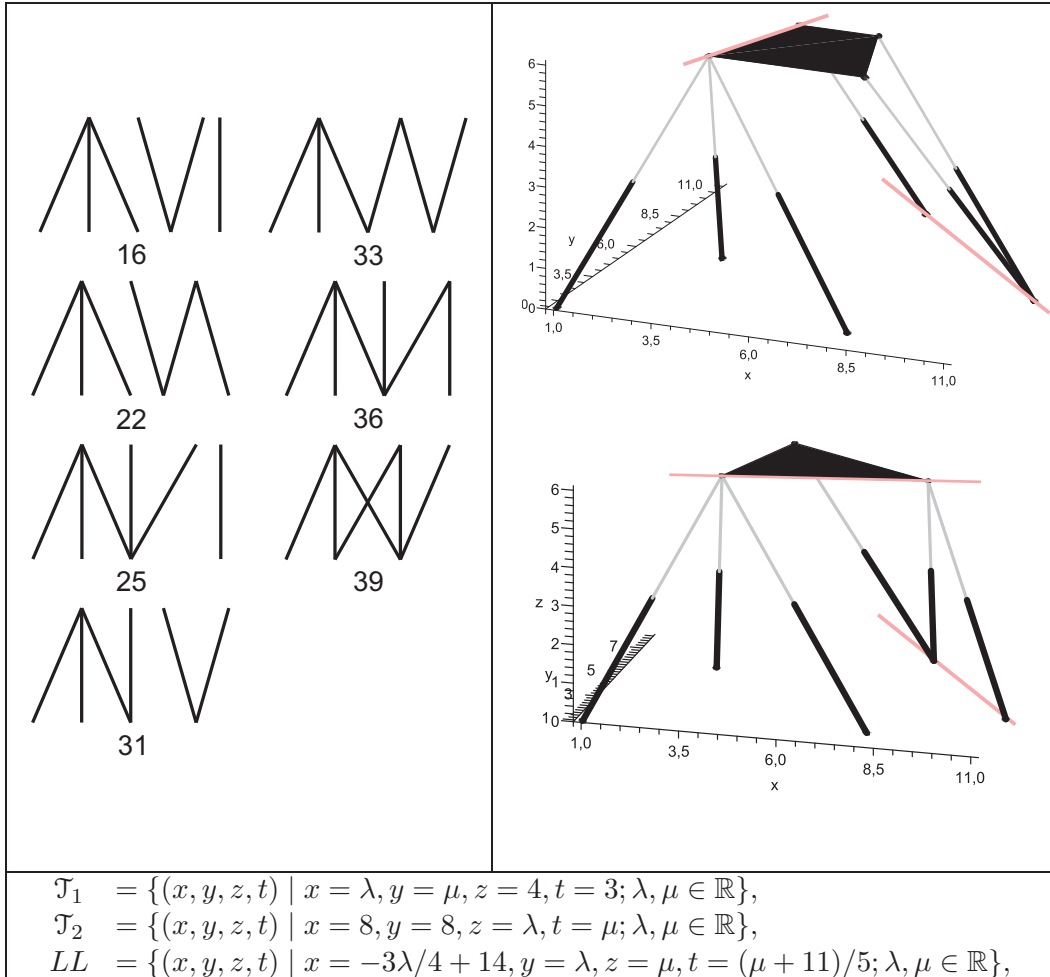
7.4 Classification of doubly-planar Stewart-Gough platforms



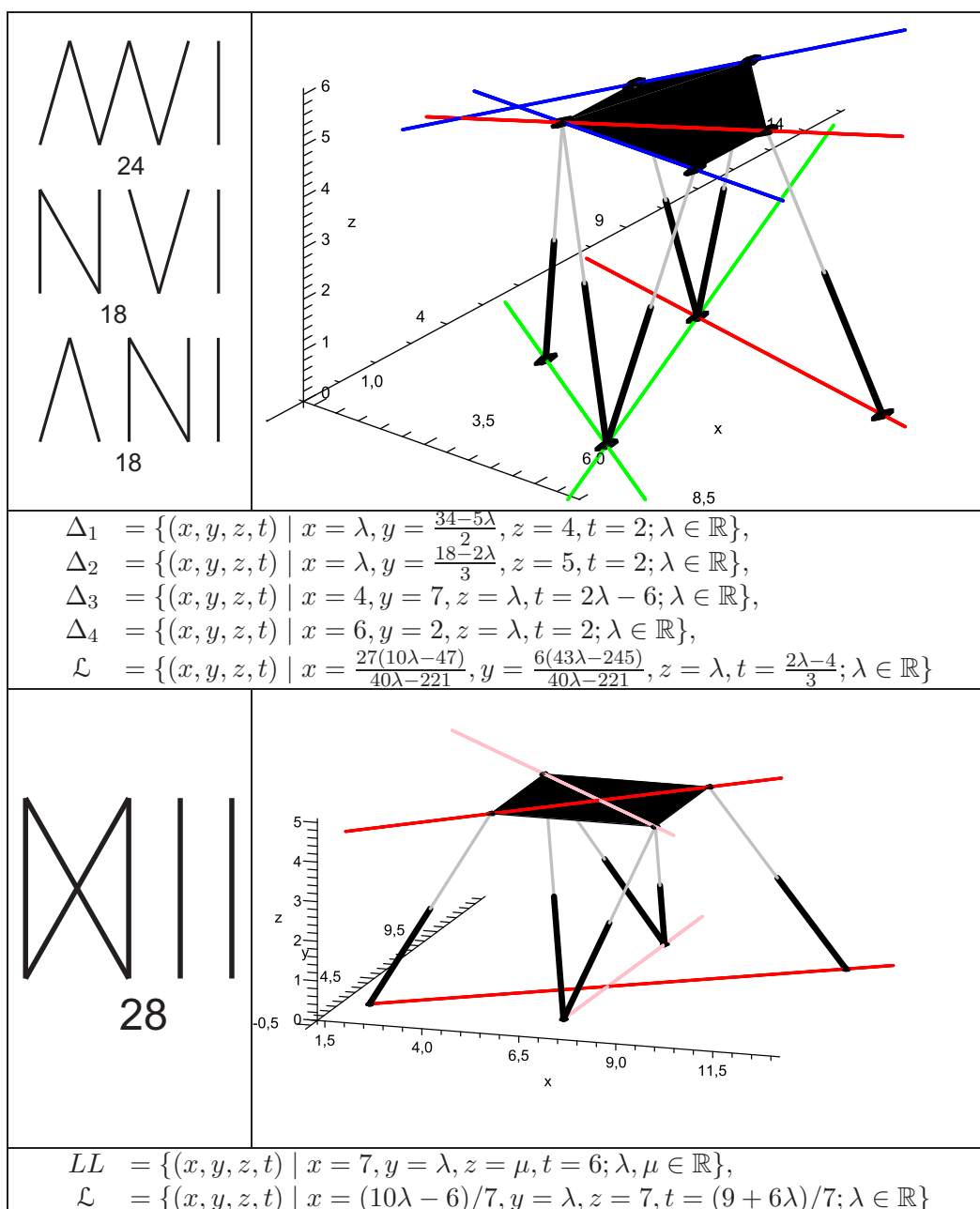
7.4 Classification of doubly-planar Stewart-Gough platforms

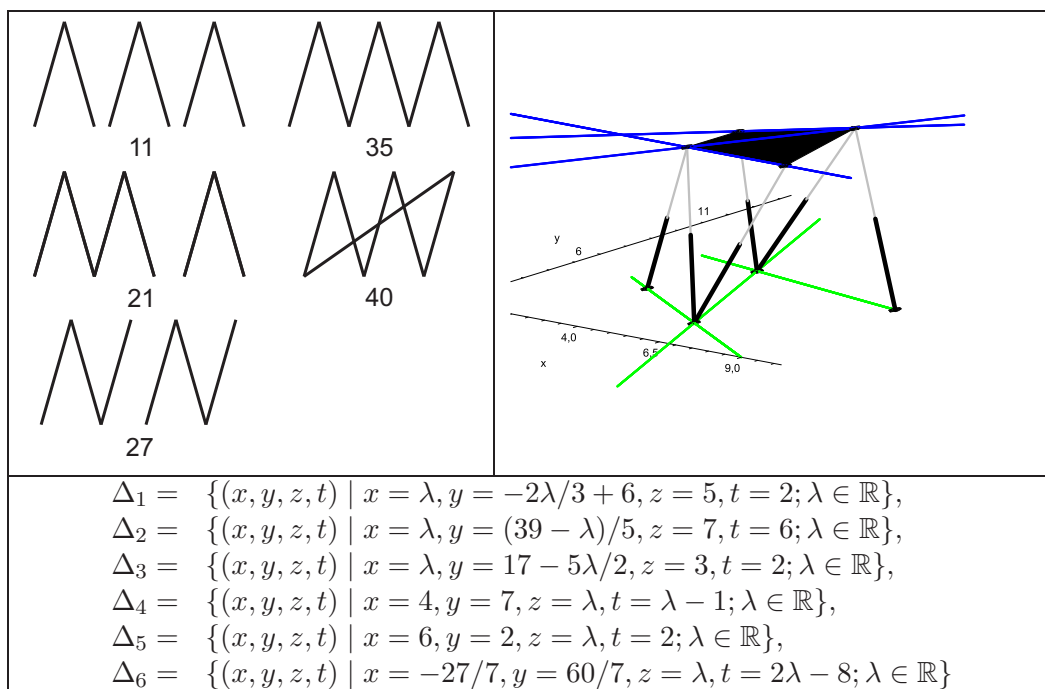


7.4 Classification of doubly-planar Stewart-Gough platforms



7.4 Classification of doubly-planar Stewart-Gough platforms





7.4.2 Families of doubly-planar 3-3 manipulators

Next, the three families of manipulators corresponding to the three 3-3 manipulators are presented. They are called flagged, partially flagged and octahedral manipulators [1, 2, 46]. It was shown in [12] that the singularities of any doubly-planar platform can be written as a linear combination of the 3-3 manipulator singularity polynomials. Therefore, these three manipulators can be seen as the basis of all the doubly-planar Stewart-Gough platforms from the singularities point of view.

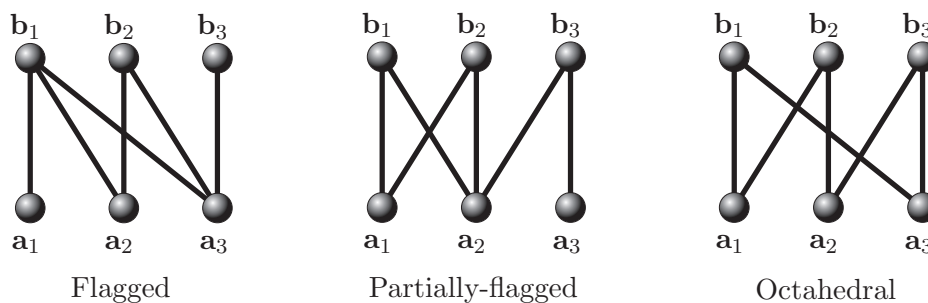


Figure 7.9: The basic 3-3 Stewart-Gough manipulators. They are named, from left to right, flagged, partially flagged and octahedral manipulators.

All three families are obtained applying Point-Line singularity-invariant leg rear-

7.4 Classification of doubly-planar Stewart-Gough platforms

rangements.

The flagged family of manipulators consists of 39 manipulators with different topologies whose forward kinematics can be solved by 3 trilaterations and their singularities can be interpreted geometrically as the degeneration of three tetrahedra (see [2] for details). The singularity-invariant curves for all members of this family are defined by two Point-Plane solutions and one Line-Line solution. This family first appeared in [10].

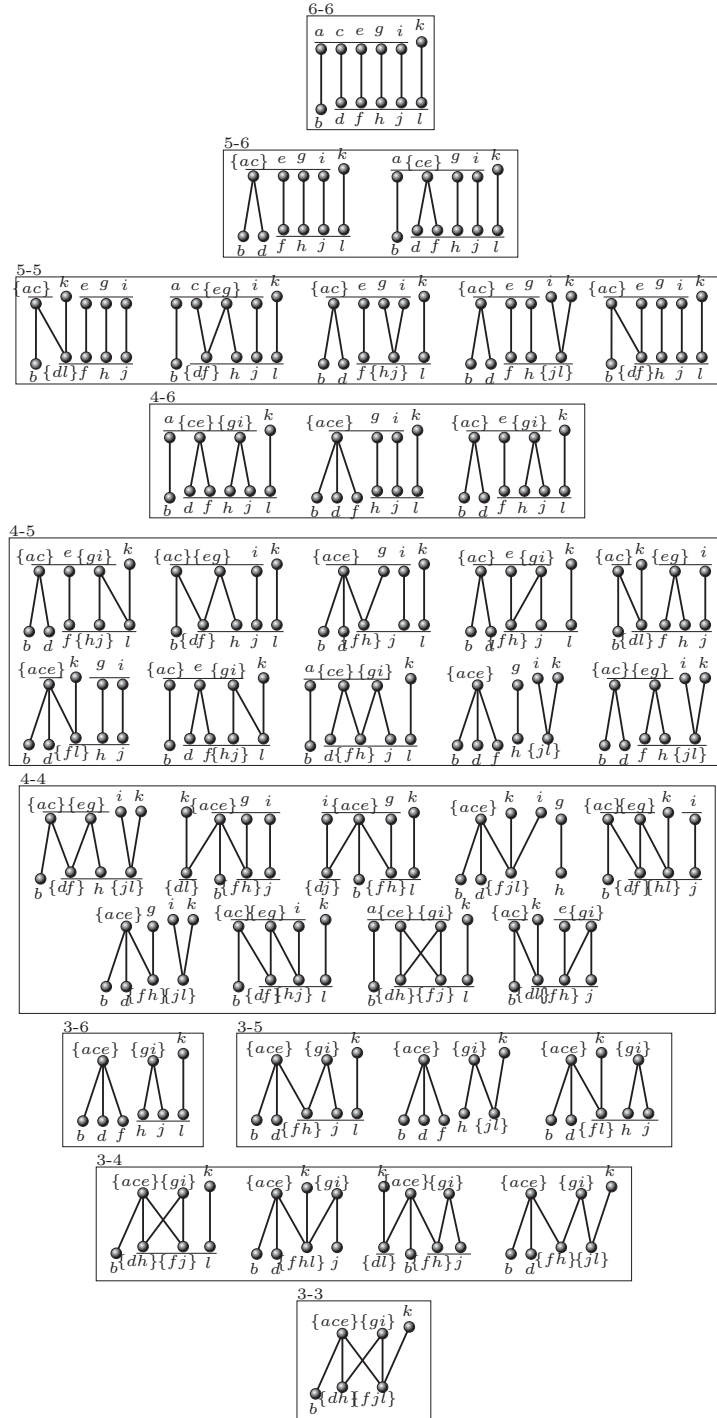
The partially flagged family of manipulators has 46 members, their forward kinematics can be also solved with three trilaterations and their singularities can be also interpreted geometrically as the degeneracy of 3 tetrahedra. Thus, the two families are quite similar, but not equivalent because the singularity-invariant curves are defined, in this case, by a Point-Plane, a Point-Line and a Line-Line solution.

Finally, the members of the octahedral family of manipulators have 16 solutions of the forward kinematics (with a characteristic polynomial of degree 8) and its singularities can be geometrically interpreted as the intersection of four planes. This family, which first appeared in [84], has 22 members.

Additionally to these families, in the table of the previous section, 12 families of manipulators have been enumerated. This is the first classification of manipulators according to their kinematic properties, and also the first that takes into account only doubly-planar Stewart-Gough platforms, which are common in most implementations.

7.4 Classification of doubly-planar Stewart-Gough platforms

Table 7.3: Family of flagged parallel manipulators



7.4 Classification of doubly-planar Stewart-Gough platforms

Table 7.4: Family of partially flagged parallel manipulators

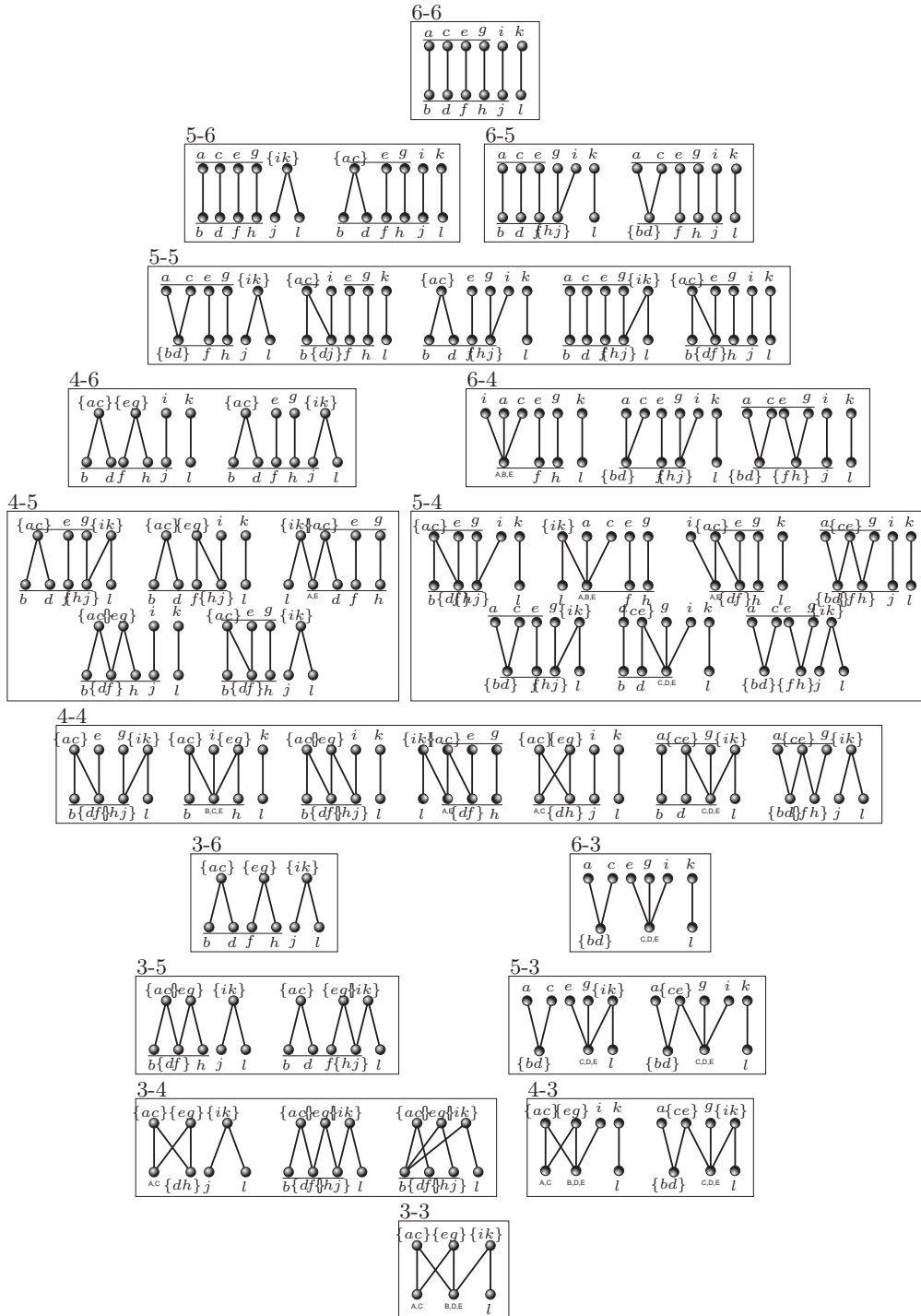
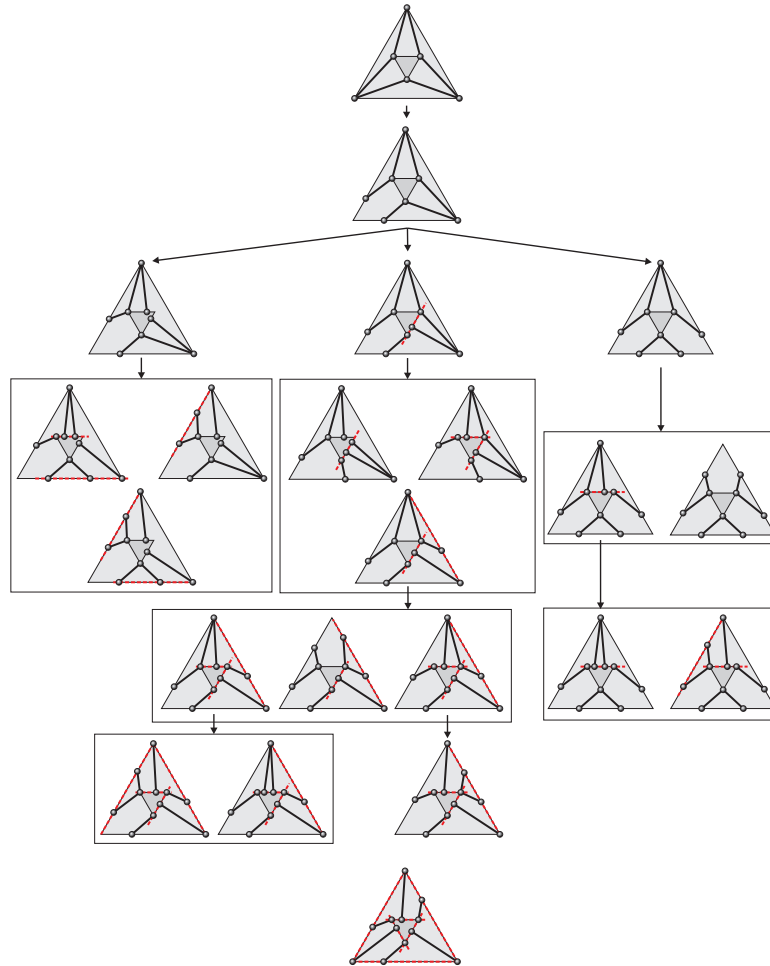


Table 7.5: Family of octahedral manipulators



7.5 Rewriting the Jacobian matrix determinant

Matrix \mathbf{P} defined in (7.6) has an aspect similar to the corresponding matrices defining singularity-invariant leg rearrangements for the Line-Plane (equation (5.12) in Chapter 5) or for the Line-Body (equation (6.3) in Chapter 6) components. As a consequence, there is the intuition that matrix \mathbf{P} can be transformed into a 9×9 matrix by replacing the last row by 3 extra rows depending only on pose parameters.

Let matrix $\widehat{\mathbf{T}}$ be matrix \mathbf{P} with the last row removed and

$$\mathbf{T} = \begin{pmatrix} r_1(\mathbf{X}) \\ r_2(\mathbf{X}) \\ r_3(\mathbf{X}) \\ \widehat{\mathbf{T}} \end{pmatrix}$$

so that $\det(\mathbf{J}) = \det(\mathbf{T})$. While it has been checked that all the coefficients of $\det(\mathbf{J})$ are minors of matrix $\widehat{\mathbf{T}}$, until the moment, it has not been possible to find $r_1(\mathbf{X})$, $r_2(\mathbf{X})$ and $r_3(\mathbf{X})$ so that $\det(\mathbf{J}) = \det(\mathbf{T})$.

7.6 Architectural Singularities

7.6.1 Algebraic characterization

Consider matrix $\widehat{\mathbf{T}}$, that is, \mathbf{P} without its last row

$$\widehat{\mathbf{T}} = \begin{pmatrix} -z_1 & -t_1 & x_1 & y_1 & x_1z_1 & y_1z_1 & x_1t_1 & y_1t_1 & 1 \\ -z_2 & -t_2 & x_2 & y_2 & x_2z_2 & y_2z_2 & x_2t_2 & y_2t_2 & 1 \\ -z_3 & -t_3 & x_3 & y_3 & x_3z_3 & y_3z_3 & x_3t_3 & y_3t_3 & 1 \\ -z_4 & -t_4 & x_4 & y_4 & x_4z_4 & y_4z_4 & x_4t_4 & y_4t_4 & 1 \\ -z_5 & -t_5 & x_5 & y_5 & x_5z_5 & y_5z_5 & x_5t_5 & y_5t_5 & 1 \\ -z_6 & -t_6 & x_6 & y_6 & x_6z_6 & y_6z_6 & x_6t_6 & y_6t_6 & 1 \end{pmatrix}. \quad (7.18)$$

When this matrix loses rank, the manipulator is architecturally singular. Alternatively, if matrix \mathbf{T} would exist, it would be clear that the rank deficiency of $\widehat{\mathbf{T}}$ would imply that all coefficients of the singularity polynomial are zero.

Then, in a similar way as in previous chapters, suppose that the rearrangement is done to only one of the legs (say \mathbf{l}_6). Then, for any new position of its attachments, the locus of architectural singularities is defined by those (x, y, z, t) for which $\widehat{\mathbf{T}}$ loses rank. Again, applying Gaussian Elimination, the last row of the resulting matrix has the form

$$\frac{1}{P_{6789}}(0, \dots, 0, P_{789}, P_{689}, P_{679}, P_{678})$$

where P_{6789} is the determinant of $\widehat{\mathbf{T}}$ after deleting its last row, and columns 6,7,8 and 9.

The 6th leg attachments are $\mathbf{a} = (x, y, 0)$ and $\mathbf{b} = \mathbf{p} + \mathbf{R}(z, t, 0)$. Then, the condition

$$P_{789} = P_{689} = P_{679} = P_{678} = 0 \quad (7.19)$$

define the locus of architectural singularities for the sixth leg (assuming $P_{6789} \neq 0$). By construction, the attachments of the other five legs must satisfy this condition. It can be proved that the above system has 6 solutions. The additional sixth solution correspond to an architectural singularity. Such architectural singularity was first studied by Bricard [21], Borel [7] and Duporcq [31, 32], and lately was revisited by Karger in [53].

7.6.2 Geometric interpretation

French mathematicians at the end of XIX century studied the feasible spherical paths that a body supported by six legs can perform [7, 21, 31]. They provided several mathematic interpretations of the singularity point found in the previous section. Next, the one presented by Ernest Duporcq in [32] is described with a numerical example, because it is highly related to the existence of the cubic curve that defines the singularity-invariant leg rearrangements. Indeed, it will be shown how this point on the cubic curve is a very special point that is geometrically defined given 5 of the legs of the manipulator.

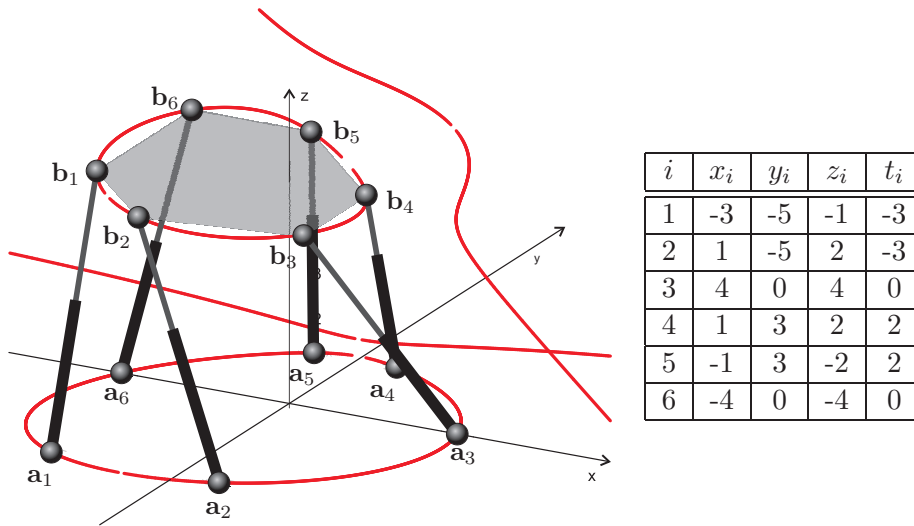


Figure 7.10: A doubly-planar Stewart-Gough platform and its corresponding attachment coordinates $(\mathbf{a}_i = (x_i, y_i, 0)^T$ and $\mathbf{b}_i = \mathbf{p} + \mathbf{R}(z_i, t_i, 0)^T$). In addition, the corresponding cubic curves defining its singularity-invariant leg rearrangements are also plotted.

Consider the example in Fig 7.10. After performing Gaussian Elimination on the

corresponding matrix \mathbf{P} , the system of equations that define the singularity-invariant leg rearrangements is

$$\left. \begin{aligned} 9xt - 10yz - 42x + 230y + 42z - 345t &= 0 \\ yt + 48y - 75t &= 0 \\ -9xz + yz + 6x + 598y - 6z - 960t + 144 &= 0 \end{aligned} \right\} \quad (7.20)$$

Then, the equations of the platform and base cubic curves are:

$$-59z^2t - 23zt^2 - 80t^3 + 168z^2 + 46zt + 302t^2 + 960t - 2688 = 0,$$

and

$$-79x^2y + 46xy^2 - 115y^3 + 525x^2 - 138xy + 249y^2 + 2992y - 8400 = 0,$$

respectively. The cubics are also represented in Fig. 7.10.

Now, consider that the sixth leg is rearranged. The locus of architectural singularities has been algebraically defined in the previous section as the points that satisfy condition (7.19), which are the solution of

$$\left. \begin{aligned} -3xz + 7yz + 66x - 254y - 54z + 384t &= 0 \\ -10xz + 21xt + 122x - 310y - 82z + 475t &= 0 \\ yt + 48y - 75t &= 0 \\ -5xz - 2x + 370y + z - 592t + 84 &= 0 \end{aligned} \right\} \quad (7.21)$$

It has 6 solutions, 5 corresponding the the other leg attachments and the sixth is

$$\left\{ x = \frac{237}{1553}, y = \frac{5019}{1553}, z = \frac{467}{774}, t = \frac{1673}{774} \right\}. \quad (7.22)$$

The geometric interpretation of this point given by Duporcq is based on the fact that you can always determine 3 special points on the cubic curves attached to the base and the platform. Then, the 5 base and platform attachments, plus that 3 special points, on the base and on the platform, define a pencil of cubics through these 8 points. Any pencil of cubic curves through 8 points intersect all at one 9th point, and this particular point is the one that gives the architectural singularity [32, n°182]. The idea is that, given 5 couples of corresponding points (defined by the 5 legs), a 6th couple can be computed independently of the pose of the platform, and thus, it corresponds to an architectural singularity. Next, this point will be derived in detail for this example.

Consider the systems of equations in (7.21) or in (7.20). Each equation of the system define a *correlation*, that is, given the coordinates of a point in the plane (z, t) , the equation defines a line on the plane (x, y) , and vice-versa. Then, two of these equations define what in [32, n°181] is called a *rational quadratic transformation* between points, because given a point in the plane (z, t) , the two equations define two lines that intersect at one point on the plane (x, y) . For a generic case, that is, for non-degenerate correlations, any of these transformations have always 3 singular points, that is, points for which the two lines coincide and thus, do not intersect at one point.

Consider the first and the third equations in system (7.20) (the results are independent of this choice). The rational quadratic transformation defined by these two equations is

$$\begin{aligned} (9t - 42)x + (230 - 10z)y + 42z - 345t &= 0 \\ (6 - 9z)x + (z + 598)y + 144 - 6z - 960t &= 0 \end{aligned} \quad (7.23)$$

so that, given a value of (z, t) , the above equations correspond to two lines on the plane (x, y) . The three singular points α_P , β_P and γ_P for which the two lines are coincident can be computed by imposing the coefficients of the lines to be proportional, that is, imposing

$$\begin{aligned} \begin{vmatrix} 9t - 42 & 230 - 10z \\ 6 - 9z & z + 598 \end{vmatrix} &= 0, \\ \begin{vmatrix} 230 - 10z & 42z - 345t \\ z + 598 & 144 - 6z - 960t \end{vmatrix} &= 0, \\ \begin{vmatrix} 9t - 42 & 42z - 345t \\ 6 - 9z & 144 - 6z - 960t \end{vmatrix} &= 0. \end{aligned}$$

The solutions of this system are the singular points of the quadratic transformation,

$$\alpha_P = \left(2, \frac{21}{5}\right), \quad \beta_P = \left(\frac{2300}{307}, \frac{896}{307}\right), \quad \gamma_P = \left(\frac{46}{3}, \frac{17}{6}\right),$$

which, at the same time, belong to the platform cubic curve. Then, the eight points \mathbf{b}_i for $i = 1, \dots, 5$, α_P , β_P and γ_P define a pencil of cubics. In Fig. 7.11-(top) all these points and the pencil of cubics are plotted, for this example.

Any pencil of cubics through 8 points intersect at a 9th point, which can be computed for example, as the intersection point of any two of the cubics of the pencil. In

Fig. 7.11-(top) it is represented by the big red dot and has coordinates

$$\left(\frac{467}{774}, \frac{1673}{774} \right). \quad (7.24)$$

The same computations can be done for the base attachments. Choosing the same polynomials, the singular points on the base are

$$\alpha_B = \left(1, \frac{105}{23} \right), \quad \beta_B = \left(\frac{4945}{449}, \frac{15087}{2245} \right), \quad \gamma_B = (25, 7),$$

and the pencil of cubics is shown in Fig. 7.11-(bottom). The singular point given by the intersection of all the cubics of the pencil have base coordinates

$$\left(\frac{237}{1553}, \frac{5019}{1553} \right). \quad (7.25)$$

Note that both singular points are in correspondence, in other words, are solution of the system (7.20), and coincide with the solution given in (7.22). See [32, pp.133] for details.

7.6.3 Comparison with previous results

In most of the literature, the architectural singularity for the Plane-Plane component is characterized by all base and platform attachments being on conics, and in addition, in projective correspondence. But such characterization is far from being general.

On the one hand, when all the base and platform attachments belong to a base and a platform conic, respectively, singularity-invariant leg rearrangements are defined as in the general case (because 6 points can belong to a conic and a cubic at the same time). Therefore, as in the general case, the attachments belong to a cubic and the condition of being on the same conic has nothing to do with the singularity condition.

On the other hand, when a projectivity between base and platform attachments exists, singularity-invariant leg rearrangements are defined by the roots of system (7.8), which gives exactly the projectivity as solution. In other words, leg attachments can be rearranged to any point of the base and platform planes without modifying the singularity locus as long as the attachments belong to the projectivity. Then, architectural singularities will occur if, and only if, all the base and platform attachments belong to conics.

7.6 Architectural Singularities

The architecturally singular condition found here is more general, and the presented methodology to find it gives the solution independently of the existence of such projectivity (contrary to other characterizations like the one in [53]).

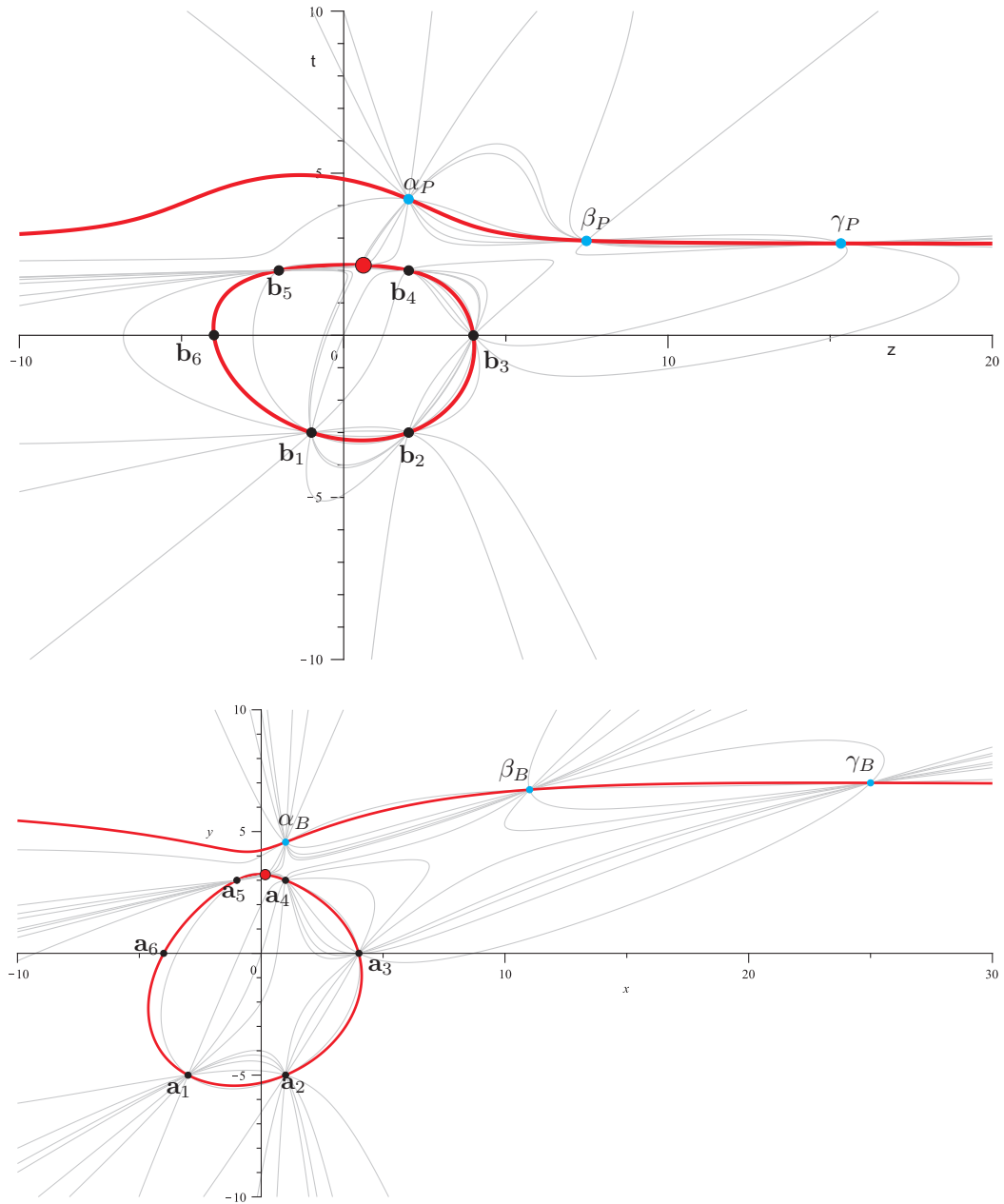


Figure 7.11: The pencil of cubics through the first five platform and base attachments and the 3 singular points (top and bottom respectively). They all intersect at another point (represented by the big red dot) which corresponds to the platform and base location of the sixth leg that leads to an architectural singularity.

Chapter 8

The Plane-Body and the Body-Body components

All singularity-invariant leg rearrangements have already been obtained for all the rigid components, except for the Plane-Body and the Body-Body. In this chapter it will be explained why singularity-invariant leg rearrangements are not possible for generic Plane-Body or Body-Body components.

Until Chapter 5, obtaining the a singularity-invariant leg rearrangements by finding an affine relationship, entails solving the system of forward kinematics equations,

$$(\mathbf{a}_i - \mathbf{b}_i)^2 = l_i^2, \text{ for } i = 1, \dots, 6$$

plus one equation involving the location of the new attachments for the rearranged leg,

$$(\mathbf{a} - \mathbf{b})^2 = d^2.$$

To derive its associated linear system, the same simplifications have to be used for all the cases. First, using the orthogonality of the rotation matrix, 6 equations can be used to simplify the quadratic terms of all the orientation variables

$$\begin{aligned} i_x^2 + i_y^2 + i_z^2 &= 1, & \mathbf{i} \cdot \mathbf{j} &= 0, \\ j_x^2 + j_y^2 + j_z^2 &= 1, & \mathbf{i} \cdot \mathbf{k} &= 0, \\ k_x^2 + k_y^2 + k_z^2 &= 1, & \mathbf{j} \cdot \mathbf{k} &= 0. \end{aligned}$$

Secondly, the introduction of additional unknowns allows the linearization of all bilinear

terms by simple variable changes

$$\begin{aligned} u &= \mathbf{p} \cdot \mathbf{i} = p_x i_x + p_y i_y + p_z i_z, \\ v &= \mathbf{p} \cdot \mathbf{j} = p_x j_x + p_y j_y + p_z j_z, \\ w &= \mathbf{p} \cdot \mathbf{k} = p_x k_x + p_y k_y + p_z k_z \end{aligned}$$

and finally, subtracting the first equation from all the others, quadratic terms in p_x , p_y and p_z are eliminated.

The matrix associated with the linear system, after some manipulation using row operations, has always been named \mathbf{P} and has a regular appearance (matrix (5.13) for the Line-Plane component, matrix (6.3) for the Line-Body component and matrix (7.6) for the Plane-Plane component).

In all cases, singularity-invariant leg rearrangements are defined by the rank deficiency of matrix \mathbf{P} . In the next sections, the same matrix will be analyzed for the Plane-Body and the Body-Body components to conclude that no singularity-invariant leg rearrangements are possible for generic instances of these components.

8.1 The Plane-Body component

The Plane-Body component consists of 6 legs, whose base attachments have coordinates $\mathbf{a} = (x_i, y_i, z_i)^T$ and the corresponding platform attachments lie in a plane, and thus, have local coordinates $\tilde{\mathbf{b}}_i = (r_i, s_i, 0)^T$, for $i = 1, \dots, 6$. So, the space of leg attachments is a 5-dimensional space defined by $(x, y, z, r, s) \in \mathbb{R}^5$.

Using the same equations and simplifications explained above, it can be checked that the corresponding \mathbf{P} matrix for the Plane-Body component is

$$\begin{pmatrix} -r_1 & -s_1 & x_1 & y_1 & z_1 & r_1 x_1 & r_1 y_1 & r_1 z_1 & s_1 x_1 & s_1 y_1 & s_1 z_1 & 1 \\ -r_2 & -s_2 & x_2 & y_2 & z_2 & r_2 x_2 & r_2 y_2 & r_2 z_2 & s_2 x_2 & s_2 y_2 & s_2 z_2 & 1 \\ -r_3 & -s_3 & x_3 & y_3 & z_3 & r_3 x_3 & r_3 y_3 & r_3 z_3 & s_3 x_3 & s_3 y_3 & s_3 z_3 & 1 \\ -r_4 & -s_4 & x_4 & y_4 & z_4 & r_4 x_4 & r_4 y_4 & r_4 z_4 & s_4 x_4 & s_4 y_4 & s_4 z_4 & 1 \\ -r_5 & -s_5 & x_5 & y_5 & z_5 & r_5 x_5 & r_5 y_5 & r_5 z_5 & s_5 x_5 & s_5 y_5 & s_5 z_5 & 1 \\ -r_6 & -s_6 & x_6 & y_6 & z_6 & r_6 x_6 & r_6 y_6 & r_6 z_6 & s_6 x_6 & s_6 y_6 & s_6 z_6 & 1 \\ -r & -s & x & y & z & rx & ry & rz & sx & sy & sz & 1 \end{pmatrix}. \quad (8.1)$$

Singularity-invariant leg rearrangements for the Plane-Body component would be defined by those (x, y, z, r, s) that make \mathbf{P} lose rank. Such condition can be translated into a system of equations by applying Gaussian Elimination. As \mathbf{P} is a 7×12 matrix, the last row of the resulting matrix has 6 elements different from zero. In other words, the singularity-invariant leg rearrangements would be defined by the solutions of a system of 6 equations in the 5 unknowns (x, y, z, r, s) . For any generic case, this is an overdetermined system that has no solution, and so, there are no singularity-invariant leg rearrangements for a generic Plane-Body manipulator.

8.2 The Body-Body component

The generic Stewart-Gough platform also consists of 6 legs with base attachments $\mathbf{a} = (x_i, y_i, z_i)^T$ and platform attachments $\tilde{\mathbf{b}}_i = (r_i, s_i, t_i)^T$, for $i = 1, \dots, 6$.

Repeating the same steps as above, the associated linear system leads to the following \mathbf{P} matrix

$$\begin{pmatrix} -r_1 & -s_1 & -t_1 & x_1 & y_1 & z_1 & r_1x_1 & r_1y_1 & r_1z_1 & s_1x_1 & s_1y_1 & s_1z_1 & t_1x_1 & t_1y_1 & t_1z_1 & 1 \\ -r_2 & -s_2 & -t_2 & x_2 & y_2 & z_2 & r_2x_2 & r_2y_2 & r_2z_2 & s_2x_2 & s_2y_2 & s_2z_2 & t_2x_2 & t_2y_2 & t_2z_2 & 1 \\ -r_3 & -s_3 & -t_3 & x_3 & y_3 & z_3 & r_3x_3 & r_3y_3 & r_3z_3 & s_3x_3 & s_3y_3 & s_3z_3 & t_3x_3 & t_3y_3 & t_3z_3 & 1 \\ -r_4 & -s_4 & -t_4 & x_4 & y_4 & z_4 & r_4x_4 & r_4y_4 & r_4z_4 & s_4x_4 & s_4y_4 & s_4z_4 & t_4x_4 & t_4y_4 & t_4z_4 & 1 \\ -r_5 & -s_5 & -t_5 & x_5 & y_5 & z_5 & r_5x_5 & r_5y_5 & r_5z_5 & s_5x_5 & s_5y_5 & s_5z_5 & t_5x_5 & t_5y_5 & t_5z_5 & 1 \\ -r_6 & -s_6 & -t_6 & x_6 & y_6 & z_6 & r_6x_6 & r_6y_6 & r_6z_6 & s_6x_6 & s_6y_6 & s_6z_6 & t_6x_6 & t_6y_6 & t_6z_6 & 1 \\ -r & -s & -t & x & y & z & rx & ry & rz & sx & sy & sz & tx & ty & tz & 1 \end{pmatrix}. \quad (8.2)$$

This is a 7×16 matrix whose last row, after Gaussian Elimination, has 10 non-zero elements. Then, for this case, singularity-invariant leg rearrangements are defined by the zeros of a system of 10 equations in the 6 unknowns (x, y, z, r, s, t) .

In conclusion, if any of the legs is relocated to the new attachments $\mathbf{a} = (x, y, z)^T$ and $\tilde{\mathbf{b}} = (r, s, t)^T$, the resulting leg rearrangement is singularity-invariant if, and only if, the 10 polynomials do simultaneously vanish.

This is an overdetermined system that has no solution for a generic case. We need to impose at least 5 more scalar equations to obtain a 1-dimensional set of solutions. For example, non-generic manipulators could lead to cases where such overdetermined systems have solutions. The important point here is that, for any of those cases, the

8.3 Example of a non-generic case: a decoupled Stewart-Gough platform

rank deficiency of matrix \mathbf{P} would characterize all possible singularity-invariant leg rearrangements. In conclusion, all the generic singularity-invariant leg rearrangements have been classified in this work and any non-generic case can be obtained through the study of the matrix \mathbf{P} .

8.3 Example of a non-generic case: a decoupled Stewart-Gough platform

Consider the Plane-Body component in Fig. 8.1. It contains a Point-Plane subcomponent and 3 legs, and only the base attachments are all coplanar. The doubly-planar version with the same topology appears in Section 7.4 under number 8, and it turns out that the singularity-invariant leg rearrangements that can be done are exactly the same as in the doubly-planar version.

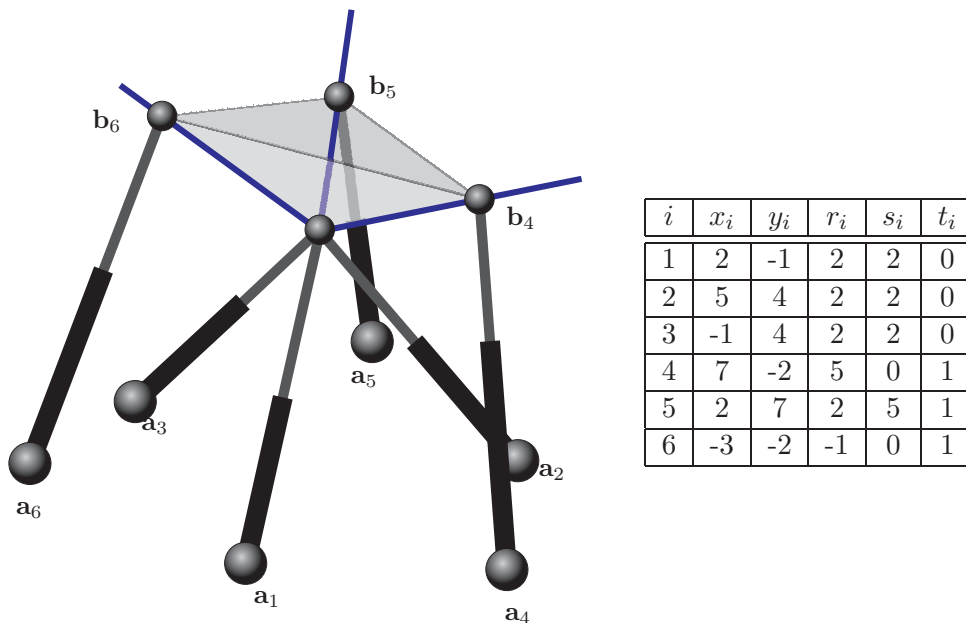


Figure 8.1: A decoupled manipulator with non-planar platform and its corresponding attachment coordinates ($\mathbf{a}_i = (x_i, y_i, 0)$ and $\mathbf{b}_i = \mathbf{p} + \mathbf{R}(r_i, s_i, t_i)^T$). In blue, its singularity-invariant leg rearrangement lines.

This manipulator is said to be decoupled because the three legs forming the tripod give the position of the platform, while the three remaining ones orient it. When the tripod is rigid, *i. e.*, fixed at a position, this manipulator is also known as spherical

8.3 Example of a non-generic case: a decoupled Stewart-Gough platform

[6, 39]. Note that when \mathbf{b}_4 , \mathbf{b}_5 and \mathbf{b}_6 are collinear, the manipulator contains a Line-Plane component (see the example in Section 5.9.1), and when they are coplanar with the 4th attachment, it contains a Plane-Plane component.

After performing Gaussian Elimination on the corresponding matrix \mathbf{P} , only six non-zero elements remain at the last row. That is, a leg rearrangement will be singularity-invariant if it fulfills the following 6 conditions

$$\begin{aligned}
 -2xr + yr + 4x - 2y + 6r - 6s + 18t &= 0, \\
 -4xr/3 + xs + 2x/3 + 6r - 6s + 12t &= 0, \\
 1/5(17xr + ys - 34x - 10y - 34r + 34s - 207t) &= 0, \\
 5xr/3 + xt - 10x/3 - 5r + 5s - 17t &= 0, \\
 9xr/5 + yt - 18x/5 - 18r/5 + 18s/5 - 89t/5 &= 0, \\
 -1xr/2 + x + r - 3s/2 + 9t/2 + 1 &= 0.
 \end{aligned}$$

This system of equations has 4 sets of solutions:

$$\begin{aligned}
 \mathcal{T} &= \{(x, y), (r, s, t) \mid \\
 &\quad x = \lambda, y = \mu; r = 2, s = 2, t = 0, \lambda, \mu \in \mathbb{R}\}, \\
 \Delta_1 &= \{(x, y), (r, s, t) \mid \\
 &\quad x = 2, y = 7; r = 2, s = 2 + 3\lambda, t = \lambda, \lambda \in \mathbb{R}\}, \\
 \Delta_2 &= \{(x, y), (r, s, t) \mid x = 7, y = -2; \\
 &\quad r = 5 - 3\lambda/2, s = \lambda, t = 1 - \lambda/2, \lambda \in \mathbb{R}\}, \\
 \Delta_3 &= \{(x, y), (r, s, t) \mid x = -3, y = -2; \\
 &\quad r = 2 - 3\lambda, s = 2 - 2\lambda, t = \lambda, \lambda \in \mathbb{R}\}.
 \end{aligned}$$

The first one corresponds to the tripod component and it means that base attachments can be rearranged to any point of the base plane as long as its corresponding platform attachment is the vertex of the tripod. The other 3 sets correspond to point-line correspondences as before, depicted as red lines in Fig. 8.1. This means that \mathbf{b}_4 , \mathbf{b}_5 and \mathbf{b}_6 can be relocated to any other point of the blue lines (as long as their corresponding base attachments remain the same).

8.3 Example of a non-generic case: a decoupled Stewart-Gough platform

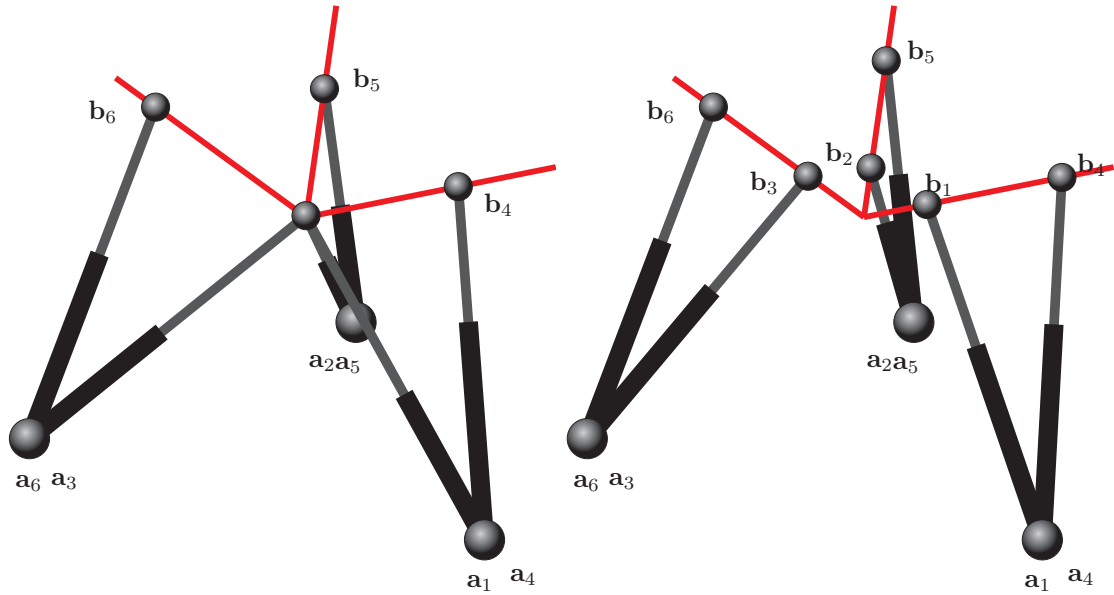


Figure 8.2: Singularity-invariant leg rearrangements from the example in Fig. 8.1.

In Fig. 8.2 we show two possible singularity-invariant leg rearrangements of the manipulator at hand. For all of them, the decoupling properties remain the same as they are all equivalent manipulators.

Chapter 9

Conclusions: contributions and prospects for further research

To the best of our knowledge, the concept of singularity-invariant leg rearrangements is new. This concept has allowed us not only to contribute to new geometric interpretations of singularities, but also to the detection of kinematic equivalences, and to provide a new geometric point of view to architectural singularities.

A complete characterization of all possible singularity-invariant leg rearrangements for Stewart-Gough platforms has been done. On the one hand, three of the possible rigid components of a Stewart-Gough platform, the Point-Line, the Point-Plane and the Line-Line, admit any leg rearrangement that preserves the lines and the planes to which their attachments belong. On the other hand, the rest of rigid components only admit rearrangements that preserve some extra geometric constraints. Although this may seem more restrictive, it provides a lot of geometric information about the kinematics of the platform, by, among other things, allowing to identify the complexity of its singularity locus at a glance.

Despite its simplicity, the Point-Line singularity-invariant leg rearrangements have been proved to be very powerful to detect equivalences and to perform complex rearrangements, specially when several of these rearrangements are applied simultaneously. Unfortunately, these rearrangements alone are incomplete because they cannot be applied to manipulators with no multiple spherical joints. This has been proved, for example, for the Line-Line component, whose singularity-invariant leg rearrangements require an in-depth independent analysis for the general case. In addition, leg rear-

rangements in Point-Line components have also been used to obtain parameterizations of self-motions of some architecturally singular versions of well-known manipulators, such as the Griffis-Duffy type I and the Zhang-Song platform.

The most fruitful singularity-invariant leg rearrangements have been obtained through the analysis of the Line-Plane component, in the sense that they have led to a lot of unknown properties of this component. Indeed, this analysis permitted to identify different topologies, each of them with different degree for its characteristic polynomial. In addition, this analysis has also provided a geometric interpretation of type II singularities and a measure of distance to architectural singularities. All these results had never appeared before in the literature. Its generalization to Line-Body components have revealed a more complex correspondence between the platform line and a cubic space curve attached to the base. In addition, for this component, a very interesting property has been found: in a singular position, it is always possible to relocate a leg through a singularity-invariant rearrangement so that it has zero length. This provides a connection between type I and type II singularities of the platform, but more research has to be done to generalize this result to more general components like the Plane-Plane component.

The singularity-invariant leg rearrangements for the Plane-Plane component have revealed a hidden geometric world to explore. The correspondence between the planar cubic curves attached to the base and the platform can be seen as a generalization of all the other singularity-invariant leg rearrangements on components involving points, lines and planes. Factorizations of such cubics provide kinematic simplifications, and its generic architectural singularity can be seen as a particular degenerate rearrangement.

The remaining Line-Body and Body-Body components have been shown not to admit any singularity-invariant leg rearrangement in general, but for some non-generic cases such rearrangements exist and tools have been provided to compute them.

Regarding the classifications of Stewart-Gough platforms, two types of classifications have been done in this thesis. On the one hand, families of manipulators with the same singularities have been generated for all doubly-planar Stewart-Gough platforms. To this end, the Faugère and Lazard classification, using bipartite graphs, is used to identify each architecture. Then, they are all grouped into families where each member has the same forward kinematic solution and essentially, the same singularity locus.

On the other hand, a different type of classification is done, which finds classes inside the same architecture. Indeed, for the Line-Plane, three types of singularity loci with different topology have been found, each one corresponding to different degrees of the characteristic polynomial, but them all corresponding to the same bipartite graph, that is, to the same type of architecture. For the Line-Body and the Plane-Plane components, classifications depending on the factorizations of the cubic curves that define their singularity-invariant leg rearrangements have been done. It is still an open problem to elucidate if they all correspond to different characteristic polynomial degrees.

Finally, several applications have been reported. An octahedral manipulator kinematically equivalent to a 6-6 parallel platform with only simple spherical joints has been presented and its implementation briefly described. It has also been presented the first optimizations done using singularity-invariant leg rearrangements. More research can be done to study the impact of such rearrangements in other indexes like the condition number or the volume of the static workspace. In short, the optimizations that can be done using singularity-invariant leg rearrangements present an interesting paradigm to be taken into account in the future.

In conclusion, singularity-invariant leg rearrangements are proved to be a powerful tool for the study of several aspects of robot kinematics. We hope that the obtained results will encourage other researchers to follow this new research line.

Appendix A

Cayley-Menger determinants and Distance Geometry

Cayley-Menger determinants play a fundamental role in the so-called Distance Geometry, a branch of Geometry devoted to the characterization and study of sets of points on the basis of only their pairwise distances (see [73] for a complete review of these determinants and their generalizations). Hence, Distance Geometry has immediate relevance where distances between points are determined or considered, as for example, the resolution of the forward kinematics problem of parallel manipulators.

Let us define:

$$D(\mathbf{p}_1, \dots, \mathbf{p}_n; \mathbf{q}_1, \dots, \mathbf{q}_n) = \begin{vmatrix} 0 & 1 & \dots & 1 \\ 1 & s_{1,1} & \dots & s_{1,n} \\ \vdots & \vdots & \ddots & \vdots \\ 1 & s_{n,1} & \dots & s_{n,n} \end{vmatrix}, \quad (\text{A.1})$$

with $s_{i,j} = \|\mathbf{p}_i - \mathbf{q}_j\|^2$. This determinant is known as the *Cayley-Menger bi-determinant* of the point sequences $\mathbf{p}_1, \dots, \mathbf{p}_n$, and $\mathbf{q}_1, \dots, \mathbf{q}_n$. When the two point sequences are the same, it will be convenient to abbreviate $D(\mathbf{p}_1, \dots, \mathbf{p}_n; \mathbf{p}_1, \dots, \mathbf{p}_n)$ by $D(\mathbf{p}_1, \dots, \mathbf{p}_n)$, which is simply called the *Cayley-Menger determinant* of the involved points.

The square volume $V^2(\mathbf{p}_1, \dots, \mathbf{p}_{k+1})$ of the k -dimensional simplex defined by the $k + 1$ points $\mathbf{p}_1, \dots, \mathbf{p}_{k+1}$ can be expressed as follows:

$$V^2(\mathbf{p}_1, \dots, \mathbf{p}_{k+1}) = \frac{(-1)^{k+1}}{2^k (k!)^2} D(\mathbf{p}_1, \dots, \mathbf{p}_{k+1}). \quad (\text{A.2})$$

The direct consequence of the above property is that any Cayley-Menger determinant involving 5 or more points will be proportional to a degenerate volume, because any set of points embedded in \mathbb{R}^3 have degenerate volumes in 4 or higher dimensions.

There are several other properties of Cayley-Menger determinants that can be very useful to the geometric interpretation of results obtained using this methodology [98]. For example,

$$D(\mathbf{p}_1, \mathbf{p}_2, \mathbf{p}_3; \mathbf{q}_1, \mathbf{q}_2, \mathbf{q}_3) = ((\mathbf{p}_1 - \mathbf{p}_3) \times (\mathbf{p}_2 - \mathbf{p}_3)) \cdot ((\mathbf{q}_1 - \mathbf{q}_3) \times (\mathbf{q}_2 - \mathbf{q}_3)), \quad (\text{A.3})$$

which means that $D(\mathbf{p}_1, \mathbf{p}_2, \mathbf{p}_3; \mathbf{q}_1, \mathbf{q}_2, \mathbf{q}_3)$ is the product of the areas of the two triangles defined by the two sets of points, and

$$D(\mathbf{p}_1, \mathbf{p}_2, \mathbf{p}_3, \mathbf{p}_4; \mathbf{q}_1, \mathbf{q}_2, \mathbf{q}_3, \mathbf{q}_4) = |\mathbf{p}_1 - \mathbf{p}_4, \mathbf{p}_2 - \mathbf{p}_4, \mathbf{p}_3 - \mathbf{p}_4| \cdot |\mathbf{q}_1 - \mathbf{q}_4, \mathbf{q}_2 - \mathbf{q}_4, \mathbf{q}_3 - \mathbf{q}_4|, \quad (\text{A.4})$$

which again means that the bi-determinant is the product of the volumes of the 2 tetrahedra formed by the two sets of points.

The Jacobi's theorem can be applied to a Cayley-Menger determinants to simplify its expansion [104]. In this context, a simple minor M_{ij} of a matrix is defined as the determinant of the matrix after deleting the i th row and the j th column.

Jacobi's Theorem. *Given a $n \times n$ matrix $\mathbf{A} = (a_{ij})$, consider the following submatrices*

$\mathbf{M}_{(r)}$ *It is the $(n - r) \times (n - r)$ matrix determinant obtained from the determinant of the matrix \mathbf{A} after deleting rows i_1, \dots, i_r and columns k_1, \dots, k_r , with sign $(-1)^{i_1 + \dots + i_r + k_1 + \dots + k_r}$.*

Δ_r *It is the r -minor of the cofactor matrix. That is, if $\mathbf{A}_{ij} = (-1)^{i+j} M_{ij}$ is the ij 's cofactor of the matrix \mathbf{A} , Δ_r is the determinant of the matrix defined by the first r rows and columns of the matrix (\mathbf{A}_{ij}) .*

Then, the Jacobi's theorem states that

$$\Delta_r = |\mathbf{A}|^{r-1} \mathbf{M}_{(r)}$$

where $|\mathbf{A}|$ stands for the determinant of the matrix \mathbf{A} .

For $r = 1$, it can be checked that the Jacobi's theorem gives the trivial relation $\mathbf{A}_{11} = \mathbf{A}_{11}$. Otherwise, for $r = 2$, Jacobi's theorem says

$$\Delta_2 = |\mathbf{A}| \mathbf{M}_{(2)} \implies |\mathbf{A}| = \frac{\mathbf{A}_{11} \mathbf{A}_{22} - \mathbf{A}_{12} \mathbf{A}_{21}}{\mathbf{M}_{(2)}}$$

where

$$\mathbf{M}_{(2)} = (-1)^{1+2+1+2} \begin{vmatrix} a_{33} & \dots & a_{3n} \\ \vdots & & \vdots \\ a_{n3} & \dots & a_{nn} \end{vmatrix}$$

supposing that the chosen indexes to delete, i_1 and i_2 , are 1 and 2.

Consider now that \mathbf{A} is the matrix of the Cayley-Menger determinant of 5 points, so that $|\mathbf{A}| = D(\mathbf{p}_1, \mathbf{p}_2, \mathbf{p}_3, \mathbf{p}_4, \mathbf{p}_5)$. Note that any minor \mathbf{M}_{ii} will correspond to the Cayley-Menger determinant of the four points $\{\mathbf{p}_1, \mathbf{p}_2, \mathbf{p}_3, \mathbf{p}_4, \mathbf{p}_5\} \setminus \mathbf{p}_i$. On the other hand, a minor \mathbf{M}_{ij} for $i \neq j$ gives the bi-determinant of the two sets $\{\mathbf{p}_1, \mathbf{p}_2, \mathbf{p}_3, \mathbf{p}_4, \mathbf{p}_5\} \setminus \mathbf{p}_i$ and $\{\mathbf{p}_1, \mathbf{p}_2, \mathbf{p}_3, \mathbf{p}_4, \mathbf{p}_5\} \setminus \mathbf{p}_j$.

Then, for a 5-point Cayley-Menger determinant, one can directly apply Jacobi's theorem for $r = 2$ to the following partition of the Cayley-Menger determinant:

$$D(\mathbf{p}_1, \mathbf{p}_2, \mathbf{p}_3, \mathbf{p}_4, \mathbf{p}_5) = \begin{vmatrix} 0 & 1 & 1 & 1 & | & 1 & 1 \\ 1 & 0 & s_{1,2} & s_{1,3} & | & s_{1,4} & s_{1,5} \\ 1 & s_{2,1} & 0 & s_{2,3} & | & s_{2,4} & s_{2,5} \\ 1 & s_{3,1} & s_{3,2} & 0 & | & s_{3,4} & s_{3,5} \\ \hline 1 & s_{4,1} & s_{4,2} & s_{4,3} & | & 0 & s_{4,5} \\ 1 & s_{5,1} & s_{5,2} & s_{5,3} & | & s_{5,4} & 0 \end{vmatrix} = \frac{\mathbf{A}_{55}\mathbf{A}_{66} - \mathbf{A}_{56}\mathbf{A}_{65}}{D(\mathbf{p}_1, \mathbf{p}_2, \mathbf{p}_3)},$$

that is,

$$D(\mathbf{p}_1, \mathbf{p}_2, \mathbf{p}_3, \mathbf{p}_4, \mathbf{p}_5) = \frac{D(\mathbf{p}_1, \mathbf{p}_2, \mathbf{p}_3, \mathbf{p}_4)D(\mathbf{p}_1, \mathbf{p}_2, \mathbf{p}_3, \mathbf{p}_5) - D(\mathbf{p}_1, \mathbf{p}_2, \mathbf{p}_3, \mathbf{p}_4; \mathbf{p}_1, \mathbf{p}_2, \mathbf{p}_3, \mathbf{p}_5)^2}{D(\mathbf{p}_1, \mathbf{p}_2, \mathbf{p}_3)}. \quad (\text{A.5})$$

In conclusion, Jacobi's theorem is used to express Cayley-Menger determinants as a function of lower degree Cayley-Menger determinants. This is used in [77, 78, 79] to solve the kinematics of both serial and parallel robots using Distance Geometry. During the development of the present thesis, it was used to proof several singularity-invariant leg rearrangements of some of the rigid components [9], but here it is only applied to the Point-Plane component in Section 4.6 in the 4th chapter.

Appendix B

Cross-ratios and Projective Geometry

One of the objectives of the present work is to give a common framework to deal with architectural singularities, whose characterizations found until the moment deal with projective invariants that must be preserved between the platform and the base attachments in their local coordinates. In this context, it could be useful to interpret the leg rearrangements in terms of Projective Geometry. To this end, next a brief review of some basic concepts and some of the theorems used in this thesis is presented.

The cross-ratio of four points on a line¹ $\mathbf{p}_i = (n_i, 0, 0)$, for $i = 1, \dots, 4$, is defined as:

$$\{\mathbf{p}_1, \mathbf{p}_2; \mathbf{p}_3, \mathbf{p}_4\} = \frac{(n_3 - n_1)(n_4 - n_2)}{(n_4 - n_1)(n_3 - n_2)}. \quad (\text{B.1})$$

Likewise, for a pencil of lines l_1, l_2, l_3, l_4 with focus \mathbf{v} , their cross-ratio $\{l_1, l_2; l_3, l_4\}$ can be defined as the cross-ratio of the four points resulting from intersecting these four lines with an arbitrary line, in general position, lying in the same plane [23, Section IV.3] (points $\mathbf{p}_1, \mathbf{p}_2, \mathbf{p}_3$ and \mathbf{p}_4 in Fig. B.1).

The cross-ratio of four points lying on a conic is defined as the cross-ratio of the pencil of lines formed by joining the four points with any other different point of the conic. Chasles's Theorem states that the value of this cross-ratio is independent of the position of the pencil focus on the conic [89, Section V].

¹The set of points of a fixed line a is called *range of points*, having a as its axis; dually, the set of all lines through a fixed point A is called *pencil of lines*, having A as its vertex [89].

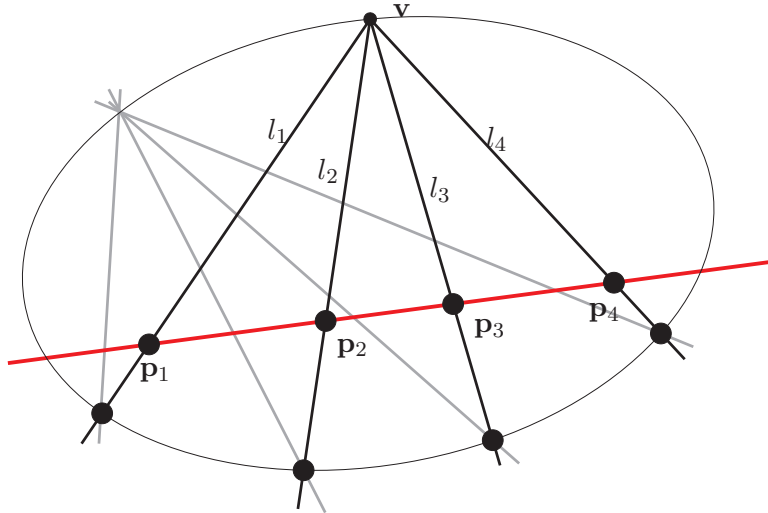


Figure B.1: A range of points on a line, and a pencil of lines through them, and four points on a conic.

Pencils of lines, ranges of points and conics are all one-dimensional projective domains. Thus, their elements (lines or points) can be defined by a single non-homogeneous coordinate which is called the projective parameter.

Theorem *Given a one-to-one correspondence between two one-dimensional projective domains, the three following statements are equivalent:*

1. *The correspondence is projective.*
2. *The cross-ratio of any four elements is equal to the cross ratio of the four corresponding elements, taken in the corresponding order. Actually, the cross-ratio can be used to define the correspondence.*
3. *The correspondence is associated with a bilinear relation between their projective parameters θ and θ' of the form*

$$\theta' = \frac{\alpha\theta + \beta}{\gamma\theta + \delta}, \text{ with } \alpha\delta - \beta\gamma \neq 0. \quad (\text{B.2})$$

All these concepts of plane Projective Geometry are used in Chapter 5 in some of the geometrical interpretations of the singularity-invariant leg rearrangements and for the architectural singularity characterization. All the one-to-one correspondences that appear in this thesis can be defined in a Projective Space.

Bibliography

- [1] M. Alberich-Carramiñana, M. Garolera, F. Thomas, and C. Torras. Partially-flagged parallel manipulators: Singularity charting and avoidance. *IEEE Transactions on Robotics*, 25(4):771–784, 2009.
- [2] M. Alberich-Carramiñana, F. Thomas, and C. Torras. Flagged parallel manipulators. *IEEE Transactions on Robotics*, 23(5):1013–1023, 2007.
- [3] P. Ben-Horin and M. Shoham. Singularity condition of six degree-of-freedom three-legged parallel robots based on Grassmann-Cayley algebra. *IEEE Transactions on Robotics*, 22(4):577–590, 2006.
- [4] P. Ben-Horin and M. Shoham. Singularity of Gough-Stewart platforms with collinear joints. In *12th IFToMM World Congress*, 2007.
- [5] P. Ben-Horin and M. Shoham. Application of Grassmann-Cayley algebra to geometrical interpretation of parallel robot singularities. *International Journal of Robotics Research*, 28(1):127–141, 2009.
- [6] I. A. Bonev and C. M. Gosselin. Analytical determination of the workspace of symmetrical spherical parallel mechanisms. *IEEE Transactions on Robotics*, 22(5):1011–1017, 2006.
- [7] E. Borel. Mémoire sur les déplacements à trajectoires sphériques. *Mémoires présentés par divers savants à l'Académie des Sciences de l'Institut National de France*, 33(1):1–128, 1908.
- [8] J. Borràs and F. Thomas. Kinematics of the line-plane subassembly in Stewart platforms. In *IEEE International Conference on Robotics and Automation*, pages 4094–4099, 2009.

- [9] J. Borràs, F. Thomas, and C. Torras. Analysing the singularities of 6-SPS parallel robots using virtual legs. In *Second International Workshop on Fundamental Issues and Future Research Directions for Parallel Mechanisms and Manipulators*, pages 145–150, 2008.
- [10] J. Borràs, F. Thomas, and C. Torras. Architecture singularities in flagged parallel manipulators. In *IEEE International Conference on Robotics and Automation*, pages 3844–3850, 2008.
- [11] J. Borràs, F. Thomas, and C. Torras. On Δ -transforms. *IEEE Transactions on Robotics*, 25(6):1225–1236, 2009.
- [12] J. Borràs, F. Thomas, and C. Torras. Straightening-free algorithm for the singularity analysis of Stewart-Gough platforms with collinear/coplanar attachments. In *International Workshop on Computational Kinematics*, 2009.
- [13] J. Borràs, F. Thomas, and C. Torras. Architectural singularities of a class of pentapods. *Mechanism and Machine Theory*, 2010. Accepted with minor revisions.
- [14] J. Borràs, F. Thomas, and C. Torras. A family of quadratically-solvable 5-SPU parallel robots. In *IEEE International Conference on Robotics and Automation*, pages 4703–4708, 2010.
- [15] J. Borràs, F. Thomas, and C. Torras. Singularity-invariant families of 5-SPU platforms. *IEEE Transactions on Robotics*, 2010. Conditionally accepted.
- [16] J. Borràs, F. Thomas, and C. Torras. Singularity invariant leg rearrangements in doubly-planar Stewart-Gough platforms. In *Robotics: Science and Systems VI*. The MIT Press, 2010.
- [17] J. Borràs, F. Thomas, and C. Torras. Singularity-invariant leg rearrangements in Stewart-Gough platforms. In *International Symposium on Advances in Robot Kinematics*, pages 421–428, 2010.
- [18] J. Borràs and F. Thomas. Singularity-invariant leg substitutions in pentapods. In *IEEE/RSJ International Conference on Intelligent Robots and Systems*, pages 2766–2771, 2010.

- [19] P. Bosscher and I. Ebert-Uphoff. A novel mechanisms for implementing multiple collocated spherical joints. In *IEEE International Conference on Robotics and Automation*, pages 336–341, 2003.
- [20] G. F. Bär and G. Weiß. Kinematic analysis of a pentapod robot. *Journal for Geometry and Graphics*, 10(2):173–182, 2006.
- [21] R. Bricard. Mémoire sur les déplacements à trajectoires sphériques. *Journal de l'École Polytechnique*, 11(2):1–93, 1906.
- [22] M. Chasles. Sur les six droites qui peuvent être les directions de six forces en équilibre. *Comptes Rendus, Journal de Mathématiques Pures et Appliquées*, page 1094, 1851.
- [23] R. Courant and H. Robbins. *What is Mathematics?* Oxford Univesity Press, 1996.
- [24] G. M. Crippen and T. F. Havel. *Distance Geometry and Molecular Conformation*. Taunton, U.K.: Res. Studies, 1988.
- [25] A. Dandurand. The rigidity of compound spatial grids. *Structural Topology*, 10:41–56, 1984.
- [26] B. Dasguptaa and T.S. Mruthyunjayab. The Stewart platform manipulator: a review. *Mechanism and Machine Theory*, 35:15–40, 2000.
- [27] P. Dietmaier. The Stewart-Gough platform of general geometriy can have 40 real postures. In *International Symposium on Advances in Robot Kinematics*, pages 1–10, 1998.
- [28] P. Donelan. Singularities in robot kinematics - a publications database, 2007. [Online; accessed 1-December-2008].
- [29] H. Dörrie. *100 Great Problems of Elementary Mathematics. Their History and Solution*. New York: Dover, 1965.
- [30] D.M. Downing, A.E. Samuel, and K.H. Hunt. Identification of the special configurations of the octahedral manipulator using the pure condition. *International Journal of Robotics Research*, 21(2):147–159, 2002.

- [31] E. Duporcq. Sur la correspondance quadratique et rationnelle de deux figures planes, et sur un déplacement remarquable. *Comptes Rendus, Journal de Mathématiques Pures et Appliquées*, pages 1405–1406, 1896.
- [32] E. Duporcq. *Premiers principes de géométrie moderne*. Éditions Jacques Gabay, 1995.
- [33] J.C Faugère and D. Lazard. Combinatorial classes of parallel manipulators. *Mechanism and Machine Theory*, 30(6):765–776, 1995.
- [34] X-S. Gao, D. Lei, Q. Liao, and G-F. Zhang. Generalized Stewart-Gough platforms and their direct kinematics. *IEEE Transactions on Robotics*, 21(2):141–151, 2005.
- [35] Z. Geng and L. S. Haynes. A 3-2-1 kinematic configuration of a Stewart platform and its application to six degree of freedom pose measurements. *Robotics and Computer-Integrated Manufacturing*, 11(1):23–34, 1994.
- [36] C.G. Gibson and K. H. Hunt. Geometry of screw systems-I, screws: Genesis and geometry. *Mechanism and Machine Theory*, 25(1):1–10, 1990.
- [37] C.G. Gibson and K.H. Hunt. Geometry of screw systems-II, screws: classification of screw systems. *Mechanism and Machine Theory*, 25(1):11–27, 1990.
- [38] C. Gosselin and J. Angeles. Singularity analysis of closed-loop kinematic chains. *IEEE Transactions on Robotics*, 6(3):281–290, 1990.
- [39] C. M. Gosselin and E. St.-Pierre. Development and experimentation of a fast 3-DOF camera-orienting device. *International Journal of Robotics Research*, 16(5):619–630, 1997.
- [40] V.E. Gough and S.G. Whitehall. Universal tyre test machine. In *Proceedings 9th Int. Technical Congress F.I.S.I.T.A.*, volume 117, pages 117–135, 1962.
- [41] R. Di Gregorio. Singularity-locus expression of a class of parallel mechanisms. *Robotica*, 20:323–328, 2002.
- [42] M. Griffis and J. Duffy. Method and apparatus for controlling geometrically simple parallel mechanisms with distinctive connections. *US Patent 5,179,525*, 1993.

- [43] G.J. Hamlin and A.C. Sanderson. *Tetrobot: A Modular Approach to Reconfigurable Parallel Robotics*. Kluwer Academic Publishers, Norwell, 1999.
- [44] J. Hesselbach, M. Krefft, and H. Brüggemann. Reconfigurable parallel robots: Combining high flexibility and short cycle times. *Production Engineering WGP e. V.*, XIII(1):109–112.
- [45] J. Hubert and J.P. Merlet. Singularity analysis through static analysis. In *International Symposium on Advances in Robot Kinematics*, pages 13–20, 2008.
- [46] K.H. Hunt and P.R. McAree. The octahedral manipulator: geometry and mobility. *International Journal of Robotics Research*, 17(8):868–885, 1998.
- [47] M. Husty. An algorithm for solving the direct kinematics of Stewart-Gough-type platforms. Technical report, Rapport de Recherche TR-CIM-94-7, Université McGill, 1994.
- [48] M. Husty, S. Mielczarek, and M. Hiller. A redundant spatial Stewart-Gough platform with a maximal forward kinematics solution set. In *International Symposium on Advances in Robot Kinematics*, pages 147–154, 2002.
- [49] M.L. Husty and A. Karger. Architecture singular parallel manipulators and their self-motions. In *International Symposium on Advances in Robot Kinematics*, pages 355–364, 2000.
- [50] M.L. Husty and A. Karger. Self-motions of Griffis-Duffy type parallel manipulators. In *IEEE International Conference on Robotics and Automation*, pages 7–12, 2000.
- [51] C. Innocenti and V. Parenti-Castelli. Exhaustive enumeration of fully-parallel kinematic chains. *Proc. ASME 1994 International Annual Winter Meeting (Dynamic System and Control)*, 55(2):1135–1141, 1994.
- [52] A. Karger. Singularities and self-motions of equiform platforms. *Mechanism and Machine Theory*, 36(7):801–815, 2001.
- [53] A. Karger. Architecture singular planar parallel manipulators. *Mechanism and Machine Theory*, 38:1149–1164, 2003.

- [54] A. Karger. Architecturally singular non-planar parallel manipulators. *Mechanism and Machine Theory*, 43:335–346, 2008.
- [55] A. Karger and M. Husty. Singularities and self-motions of Stewart-Gough platforms. In *Proc. of Computational Methods in Mechanisms, NATO Advanced Study Institute*, pages 279–288, 1997.
- [56] X. Kong. Generation of singular 6-SPS parallel manipulators. In *Proc. of ASME Design Engineering Technical Conferences*, pages DETC98/MECH–5952, 1998.
- [57] X. Kong and C.M. Gosselin. Classification of 6-SPS parallel manipulators according to their components. In *Proc. of ASME Design Engineering Technical Conferences*, pages DETC2000/MECH–14105, 2000.
- [58] X. Kong and C.M. Gosselin. Generation of architecturally singular 6-SPS parallel manipulators with linearly related planar platforms. In *International Workshop on Computational Kinematics*, 2001.
- [59] P. Kovács and G. Hommel. On the tangent-half-angle substitution. In *International Workshop on Computational Kinematics*, pages 27–39, 1993.
- [60] M. Krefft, J. Hesselbach, G. Herrmann, and H. Brüggemann. VARIOPOD: A reconfigurable parallel robot with high flexibility. In *Proc. of ISR Robotik, Joint Conference on Robotics*, 2006.
- [61] D. Lazard. Stewart platforms and Gröbner basis. In *International Symposium on Advances in Robot Kinematics*, pages 136–142, 1992.
- [62] J. Lee, J. Duffy, and K.H. Hunt. A practical quality index based on the octahedral manipulator. *International Journal of Robotics Research*, 17(10):1081–1090, 1998.
- [63] H. Li, C.M. Gosselin, M.J. Richard, and B.M. St-Onge. Analytic form of the six-dimensional singularity locus of the general Gough-Stewart platform. *Journal of Mechanical Design*, 128(1):279–287, 2006.
- [64] O. Ma and J. Angeles. Architecture singularities of platform manipulators. In *IEEE International Conference on Robotics and Automation*, volume 2, pages 1542–1547, 1991.

- [65] J.M. McCarthy. *Geometric Design of Linkages*. 2000.
- [66] J-P. Merlet. Singular configurations of parallel manipulators and grassmann geometry. *International Journal of Robotics Research*, 8(5):45–56, 1989.
- [67] J-P. Merlet. Determination of the orientation workspace of parallel manipulators. *Journal of Intelligent and Robotic Systems*, 13(2):143–160, 1995.
- [68] J-P. Merlet. *Parallel Robots*. Springer, 2000.
- [69] J-P. Merlet. Solving the forward kinematics of a Gough-type parallel manipulator with interval analysis. *International Journal of Robotics Research*, 23(3):221–236, 2004.
- [70] J-P. Merlet. Jacobian, manipulability, condition number, and accuracy of parallel robots. *Journal of Mechanical Design*, 128:199–206, 2006.
- [71] J-P. Merlet. Alias: an interval analysis based library for solving and analyzing system of equations. <http://www-sop.inria.fr/coprin/logiciels/ALIAS/ALIAS-C++/ALIAS-C++.html>, 2007.
- [72] J-P. Merlet. Parallel robots. Notes from EURON Winter School: Parallel robots: theory and applications, 2007.
- [73] D. Michelucci and S. Foufouy. Using Cayley-Menger determinants for geometric constraint solving. *Proc. ACM Symposium on solid modeling and applications*, pages 285–290, 2004.
- [74] S. Mielczarek, M. Husty, and M. Hiller. Designing a redundant Stewart-Gough platform with a maximal forward kinematics solution set. In *Proc. of MUSME, the International Symposium on Multibody Systems and Mechatronics*, page M31, 2002.
- [75] J.J. Milne. *An elementary treatise on cross-ratio geometry with historical notes*. Cambridge University Press, 1911.
- [76] R. Neugebauer, M. Schwaar, St. Ihlenfeldt, G. Pritschow, C. Eppler, and T. Garber. New approaches to machine structures to overcome the limits of classical

- parallel structures. *CIRP Annals - Manufacturing Technology*, 51(1):293–296, 2002.
- [77] J. M. Porta, L. Ros, F. Thomas, and C. Torras. A branch-and-prune solver for distance constraints. *IEEE Transactions on Robotics*, 21(2):176–187, 2005.
- [78] J.M. Porta, L. Ros, and F. Thomas. Inverse kinematics by distance matrix completion. In *International Workshop on Computational Kinematics*, 2005.
- [79] J.M. Porta, L. Ros, and F. Thomas. On the trilaterable six-degree-of-freedom parallel and serial manipulators. In *IEEE International Conference on Robotics and Automation*, pages 960 – 967, 2005.
- [80] J.M. Porta, L. Ros, and F. Thomas. A linear relaxation technique for the position analysis of multiloop linkages. *IEEE Transactions on Robotics*, 25(2):225–239, 2009.
- [81] PI-Piezo Nano Positioning. Parallel kinematics: Hexapods & tripods. http://www.physikinstrumente.com/en/products/hexapod_tripod/.
- [82] M. Raghavan. The Stewart platform of general geometry has 40 configurations. *Journal of Mechanical Design*, 115(2):277–282, 1993.
- [83] J.D. Robinson and M.J.D. Hayes. The kinematics of a-pair jointed serial linkages. In *Proceedings of the ASME 2010 International Design Engineering Technical Conferences & Computers and Information in Engineering Conference*, 2010.
- [84] N. Rojas, J. Borràs, and F. Thomas. A distance-based formulation of the octahedral manipulator kinematics. In *IFTToMM Symposium on Mechanism Design for Robotics*, 2010.
- [85] N. Rojas and F. Thomas. The forward kinematics of 3-RPR planar robots: A review and a distance-based formulation. *IEEE Transactions on Robotics*, 27(1):143–150, 2011.
- [86] F. Ronga and T. Vust. *Stewart platforms without computer?* Preprint, Université de Genève, 1992.

- [87] O. Röschel and S. Mick. Characterisation of architecturally shaky platforms. In *International Symposium on Advances in Robot Kinematics*, pages 465–474, 1998.
- [88] T. Schmidt-Kaler. The hexapod telescope: A new way to very large telescopes. *ESO Conference on Progress in Telescope and Instrumentation Technologies*, 1992.
- [89] J.G. Semple and G.T. Kneebone. *Algebraic Projective Geometry*. Oxford University Press, 1952.
- [90] S-K. Song and D-S. Kwon. A tetrahedron approach for a unique closed-form solution of the forward kinematics of six-dof parallel mechanisms with multiconnected joints. *Journal of Robotic Systems*, 19(6):269–281, 2002.
- [91] B. Mayer St-Onge and C. Gosselin. Singularity analysis and representation of the general Gough-Stewart platform. *International Journal of Robotics Research*, 19(3):271–288, 2000.
- [92] E. Staffetti and F. Thomas. Kinestatic analysis of serial and parallel robot manipulators using Grassmann-Cayley algebra. In *International Symposium on Advances in Robot Kinematics*, pages 17–26, 2000.
- [93] C. Stechert and H.-J.Franke. Requirement-oriented configuration of parallel robotic systems. In *Proc. of The 17th CIRP Design Conference 2007, The Future of Product Development*, pages 259–268, 2007.
- [94] D. Stewart. A platform with 6 degrees of freedom. In *Proc. of The Institution of Mechanical Engineers*, volume 180, pages 371–386, 1965/66.
- [95] R.S. Stoughton and T. Arai. A modified Stewart platform manipulator with improved dexterity. *IEEE Transactions on Robotics*, 9(2):166–173, 1993.
- [96] J.C. Taylor. Correction of the general deformity with the Taylor Spatial Frame Fixator. <http://www.jcharlestaylor.com/spat/00spat.html>.
- [97] The CUIK project home page. <http://www.iri.upc.edu/research/webprojects/cuikweb/>.
- [98] F. Thomas and L. Ros. Revisiting trilateration for robot localization. *IEEE Transactions on Robotics*, 21(1):93–101, 2005.

- [99] C. Torras, F. Thomas, and M. Alberich-Carramiñana. Stratifying the singularity loci of a class of parallel manipulators. *IEEE Transactions on Robotics*, 22(1):23–32, 2006.
- [100] L-W. Tsai. *Robot Analysis. The Mechanics of Serial and Parallel Manipulators*. John Wiley and Sons, 1999.
- [101] K. J. Waldron, M. Raghavan, and B. Roth. Kinematics of a hybrid series-parallel manipulation system. *ASME Journal of Dynamic Systems, Measurement, and Control*, 111(2):211–221, 1989.
- [102] M. Wecka and D. Staimera. Parallel kinematic machine tools. current state and future potentials. *CIRP Annals - Manufacturing Technology*, 51(2):671–683, 2002.
- [103] G. Weiß and G.F. Bär. Singularity investigation of a 5-leg milling robot. In *EuCoMeS, 1st European Conference on Mechanism Science*, 2006.
- [104] E.W. Weisstein. “Jacobi’s theorem”, from mathworld—a wolfram web resource. <http://mathworld.wolfram.com/JacobisTheorem.html>.
- [105] N. White. The bracket of 2-extensors. *Congressus Numerantium*, 40:419–428, 1983.
- [106] K. Wohlhart. Architectural shakiness or architectural mobility of platforms. In *International Symposium on Advances in Robot Kinematics*, pages 365–374, 2000.
- [107] K. Wohlhart. Synthesis of architecturally mobile double-planar platforms. In *International Symposium on Advances in Robot Kinematics*, pages 473–482, 2002.
- [108] K. Wohlhart. Mobile 6-SPS parallel mainpulators. *Journal of Robotic Systems*, 20(8):509–516, 2003.
- [109] A. Wolf and M. Shoham. Investigation of parallel manipulators using linear complex approximation. *Journal of Mechanical Design*, 125:564–572, 2003.
- [110] T. Yoshikawa. Manipulability of robotic mechanisms. *International Journal of Robotics Research*, 4(2):3–9, 1985.

BIBLIOGRAPHY

- [111] C. Zhang and S.M. Song. Forward kinematics of a class of parallel (Stewart) platforms with closed-form solutions. *Journal of Robotic Systems*, 9(1):93–112, 1992.
- [112] Y. Zhu, L.D. Senevirante, and S.W. Earles. A new structure of invariant for 3D point sets from a single view. In *IEEE International Conference on Robotics and Automation*, pages 1726–1731, 1995.